



<https://theses.gla.ac.uk/>

Theses Digitisation:

<https://www.gla.ac.uk/myglasgow/research/enlighten/theses/digitisation/>

This is a digitised version of the original print thesis.

Copyright and moral rights for this work are retained by the author

A copy can be downloaded for personal non-commercial research or study,
without prior permission or charge

This work cannot be reproduced or quoted extensively from without first
obtaining permission in writing from the author

The content must not be changed in any way or sold commercially in any
format or medium without the formal permission of the author

When referring to this work, full bibliographic details including the author,
title, awarding institution and date of the thesis must be given

Enlighten: Theses

<https://theses.gla.ac.uk/>
research-enlighten@glasgow.ac.uk

Overpressure in the Central North Sea

A thesis submitted for the degree of
Doctor of Philosophy

by

David Darby

B. Sc. Glasgow University

Department of Geology and Applied Geology
University of Glasgow

September 1995

ProQuest Number: 13815360

All rights reserved

INFORMATION TO ALL USERS

The quality of this reproduction is dependent upon the quality of the copy submitted.

In the unlikely event that the author did not send a complete manuscript and there are missing pages, these will be noted. Also, if material had to be removed, a note will indicate the deletion.



ProQuest 13815360

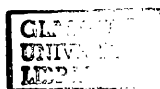
Published by ProQuest LLC (2018). Copyright of the Dissertation is held by the Author.

All rights reserved.

This work is protected against unauthorized copying under Title 17, United States Code
Microform Edition © ProQuest LLC.

ProQuest LLC.
789 East Eisenhower Parkway
P.O. Box 1346
Ann Arbor, MI 48106 – 1346

Therist
10265
Copy 1



Abstract

The Central Graben of the North Sea is characterised by high levels of overpressure. This causes drilling problems and may control the migration and entrapment of hydrocarbons. Pressure measurements from repeat formation tests, mud weight and drilling gas levels have been compiled and interpreted, and integrated with the structural, lithostratigraphic and diagenetic framework of the basin. Interpretation of this data reveals that Jurassic sandstones in the region are divided into a boxwork of pressure cells. These are bodies of rock which are internally in hydraulic communication but externally isolated from adjacent cells by pressure seals. Pressure seals in the region are lithological and vary with depth, in contrast to previous hypotheses of diagenetic or temperature controls. The magnitude of overpressure in a pressure cell is controlled by the structural position of the cell, with high overpressures (close to the lithostatic pressure) occurring in structurally-elevated cells on an axial horst. Lateral hydraulic communication between deep regions and structurally-elevated positions increases the fluid pressure in the permeable sandstones in the elevated regions. This leads to focused vertical fluid flow through the thin aquitard at these elevated regions, which are termed "Leak Points". Here, the pressure seal occurs at the top of the permeable Jurassic sandstone, while in adjacent off-structure regions the pressure seal occurs in the Kimmeridge Clay Fm., the region's petroleum source rock. Analysis of density and sonic log data demonstrates excess mudstone porosity in the overpressured cells, suggesting that disequilibrium compaction is a cause of overpressure in the region. The location of pressure seals within gas-mature source rocks suggests hydrocarbon generation may also play an important role in causing overpressure. Quantitative computer modelling of the basin supports the data-driven model, emphasising lateral flow in Jurassic sandstones beneath the pressure seal and focused vertical flow across formations at structurally-elevated points. The model shows that rapid Cenozoic sedimentation, coupled to low permeability of the mudstone-dominated basin, has led to disequilibrium compaction due to restricted fluid flow. The model suggests that overpressuring began at 40 Ma in Jurassic sandstones of the Graben axis. A link between overpressure-controlled fluid flow and the K-Ar dates of authigenic illite in the Jurassic sandstones is delineated. Measured illite dates coincide with modelled periods of declining fluid flow. A link to the incursion of organic acids from adjacent mudstones into the sandstones is proposed, with the supply of organic acids controlled by the compaction and overpressure in the basin. The distribution of porosity within Jurassic sandstones is examined and is shown to be controlled by the complex distribution of overpressure. Overpressure supports the development of secondary porosity. Products of mineral dissolution are preferentially removed from Leak Points due to enhanced vertical fluid flow. This results in 10-12 % excess porosity at 4.6 km depth. Overpressure is a dynamic system, with basin-scale structures such as pressure cells being caused by microscopic changes in pore size. The basin-scale overpressure systems in turn effect pore-scale alterations on the basin. Overpressure is an expression of the complex dynamic interaction of coupled hydrogeological and geochemical processes active throughout the evolution of the basin.

Thesis Declaration

The material presented in this thesis is the result of research carried out between October 1992 and September 1995 in the Department of Geology and Applied Geology, University of Glasgow, under the supervision of Dr. Stuart Haszeldine.

This thesis is based on my own independent research and any published or unpublished material used by me has been given full acknowledgement in the text.

David Darby
September 1995

We certify that David Darby has undertaken the bulk of the work involved in this thesis. Specifically, background geology, data collation and analysis, and computer modelling. We have assisted with advice and help of a general, technical, conceptual nature, as would be expected in the course of normal Ph.D supervision. David Darby has written the thesis himself, and is responsible for its content.

R.S. Haszeldine

G.D. Couples

M. Wilkinson

To Sharon

The geologic approach is certainly primary and fundamental, underlying the attitude and outlook that best support all others, including the insights of poetry and the wisdom of religion. Just as the earth itself forms the indispensable ground for the only kind of life we know, providing the sole sustenance of our minds and bodies, so does empirical truth constitute the foundation for higher truths....I see more poetry in a chunk of quartzite than in a make-believe wood-nymph, more beauty in the revelations of a verifiable intellectual construction than in whole misty empires of obsolete mythology.

Edward Abbey, from The Journey Home

Acknowledgements

My first acknowledgement is to Dr R Stuart Haszeldine. Dr Haszeldine created this fascinating project and has guided its progress throughout the past three years. He has continually astounded me with his creativity and perception. I thank him for his guidance and for allowing me the space to pursue my own interests in this project. I consider myself fortunate to have served my "apprenticeship" with a scientist of his calibre. The Natural Environment Research Council have funded this study. NERC has also kindly provided travel and subsistence funds for numerous conferences.

I would like to thank the "gurus" who have guided me through this research. Dr Gary D. Couples, the "off-on" joint supervisor of this project, is thanked for his continual interest and encouragement of this work. His professionalism and approachability have improved this thesis beyond compare. I owe a particular debt to Gordon Holm of Hydrocarbon Management International Ltd, whose insight, enthusiasm and experience still leaves me in awe. Dr. Mark Wilkinson of Glasgow University has encouraged the synergy between my project and his diagenetic research, which has added enormously to this thesis. Mark has allowed me to share his knowledge and scientific interests, and has given me a model for exactly how rigorous research should be conducted. Dr Tony Fallick of the Scottish Universities Research and Reactor Centre has reviewed and refined the "illite story" of Chapter Six

Platte River Associates are thanked for allowing me use of the BasinMod 1D and 2D basin modelling computer codes, which were provided free of charge. Particular thanks are due to Jay and China Leonard. I would also like to thank IGI Ltd who have provided invaluable support and insight. Technical support for this hi-tech monstrosity has been provided by Dr. Colin Farrow, Jim Kavanagh and Pete Ainsworth.

Elf Enterprise Caledonia have provided access to confidential and released pressure data. E.E. Cal. provided desk space, computers and expenses for a three-month period during which I gathered data in their Aberdeen headquarters. The efficiency and generosity of their staff provided a head start for this project. I would particularly like to thank John Lasocki, Roger Hinton and Francois Issard. E.E. Cal. have also funded the wider study of Central North Sea diagenesis which added so much to the interest and significance of this project.

This project has benefited from comments by many scientists at conferences in Britain and the USA. For the encouragement and interest they have shown, I would particularly like to thank Larry Cathles of Cornell University, Jean Whelan of Woods Hole, Christian Hermanrud and Lars Wensaas of Statoil, Sebastian Bell and Dale Issler of the Canadian Geological Survey, Indu Meshri of Amoco, and Brett Mudford of Unocal.

Although this project has been helped by many excellent scientists, this thesis would never have been completed without the support of my friends. I cannot even begin to acknowledge the debt I owe to my parents for their support and love; I hope they can feel my gratitude. The Glasgow Geology department has been a wonderful place to work; my thanks go out to the students and staff, past and present, especially Campbell, Gary, Karen, Wobbly, Helen and Carolyn. Thanks too to Johnny Hull, Kate Powney and Andy Cavanagh, whose student projects were fun (for me at least). My special thanks must go to Chris McKeown whose friendship and wit has made each day a little sunnier.

My greatest thanks go to my friend and lover Sharon.

Contents

	<i>Page Number</i>
Abstract	(i)
Thesis declaration	(ii)
Acknowledgements	(iii)
Contents	(iv)
Figure List	(vii)
Chapter 1 Introduction	1
1.1 Context of thesis	2
1.2 Aims of thesis	3
1.3 Layout of thesis and methodology employed in research	4
1.4 Study area of thesis: the Central North Sea	5
1.4.1 <i>Location of Central North Sea wells</i>	5
1.4.2 <i>Tectonic setting of the Central North Sea</i>	6
1.4.3 <i>Central North Sea lithostratigraphy</i>	7
1.4.4 <i>Previous studies of Central North Sea overpressure</i>	9
Chapter 2 Background Theory	21
2.1 Physical principles of overpressure in the geological environment	22
2.2 Fluid flow in the subsurface	23
2.3 Overpressure in the Earth's crust	24
2.3.1 <i>Near-surface overpressuring</i>	24
2.3.2 <i>Overpressure in sedimentary basins</i>	24
2.3.3 <i>Overpressure in the deep crust</i>	25
2.4 Overpressure in sedimentary basins: a global overview	25
2.5 The pressure cell paradigm	26
2.6 Pressure seals	28
2.7 Origins of overpressure	30
2.7.1 <i>External effects</i>	30
2.7.2 <i>Internal effects</i>	31
2.8 Paradigms of overpressure	33
2.9 Summary	34
Chapter 3 Pressure Cells and Pressure Seals in the Central North Sea	42
3.1 Introduction	43

3.2	Pressure data	43
3.2.1	<i>Direct pressure measurements</i>	44
3.2.2	<i>Indirect pressure measurements</i>	46
3.2.3	<i>Leak-Off Tests</i>	48
3.2.4	<i>Correction of depths</i>	49
3.3	Pressure distribution in the Central North Sea	49
3.3.1	<i>Basin-scale pressure distribution</i>	49
3.3.2	<i>Cenozoic mudstones</i>	49
3.3.3	<i>Palaeocene sandstones</i>	50
3.3.4	<i>Cretaceous Chalk</i>	50
3.3.5	<i>L. Cretaceous - Triassic</i>	50
3.4	Discussion of the pressure distribution	52
3.4.1	<i>Cenozoic</i>	52
3.4.2	<i>Cretaceous Chalk</i>	52
3.4.3	<i>L Cretaceous - Triassic</i>	53
3.5	The problems presented by the pressure distribution	56
3.6	A model of Central North Sea overpressure	57
3.6.1	<i>Potential energy of fluids in the Central North Sea</i>	57
3.6.2	<i>Intra-cell and inter-cell flow beneath the pressure seal</i>	59
3.6.3	<i>Lateral permeability considerations</i>	61
3.6.4	<i>Pressure seals in the dynamic model</i>	63
3.6.5	<i>Vertical fluid flow through the pressure seal: Leak Points</i>	64
3.6.6	<i>Case studies of Leak Points</i>	64
3.6.7	<i>Additional supportive evidence for the dynamic model</i>	66
3.6.8	<i>The role of Zechstein salt</i>	67
3.7	Implications for hydrocarbon migration and entrapment	68
3.8	Summary	69
Chapter 4	Causes of Overpressure in the Central Graben	103
4.1	Introduction	104
4.2	Disequilibrium compaction	105
4.2.1	<i>Sonic log measurements of porosity</i>	106
4.2.2	<i>Density measurements</i>	107
4.2.3	<i>Caliper logs</i>	108
4.2.4	<i>The sub-seal porosity anomaly: primary or secondary?</i>	109
4.2.5	<i>Assumptions of this approach</i>	110
4.3	Hydrocarbon generation	111
4.3.1	<i>Pressure distribution</i>	112
4.3.2	<i>Magnitude of minimum stress</i>	113
4.3.3	<i>Pressure sealing and pressure generation in the Kimmeridge Clay</i>	115

4.3.4	<i>Hydrocarbon generation in HPHT regions</i>	118
4.4	Aquathermal pressuring	119
4.5	Clay Mineral dehydration	120
4.6	A synthetic model for Central North Sea overpressures	121
4.7	Summary	123
Chapter 5	A model investigation of Central North Sea Overpressure	140
5.1	Introduction	141
5.2	Review of existing model approaches	142
5.3	Choice of methodology: the philosophy of modelling	144
5.4	One-dimensional models	145
5.4.1	<i>Aims of the one-dimensional model investigation</i>	145
5.4.2	<i>Data</i>	146
5.4.3	<i>One-dimensional model methodology</i>	147
5.4.4	<i>Evaluation of sensitivity to variations</i>	147
5.4.5	<i>One-dimensional model results</i>	148
5.4.6	<i>Discussion and conclusions</i>	150
5.5	Two-dimensional models	151
5.5.1	<i>Aims of two-dimensional model investigations</i>	151
5.5.2	<i>Data</i>	152
5.5.3	<i>Two-dimensional model methodology</i>	153
5.5.4	<i>Two-dimensional model results</i>	154
5.5.5	<i>Model hydrocarbon generation and migration</i>	155
5.5.6	<i>Evaluation of sensitivity to variations</i>	156
5.5.7	<i>Discussion</i>	160
5.6	Conclusions	161
Chapter 6	Overpressure-related aspects of diagenesis in the Central Graben	204
6.1	Introduction	205
6.2	Current conceptual models of diagenesis	206
6.2.1	<i>Diagenesis and overpressure</i>	207
6.2.2	<i>Review of diagenesis of the Fulmar sandstones</i>	208
6.2.3	<i>Summary</i>	209
6.3	Authigenic illite and overpressure in the Central Graben	210
6.3.1	<i>Methodology and results</i>	210
6.3.2	<i>Discussion</i>	212
6.3.3	<i>Conclusions</i>	215
6.4	Overpressure and porosity distribution in the Central Graben	216
6.4.1	<i>Methodology</i>	218

6.4.2	<i>Results</i>	219
6.4.3	<i>Discussion</i>	220
6.4.4	<i>Conclusions</i>	224
6.5	Conclusions: a model for Central North Sea overpressure-related diagenesis	225
Chapter 7	Conclusions	249
7.1	Introduction	250
7.2	Research conclusions	250
7.2.1	<i>The distribution of overpressure in the Central Graben</i>	250
7.2.2	<i>Origins of overpressure</i>	252
7.2.3	<i>Development of a quantitative process-based model</i>	253
7.2.4	<i>Overpressure and diagenesis</i>	254
7.3	Thesis methodology: steps forward	255
7.4	Assumptions made in the research	255
7.5	Further work suggested by this thesis	257
7.6	Concluding statement	259
	Bibliography	261
	Appendix	285

List of Figures

Figure Number	Title	Page Number
Chapter 1		
1.1	Definition of North Sea pressure compartments from Hunt (1990)	11
1.2	Location map of Central Graben	12
1.3	Division of Central Graben into Quads and Blocks, and location of study wells	13
1.4	Late Jurassic tectonic elements of Central Graben	14
1.5	Cross-sections of northern Central Graben	15
1.6	Cross-sections of southern Central Graben	16
1.7	Stratigraphic column of the Central Graben	17
1.8	Stratigraphic column of the Humber Group	18
1.9	Stratigraphic cross-section of the Humber Gp.	19
Chapter 2		
2.1	Mohr circle diagram of principal stresses and pore pressure	35
2.2	Hydrogeological regimes of a sedimentary basin	35
2.3	Occurrence of overpressure in the Earth's crust	36
2.4	Pressure cell definition	37
2.5	Example pressure-depth plot	38
2.6	Maximum time a pressure seal may confine excess pressure	39
2.7	Fluid pressure changes in response to loading	40
2.8	Mudstone bulk composition during dehydration	41
Chapter 3		
3.1	Example RFT logs	71
3.2	Use of gas levels and mudweight as qualitative pressure interpretation	72
3.3	Central North Sea Leak-Off Test Logs	73
3.4	Regional RFT pressure-depth plot	74
3.5	Map of pressure distribution in Palaeocene sands	75
3.6	Palaeocene RFT pressure-depth plot	76
3.7	Map of distribution of pressure in Cretaceous Chalk	77
3.8	Cretaceous Chalk RFT pressure-depth plot	78
3.9	Map of overpressure in Jurassic and Triassic sandstones in the Central Graben	79
3.10	Pressure-depth plot of RFTs in Jurassic and Triassic sandstones of the Central Graben	80
3.11	Pressures in well 22/30a-1	81
3.12	Pressures in well 29/5b-4	82
3.13	Pressures in well 29/10-2	83
3.14	Pressures in well 29/5a-3	84
3.15	Pressures in well 22/27a-1	85
3.16	Pressures in well 22/24a-1	86
3.17	Pressures in well 23/26a-7	87
3.18	Pressures in well 23/26a-2	88
3.19	Pressures in well 30/1c-2	89
3.20	Pressure cells in Jurassic sandstones of the East Forties basin	90
3.21	Detail plot of cell relationships in Blocks 29/5 - 22/30	91
3.22	A pressure cell on the Jaeren High	92
3.23	Pressure cells on the Forties-Montrose High	93
3.24	Pressure cells in Jurassic sandstones in Quad 30	94
3.25	Map of pressure cells in sub-Cretaceous stratigraphy	95
3.26	Potentiometric map of central study area	96
3.27	Cartoon of hydraulic connectivity and resultant pressure relationships	97
3.28	Temperature and heat flow variation in the Central Graben	98
3.29	Hydrocarbon distribution and the dynamic pressure model	99
3.30	Hydrocarbon entrapment and retention in HPHT regions	100
3.31	The dynamic nature of hydrocarbon entrapment	101
3.32	Summary cartoon of Central North Sea overpressure	102
Chapter 4		
4.1	Sonic and density logs from well 22/30a-1	124
4.2	Sonic and density logs from well 22/27a-1	125
4.3	Sonic and density logs from well 29/10-2	126
4.4	Sonic and density logs from well 23/26a-2	127
4.5	Pressure and wireline logs from the Gullfaks area, Northern North Sea	128
4.6	Sonic logs and effective stress in well 23/26a-2	129
4.7	Caliper logs of well 29/10-2	130
4.8	Caliper logs of well 23/26a-2	130
4.9	Graph of LOT pressures vs depth	131
4.10	Pressures and stresses in the Piceance Basin, Rocky Mountains	132
4.11	Three-stage evolution of Kimmeridge Clay overpressure	133
4.12	Volume changes during hydrocarbon generation	134
4.13	Formation pressures in the Williston Basin, Canada	135
4.14	Solubility of natural gas in formation water	136
4.15	Volume changes affecting hydrocarbons in HPHT environments	137
4.16	Effective stress in a dipping sandstone	138

Chapter 5

5.1 Data available for model calibration	163
5.2 Modelled and observed temperature in well 22/30a-1	164
5.3 Sensitivity of model pressures to thermal input variables	165
5.4 Sensitivity of model maturity to thermal input variables	166
5.5 Sensitivity of model pressure to variation in density and porosity	167
5.6 Subsidence curve of well 22/30a-1	168
5.7 Subsidence curve of well 29/10-2	169
5.8 Model porosity and permeability for Valanginian mudstones in well 22/30a-1	170
5.9 Model porosity and permeability for Valanginian mudstones in well 29/10-2	171
5.10 Model porosity and permeability for Aptian-Albian mudstones in well 22/24a-1	172
5.11 Model pressure-depth profiles for well 22/30a-1	173
5.12 Model pressure-depth profiles for well 29/10-2	174
5.13 Model pressure-depth profiles for well 22/24a-1	175
5.14 Modelled and observed pressures in the Central Graben	176
5.15 Model porosity and permeability for Maastrichtian Chalks in well 29/10-2	177
5.16 Model porosity and permeability for Maastrichtian Chalks in well 22/24a-1	178
5.17 Initial input cross-section for two-dimensional model	179
5.18 Initial input cross-section for two-dimensional model showing lithostratigraphic horizons	180
5.19 Cross-section calculation grid for two-dimensional model	181
5.20 Modelled and observed pressure-depth profile for well 22/30a-1	182
5.21 Modelled and observed pressure-depth profile for well 23/27-6	183
5.22 Cross-section of modelled overpressure	184
5.23 Simulated water flow directions in the model cross-section	185
5.24 Model pressure-depth profile for off-structure pseudowell	186
5.25 Modelled porosity-depth profiles for well 22/30a-1 and off-structure pseudowell	187
5.26 Evolution of model aquitard porosity and permeability of well 22/30a-1	188
5.27 Modelled timing of overpressure development for Fulmar Fm. of well 22/30a-1	189
5.28 Modelled timing of overpressure development for Fulmar Fm. of well 23/27-6	190
5.29 Evolution of modelled overpressure with time and burial history for off-structure pseudowell	191
5.30 Modelled timing of hydrocarbon generation and associated overpressuring in Kimmeridge Clay	192
5.31 Modelled timing of hydrocarbon accumulation in Fulmar Fm. of well 22/30a-1	193
5.32 Cross-section of modelled hydrocarbon migration and accumulation	194
5.33 Water flow directions in simulation representing lateral shale-out of Fulmar Fm.	195
5.34 Oil accumulation and flow paths at 30 Ma in simulation representing lateral shale-out of Fulmar Fm.	196
5.35 Modelled and observed pressure-depth profiles in well 23/27-6 in simulation with discontinuous Palaeocene	197
5.36 Modelled oil accumulation in simulation with discontinuous Palaeocene sandstones	198
5.37 Oil migration and accumulation in open-fault model at 30 Ma	199
5.38 Modelled and observed pressures in well 23/27-6 for low-permeability mudstones	200
5.39 Summary cartoon of model investigation findings	201

Chapter 6

6.1 Relationship between illite dates and modelled overpressure evolution in NW Hutton area	227
6.2 Published diagenetic sequences for Fulmar Fm. in Central Graben	228
6.3 Location of study wells	229
6.4 SEM and TEM images of authigenic illite from the Fulmar Fm.	230
6.5 XRD pattern for < 0.1 micron clay fraction from Fulmar Fm.	231
6.6 Modelled subsidence curves for study wells	232
6.7 Simulated overpressure for wells 22/30a-1 and 23/27-6	233
6.8 Modelled depth of burial and temperature for well 23/27-6	234
6.9 Summary cartoon of relationship between structure, overpressure and illite growth	235
6.10 Evolution of effective stress through time	236
6.11 Relationship of porosity to changes in effective stress	237
6.12 Effective stress and the Maximum Potential Porosity (MPP) concept	238
6.13 MPP and relationship between porosity and overpressure	239
6.14 Porosity data from Fulmar Fm. cores	240
6.15 Modelled overpressure, porosity and MPP for well 23/27-6	241
6.16 Modelled overpressure, porosity and MPP for well 22/30a-1	242
6.17 Distribution of feldspar as a function of depth in Fulmar Fm.	243
6.18 Thin sections and SEM images of porosity in the Fulmar Fm.	244
6.19 Evolution of Fulmar Fm. poroperm during late diagenesis	245
6.20 Summary cartoon of overpressure-related diagenesis in the Central Graben	246

Chapter 7

7.1 Summary cartoon of thesis conclusions	260
---	-----

Appendix

A.1 Compaction curves of standard model lithologies in hydro pressured conditions	293
A.2 Porosity-permeability relationships of standard model lithologies	294
A.3 Model fault permeability	295

Tables

5.1 Model input lithological parameters	202
5.2 Model hydrocarbon generation parameters	203
5.3 Sensitivity analysis results for two-dimensional model	203
6.1 Radiogenic K-Ar dates from illite in the Fulmar Fm.	247
6.2 Statistical analysis of porosity data from the Fulmar Fm.	248
A.1 Symbols used in equations	

Chapter One

Introduction

- 1.1** **Context of thesis**

- 1.2** **Aims of thesis**

- 1.3** **Layout of thesis and methodology employed
in research**

- 1.4** **Study area of thesis: the Central North Sea**
 - 1.4.1* *Location of Central North Sea wells*
 - 1.4.2* *Tectonic setting of the Central North Sea*
 - 1.4.3* *Central North Sea lithostratigraphy*
 - 1.4.4* *Previous studies of Central North Sea overpressure*

1.1 Context of thesis

Overpressure is defined as fluid pressure above normal hydrostatic pressure. Overpressured fluids have been recognised in many sedimentary basins worldwide. Overpressure forms a hazard for drilling for hydrocarbons in basins. High fluid pressures can cause blowouts on drilling rigs, and may cause injury to personnel. The occurrence of overpressure suggests that fluid flow is restricted. It thus carries implications for hydrocarbon migration and provides a clue to the hydrogeological regime of the basin.

The presence of fluid pressures above hydrostatic pressure implies that low-permeability restrictions to free fluid flow exist. Without a restriction, fluid pressures will remain at hydrostatic pressure. The recognition that overpressure requires inhibition of fluid flow by a low-permeability barrier allowed Bradley (1975) to propose the concept of a “pressure seal”. A pressure seal, as defined by Bradley (1975), is a zone of rock that prevents fluid flow. Accordingly, a seal hydraulically isolates regions of a basin. The basin is compartmentalised by seals into “pressure cells” or “pressure compartments”. In this model, fluids remain **static**, trapped within pressure cells until fracturing of the pressure seal occurs. This model of the hydrogeology of the deep regions of sedimentary basins has been applied to many basins world-wide (Hunt, 1990; Powley, 1990; Ortoleva & Al-Shaieb, Z. 1994). Pressure seals in these basins are inferred to be zones of rock where diagenetic cementation has lowered permeability to extremely low values. These cemented seals are claimed to be horizontal and discordant with stratigraphy (Hunt 1990).

However, the interpretation of a basin as a series of hydraulically-isolated compartments appears to contradict a fundamental tenet of hydrogeological thought—that there are no absolutely impermeable geological materials. Bredehoeft *et al.*, (1994), Deming (1994) and Neuzil, (1995) have shown that overpressure in sedimentary basins may be perceived as a **dynamic** phenomena. In this “dynamic” paradigm, fluid flow is retarded by low (but finite) permeability barriers. Overpressure is a disequilibrium that arises due to transient perturbation of flow by aspects of the dynamic evolution of the basin. Such aspects include rapid subsidence or fluid generation (Neuzil 1995). In this model, pressure seals are formed by low-permeability lithologies such as mudstones.

Interpretation of a basin in terms of the “pressure cell” model raises many important questions. Where are the pressure seals? What are the lithological or diagenetic characteristics that formed the seals? When did the seals form? Have the seals exerted

an effect on palaeo-fluid flow, and thus on diagenesis and hydrocarbon migration? Interpretation of a basin in terms of the “dynamic” model raises different questions. What are the origins of disequilibrium? What is the interplay between the rate of perturbation and the rate of re-equilibrating flow? Questions raised by overpressure are central to the understanding of fluid flow in sedimentary basins.

The Central North Sea has been cited as an example of a basin that is compartmentalised into pressure cells (Fig. 1.1; Hunt 1990). The Central North Sea is characterised by extremely high levels of overpressure (Cayley, 1987). It thus provides a case study for testing of the “pressure cell” model and its implications. This thesis attempts to understand the distribution, origins and effects of overpressure in the Central North Sea.

1.2 Aims of thesis

This thesis will present the data, interpretation and results of a research project aimed at clarifying the phenomena of overpressure in the Central North Sea. A data-driven approach to one case-study basin has been chosen to allow building and testing of hypotheses in a region of economic interest.

The aims of this research project are:

1. To delineate overpressure in the Central North Sea and to identify pressure cells and pressure seals. This project will allow identification of the controls on overpressure distribution in the area and the controls on the morphology and distribution of pressure seals. It will allow testing of the hypothesis that pressure seals in the region are planar zones that cross-cut stratigraphy (Hunt 1990).
2. To identify the mechanisms of pressure seal formation in the region. This project will allow testing of the rival hypotheses that pressure seals are diagenetic in origin (e.g. Hunt, 1990; Whelan *et al.*, 1994), or are lithological (e.g. Mello *et al.*, 1994).
3. To identify the origins of overpressure in the area. This task forms a necessary stage of pressure evaluation (Deming 1994) and allows testing of the hypothesis that overpressure and pressure seals are essentially transient in nature.

4. To examine the impact of overpressure on diagenesis in the region. This project will evaluate the impact of pressure seals and overpressure on palaeo-fluid flow (e.g. Hunt 1990).
5. The overall aim of the research is to gain insight into the fundamental controversy of overpressure (Section 2.9; Neuzil 1995): is overpressure a *static*, stable phenomena where regions exist in hydrogeological isolation (e.g. Hunt 1990) or is it a *dynamic* process in a hydraulically-continuous medium (e.g. Bredehoeft *et al*1994)?

1.3 Layout of thesis and methodology employed in research

Overpressure is a facet of fluid flow and the geodynamics of the basin. As such, it is intrinsically multi-disciplinary and may reflect many varied aspects of the basin. Accordingly, a multi-disciplinary approach has been employed to achieve the aims of this research project.

Chapter Two reviews a selection of existing publications to present background theory on overpressures. This chapter attempts to provide a context for the general reader. The physical principles of overpressure are presented. The terminology employed in this thesis is defined. The distribution and origins of overpressure are reviewed. The "static" and "dynamic" conceptual models of overpressure and pressure seals are discussed.

Chapter Three presents a new compilation and interpretation of pressure data from the Central North Sea. Pressure cells and pressure seals have been delineated, and integrated with the lithostratigraphic and structural framework of the basin.

Chapter Four presents new work defining the possible origins of overpressure in the region. It presents additional description of pressure data and ancillary lithological data. This data has been linked to a critical review of possible overpressuring mechanisms.

Chapter Five presents new work comprising computer simulations of fluid flow, hydrocarbon generation and basin evolution in the Central Graben. Computer simulation has been used to synthesise the empirical observations of overpressure and to provide a quantitative analysis of the processes controlling overpressure throughout

the history of the region. The *Appendix* presents the mathematical basis for the computer simulation, with a critical review of the technical basis of the model.

Chapter Six uses this quantitative simulation to provide a new framework for examining palaeo-fluid flow. Potassium-argon age-dates from authigenic minerals, porosity data and petrographic observations have been integrated with this quantitative framework to examine the effect of overpressure on palaeo-fluid flow.

Chapter Seven presents a critical summary of the findings of the research and delineates areas deserving further work.

1.4 Study area of thesis: the Central North Sea

The Central Graben of the North Sea is located 240 km east of Scotland (Fig 1.2). The study area consists of Quadrants 22, 23, 29 and 30 of the UK Central North Sea. This section will review the structure, lithostratigraphy and hydrogeology of the area.

1.4.1 Location of Central North Sea Wells

Pressure and lithological data in this project is derived from hydrocarbon exploration wells. The UK Sector of the North Sea is divided into *Quadrants*. Quadrants are subdivided into 30 *Blocks*, which are identified by a Quadrant Number and a Block Number. Block numbers progress from West to East across a Quadrant, and from North to South. Thus the block in the south-east corner of Quadrant 22 is identified by number 22/30. Each block may be licensed to an exploration company, who is permitted to drill exploration wells. Blocks may be further subdivided into sections licensed to separate companies (e.g. Block 22/30a). Within each block, exploration *wells* are numbered chronologically. The first well drilled in a block is given the number 1, the second the number 2, and so on. North Sea wells are identified by a code number in the form QUADRANT NUMBER/BLOCK NUMBER-WELL NUMBER. As an example, Well 22/30a-1 is the first well to be drilled in Block 30a of Quadrant 22.

The study area consists of Quadrants 22, 23, 29 and 30. This project will follow the nomenclature, detailed above, as it allows immediate location of any well specified in the text. A map of well locations is shown as Fig. 1.3

1.4.2 Tectonic setting of the Central North Sea

The Central Graben of the North Sea is the NNW-SSE trending southern arm of the tripartite North Sea rift. From its intersection with the Outer Moray Firth Basin at 58°N, the Central Graben extends 500 km southwards. The Central North Sea exhibits a polyphase structural evolution (Sears *et al.*, 1993). The basement framework was developed during the Caledonian orogeny, giving rise to NE-SW trending diffuse shear zones. These zones experienced repeated reactivation throughout the Mesozoic and the Cenozoic. A late Jurassic- early Cretaceous reorientation of stress led to reactivation of faults to form transpressional and transtensional features.

Rifting occurred from the Hauterivian to the Sinemurian, with fault-controlled sedimentation (Rattee & Hayward, 1993). Failure of the rift in the Portlandian transferred extension into the Atlantic margin and thus post-rift thermal sag deposition dominated the Cretaceous and Cenozoic. Post-rift structural modifications include halokinesis, structural inversion, gravitational collapse and compaction (Rattee & Hayward 1993).

Late Jurassic extension in the Central Graben resulted in a series of NE-dipping tilted fault blocks, bounded by NW-SE oriented faults (Roberts *et al.*, 1990). A structural map of the late Jurassic tectonic elements is shown as Fig 1.4. The basin can be divided into two, into an eastern and a western graben, separated by the axial Forties-Montrose High. A subdivision of the Central Graben into four structural subareas has been proposed (Roberts *et al.* 1990); this subdivision is shown on Fig 1.4, and cross-sections of each area are shown in Figs 1.5 and 1.6.

- Area 1: a northern subarea bounded in the east by the Jaeren High and in the North by the complex triple junction of the tripartite Graben system. This region comprises a simple Graben termed the West Forties Basin. The Forties-Montrose High in this region is a horst separating a second Graben, termed the Fisher Bank Basin. (Fig 1.5a)
- Area 2: a central zone of structural complexity formed by (from west to east): a series of three 10-km wide westerly-dipping half-Grabens, the true Central Graben, and the SE Forties Basin. This eastern basin is a half-Graben, the crest of which forms the offset continuation of the axial Forties-Montrose High. (Fig 1.5b).

- Areas 3 and 4 (Fig 1.6) form Quadrant 30 of the study area. These subareas are poorly resolved on regional seismic but, as in the northern areas, the region can be divided into a western "Central" Graben and an eastern basin termed the "East Forties Basin" in this project. The basins are separated by an eroded Jurassic High forming the southern extension of the Forties-Montrose High. This axial horst is termed the "Josephine Ridge".

1.4.3 Central North Sea lithostratigraphy

The lithostratigraphy of the study region has been presented by Cayley (1987), and more detailed analyses of the Jurassic section have been presented by Donovan *et al.* (1993) and Price *et al.* (1993). The stratigraphic section reaches from Devonian Old Red Sandstone that forms the basement to the Central North Sea (Cayley, 1987) to Recent, and will be discussed in this section by stratigraphic unit. A stratigraphic log of the Central Graben (after Cayley, 1987) is shown in Fig 1.7. As the Jurassic is the interval of greatest interest to this research, a detailed summation of Jurassic lithostratigraphy is presented.

The *Permian* deposits in the Central Graben are dominated by the presence of a Zechstein evaporite basin that underlies much of the study area (Taylor, 1984). The Zechstein evaporites in this basin form a thick ductile base to the basin. The salt forms a mobile layer and a shallow detachment structure that has determined the sedimentation and structural geometry of much of the Mesozoic section. Penge *et al.* (1993) have identified detached "rafts" of Mesozoic sediments on the eastern flank of the Forties-Montrose High, where large fault blocks have translated, rotated and distorted on ductile salt. Similar domination by halokinesis of the structural evolution of the Jaeren High has been noted by Hoiland *et al.* (1993).

The *Triassic* of the Central North Sea can be divided into a lower siltstone-mudstone unit termed the Smith Bank Fm., and an upper sandstone unit termed the Skaggerak Fm. Synforms forming in the extending Zechstein salt filled with thick clastics, forming "pods" of Smith Bank mudstones (Wakefield *et al.*, 1993). Dissolution of salt crests led to "interpod" topographic lows that determined the patterns of drainage during Skagerrak Fm deposition. This halokinetic control of the drainage pattern extended into the Jurassic, forming the Triassic-Jurassic "pod-interpod" geometry of sandbodies on the Western Platform and the Forties-Montrose High. Early Fe-rich

chloritisation of grains and inferred overpressuring results in the preservation of good reservoir quality to 4km depths, termed the Marnock facies (Smith *et al.*, 1993).

Jurassic sediments are divided into a lower Jurassic non-marine sandy siltstone formation, termed the Pentland Fm (Donovan *et al*1993), and an upper Jurassic sandstone-siltstone-mudstone group termed the Humber Group. A lithostratigraphic system for the Humber Gp. (Fig. 1.8) has been presented by Price *et al*(1993). Mudstones are assigned to one of three formations on the basis of lithostratigraphy: the Heather Fm, the organic-rich Kimmeridge Clay Fm (the source of the region's hydrocarbons, Cornford 1994), and the Mandal Fm (the uppermost radioactive mudstone formation). Upper Jurassic sandstones may be divided by geographical position (Fig 1.3) into the Puffin Fm, the Fulmar Fm, and the Ula Fm (Price 1993). For the purposes of this study the term "Fulmar Fm" will be applied to all Upper Jurassic sandstones in the UK Sector of the Central Graben. This follows the precedent of Roberts *et al*(1990) and Donovan *et al*(1993), who applied the term to all non-coal-bearing Upper Jurassic sandstones encountered in the Central Graben. Basin-wide correlation of the Humber Group is presented in Fig 1.9, after Price *et al*(1993). It is likely that the extensive Puffin Fm. passes laterally into basinal mudstones (Price *et al*1993) in the deeper axial parts of the Graben.

The Fulmar Formation is the main stratigraphic unit examined in this study. These sandstones form the principal hydrocarbon exploration target in the pre-Cretaceous strata of the Central Graben. Accordingly abundant pressure information and conventional core are obtained from this stratigraphic interval. The sandstones are marine sequences interpreted as having been deposited in a prograding shore face or as migrating storm-dominated shelf sandsheets. The Fulmar Fm is characterised by 1) large thickness and massive nature; 2) restriction to the basin margins; 3) localised occurrence, passing rapidly laterally and basinwards into mudstones; 4) mineralogical immaturity. The sandstones range in age from early Oxfordian to Kimmeridgian. Sketch maps of Fulmar sandstone extent are presented by Roberts *et al*(1990). The Fulmar Fm on the Western Platform is intimately related to halokinesis in the same manner as suggested for the Skagerrak Fm (Price *et al*1993), forming sandstones that are fully encased in mudstones and which form "pod-interpod" stratigraphic traps for hydrocarbons (Wakefield *et al*1993).

A sequence stratigraphic control on Middle and Upper Jurassic sandstone distribution was noted by Donovan *et al*(1993), who showed that unconformities within the Fulmar Fm play a major role in modifying the original thicknesses and geographic distribution of the formation. An upper member on the Western Margin of the Graben

was distinguished from a lower member on the basis of age and geographical location; no lithological variation was noted.

The *Cretaceous* of the Central North Sea marks the transition from continental/marginal-marine sedimentation in failed rifting conditions to quieter, fully marine conditions. The Lower Cretaceous consists of Valanginian-Albian grey mudstones and marls termed the Cromer Knoll Group. The upper boundary of the Cromer Knoll Group is marked by the Plenus Marl Fm. The Upper Cretaceous is formed by the Chalk Group, consisting of the Hod (distinguished by clastic input forming silt horizons), Tor and Ekofisk Fms.

The *Cenozoic* of the study area is dominated by rapid subsidence and rapid clastic sedimentation. Large-scale uplift of Scotland in the Palaeocene led to sand deposition across the region in large submarine fans, which now form the Palaeocene Maureen, Andrew and Forties sandstone formations (Reynolds, 1994). These sandstones form major hydrocarbon reservoirs in the northern Central Graben. Increasing subsidence, accelerating sedimentation rates and increasing water depths from the Palaeocene to the present day led to deposition of the thick mudstone formations of the Hordaland and Nordaland Groups.

1.4.4 Previous studies of Central North Sea overpressure

The areal distribution of overpressure in the Jurassic and Triassic sandstones of the Central North Sea has been described by Cayley (1987) and by Gaarenstroom *et al.* (1993). Extremely high levels of overpressure are observed, with fluid pressures approaching the lithostatic pressure. The relationship of overpressure to depth has been presented by Gaarenstroom *et al.* (1993); the presence of distinct pressure gradients implies the presence of pressure cells (Section 1.1). Gaarenstroom *et al.* (1993) presented a generalised model which suggested that fault blocks in the Central North Sea delimit pressure cells, and accordingly that the lateral seals to pressure cells are faults. This model suggested that the Central North Sea contains the potential for several different overpressuring mechanisms (Section 2.7), and that pressure distribution is controlled by restriction of fluid flow. The major control on this restriction was suggested to be pressure-induced and tectonically-induced fracturing of the pressure seal. Both Cayley (1987) and Gaarenstroom *et al.* (1993) suggest that overpressure may have affected hydrocarbon migration.

Leonard (1993) presented a model for the distribution of overpressure in terms of depth and area for the Norwegian Sector of the Central North Sea. This work showed that the hydrogeology of the area is divided into pressure cells and that the pressure seals to these cells are planar, horizontal cemented zones that cross-cut stratigraphy. In this aspect the study was similar to the earlier study by Hunt (1990) which delineated an upper and lower pressure cell in the Central Graben, separated from an overlying normally-pressured zone by cemented seals. Hunt (1990) stated that well 30/6-2 cored a silica-cemented zone at the same depth as a pressure seal in the Cretaceous Chalk. However, no detailed analysis of the seals in the region has been presented.

The data of Gaarenstroom *et al*(1993) was used by Engelder & Fischer (1994) to demonstrate that the magnitude of the minimum horizontal stress increases with depth and to suggest that fluid generation at depth due to hydrocarbon generation was changing the stress state in the region. A map showing the orientation of the maximum horizontal stress (derived from borehole breakouts) in NW Europe was presented by Van Balen & Cloetingh (1994). This showed a general NW-SE orientation of maximum horizontal stress in the Central Graben. This pattern is identical to a more detailed study of the crustal stress in the northern North Sea (Lindholm *et al.*, 1995) which found that the regional stress field is dominated by NW-SE compression related to ridge push.

Thus previous studies of the pressures in the Central North Sea demonstrate that the region is highly overpressured, is compartmentalised into pressure cells, and contains pressure seals that are diagenetic and have a horizontal, discordant morphology. Moreover, the high overpressures may have affected hydrocarbon migration and entrapment. However, the morphology and extent of the pressure seals in the UK sector of the Central North Sea has not been documented; the mechanisms of seal formation are unknown; the origins of overpressure are unclear and unquantified; and the timing of the onset of overpressure, and the control of overpressure on palaeo-fluid flow is unknown. The Central North Sea provides an excellent natural laboratory for the study of overpressure. This thesis sets out to test these concepts and problems.

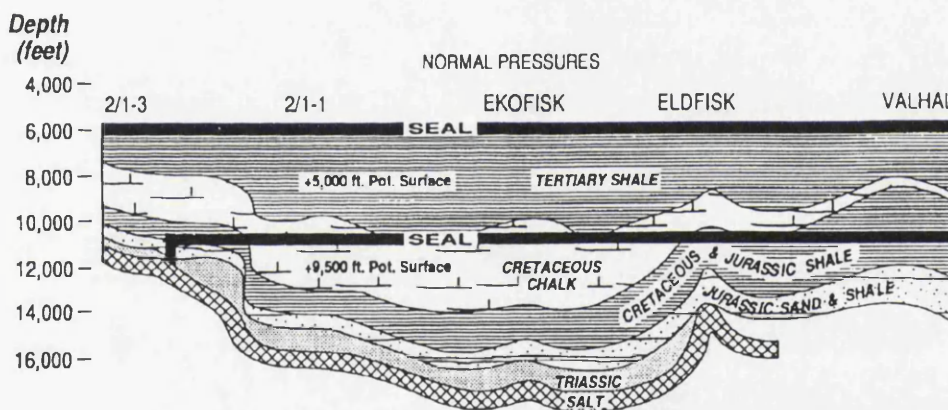
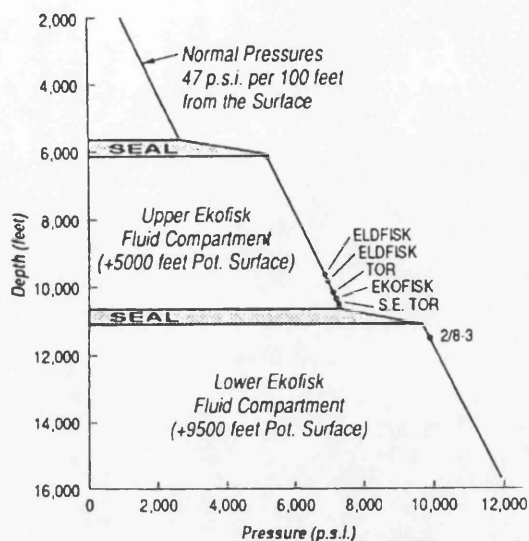


Fig 1.1 Definition of Central North Sea pressure compartments from Hunt (1990)

RFT measurements define three hydrogeological zones in the Central Graben. An upper, normally pressured regime is undelained by two pressure compartments (or cells) termed the Upper and Lower Ekofisk Fluid Compartments. The zones are separated by pressure seals, which are depicted as horizontal, diagenetically-cemented low-permeability bands. The seals extend across the Graben and are discordant with stratigraphy.

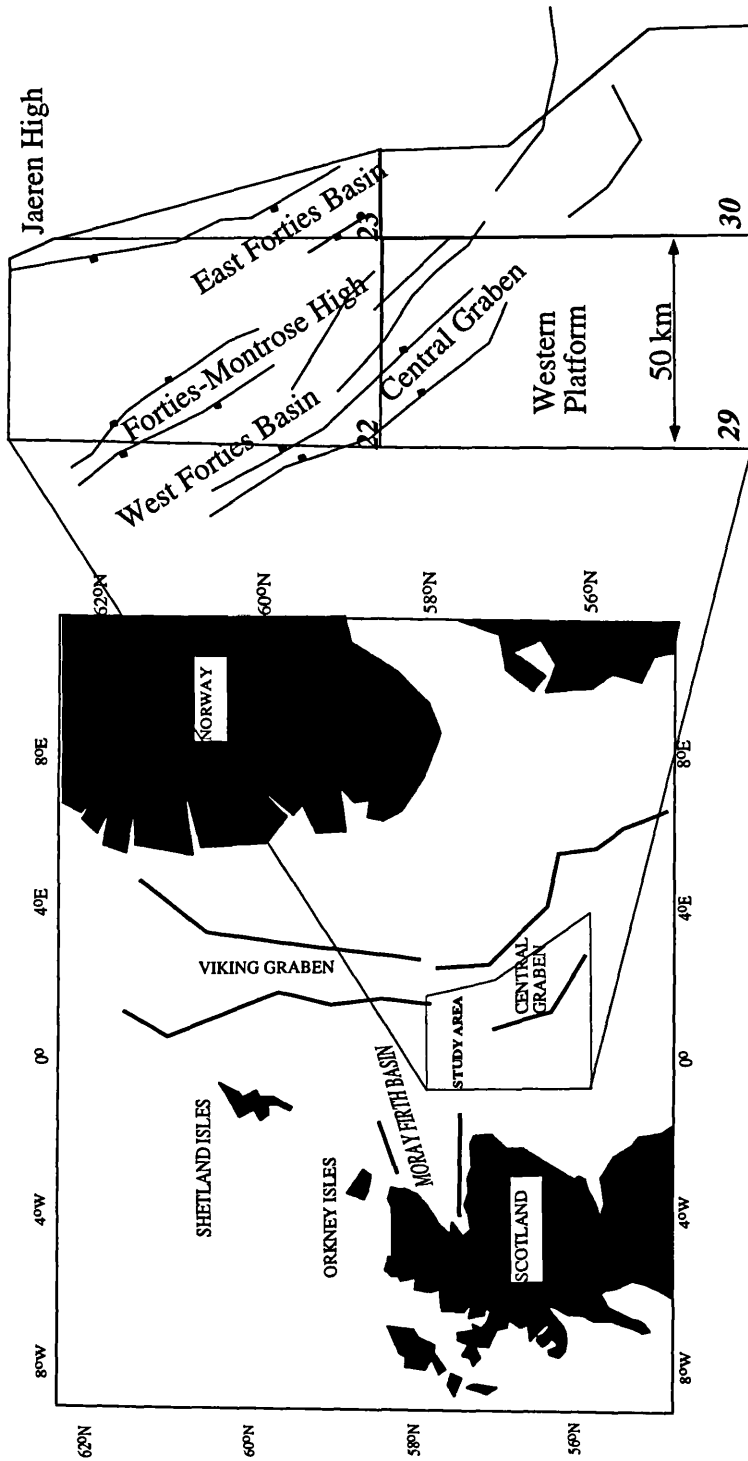


Figure 1.2 Location Map of the Central Graben

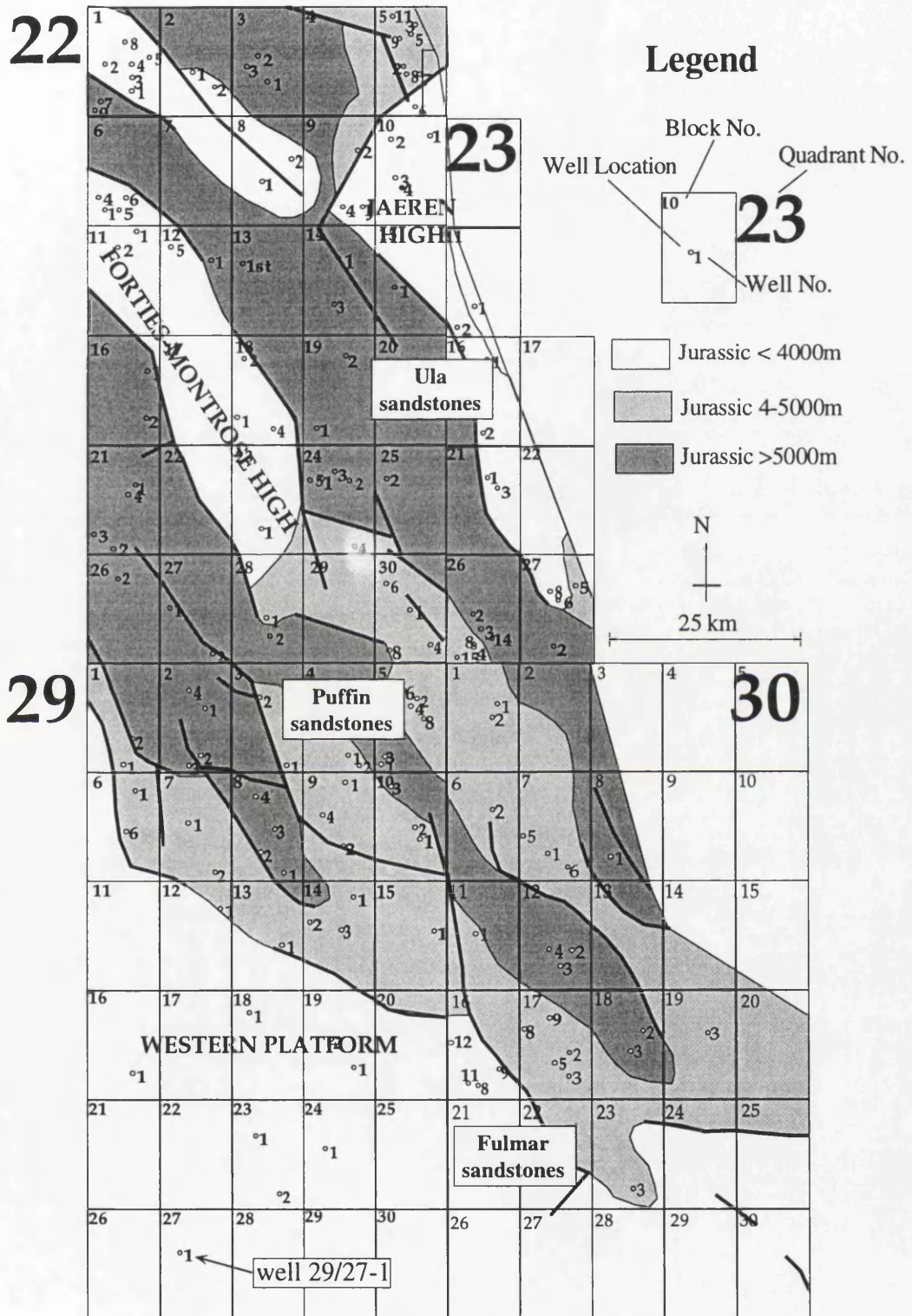


Figure 1.3 Division of the Central Graben into Quadrants and Blocks. Well location can be found by Quad No./Block No.-Well No. code system. Example box in legend shows well 29/27-1. Upper Jurassic sandstones may be divided into Ula, Puffin and Fulmar Fms on the basis of geographic location.

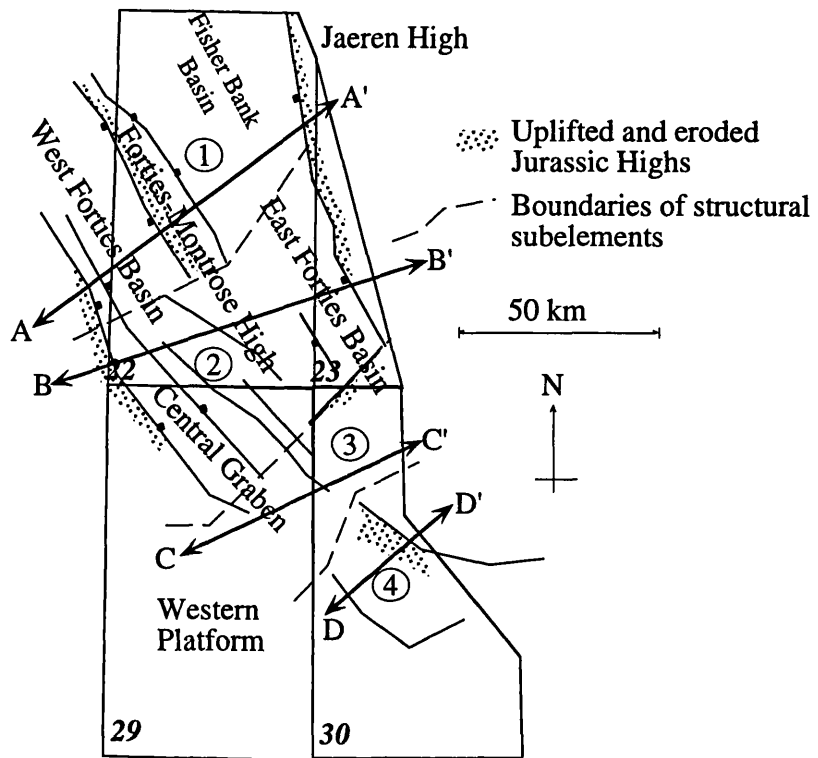


Fig 1.4 Late Jurassic tectonic elements of the Central Graben (after Roberts et al 1990). Numbers in circles represent the tectonic subelements identified; lines A-A', B-B' and C-C' show locations of structural cross-sections of Figs 1.5 and 1.6. The Graben can broadly be divided in two, into an eastern Graben (the East Forties Basin) and a western Graben (the Central Graben proper), separated by the axial Forties-Montrose High. The Forties-Montrose High continues into the south of the study area: note the presence of an eroded Jurassic high in the NW and centre of Quadrant 30.

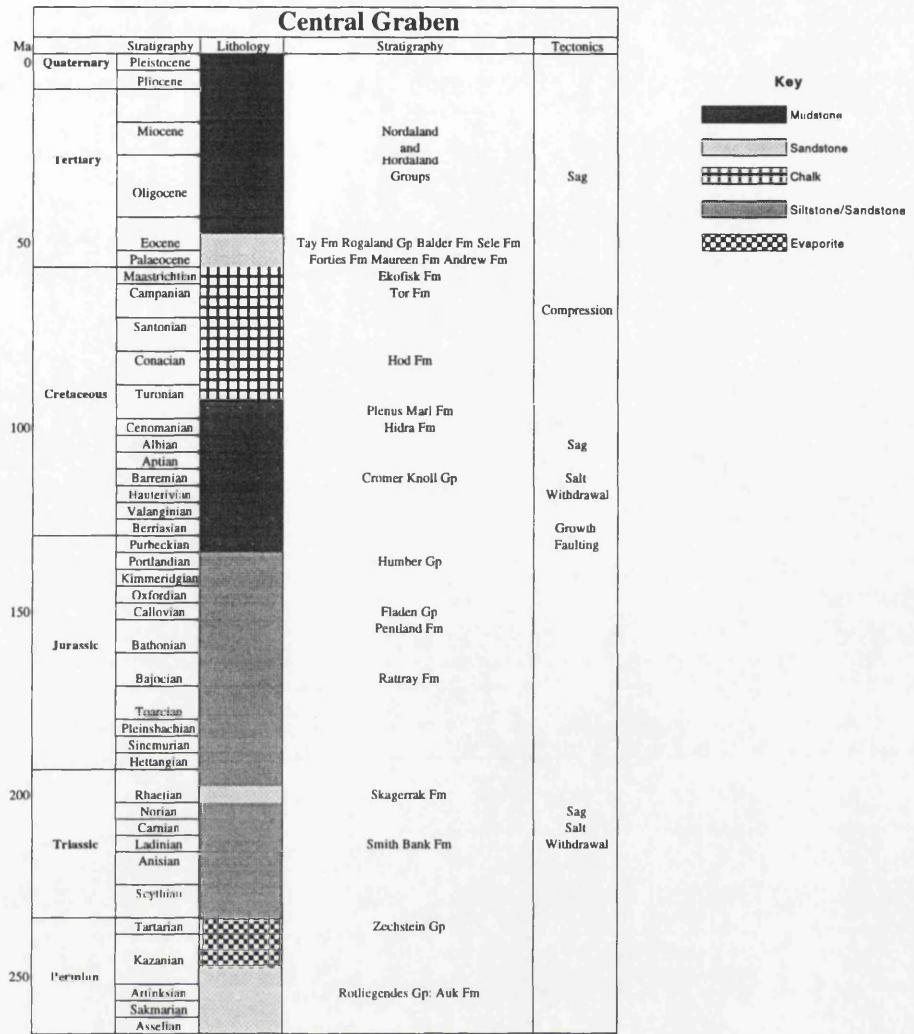


FIGURE 1.7 STRATIGRAPHIC COLUMN OF THE CENTRAL GRABEN (AFTER ROBERTS ET AL 1990).

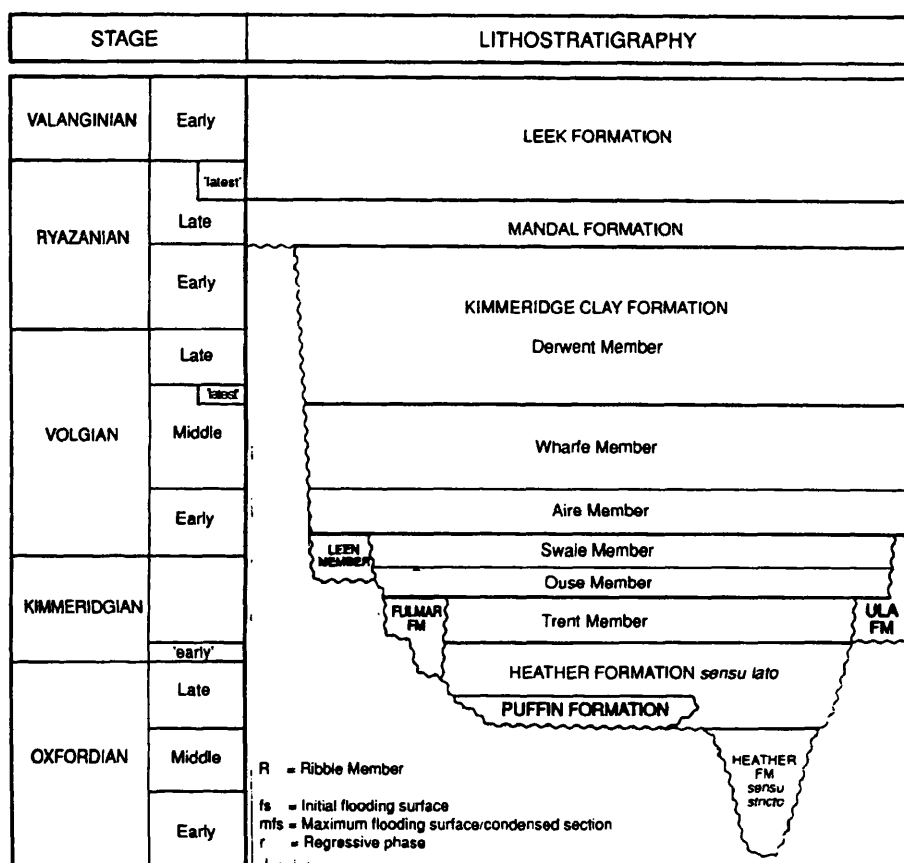


Figure 1.8 Stratigraphic column of the Humber Group (after Price *et al* 1993). Sandstones of the Fulmar and Puffin Fms will be termed the "Fulmar Fm." in this thesis, as the division is made on geographic location, and is not used in all studies (e.g. Roberts *et al* 1990).

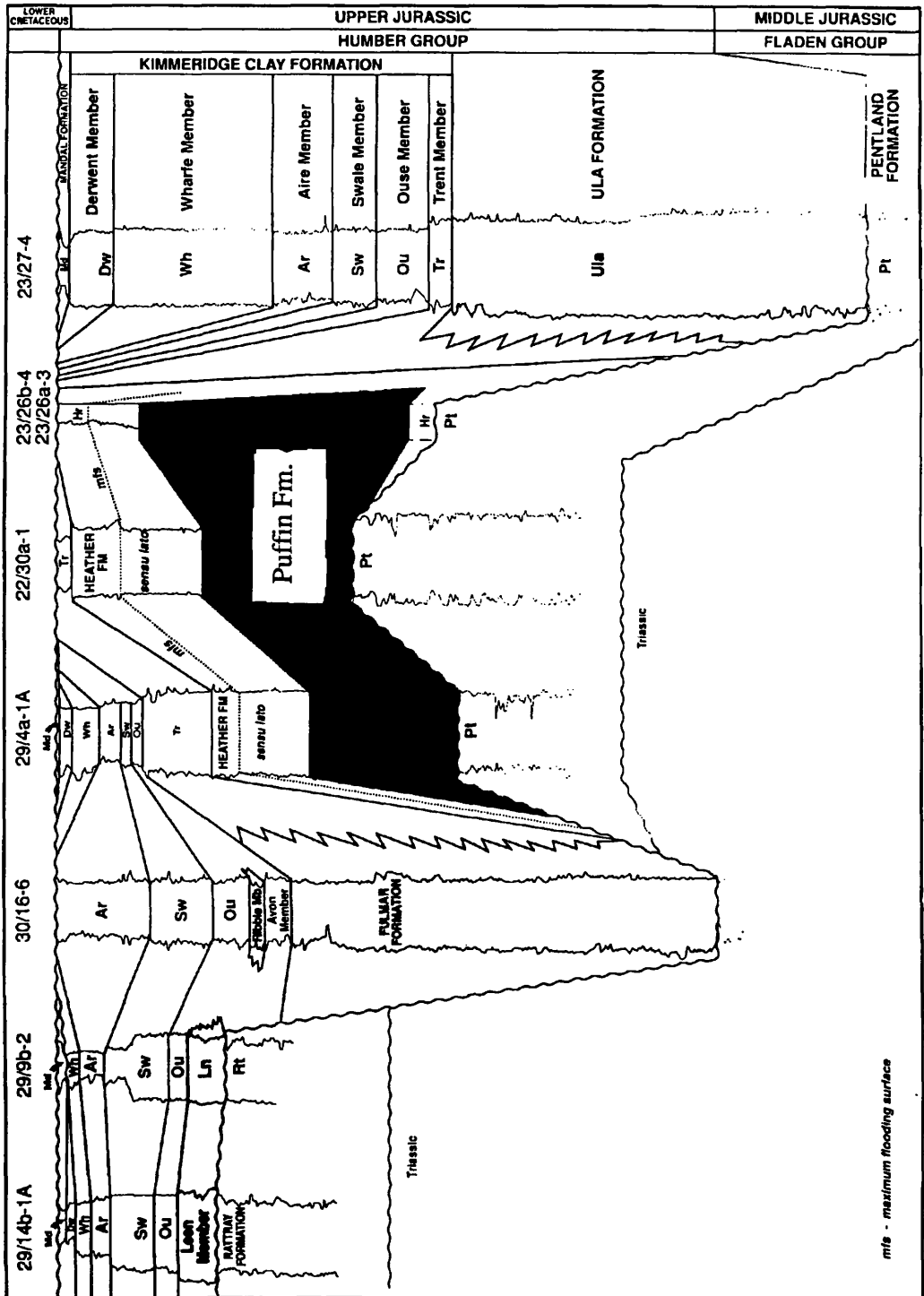


Figure 1.9 Stratigraphic cross-section of the Humber Gp. in the Central Graben (after Donovan *et al* 1993)

Chapter Two

Background Theory

- 2.1 Physical principles of overpressure in the geological environment**
- 2.2 Fluid flow in the subsurface**
- 2.3 Overpressure in the Earth's Crust**
 - 2.3.1 Near-surface overpressuring*
 - 2.3.2 Overpressure in sedimentary basins*
 - 2.3.3 Overpressure in the deep crust*
- 2.4 Overpressure in sedimentary basins: a global overview**
- 2.5 The Pressure Cell Paradigm**
- 2.6 Pressure Seals**
- 2.7 Origins of overpressure**
 - 2.7.1 External effects*
 - 2.7.2 Internal effects*
- 2.8 Paradigms of overpressure**
- 2.9 Summary**

This introductory Chapter aims to provide a background to the scientific basis and aims of this thesis. This Chapter comprises:

- A brief summary of the physical principles of pressure in the geological environment.
- A review of the occurrence of abnormal pressures in the Earth's crust, and a review of the theories concerning the origins and distribution of overpressure.

2.1 Physical principles of pressure in the geological environment

The physics of pressure in a fluid were first defined in 1653 by the French natural philosopher Blaise Pascal (1623-1662). Pascal's Law states that "Pressure applied to an enclosed fluid is transmitted undiminished to every portion of the fluid and the walls of the confining vessel". Pascal's Law defines the science of hydrostatics, the study of fluids at rest.

The fluid-saturated geological environment is governed by a series of pressures. The weight of a static column of water exerts a pressure termed *hydrostatic* pressure. It is a function of the height and density of the fluid column. It is expressed by the equation

$$P_h = \rho \cdot g \cdot h$$

where P_h = hydrostatic pressure (N m^{-2})

ρ = average fluid density (kg m^{-3})

g = acceleration due to gravity (m s^{-2})

h = vertical height of the water column (m)

The weight of the column of rock exerts a notional pressure termed *overburden pressure* (sometimes termed lithostatic pressure). It is defined as

$$S = \rho_b \cdot g \cdot h$$

where S = overburden pressure (N m^{-2})

ρ_b = rock average bulk density (kg m^{-3})

g = acceleration due to gravity (m s^{-2})

h = vertical height of the sediment column (m)

Overburden pressure is often taken as an approximation to the vertical stress S_V acting on a unit of rock (Anderson, 1951; Engelder, 1993). Geological bodies are acted upon by three principal stresses. Anderson (1951) proposed a classification of the tectonic stresses acting on a rock. In his classification, S_V is the vertical stress, arising from the overburden load; S_H is the maximum horizontal stress, and S_h is the minimum horizontal stress. S_V is the maximum principal stress in a normal-fault regime. S_H and S_h are constrained by the rock strength to lie within definite limits related to S_V (Engelder 1993).

Formation pressure (or pore pressure) is the pressure of the fluid contained in the pore spaces of the rock at any given depth. When formation pressure is equal to hydrostatic pressure, the formation pressure is termed "normally pressured" or "hydropressedured". In a subsiding basin, where S_V is increasing, this situation implies that there is a free connection between pores to the atmosphere. Fluid can move freely in response to changes in stress.

Overpressure is defined as a condition where fluid pressure exceeds the hydrostatic pressure. This situation implies that pores do not have a totally free connection to the atmosphere, and that the total stress acting on the rock matrix is partially transferred to the pore fluid. Where pore fluids are totally prevented from draining away, with no connection to the atmosphere, the stresses exerted on the rock matrix are distributed over the fluid and matrix. The *hydrostatic* conditions in such a closed system is governed by Pascal's Law.

Pore fluids have a profound effect on the stresses acting on the rock (Biot, 1941; Hubbert & Rubey, 1959; Terzaghi, 1943). The recognition of the role of fluids in modifying stresses applied to a porous, fluid-filled rock has led to the concept of effective stress (Biot, 1941; Terzaghi, 1943). Stresses in porous rocks obey the law

$$\sigma_{ij}^* = \sigma_{ij} - \delta_{ij} P_p$$

$$\Rightarrow \sigma_{ij}^* = \begin{bmatrix} \sigma_{11} & \sigma_{12} & \sigma_{13} \\ \sigma_{21} & \sigma_{22} & \sigma_{23} \\ \sigma_{31} & \sigma_{32} & \sigma_{33} \end{bmatrix} - \begin{bmatrix} 1 & 0 & 0 \\ 0 & 1 & 0 \\ 0 & 0 & 1 \end{bmatrix} \begin{bmatrix} P_p & 0 & 0 \\ 0 & P_p & 0 \\ 0 & 0 & P_p \end{bmatrix}$$

where σ_{ij}^* = effective stress, σ_{ij} = total stress, δ_{ij} = Kronecker Delta and P_p = pore pressure.

Tensile effective stress conditions ($\sigma_{ij}^* = \sigma_{ij} - \delta_{ij}P_p \rightarrow 0$) can arise if pore pressure is increased to values approaching the lithostatic pressure. These conditions lead to rock failure and crack propagation (Fig 2.1; Hubbert & Rubey 1959). In practice, rock failure occurs when P_p achieves approximately 85% of S_v (Engelder 1993). This value is analogous to the *fracture pressure* used in drilling terminology, which is the fluid pressure at which hydraulic fractures are produced during drilling. This value is dependent on lithology (Mouchet & Mitchell, 1989)

2.2 Flow of water in the subsurface

Water flow in the subsurface is driven by imbalances of energy. These can be imbalances in potential energy, imbalances in thermal energy, or imbalances in chemical energy. Imbalances in thermal energy may arise due to spatial variation in temperature in a basin, while imbalances in chemical energy may arise due to differences in dissolved solids in water. This discussion will deal with potential energy.

Potential energy of a fluid is defined as

$$\Phi_w = P_p - \rho \cdot g \cdot h$$

where P_p = the formation pressure. In a *hydrostatic* environment, formation pressure is equal to hydrostatic pressure, and thus fluid potential between any two points is zero. There is no driving force for water movement, neglecting other imbalances. Where fluid potential between two points is non-zero, the environment is termed *hydrodynamic* and the fluid experiences a force that will induce movement. Note that the potential energy of a fluid is dependent on density and so flow can be driven by salinity variations and by buoyancy. The migration of petroleum fluids, which are less dense than water, is thus governed by additional forces. However, this discussion will consider only the water potential.

The rates of fluid movement are determined by Darcy's Law:

$$q = \frac{-k_{\phi}}{\mu} \frac{\partial P_p}{\partial l} \Phi_w$$

where q = Darcy flux per unit cross-sectional area of rock (ms^{-1}), $-k_{\phi}$ = intrinsic permeability (m^2), μ = dynamic viscosity ($\text{kg m}^{-1} \text{s}^{-1}$) and Pp = pressure and l = distance (m)

The importance of rock permeability to fluid flow is obvious in this fundamental equation. If permeability is zero, no fluid flow can occur regardless of fluid potential energy. If permeability is non-zero, fluid flow will occur in response to variations in fluid potential energy. In the subsurface, variations in fluid potential can occur due to numerous factors.

Inhomogeneities in topographic elevation can induce flow of meteoric water from elevated recharge areas into low-lying basins (Garven, 1989; Hubbert, 1940). A summation of flow regimes in a sedimentary basin is presented in Fig 2.2.

Continued subsidence and sedimentation in a sedimentary basin increases the vertical stress on the sediments, and the basin will seek to deform in response to this increase of stress by compaction of porosity. The porosity change associated with burial requires an expulsion of porewater. If this expulsion is restricted, the pore fluid assumes a portion of the load and becomes overpressured. Heating may liberate water bound to mineral surfaces (Burst, 1969). These processes, amongst many others discussed in Section 2.7, increase fluid potential and raise fluid pressure.

2.3 Overpressure in the Earth's crust

Overpressured fluids have been observed to occur at various geodynamic and geographical locations in the Earth's crust, and occur at various depths (Fig 2.3). A review of the occurrence of overpressure in the crust is informative and illustrates the diversity of overpressured environments:

2.3.1 Near-surface overpressuring in sedimentary sequences

Evidence of shallow overpressures may be observed in outcropping sandstones as convoluted bedding, formed by disruptive dewatering of rapidly-deposited sediments. This overpressuring occurs within the first few metres of burial, in soft sediments prior to lithification. Extremely high fluid pressures at shallow depths can also be induced by earthquakes (Berry, 1973). Fault patterns in Palaeogene clays have been used to infer hydraulic fracturing by high fluid pressures during shallow burial (<500m) (Henriet *et al.*, 1991).

2.3.2 Overpressure in sedimentary basins

Fluid pressures in sedimentary basins above approximately 1500m burial depth are generally hydrostatic (Hunt, 1990), reflecting free fluid flow and energy equilibrium. Below this depth, fluid flow becomes increasingly restricted and overpressures are commonly encountered in the deeper regions of sedimentary basins world-wide (Hunt 1990). Fluid pressure may achieve values equal to the lithostatic pressure (Hunt 1990). Overpressure in a sedimentary basin is the focus of this research project, and so the phenomena of overpressure in this form of geological environment will be discussed in more detail below.

2.3.3 Overpressure in the deep crust

High fluid pressures also occur deep in the crystalline crust of the Earth (Neuzil, 1995; Yardley & Valley, 1994). Fluid pressures equivalent to lithostatic pressure are implied for zones of active metamorphism (Ferry & Dipple, 1991). Stable crystalline crust may be perceived as containing disconnected fluid, occurring in isolated pores or inclusions. The crust may then form a sink for downward-moving fluids. Alternatively, the deep crust may contain an interconnected pore fluid at lithostatic pressure. The evidence for a highly-pressured interconnected fluid is primarily geophysical. The presence of open fluid-filled fractures is inferred from shear waves (Muir-Wood, 1988). Frequent low-velocity zones at 7-12 km depth (Berry & Mair, 1977) also suggest high-pressure interstitial fluids. However, the crust may be too permeable for lithostatic pressures to occur ubiquitously: It is necessary to keep fluids "bottled up" in a closed, or nearly-closed, system, or fluid flow over geological time will equilibrate pressure at the stable, low-energy state of hydrostatic pressure. (Bailey, 1994) has suggested that impermeable barriers may develop in the mid-crust due to the presence of immiscible fluids. Deep drilling in the European continental crust as part of the KTB Project (Zoback *et al.*, 1993) has found hydrostatically-pressured fluids down to the maximum drilling depth at that time of 4 km. The presence, movement and pressure of fluids in the deep crystalline crust is not yet clear.

2.4 Overpressures in sedimentary basins: a global overview

Overpressures have been recognised in the deeper regions of many sedimentary basins across the world (Hunt, 1990; Law & Ulmishek, *in press*). High fluid

pressures are encountered in rocks of a range of ages from Devonian to Pliocene, and in a range of geodynamic settings. A thorough review of the global distribution of overpressure would require a volume to itself (see Law & Ulmishek *in press*); however, a brief review is informative.

Overpressure in rocks of *Cenozoic* age have been encountered in the Niger (Hunt 1990) and Nile Deltas (Nashaat, *in press*) of Africa; the Uinta Basin of the Rocky Mountains of America (Bredehoeft *et al.*, 1994; Spencer, 1987); the Gulf Coast of America (Dickinson, 1953); the Beaufort-Mackenzie Basin (Tang & Lerche 1992) of Canada; and the Yinggehai Basin of the South China Sea (Funing, *in press*), the Akita Basin (Okui *et al.*, *in press*) and Nagaoka Plain (Magara, 1968) of Japan and other unspecified basins (see Bour & Lerche, 1994) of SE Asia.

Overpressures in rocks of *Mesozoic* age occur in the Viking Graben (Chiarelli & Duffaud, 1980), Central Graben (Cayley, 1987) and Adriatic (Carlin & Dainelli, *in press*) of Europe; the Scotian Shelf, Scotian Basin (Yassir & Bell, 1994), Sable Basin (Williamson & Smyth, 1992) and Jeanne D'Arc Basin (Williamson *et al.* 1994) of Canada; the Piceance, Greater Green River, Powder River and Bighorn Basins of the Rocky Mountains (Spencer, 1987); and the Middle Caspian (Malysheva 1994), Carpathian (Herman *et al.*, *in press*), and W Siberian (Goloshubin & Galchenko, *in press*) Basins of the CIS.

Overpressure in rocks of *Palaeozoic* age is less common; nevertheless, high levels of overpressure are noted for the Williston (Meissner, 1988), Anadarko (Dewers & Ortoleva, 1994) and Eastern Delaware Basins (Luo *et al.*, 1994) of the USA; the SE Peri-Caspian (Keller, *in press*) and Timan-Pechara (Oknova, *in press*) Basins of the CIS; and the Sichuan Basin of China (Da-Jun & Yun-Ho, *in press*).

Thus overpressures occur in basins of widely varying ages and geodynamic setting. Overpressures may be encountered in young, rapidly subsiding grabens, passive margins and deltas, stable Palaeozoic intracratonic basins that have been tectonically quiescent for much of the Mesozoic and Cenozoic, uplifted and eroded Cenozoic basins, and in intracratonic basins that may be being tectonically deformed at the present day (such as the Sichuan Basin, linked to the evolution of the Himalayas).

2.5 The Pressure Cell Paradigm

The occurrence of overpressured fluids in deep sedimentary basins implies that fluids do not have a free connection to the surface. Bradley (1975) argued that overpressure implies the presence of low-permeability rocks that restrict fluid flow. He termed these rocks "pressure seals". A similar line of reasoning was used later for the deep crust by Bailey (1994). Without a seal, fluid pressures would equalise at the stable, low-energy state of hydrostatic pressure over geological time (Bradley, 1975; Deming, 1994). The concept of a seal allowed Hunt (1990), on the basis of Bradley (1975) and Powley (1980), to propose a new paradigm in the hydrogeology of sedimentary basins: pressure cells.

Pressure cell and pressure compartment are synonymous terms which denote a volume of rock containing overpressured fluid. The term pressure cell will be used in this project. The fluids in a pressure cell are internally in pressure communication; that is, fluids are connected within the cell. The overpressured fluids are internally in hydrostatic energy conditions. These conditions are inferred from examination of pressure gradients in the cell. Identical pressure gradients and identical magnitudes of overpressure are encountered everywhere within a pressure cell (Dahlberg, 1982; Hunt, 1990). Fig 2.4 illustrates the concept and identification of a pressure cell.

In contrast, each pressure cell is hydraulically isolated from neighbouring pressure cells. This implies that fluids in each cell are not in pressure communication, that barriers to fluid flow exist between the cells, and that there is a difference in hydrodynamic energy between cells. These conditions are inferred from differing magnitudes of overpressure between cells (Fig 2.4). Accordingly, the definition of pressure cells is achieved through a graph of pressure against depth (a pressure-depth plot), which forms a principal interpretative method in pressure analysis (Dahlberg 1987, Mouchet & Mitchell 1991) and allows graphical depiction of pressure gradients. Fig 2.5 shows an example pressure-depth plot.

The low-permeability barriers to free fluid flow that exist between pressure cells are termed pressure seals in the pressure cell paradigm. Pressure seals are defined on the basis of a change in the measured pressure gradient. Thus both pressure cells and pressure seals are defined on the basis of their pressure characteristics and not their intrinsic lithological characteristics. A pressure seal is thus equivalent to a "*transition zone*", as used in drilling terminology. A transition zone is a zone of changing pore pressure encountered when a well is drilled. As pressure seals are implied to restrict fluid flow, they are *aquitards* in hydrogeological terminology.

Overpressure terminology is diverse due to the multi-disciplinary interest it attracts, from drilling engineers, petroleum geologists, physicists, and hydrogeologists. Each discipline describes the observed phenomena in different terms. It is necessary to clarify the terminology of overpressure for this research project. For this project, "pressure seal" (Fig 2.5) will be used to define a zone of rock containing fluids with constant pore pressure gradients at the present day that are in excess of hydrostatic *gradient*, and below which *constant hydrostatic gradients are maintained in overpressured fluids*. It is thus precisely applied to a zone of rapidly changing pressure (a "transition zone" in drilling terminology) delineating the boundaries to a pressure cell. The definition of a pressure seal in this project is purely on the basis of pressure gradients. No lithological characteristics are implicitly assumed in this definition. The term aquitard will be applied to a zone of low-permeability rocks. Aquitards in overpressured basins commonly exhibit a pore pressure gradient greater than a hydrostatic gradient. Thus in practise, pressure seals are a subset of aquitards.

An important implication of this definition is that pore pressure gradients are not hydrostatic across pressure seals, and so hydrodynamic conditions exist. Accordingly, fluid flow will occur if permeability is non-zero (Deming 1994). It should be noted clearly that in this project, the use of the terms pressure cell and pressure seal do not imply the presence of an *impermeable* seal. Accordingly there is an implication that fluid flow can occur between cells. A pressure seal is not synonymous with the seal or caprock to a hydrocarbon accumulation. The flow of petroleum fluids is governed by capillary entry pressures which will not apply to the flow of a wetting-phase fluid in a hydraulically-continuous system. Pressure cell and pressure seal are useful terms that imply the precise hydrogeological conditions defined above.

2.6 Pressure Seals

The unusual hydrogeological conditions indicated by a pressure seal have led to a growing body of research into the petrological characteristics of the seal, and the mechanisms by which pressure seals can form. Two main schools of thought can be determined. The first school considers the unusual hydrogeological conditions of pressure seals to be caused by the unusual lithological characteristics of seals, such as cemented or compacted zones. These characteristics are diagenetic in origin. The second school considers pressure seals to be essentially unaltered lithologies, whose sealing characteristics are determined by physical lithological parameters. It is informative to review the evidence advanced in support of these contrasting schools.

2.6.1 Diagenetic pressure seals

Pressure seals in zones of calcite and silica-cemented rocks have been inferred by Hunt (1990) for the Central North Sea (Fig 1.1), the Cook Inlet of Alaska and offshore Louisiana. These seals are claimed to be planar, horizontal, and are discordant with stratigraphy. They occur at constant depths of approximately 3000m. Depth to the pressure seal appears to be related to geothermal gradient. Similar horizontal seals have been noted for the Anadarko Basin of Oklahoma (Tiggert & Al-Shaieb, 1990). These seals are an unusual basinal phenomena which clearly limit fluid movement. Permeability is reduced to near-zero levels by cementation (Hunt 1990).

Hunt's (1990) paper provided a global overview of seals, and posed fundamental questions. What controls the depth to a seal? How do seals remain at constant depth as the basin subsides? How do the cements form? Answering these questions by identification of the mechanisms of diagenetic alteration that can form a diagenetic pressure seal have been undertaken by several authors. Study is almost ubiquitously hampered by lack of core across pressure seals, which prevents direct observation of the seal.

Tiggert & Al-Shaieb (1990) showed that the pressure seal zone in the Anadarko Basin consists of diagenetic bands of calcite and silica. Dewers & Ortoleva (1990) suggested that this banding, and associated loss of permeability, arises from geochemical self-organisation within a sedimentary basin. Weedman *et al.*, (1992) demonstrated that compaction of high-porosity zones within sandstones leads to low-permeability zones that form pressure seals in the Tuscaloosa Fm, Louisiana. An alternative, organically-mediated form of diagenetic permeability reduction has been proposed by Whelan *et al.*, (1994). These workers suggested that the pressure drop across the transition zone causes separation of oil and gas, and deposition of asphalt. Permeability is reduced by bitumen plugging of pore space, inorganic alteration, and gas-water capillary effects.

2.6.2 Lithostratigraphic pressure seals

Active generation of overpressure due to geologic processes may lead to the appearance of a pressure seal in a low-permeability lithology despite considerable leakage across the seal (Deming 1994; Neuzil 1995). Thus mechanisms for lowering seal permeability to near-zero values may not be required in young basins. Pressure seals can thus be formed by conventional, well-documented basin processes that form low-permeability restrictions to fluid flow. These can include the presence of mudstone strata; calcite concretionary laminae (Wilkinson, 1990); zones of silica cement (Jansa & Urrea, 1992); and sequence stratigraphic bounding surfaces (Van Wagoner *et al* 1990). It can be noted that the pressure seals of Weedman *et al* (1992) are formed by a common permeability-reducing process in sedimentary rocks (e.g. Bjørlykke, 1984) that should not be considered to be responsible for basin-wide overpressuring. Equally, the calcite-cemented zones identified in the Ekofisk area of the Central North Sea by Hunt (1990) are coincident with a discontinuous sequence-stratigraphic hardground within the Cretaceous Chalk (Pekot & Gerril, 1987) termed the Ekofisk-Tommeliten Tight Zone. Are pressure seals distinct geological phenomena allowing no fluid flow, or are they simple, ubiquitous permeability restrictions, formed in a variety of ways, that transiently retard fluid flow?

The origin and significance of pressure seals is thus the subject of debate. The key concept is that of time. If fluid flow must be restricted for geological periods of time (as in Palaeozoic overpressured basins), a pressure seal must be an unusual zone of rock that prevents the basin fluids from rapidly equilibrating at a stable, low-energy state. Alternatively, if an energy disequilibrium is being actively generated in the basin, it is possible that a pressure seal is a transient phenomenon with no unusual petrological manifestation that exists until the basin re-equilibrates (Fig 2.6). Pressure seals may thus absolutely prevent fluid flow or transiently restrict fluid flow, and the concept of pressure seals is intrinsically linked to a consideration of generation of overpressure (Deming, 1994).

2.7 Origin of overpressure

The widely varying ages and geodynamic settings in which overpressure may be encountered suggests that high fluid pressures may be caused by a diverse assemblage of geological processes. The origins of overpressure have been the focus of considerable research in the past forty years. As might be expected from empirical studies of widely-varying basins, no consensus has been achieved as to the "prime

cause" of overpressure. A brief summary of the literature concerning this field is presented below.

The proposed origins of overpressure can be divided into mechanisms that are external to the system, and those that are internal (Hedberg, 1966).

2.7.1 *External effects*

The principal external effect that causes overpressure is sediment loading. As sediment thickness increases, increasing vertical stress tends to cause a reduction in the porosity of the sediments. This porosity reduction requires porewater expulsion. However, if fluid escape is inhibited due to low permeability, the sediment cannot change porosity freely; stress is transferred in part to the fluid, which becomes overpressured (Rieke & Chilingarian, 1974). This causal mechanism of overpressure is termed disequilibrium compaction (or compaction disequilibrium). It is commonly assigned as the cause of overpressure in rapidly-subsiding basins such as the North Sea (Burrus *et al.*, 1991) and the Gulf Coast (Dickinson 1953). The principles of disequilibrium compaction are shown in Fig 2.7.

Other external effects may be caused by changes in tectonic stress. Uplift of the basin margins can elevate hydrological recharge areas, imparting potential energy to the basin fluids and moving water through the basin (Bjorlykke, 1993). This gives rise to overpressure due to artesian effects (e.g. Garven & Freeze, 1984). The role of lateral tectonic stresses in causing overpressure is a relatively underdeveloped field, possibly historically due to the focus on extensional tectonic settings. However, Bour *et al* (1995) have quantitatively examined the role of lateral tectonic compression in an unspecified (confidential) basin of SE Asia, and have found that lateral stress plays an important role in the magnitude and distribution of overpressure in the region. Excess pore pressures can also be caused by shear deformations if the material is normally-consolidated and undrained (de Marsily 1980).

2.7.2 *Internal effects*

Internal effects are caused by changes in the fluid volume contained within the system. An increase in fluid volume within a system that is closed in the timescale under investigation leads to an increase of fluid pressure. Mechanisms that can cause

an increase of fluid volume include the thermal expansion of water (termed aquathermal pressuring); the conversion of solid kerogen to oil and gas; and dehydrating diagenetic reactions, most notably the conversion of smectite to illite.

Aquathermal pressuring is an elegant mechanism that was thought to be a prevalent mechanism in research conducted during the 1970's (Barker, 1972; Bradley, 1975). However, the volume expansion of water upon heating is low, and has been demonstrated to be of little quantitative importance (Luo & Vasseur, 1992) in rocks with finite permeability. Darcy's Law in permeable rocks allows fluid flow that negates the small volume expansion of heated water. Aquathermal pressuring is still thought to be relevant by some studies (Miller & Luk, 1993; Wilson *et al.*, *in press*) where Darcy flow can be neglected, although the validity of neglecting flow can be questioned (Neuzil 1995).

The volume expansion associated with the conversion of solid kerogen to liquid oil, and subsequently to gas, is considered to be a major overpressuring mechanism (Hunt *et al.*, 1994; Meissner, 1980; Spencer, 1987). Overpressuring has been attributed to hydrocarbon generation in many basins worldwide. It is seen as the principal overpressuring mechanism in onshore basins in the USA (Bredehoeft *et al.*, 1994). Hydrocarbon generation has recently been advanced as an important process even in the rapidly-subsiding Gulf Coast (Birchwood & Turcotte, 1994; Hunt *et al.*, 1994).

Experimental data that quantifies the volume increase resulting from kerogen maturation has been presented by Ungerer *et al.*, (1981) (see Fig 4.12) and a numerical quantitative treatment has been presented by Lerche, (1990). There may be a 57% volume increase during gas generation. Quantification of the pressure increase resulting from the cracking of oil to gas has been presented by Barker, (1990). Pressure-induced fracturing of source rocks has been postulated as a mechanism for primary migration by Lindgreen, (1987) and Duppenbecker *et al.*, (1991), based on numerical simulation and field observation. Quantification of the role of hydrocarbon generation in the Viking Graben has been presented by Burrus *et al* (1991), and for the Green River Basin of the Rocky Mountains by Bredehoeft *et al* (1994). However, pressure change is dependent on kerogen type and expulsion efficiency (Ungerer et al 1981); these factors have not been addressed in research. The maturation-expulsion process is complex (Mann, 1993) and so accurate quantification of the role of hydrocarbon generation in basin-scale overpressuring has not been achieved.

Accordingly the evidence for hydrocarbon generation as an overpressuring process is observational. This evidence included the coincidence of overpressure with vitrinite reflectance values of 0.6% (Spencer 1987; Hunt et al 1994), and 1.0% (Holm, *in press*); the coincidence of high pressures with mature source rocks (Spencer 1987; Meissner 1980); the high hydrocarbon saturation of overpressured rocks (Spencer 1987); and the apparent absence of other mechanisms in the stable Mesozoic basins of the Rocky Mountains (Spencer 1987; Bredehoeft et al 1994) and the Palaeozoic basins of Oklahoma (Park *et al.*, 1995).

The diagenetic dehydration reaction that occurs as smectite changes to illite has been proposed as an internal overpressuring mechanism. Burst (1969) defined three zones of smectite dehydration in the Texas Gulf Coast, and noted that the upper boundary of the overpressures in the region coincided with the zone of maximum smectite dehydration (Fig 2.8). The increase of water volume (and thus pressure) rests partially on the volume and density of interlayer bound water present in mudrocks. The volume of water involved is the subject of dispute and may be very low and of equal density to porewater (Fripiat & Letellier, 1984). If so, clay mineral dehydration may be of little significance in overpressuring. Other diagenetic reactions that increase fluid volume include the conversion of gypsum to anhydrite, although this occurs at low temperatures and shallow depths, where fluid movement is freer and consequently overpressure is unlikely to result.

Thus overpressure can result from physico-geochemical changes internal to the porefluid system, or from external alterations to the system's physical environment. However, no one process has been unequivocally proven to have caused overpressure in any one basin setting (see for example Dickinson, 1953 and Hunt *et al.*, 1994 for differing interpretations of Gulf Coast overpressures), although all processes may theoretically apply.

2.8 Paradigms of overpressure

The review presented above of the characteristics of pressure seals illustrates a section of a wider debate on the significance of overpressure in the crust. The pressure cell paradigm has been used to propose the total hydraulic isolation of regions of the crust (Bradley 1975; Hunt 1990; Powley 1991; Dewers & Ortoleva 1994). In this paradigm, pressure seals prevent all fluid flow. Thus overpressured basins are essentially static until fluid pressures are high enough to fracture the pressure seal. The impermeable-seal model has also been applied to the crystalline

crust (Bailey 1994). The proponents of this "static" paradigm suggest that the presence of overpressure implies total hydraulic isolation. Without such isolation, pressures would equalise over geological time (Deming, 1994).

A contrasting paradigm is presented by Toth *et al.*, (1991), Bredehoeft *et al.*, (1994) and Neuzil (1995), who summarise thirty years of investigation of abnormally-pressured basins by hydrogeologists. In their model, termed the "hydrodynamic" model, overpressures are seen as a dynamic balance between ongoing geological processes that perturb the pressure, and fluid fluxes that dissipate the perturbations. The Earth's crust is viewed as a hydraulically-continuous system, where "pressure seals" restrict, but do not absolutely prevent, fluid flow. In this dynamic paradigm, water in sedimentary basins is always moving, albeit infinitesimally.

The two paradigms of overpressure are at present unreconciled. The static paradigm requires an impermeable seal; such a geological material has never been found. The dynamic school requires ongoing pressure-perturbing processes; these remain poorly defined and problematic, particularly in overpressured Palaeozoic basins that are tectonically static. Overpressure presents fundamental problems for geological interpretation.

2.9 Summary

The review presented above demonstrates that there are numerous unresolved problems presented by overpressure in sedimentary basins. The origins of overpressure are complex and poorly-understood. The distribution of overpressure is controlled by seals, but the geological nature of these seals are ill-defined. These problems affect geological interpretation at the present-day; the role of overpressure and the behaviour of pressure seals in the geological past, including the control of overpressure on diagenesis, exacerbates the problem. It is the aim of this thesis to address these unresolved problems in one case-study basin.

It is undeniable that overpressure exerts a major control on fluid flow in sedimentary basins. A fuller understanding of the phenomena associated with overpressure has important scientific and economic significance.

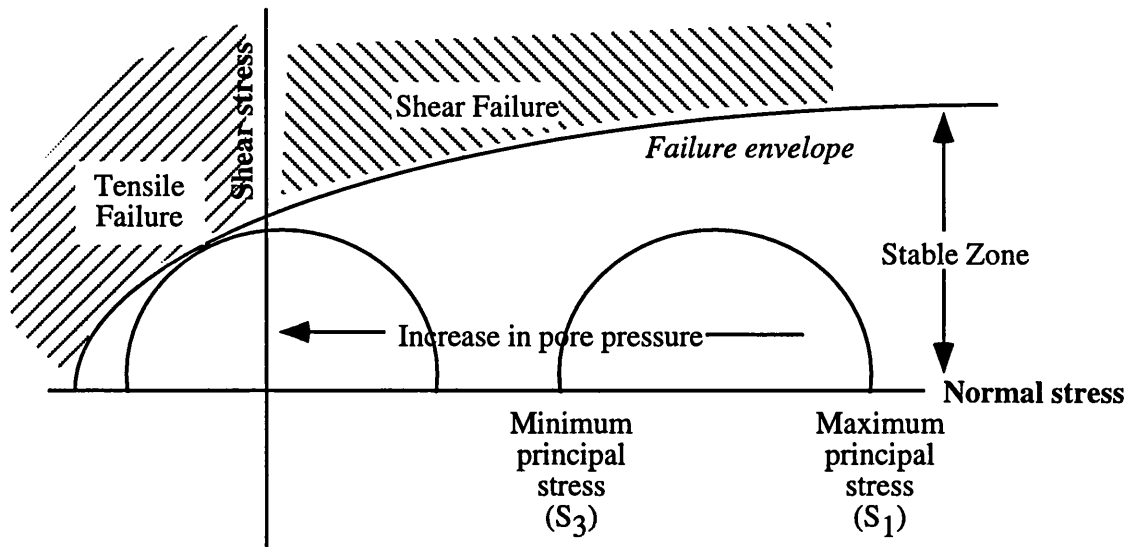


Figure 2.1 Mohr Circles depicting relationship between principal stresses, pore pressure, and rock failure. An increase in pore pressure leads to a decrease in effective stress. This moves the Mohr circle towards the origin, and towards the failure envelope.

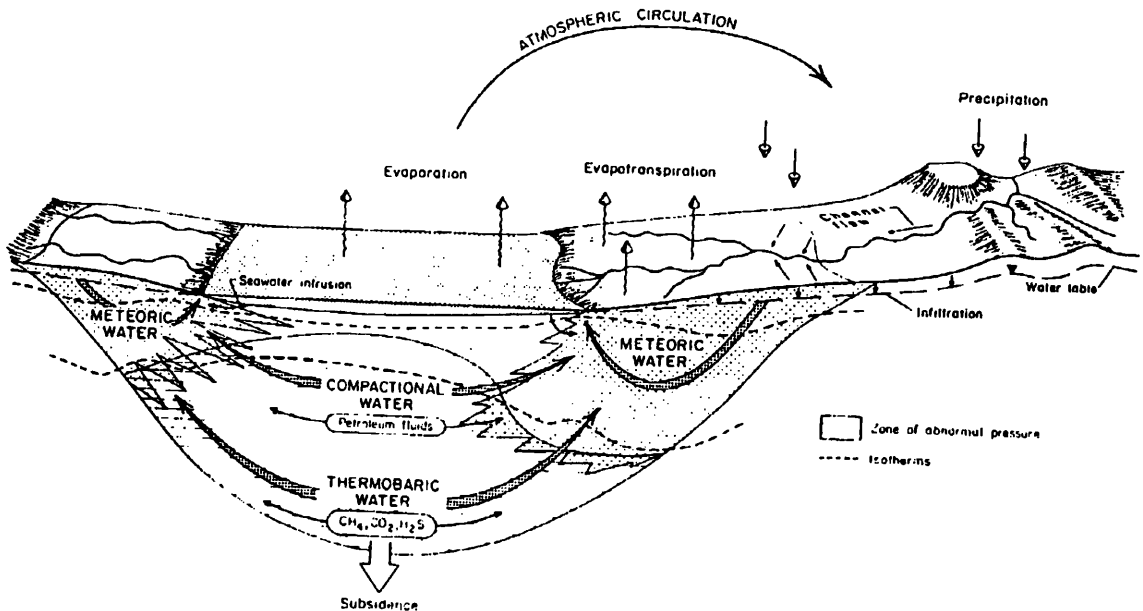


Figure 2.2 Hydrogeological regimes of a sedimentary basin (from Galloway 1984)

The basin hydrogeology can be influenced by the influx of meteoric water from uplifted basin margins; the expulsion of connate water during compaction; and the release of thermobaric water during heating. Abnormal pressures may be encountered in the deep regions of sedimentary basins.

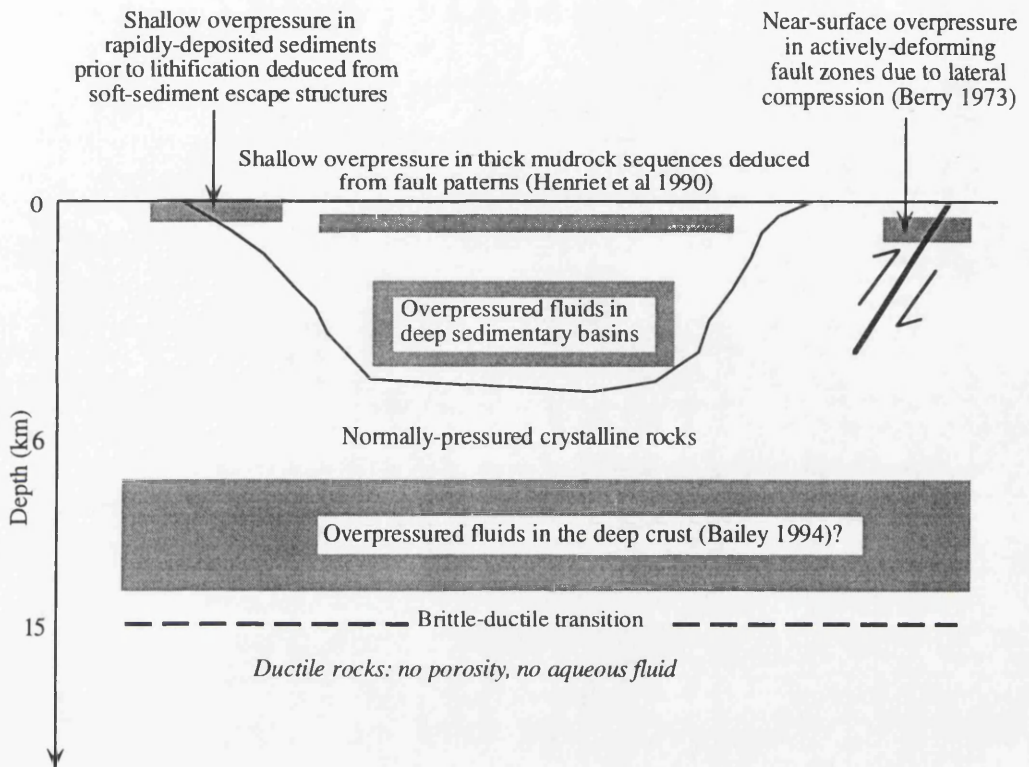


Figure 2.3 Occurrence of overpressure in the Earth's crust.

Fluids saturate the crust from close to the surface to the brittle-ductile transition zone. Overpressures can occur close to the surface (in regions of active tectonism and rapid subsidence) and at great depths in sedimentary basins. High fluid pressures may also occur deep in the crystalline crust.

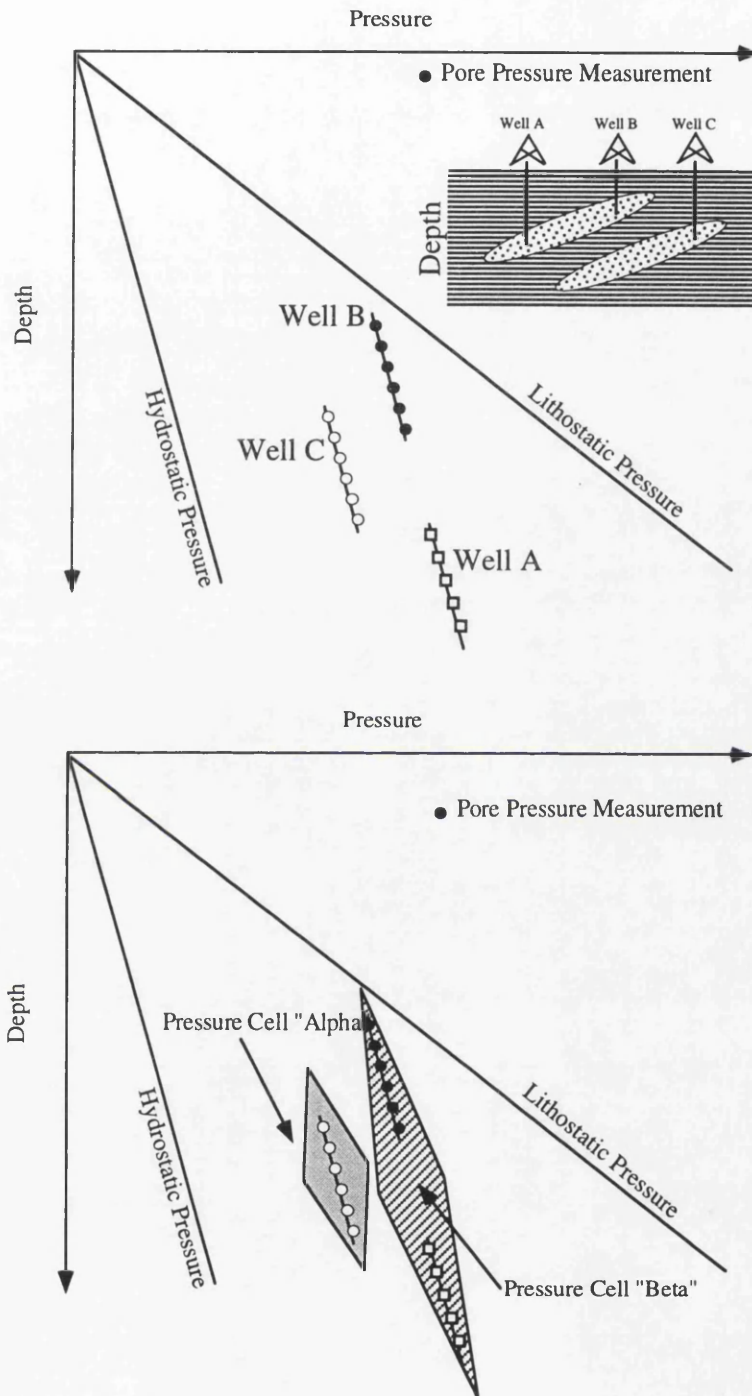


Figure 2. † If numerous pore pressure measurements are plotted on a pressure-depth plot, distinct gradients are observed. On the basis of common gradients and equal levels of overpressure, pressure cells may be defined. In this example, three wells are plotted, defining two pressure cells (Alpha and Beta). This implies that wells A and B are in pressure communication, while well C is isolated; this is revealed by the cross-section.

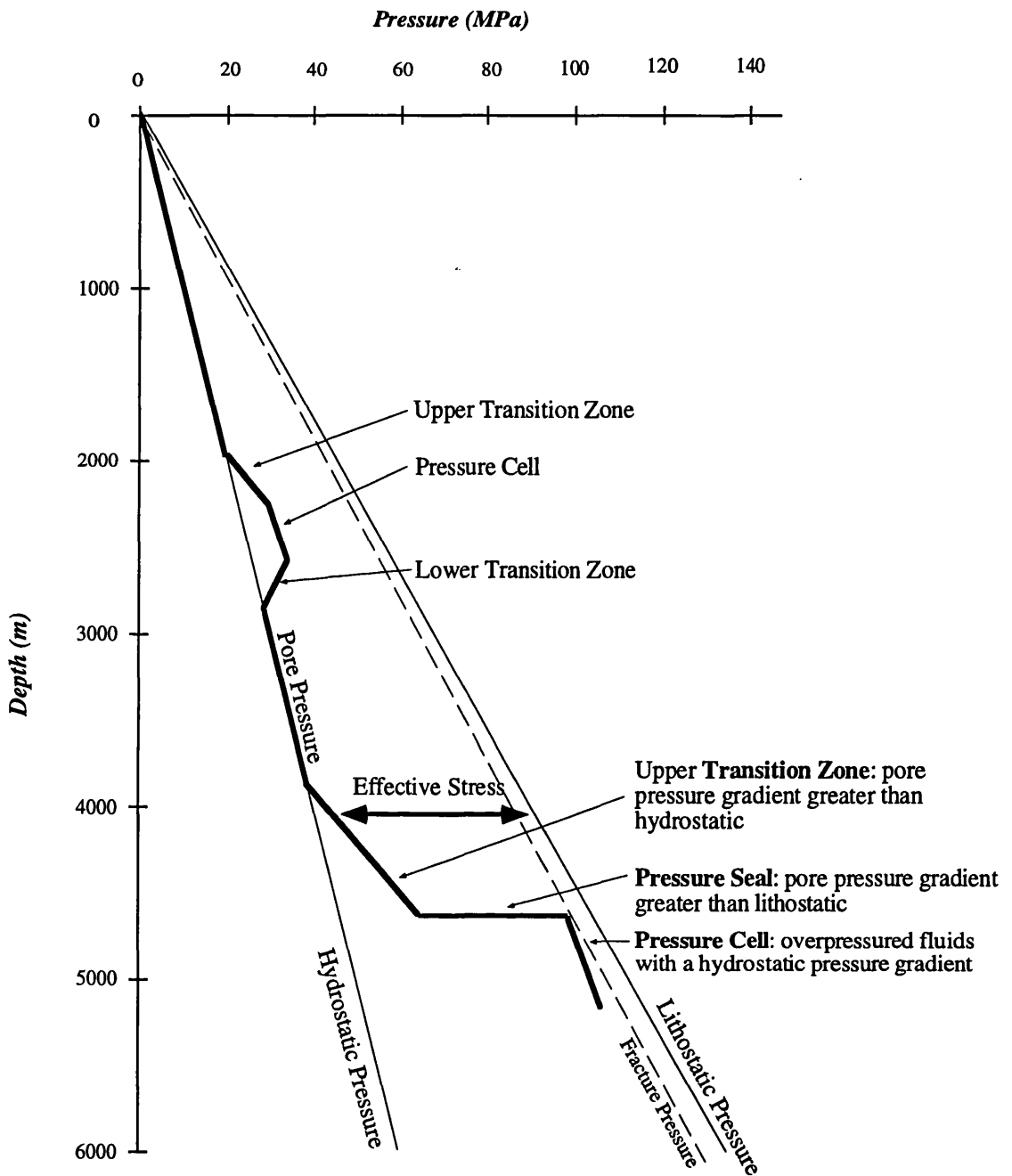


Figure 2.5 Pressure-depth plot of an example Central Graben well to illustrate terminology employed in this research project.

Two overpressured "pressure cells" of constant gradient are defined by the pressure gradients depicted in this plot. An upper cell, from 2300-2600m depth is bounded by upper and lower transition zones. A lower cell, encountered at 4600m, is bounded by a gradual transition zone at 4000-4500 m depth, and a high pressure gradient at 4600m depth. To differentiate the zone of high pressure gradients forming the boundary to a pressure cell, this zone is termed a "pressure seal".

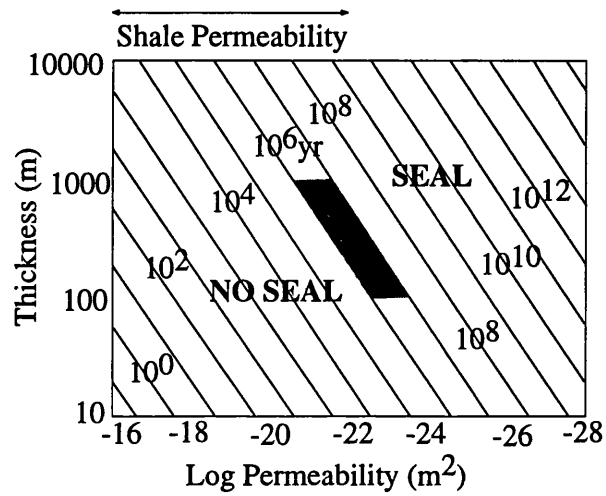


Figure 2.6 Maximum time a pressure seal may confine excess pressure (from Deming, 1994).

The plot examines the dependency of sealing time on thickness and permeability. Note that this analysis defines the time for any fluid flow to occur through the pressure seal; it does not define complete time for overpressure relaxation, which may be much longer. Shaded area shows pressure sealing behaviour of a thick shale. Thick shales may prevent fluid flow for 1-10 MY.

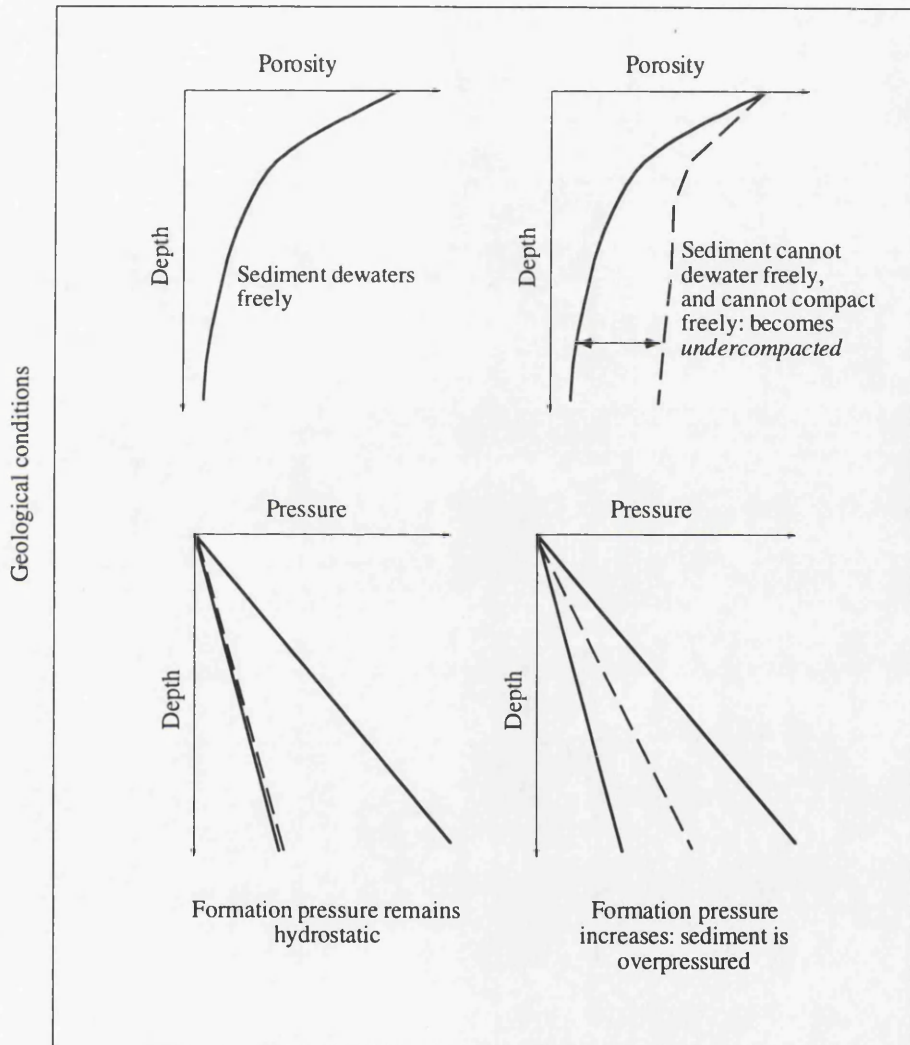
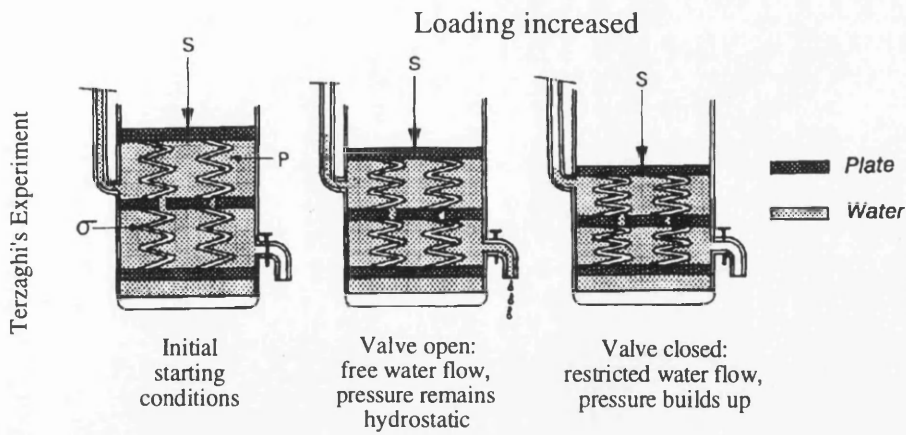


Figure 2.7 Fluid pressure changes in response to loading. Terzaghi's experiment showed that an increase in load produces an increase in fluid pressure if water escape is restricted. The geological analogy of this situation is loading due to sediment deposition. If the sediment cannot dewater freely (due to low permeability), high fluid pressures are produced and anomalous porosity occurs. The sediments are undercompacted and overpressured, a situation termed disequilibrium compaction

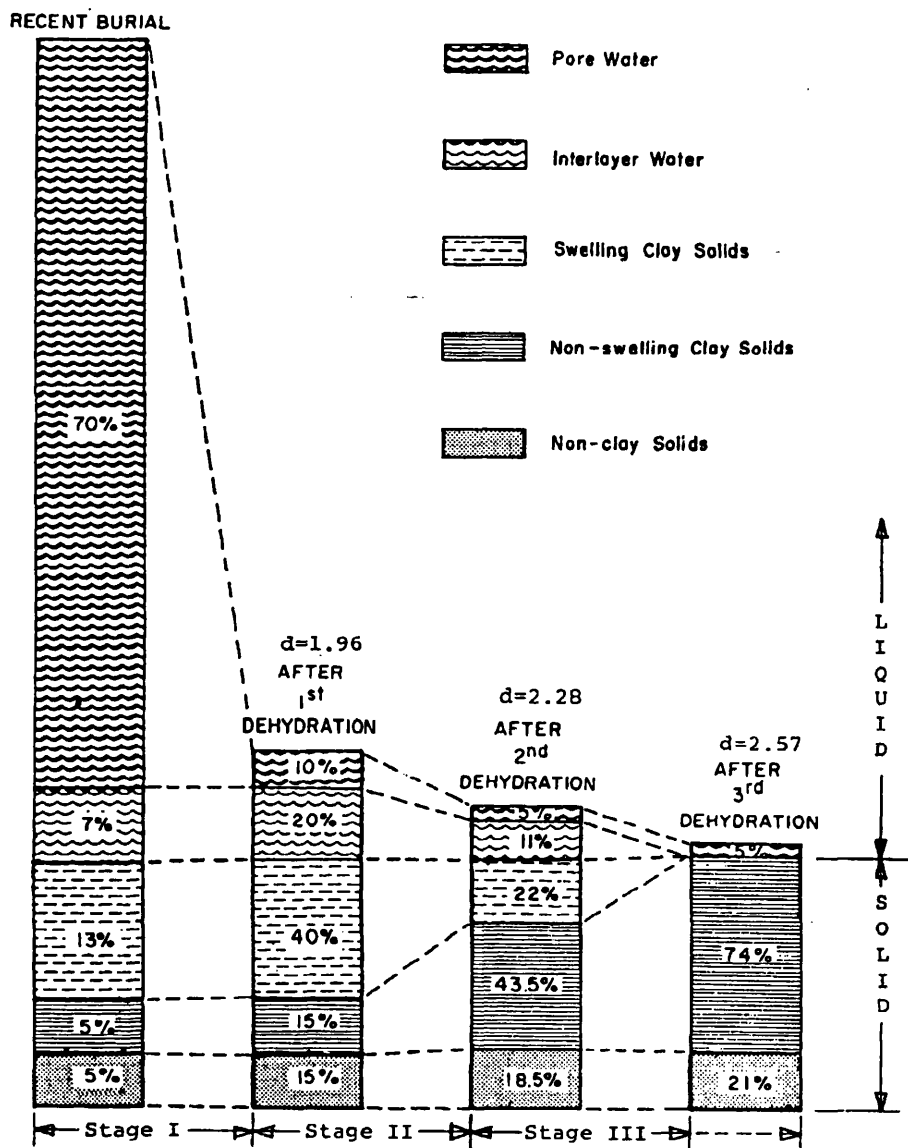


FIG. 6.—Marine shale bulk composition during dehydration.

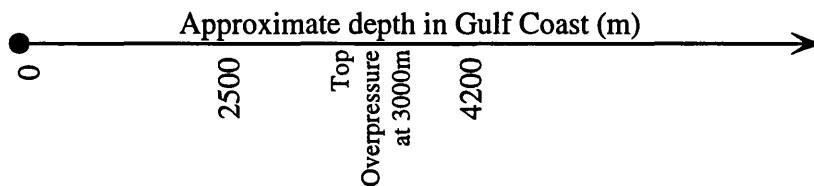


Figure 2.8 Marine mudstone bulk composition during dehydration (from Burst 1969)

Mudstones undergo most water loss soon after sedimentation. Continued burial and heating leads to the expulsion of 5% porewater and 18% interstitial (bound) water. Burst (1969) noted the coincidence of maximum Stage II dehydration with the upper boundary to overpressure in the Gulf Coast.

Chapter Three

Pressure Cells and Pressure Seals in the Central North Sea

- 3.1 Introduction**
- 3.2 Pressure Data**
 - 3.2.1 Direct Pressure Measurements*
 - 3.2.2 Indirect Pressure Measurements*
 - 3.2.3 Leak-off Tests*
 - 3.2.4 Correction of Depths*
- 3.3 Pressure Distribution in the Central North Sea**
 - 3.3.1 Basin-scale Pressure Distribution*
 - 3.3.2 Cenozoic mudstones*
 - 3.3.3 Palaeocene Sandstones*
 - 3.3.4 Cretaceous Chalk*
 - 3.3.5 L. Cretaceous- Triassic*
- 3.4 Discussion of the Pressure Distribution**
 - 3.4.1 Cenozoic*
 - 3.4.2 Cretaceous Chalk*
 - 3.4.3 L. Cretaceous- Triassic*
- 3.5 The problems presented by the pressure distribution**
- 3.6 A Model of the Distribution of Central North Sea Overpressure**
 - 3.6.1 Potential Energy of fluids in the Central North Sea*
 - 3.6.2 Intra-cell and inter-cell flow beneath the pressure seal*
 - 3.6.3 Lateral permeability considerations*
 - 3.6.4 Pressure Seals in the Dynamic Model*
 - 3.6.5 Vertical fluid flow through the pressure seal: Leak Points*
 - 3.6.6 Case Studies of Leak Points*
 - 3.6.7 Additional supportive evidence for the dynamic Model*
 - 3.6.8 The role of Zechstein Salt*
- 3.7 Implications for Hydrocarbon Migration and Entrapment**
- 3.8 Summary**

3.1 Introduction

The aims of this chapter are threefold:

- To present Central North Sea pressure data. The sources of pressure data used in this project are outlined, and the methodology of pressure interpretation employed is discussed. A consideration of the data quality is presented. The distribution of the data is shown as regional maps and sections, to illustrate the distribution of overpressure at a large scale (the basin-scale, 10km). Detailed plots of the pressure in individual wells are used to describe the overpressure distribution at a small scale (on the scale of individual reservoirs, 100-200m).
- To discuss the scientific problems posed by the complex distribution of overpressure in the region.
- To use the pressure distribution to test the applicability of the "static" paradigm of overpressure in the Central North Sea (Hunt, 1990; see Section 2.8).
- To present a qualitative model for the pressure distribution based on a synthesis of the observational data. This model forms the central thesis of this research project.

The model presented in this chapter is based on the recognition that Central North Sea overpressure represents a dynamic hydrogeological system.

3.2 Sources of Pressure Data

Pressures within the deep pre-Cretaceous strata of the Central North Sea have caused drilling problems, expensive downtime, injuries and fatalities on drilling platforms. Accordingly, government regulations and company concern have led to the acquisition of large amounts of high-quality pressure data. This data includes pre-drilling pressure prognoses, pressure evaluation while drilling, and wireline logging after well completion. The growing recognition of pressure as a severe drilling problem, and as a control on hydrocarbon migration, has meant that pressure evaluation has become a vital part of drilling a well in this region.

Pressure data coverage is intrinsically biased. Most data gathered from an exploration well is concentrated on the reservoir interval, which may form only

200m depth-extent in a 6000m deep well. Pressure data and lithological information for the remaining intervals in the well must be inferred. This problem becomes more extreme when extended to three dimensions, as information is inferred for regions away from boreholes. The implications of data bias are vital for quantitative basin modelling and are discussed in Section 5.3.

Due to the diversity of information relating to the pressures encountered during drilling a well, pressure data can be extracted from various sources. Pressure data for this study was collated from composite well logs, end-of-well completion reports, and mud logs recorded while drilling. In recent wells, pressure evaluation logs and reports compiled by pressure specialists within mudlogging companies were available to this study. Drill-stem test (DST) reports, wireline repeat-formation test (RFT) reports, and leak-off test (LOT) reports were consulted for quality control. Protocols for the interpretation of these logs are discussed below.

All data presented in this research project are derived from 108 nonconfidential wells released to the public sector. This data has been extracted from a larger database of 280 confidential wells provided by Elf Enterprise Caledonia (Fig 1.3). Confidential data has been used to check the validity of the interpretations presented in this Chapter but no confidential data is presented in this thesis.

Sources of pressure data can be divided into those that involve *direct* measurement of the fluid pressure in the rock, and those that *indirectly* allow the calculation (or inference) of fluid pressure from other data (Mouchet & Mitchell, 1989).

3.2.1 Direct Pressure Measurements

(i) Repeat-formation tests (RFTs)

An RFT is a downhole wireline tool. RFTs form the most readily-interpretable and widely-used form of pressure data. The tool measures the formation pressure at a specific well depth. A chamber with a pressure gauge is forced into contact with the borehole wall, and fluid from the formation is allowed to enter the chamber. This allows measurement of the pressure in the formation. An example of this data is shown in Fig 3.1. RFTs give detailed pressure information within a limited depth interval in the well (usually the prospective reservoir). A series of RFT pressure measurements run over 100-500m depth allows a gradient of pressure against depth to be constructed, which forms a useful analytical technique (Section 2.5). RFTs

200m depth-extent in a 6000m deep well. Pressure data and lithological information for the remaining intervals in the well must be inferred. This problem becomes more extreme when extended to three dimensions, as information is inferred for regions away from boreholes. The implications of data bias are vital for quantitative basin modelling and are discussed in Section 5.3.

Due to the diversity of information relating to the pressures encountered during drilling a well, pressure data can be extracted from various sources. Pressure data for this study was collated from composite well logs, end-of-well completion reports, and mud logs recorded while drilling. In recent wells, pressure evaluation logs and reports compiled by pressure specialists within mudlogging companies were available to this study. Drill-stem test (DST) reports, wireline repeat-formation test (RFT) reports, and leak-off test (LOT) reports were consulted for quality control. Protocols for the interpretation of these logs are discussed below.

All data presented in this research project are derived from 108 nonconfidential wells released to the public sector. This data has been extracted from a larger database of 280 confidential wells provided by Elf Enterprise Caledonia (Fig 1.3). Confidential data has been used to check the validity of the interpretations presented in this Chapter but no confidential data is presented in this thesis.

Sources of pressure data can be divided into those that involve *direct* measurement of the fluid pressure in the rock, and those that *indirectly* allow the calculation (or inference) of fluid pressure from other data (Mouchet & Mitchell, 1989).

3.2.1 Direct Pressure Measurements

(i) Repeat-formation tests (RFTs)

An RFT is a downhole wireline tool. RFTs form the most readily-interpretable and widely-used form of pressure data. The tool measures the formation pressure at a specific well depth. A chamber with a pressure gauge is forced into contact with the borehole wall, and fluid from the formation is allowed to enter the chamber. This allows measurement of the pressure in the formation. An example of this data is shown in Fig 3.1. RFTs give detailed pressure information within a limited depth interval in the well (usually the prospective reservoir). A series of RFT pressure measurements run over 100-500m depth allows a gradient of pressure against depth to be constructed, which forms a useful analytical technique (Section 2.5). RFTs

3.2.2 Indirect Pressure Measurements

(i) Mud Weight

Mud weight is the density of drilling mud used to counterbalance the pressure of the formation fluid. Drilling is conducted using a mud weight higher than formation pressure, to provide a positive pressure differential between the borehole and the formation to prevent fluids from the formation being drilled entering the borehole and causing a "blowout".

Mud weight provides a continuous record of pressure throughout the well. As such, it forms an extremely valuable source of pressure information that has been neglected in previous studies of the pressure in the Central North Sea. This is in part due to the relative inaccessibility of the data and thus the difficulties in relating mudweight to formation pressure. Mud weight gives a maximum limit to the formation pressure, except in the case of a "kick" (see below).

An increase in mud weight *may* imply an increase in formation pressure, but increases in mud weight may be implemented by the drillers if high formation pressures are expected to be encountered, to increase the safety margin. In this case, mud weight increases do not relate to fluid pressure. Alternatively, increases in mud weight may be required by the unexpected entry of the drill into a zone of high pressure, as evidenced by increasing gas levels. This second situation is valuable to allow precise location of pressure transition zones. Thus quality-control of the relationship of mud weight to formation pressure can be achieved. The monitoring and interpretation of mud gas data are fundamental to detecting transition zones. Gas in the borehole is measured by chromatographs and density measurements at the wellhead, and is continually monitored during drilling.

Drilling gas is classified into three types. **Background gas (BG)** is the gas released by the formation during drilling. An increase in BG indicates entry into a zone of lower differential pressure. If mud weight is too high, it can mask this increase. **Gas shows** occur in permeable gas-bearing formations where gas can flow into the borehole. The volume is determined by the differential pressure. **Connection Gas (CG)** is encountered when the pumps that force mud into the borehole are stopped. The equivalent density of the mud in the borehole when static is less than when the borehole is circulating. This drop in pressure may allow gas termed CG to enter the borehole. The presence of CG is typical of well imbalance. Increasing CG is encountered as transition zones are drilled.

If both BG and CG are increasing, drilling is proceeding in conditions of negative differential pressure or approaching imbalance. If an increase in mud weight reduces the volume of connection gas, the presence of abnormal pressure is confirmed (Mouchet & Mitchell 1989). The methodology employed is shown in Figure 3.2.

A significant mud-related phenomenon is provided by the case of a "kick". This occurs when formation pressure is in excess of the mud weight, and fluids begin to enter the borehole- potentially forming an extreme hazard to the drilling rig, and requiring immediate increase of mud weight to "kill" the well. The drill floor must be evacuated, causing expensive loss of time. Kicks are relatively common in the Central North Sea due to the complex pattern of pressure distribution, and the proximity of formation pressure to the fracture gradient of the rock. While unfortunate and hazardous, such kicks provide invaluable quality control on the approximation formed to formation pressure by mud weight. Killing a flowing well is the only situation where mud weight can legitimately be used as an approximation to formation pressure.

(ii) *"d"-exponent*

The "d"-exponent is a real-time pressure evaluation method widely used by mudlogging companies to monitor the pressure state in the borehole and provide a predictive indication of the proximity of transition zones. The technique is based on an integration of drilling parameters such as drilling rate, rotating speed, weight-on-bit and bit diameter into a mathematical formulation to arrive at a "formation drillability". When lithology is constant, the "d"-exponent gives an indication of porosity and differential pressure. A decrease in "d"-exponent is considered a function of increasing undercompaction, and thus increasing abnormal pressure. The "d"-exponent is an empirical technique developed in the thick shale sequences of the Gulf of Mexico (Bingham, 1964; Jordan & Shirley, 1966), and found to be extremely successful.

This technique works well in thick shale sequences that allow the construction of a standard compaction trend for the well. It is less effective in varying lithologies and non-argillaceous strata. Many companies have refined the technique, such as Agip's Sigmalog or Anadrill's "A"-exponent (Mouchet & Mitchell, 1989).

A serious criticism of this technique, for the aims of this research, is that an *a priori* assumption is made regarding the validity of the base-case "compaction trend". As discussed in section 4.2.5, compaction of argillaceous sequences is a complex subject that is poorly understood at present. Many basins world-wide do not exhibit a relationship between overpressure and undercompaction (Hunt *et al.*, 1994), and so a pressure evaluation technique such as the "d"-exponent that rests entirely on the causal link between overpressure and undercompaction must be treated with caution. If high pressures are caused by fluid volume changes such as hydrocarbon generation (Section 2.7.2), the "d"-exponent may show no relation to fluid pressure.

Nevertheless, the "d"-exponent (and related techniques) is widely used in the Central North Sea. Despite its drawbacks, it is considered reliable and drilling reports highlight the good agreement achieved between real-time predictions and wireline logs. There is a divergence between the empirical approach of drilling engineers, based on many year's experience, and scientific understanding. It is possible that formation "drillability" is more closely related to the effective stress acting on the rock than the formation's porosity (see Section 4.2.1). However, as scientific questions over the validity of the "d"-exponent have not been resolved, the technique has only been used for corroboration in this research.

3.2.3 Leak-Off Tests

A leak-off test (LOT) is used to determine the maximum safe mud weight than can be sustained by the formation without fracturing. It can thus be used as an approximation to the magnitude of the minimum stress in the well (Engelder & Fischer, 1994; Yassir & Bell, 1994). The test involves increasing the mud pressure until mud is injected into the formation (Fig. 3.3a). LOTs are carried out after setting casing, and in the Central North Sea are typically run in the Cenozoic mudstones immediately overlying the Palaeocene sandstones, and the L. Cretaceous-U. Jurassic mudstones above the Jurassic Fulmar fm. This stratigraphic bias is caused by the desire to evaluate the fracture pressure of the formation, so as to minimise damage to the underlying sandstone reservoir. Deep LOTs in Upper Jurassic/Lower Cretaceous shales in the Central Graben show a non-standard pressure profile (Fig. 3.3b). No obvious pressure "plateau" can be recognised. The LOT pressure quoted in logs and reports is thus of questionable validity. It is hypothesised that this profile is due to continued elastic deformation of the formation (Engelder & Fischer 1994).

3.2.4 Correction of depths

Well information- particularly drilling information such as mud weight- is often quoted in Measured Depth (MD). In this project, this has been standardised to True Vertical Depth Sub-Sea (TVDSS) when comparison between wells is required, to correct for well deviation and drilling floor height. TVDSS in deviated wells and side-tracks is noted from composite logs and end-of-well reports.

3.3 Pressure distribution in the Central North Sea

Quantitative pressure information from RFT measurements allows the analysis and description of the distribution of abnormal formation pressure for the principal hydrocarbon reservoirs and aquifers in the Central North Sea. This picture can be completed by the use of indirect pressure measurements. These allow the examination of the pressure distribution in poorly permeable zones of a well, where direct pressure measurements are unavailable or unreliable. In combination, this data allows the construction of a detailed description of the pressure distribution throughout the region. This distribution can be described areally by maps, and in terms of depth using pressure-depth plots. The pressure distribution is presented below by stratigraphic unit.

3.3.1 Basin-scale Pressure Distribution

On this largest scale of observation, the Central Graben can be divided into an upper, hydropressed regime, generally occurring above 3000m, and a lower, overpressured regime (Fig. 3.4). This distribution is common in sedimentary basins (see Section 2.4). The boundary between normal pressures and overpressures is diffuse, occurring between 2500m and 4000m. Pressures show a broadly depth-dependent increase throughout the region.

3.3.2 Cenozoic mudstones

Quantitative pressure data is entirely absent from the thick Quaternary and Tertiary mudstone formations of the basin. Additionally, mud weight is typically far in excess of formation pressure, and so is unindicative of pressure. The use of "d"-exponent pressure evaluation in logging reports suggests the presence of overpressures in the

Cenozoic mudstones from 1000m-3000m depth in several wells. Although the magnitude of overpressure developed in the Cenozoic mudstones is not high compared to that of pre-Cretaceous strata, it can cause drilling problems such as stuck pipes. Where resolvable, overpressure in the Cenozoic mudstones occurs from approximately 1000m depth, and formation pressures decline to lower values above the Palaeocene sandstones.

3.3.3 Palaeocene Sandstones

The porous, permeable Palaeocene sandstones are commonly hydrocarbon-bearing in the Central North Sea, and so RFTs are routinely run. The unit is normally-pressured in the north of the study area (e.g. well 22/21-4) and is overpressured towards the south of the region (Fig. 3.5). There is no relationship between Palaeocene overpressure and depth (Fig. 3.6): pressures at 2800m depth may be hydrostatic or 15MPa in excess of hydrostatic pressure. Wells 29/4a-1a and 29/4a-2 demonstrate the presence of an upper, hydro pressured formation and a lower, overpressured formation within the Palaeocene sandstones of these wells. RFTs in the northern Palaeocene sandstones define a fresh-water pressure gradient.

3.3.4 Cretaceous Chalk

Description of the pressure distribution within the Cretaceous Chalk is hampered by the paucity of quantitative data. Economic hydrocarbons have not been found in the Chalk in Quadrant 22 and so RFTs are rarely recorded. However, the upper formations of the Chalk in Quadrant 22 appear to be normally pressured. In Quadrants 23, 29 and 30, oil has been discovered in the Ekofisk and Tor formations, and so RFTs are recorded for permeable zones. These tests indicate that the Upper Chalk is overpressured in the south of the study area (Figs. 3.7 and 3.8).

3.3.5 Lower Cretaceous - Triassic

RFT measurements within Central Graben pre-Cretaceous sandstones reveal a concentric pattern of abnormal pressure in the study area (Fig. 3.9). Jurassic sandstones on the Western Platform are hydro pressured. Within the central region of the study area, overpressure increases towards the centre of the Graben from moderately overpressured marginal fault terraces (such as block 22/5b) towards

central, highly overpressured fault blocks (such as block 29/5). The distribution of overpressure is complex in detail in the East Forties Basin and the central core of the Central Graben; the concentric distribution of overpressure is complicated by the presence of the axial Forties-Montrose High and satellite fault terraces, where relatively shallow wells in this region (e.g. 22/30a-1, 30/1c-2) have encountered high levels of overpressure.

A plot of RFT pressures against depth for Jurassic reservoirs (Fig. 3.10) reveals that pressure generally increases with increasing depth in the Graben. However, when examined in detail it is evident that overpressure at any one depth may vary considerably. For example, the Fulmar sandstones of well 29/9c-4 and well 22/30a-1 occur at a similar depth of 4500m, but have 15 MPa difference in observed pressures. The magnitude of overpressure developed within pre-Cretaceous sandstones correlates to both depth and geographical position in the Graben. The presence of distinct RFT pressure-depth gradients in the pre-Cretaceous sandstones suggests compartmentalisation and division of the sandstones into pressure cells (Section 2.5).

RFTs provide an adequate description of pressure in the pre-Cretaceous aquifers of the Graben. However, a description of the pressure distribution in the Cretaceous-Jurassic shale aquitards requires a more complete examination. Figures 3.11-3.19 present detailed pressure data for wells penetrating deeply-buried Jurassic and Triassic fault blocks in the Central Graben, Forties-Montrose High and East Forties Basin. These plots allow insight into the pressure seals in the region (see Section 3.4.3 below).

A degree of complexity is revealed by the plots, with wells demonstrating several increases in pressure. A gradual increase in pressure is noted throughout the Cretaceous mudstones in all wells. A further, much larger increase in pressure to the highest pressures recorded in the well occurs either within the Kimmeridge Clay Formation (wells 29/5b-4, 23/26a-7, and 29/5a-3) or at the top of the permeable pre-Cretaceous sandstone (wells 22/30a-1, 22/27a-1, 29/10-2 and 30/1C-2). Good quality-control of mud weight is available by the presence of background and connection gases (up to 75% in some wells) suggesting balance between mud weight and formation pressure. Additional increases in pressure within the pre-Cretaceous sandstones are implied by kicks in the gas condensate reservoirs of well 29/5a-3. A strong degree of reservoir compartmentalisation is implied.

3.4 Discussion of the Pressure Distribution

3.4.1 Cenozoic

The distribution of overpressure in the Cenozoic mudstones is controlled by the low vertical permeability of these thick formations, which will inhibit vertical escape of fluids as the shales undergo compaction. Drainage of the shales downwards into the Palaeocene sandstones accounts for the reduction in pressure in the deepest shales. Faulting and deformation of the Cenozoic mudstones has been noted by Cartwright, (1994), who attributes the faulting to pressure-induced fracturing in the Oligocene. However, Figs 3.11 and 3.12 show that formation pressure and mud weight are considerably lower than LOT values in these formations. Conditions for hydraulic fracturing are not satisfied for the present day despite the accelerating subsidence rates suggested for the Cenozoic (Section 1.4.3). It seems unlikely that fractures in Cenozoic mudstones (Cartwright 1994) are related to high fluid pressures.

The distribution of abnormal pressure in the Palaeocene sandstones of the Central Graben is controlled by sandbody connectivity. The Palaeocene submarine fans are thickest in the north of Quadrant 22 (Reynolds, 1994). This thick, permeable, basin-wide sandsheet allows rapid fluid drainage towards the basin margins and consequently the unit remains hydropressured. The fans decrease in thickness and lateral extent southwards. Sand distribution is also a function of depth, with the lowermost Andrew Formation thin and discontinuous in northern Quadrants 29 and 30 (Reynolds 1994). Fluid flow in the Palaeocene is thus more restricted in the south of the Central Graben, and particularly in the lower sandstone formations, accounting for the southward increase in overpressure and the two-cell profile in well 29/4a-1.

3.4.2 Cretaceous Chalk

The distribution of overpressure in the Ekofisk and Tor Formations of the Chalk Group is also controlled by the distribution of the overlying Palaeocene sandstones. Where the sandstones are thick and free-draining in the north of the Graben, the upper Chalk formations have free vertical fluid flow. Where the Palaeocene sandstones are thin and discontinuous (and thus overpressured, as in well 29/10-2) or absent entirely (in which case the Chalk is overlain directly by overpressured Tertiary shales), vertical fluid flow in the upper Chalk is restricted and the Ekofisk and Tor Formations are overpressured.

It is hypothesised that hydro pressured Chalk overlain by free-draining Palaeocene sandstones is an unfavourable trapping configuration for hydrocarbons. The present-day distribution of hydrocarbons shows that hydrocarbons are trapped in the Chalk by immediately overlying Tertiary mudstones, as in the Ekofisk Field.

Rising pressures at the base of the Chalk Group (Hod, Herring and Flounder Formations) suggest restricted fluid flow and lower unit permeability due to the muddy nature of the lower Chalk. Mudstone and marl strata form partial barriers to vertical fluid flow.

3.4.3 Lower Cretaceous-Triassic

The pressure distribution in the sedimentary rocks that lie below the Cretaceous Chalk is complex. This complexity lends itself to examination at a range of scales. The overpressure distribution can be discussed at the basin-scale (tens of kilometres); at the scale of individual fault blocks (5-10 kilometres), a suitable scale for discussing the definition of pressure cells; or at the scale of reservoirs (100m), which serves as a suitable scale of observation for a discussion of pressure seals.

(i) Basin-scale

Analysis of the pressure distribution in the study area suggests that the pre-Cretaceous structural geology of the basin exerts a principal control on the magnitude and distribution of overpressure. The large-scale control of structure on overpressure is shown by Fig 3.9. The Western Platform, with relatively shallow pre-Cretaceous reservoirs and good lateral connectivity, is hydro pressured. Overpressure increases into the deep centre of the basin. The lower overpressures developed in the south of the study region suggest improved connectivity to the Platform, possibly due to permeable basin-margin faults (Cayley, 1987). A similar distribution has been noted for the Northern North Sea (Buhrig, 1989). Note that despite the increased coverage of pressure data available to this study, the broad distribution of pressure remains similar to that described by Cayley (1987) and Gaarenstroom *et al.*, (1993).

(ii) Block-scale: Pressure Cells

Quantitative measurement of formation pressure by RFT allows the pre-Cretaceous sandstones of the region to be divided into pressure cells on the basis of common pressure-depth gradients, and thus interpreted in terms of the "pressure cell paradigm" (Hunt 1990, see Section 2.5). Pressure cells are delineated on Figs 3.20-3.24.

The East Forties Basin (Fig 3.20) contains three distinct pressure cells. Several wells in the Basin penetrate one cell on a central fault terrace. A shallower cell on the axial Forties-Montrose High (forming the western edge of the East Forties Basin, penetrated by well 30/1c-2) is differentiated by a parallel gradient at an overpressure that is approximately 2 MPa lower. The eastern margin of the East Forties Basin forms a third cell (penetrated by well 23/27-6), which despite similar depths of 4000m to the axial High is at far lower overpressure.

One large pressure cell may be defined in the blocks 22/30-29/5 region of the Central Graben (Fig 3.21), where pressure measurements in the Fulmar sandstones of well 22/30a-1 and well 29/5b-4 (in which the sandstone is 500m deeper) form a common pressure gradient, and so are in pressure communication within a pressure cell. Other cells can be defined using the same method in the northeast of the study area on the Jaeren High (Fig 3.22); on the Forties-Montrose High (Fig 3.23); and in the south of the Central Graben in Quadrant 30 (Fig 3.24).

Fig 3.24 clearly demonstrates the division of the basin into pressure cells, and the dependency of the magnitude of pressure within each cell on structural position and geographic location. Cells on the western terraces of the Graben exhibit similar levels of overpressure regardless of depth. In contrast, cells on the axial horst are much more highly overpressured for the same depth, and the level of overpressure increases northwards along the horst in Quadrant 30.

Although data is sparse in some areas of the Graben, a map can be constructed showing the distribution of these pressure cells (Fig. 3.25). As pressure cells are defined from well information, the lateral extent of any one cell is interpretative. The compartmentalisation of the Central Graben by pre-Cretaceous fault blocks is interpreted to control the division of the basin's hydrogeological systems into pressure cells. Pressure cell distribution appears to follow the NW-SE structural grain of the Graben. Cells extend 20km NW-SE and 10km SW-NE on the Graben margins. Each fault block in the Graben appears to contain a separate pressure cell, and the bounding faults to each block form the lateral seals to cells (Fig 3.25). The

NW-SE boundaries to cells are hypothesised to be the sedimentological boundaries to the laterally-discontinuous pre-Cretaceous sandstones, which pass laterally into siltstones (Roberts *et al* 1990). These NW-SE boundaries are poorly defined.

Fluid pressure within each pressure cell increases with increasing depth of the cell, and so pressure increases from cells on the basin margins towards cells in the centre of the Graben. Significant departures from this depth-dependent overpressure trend in the Graben occur in wells penetrating the Forties-Montrose High (Figs 3.11 and 3.19). These structurally-elevated pre-Cretaceous pressure cells are anomalously highly overpressured, and exhibit fluid pressures at or close to LOT measurements of minimum stress (e.g. well 30/1c-2, Fig 3.19). The thinness or complete absence of the L Cretaceous-Jurassic mudstone aquitard on the Forties-Montrose High (Roberts *et al.*, 1990) makes this anomaly even more significant.

(iii) Reservoir-scale: Seals

The detailed description of pressure distribution within the Central Graben presented above allows insight into the pressure distribution at a 100m scale. Pressures increase in the muddy base of the Chalk Group, and continue to increase through the low-permeability aquitards of the Cretaceous and Jurassic mudstones. However, this detailed scale of observation allows discussion of the position of pressure seals *within* the regional aquitards. The analysis reveals that:

(a) Pressure seals are controlled by the presence of low-permeability lithologies.

Pressure increases, defined from increases in mudweight and mud gas, occur in the argillaceous base of the Chalk Group (e.g. Fig 3.11), the Kimmeridge Clay Fm (e.g. Fig 3.12), and the top of the Fulmar sandstone (e.g. Fig 3.19). Pressure increases also occur below intraformational mudstones in the Fulmar Fm. (Fig 3.14). A lithostratigraphic control is evident.

(b) Pressure seals do not occur at any one specific stratigraphic horizon. Although rapid increases in pressure may occur at the top (Fig 3.12), or base (Fig 3.13) of the Kimmeridge Clay Formation, increases in pressure can also occur at the top of the permeable pre-Cretaceous sandstone (e.g. Fig 3.11). This variability in seal position occurs within single pressure cells (such as the cell penetrated by wells 22/30a-1 and 29/5b-4) as well as between pressure cells (e.g. between cells penetrated by well 30/1c-2 and 23/26a-7).

- (c) A link to the geochemical processes of hydrocarbon generation is suggested by the coincidence of changes in pressure gradient and the Kimmeridge Clay source rock. The Kimmeridge Clay Fm. often contains the highest pressures developed in a well (e.g. Fig 3.12).
- (d) Pressure seals occur at a range of depths. A sharp rise in pressure from 60MPa to 80MPa is noted at the top of the Fulmar sandstone at 4100m for well 30/1c-2 in Fig 3.19; in contrast a transition from 60MPa to 100 MPa is noted at the top of the Fulmar sandstone at 4500m for well 22/30a-1 in Fig. 3.11. This suggests that pressure seal location is not controlled solely by depth-dependent processes. A link to stratigraphy is more strongly indicated.

The range of depths at which pressure seals occur in the Central Graben demonstrates that pressure seals in the region are not planar, horizontal zones that occur at constant depths across the region. Accordingly, geochemical-diagenetic models of pressure seals (Hunt, 1990) which emphasise the control of depth and temperature on pressure seal position are inapplicable to this basin. A lithostratigraphical control on pressures is preferred. Pressure seals are formed by low-permeability lithologies.

This provides an indication that the "static" model of overpressure (Hunt, 1990) is unsuitable for this basin. A prime tenet of the "static" model - the presence of horizontal seals - is refuted. The "dynamic" model (Bredehoeft *et al*, 1994; Neuzil, 1995; see Section 2.8) suggests that fluid flow is retarded by low-permeability lithologies. On the basis of the data presented above, the "dynamic" model is preferred in the Central North Sea.

3.5. Problems presented by the pressure distribution in the L. Cretaceous-Jurassic

A description of the overpressure distribution in the Central Graben reveals the structural and lithostratigraphic control on pressure. However, this discussion of the distribution in the L. Cretaceous-Triassic section highlights several problems that cannot be resolved through a simple discussion of the distribution of pressure:

- a) Structurally-elevated wells on the Forties-Montrose High are anomalously highly overpressured, with pressures close to LOT measurements of the minimum stress. This pattern is clearly unrelated to depth or to seal thickness.

- b) Some wells demonstrate a seal in the Kimmeridge Clay Fm., while others show a rapid rise in pressure in the permeable pre-Cretaceous sandstones. The control on the position of pressure seals and the morphology of well pressure-depth profiles is complex.

It is necessary to create a model for pressure distribution that accounts for these problematic phenomena. Such a model is developed in the following sections.

3.6. A Model of the Distribution of Central North Sea Overpressure

To develop a model for Central North Sea overpressure requires the development of a new paradigm. The terminology used to describe abnormal pressures infers an essentially static system. However, an understanding of the phenomenon of abnormal fluid pressure requires recognition that the hydrogeological environment of the North Sea is a dynamic system.

3.6.1 Potential energy of fluids in the Central North Sea

As a facet of a dynamic hydrogeological system, it is useful to recast the distribution of pressure in the study area in terms of fluid potential energy (Dahlberg, 1982; see Section 2.2).

Hydraulic head (H_w) was calculated from formation pressure (P_p) in the water phase as:

$$H_w = Z + \frac{P_p}{D_w \cdot g}$$

Head is related to the fluid potential energy by:

$$\Phi_w = g \cdot H_w$$

so that

$$\Phi_w = g \cdot Z + \frac{P_p}{D_w}$$

where Z = elevation below sea level; D_w = density of saline water; and g = acceleration due to gravity.

As is conventional, hydraulic head has been used as an approximation for fluid potential to construct a potentiometric surface (Dahlberg, 1982). A potentiometric surface map of the sub-seal sandstones in the mid-Central Graben is shown as Fig 3.26. An enforced assumption is that there are no lateral variations in salinity due to the paucity of formation water data in the region. This assumption may be incorrect; however it is justified as the variations in levels of overpressure in the region greatly outweigh the influence of likely variations in salinity (Gran *et al.*, 1992) in the calculation of fluid potential. Moreover, fluid pressure gradients in the water legs of Jurassic reservoirs are parallel, suggesting similar salinities.

The potentiometric map demonstrates that the distribution of fluid potential energy is complex. This complexity appears to coincide areally with the structural complexity of the region. The map reveals the presence of important lateral energy gradients.

The shallow Graben margins are zones of low potential energy, whilst the western and eastern Graben axes are zones of high potential energy. Consequently, strong potentiometric gradients are directed laterally from the Graben centres onto the south-west and northeast flanks. This pattern of energy is common in actively subsiding sedimentary basins (Magara, 1968). If fluid connectivity exists between the Graben centres and the Graben margins, then this potential can drive lateral fluid flow, allowing fluid to be expelled onto the basin margins as the basin dewater.

However, additional zones of low potential energy in the Central Graben are represented by the axial Forties-Montrose High and marginal "Puffin" horst. Most significant is the Forties-Montrose High. The presence of these zones is crucial to the basin hydrogeology.

Fluid potential energy in the Jurassic sandstones increases with increasing depth; thus fluid potential follows the Jurassic structure of the Graben. As drilled structures such as those penetrated by wells 22/30a-1 and 30/1c-2 on the High have three-dimensional hydrocarbon-trapping closure (Roberts *et al.*, 1990), it is likely that structurally closed zones of low potential energy exist along the strike of the axial horst. The marginal horst block termed the "Puffin High", penetrated by well 29/10-2, is similarly inferred to be a closed zone of low potential energy as the sub-Cretaceous rocks of the block deepen away from the well in all directions

(Gaarenstroom *et al* 1993). The presence of closed potentiometric "lows" on the axial horsts suggests that fluid escapes through the regional pressure seal at specific points (Dahlberg, 1982).

Fig 3.26 demonstrates that there is the *potential* for significant lateral fluid flow, beneath the regional pressure seal. The fluids in the sub-Cretaceous strata of the basin are out of equilibrium.

3.6.2 *Inter-cell and intra-cell flow beneath the pressure seal*

The basin fluids will seek to re-equilibrate at the stable, low-energy state of hydrostatic pressure. This re-equilibration will occur by flow, if possible, vertically towards the surface or laterally along potentiometric gradients such as those defined in Fig 3.26. The presence of potentiometric gradients implies a disequilibrium situation. This implies that either (a) fluid flow is restricted so that no re-equilibration can occur- the impermeable seal-bounded pressure cell model (Hunt, 1990); or (b) that the cause of the disequilibrium is acting at a faster rate than the re-equilibrating flow (Neuzil, 1995). Mudford *et al* (1991) have demonstrated that in the Central Graben the rate of re-equilibrating fluid flow is too slow to allow free compaction of the sediments during the rapid Cenozoic subsidence. This leads to overpressure due to disequilibrium compaction (Mudford *et al.*, 1991). The cause of the disequilibrium in the region will be investigated further in Chapter Four. In this discussion, it is sufficient to note that both possibilities (a) and (b) are tenable in the Central Graben.

Fig 3.26 shows that the crests of the horsts are in energy equilibrium with deeper, off-structure regions (as in the case of wells 22/30a-1 and 29/5b-4). This is the energy distribution implied by the coincidence of hydrostatic pressure gradients, and thus the interpretation of these wells as part of the same pressure cell. This implies a hydraulic connection between the Fulmar sandstones of the deeper terrace of well 29/5b-4 and the Fulmar sandstones of the structurally-elevated crest penetrated by well 22/30a-1. The internal permeability of the cell is sufficiently high to permit free fluid flow and equilibration of overpressure. Hydraulic connectivity and equilibration of fluid potential energy within a cell will elevate the pressures in the sandstone on the crest of the structure. Thus a hydraulic connection to deeper, highly-overpressured regions provides an explanation for the high pressures in the horsts (Fig 3.27).

An identical pattern of pressure has been presented for the crestal well 29/10-2 on the western "Puffin" Horst and the well 29/5a-1 on a neighbouring deeper terrace. Fig 3.26 suggests that the structures are in equilibrium, and so hydraulic connectivity will allow regulation of pressures: pressure will increase on the Puffin Horst and will be lowered on the adjacent terrace.

In contrast, well 30/1c-2 on the Forties-Montrose High presents a different scenario. The horst is not part of the same pressure cell as the neighbouring terrace in the East Forties Basin penetrated by wells 23/26b-4, 23/26a-7 and 23/26a-2. The two structures are separated by 2MPa pressure. Accordingly, a hydraulic connection between deep regions of the Graben and the shallow crest of the horst has not been demonstrated. The permeability of the Humber Group is too low (either due to faulting or lateral discontinuity of the Fulmar sandstone) to permit free equilibration between the structures. In this case, inter-cell flow between the sandstones on the horst and on the terraces will be restricted by the seals on the boundaries of the cells; re-equilibrating flow into the horst will be rate-limited by the lateral permeability of the faulted Humber Group. Two possible situations exist. Either (a) the pressure cell containing well 30/1c-2 and the pressure cell containing well 23/26b-4 are totally isolated; or (b) the two cells are separated by a permeability restriction that can allow slow flow between the cells. The pressure information alone cannot differentiate between these two possibilities.

If well 30/1c-2 is isolated from the rest of the Graben, it is possible to rationalise the high pressures encountered in this well by considering the structure of the Forties-Montrose High. The High dips steeply eastward (Fig 1.5; Roberts *et al* 1990) and thus the Jurassic sandstone will deepen rapidly towards the East Forties Basin. Thus a hydraulic connection between the crest of the High and deeper, highly-overpressured regions may be assumed. This accounts for the overpressure in the well in a similar manner to that demonstrated for wells 22/30a-1 and 29/5b-4.

The second possibility is intriguing. Fig 3.26 shows that hydrodynamic potential energy conditions exist between well 23/26b-4 on the terrace and well 30/1c-2 on the horst. If the basin is viewed as a hydraulically-continuous system, re-equilibrating fluid flow will occur between terrace and horst if the lateral permeability of the region is non-zero. This model provides an explanation for the high pressures (close to minimum stress) in the shallow sandstones on the horst, and the lowered pressures (distal from minimum stress) in the deeper terraces.

The potentiometric map of Fig. 3.26 reveals that the horsts are zones of low potential energy. This distribution of energy occurs despite the proximity of formation pressures in the horsts to the minimum stress, as derived from LOTs. The potential for flow into the horsts exists due to the structural elevation of the horsts. Thus the re-equilibrating flow has the potential to raise pressures in the sub-seal sandstones in the Central Graben to the minimum stress, and thus to hydraulically fracture the seal. The limiting factor for basin re-equilibration will thus be the hydraulic fracturing of the seal in structurally-elevated zones.

This dynamic model of pressure regulation in the Central Graben accounts for the complexities in the pressure distribution described above. Regulation of pressures by fluid flow between deep terraces and shallow horsts will occur as the fluid in the basin seeks to re-equilibrate. This structurally-mediated fluid flow accounts for the lack of correspondence between magnitude of overpressure and depth. It also describes the lack of correspondence between magnitude of overpressure and seal thickness. Hydraulic connectivity between sandstones at varying depths accounts for the high pressures observed in sandstones on the axial horsts.

3.6.3 Lateral permeability considerations

Section 3.7 suggested that the Central Graben may be viewed as a hydraulically-continuous system, or a series of hydraulically-isolated units. The view of the Central Graben as a dynamic, hydraulically-continuous system on a geological timescale can be challenged by considerations of lateral permeability. If impermeable rocks exist in the Graben, the basin will be divided into hydraulically-isolated zones. For the potentiometric map of Fig 3.26 to represent the actual fluid flow pattern requires finite lateral permeability. Hydraulically-isolated zones may be formed by a) the fault compartmentalisation in the region, and b) the lateral discontinuity of the permeable pre-Cretaceous sandstone formations (Donovan *et al.*, 1993). How can this challenge be addressed?

NW-SE faults bounding the fault blocks are demonstrably sealing at the present day, as they isolate distinct pressure cells. Does a fault constitute a zone of zero permeability that can totally isolate bodies of porewater over geological time? The hydrogeological role of faults is the subject of much debate, and much detailed study (e.g. Knipe, 1993). Hydrogeological studies of the North Sea often suggest hydraulic isolation of fault blocks throughout the history of the basin (Burrus *et al.*, 1991). The prime concept is that of geological time. It is contended that the faults in the Central

Graben should not be viewed as permanent, perfect seals. Rather, when examined through the lens of geological time, they should be seen as leaky permeability restrictions. It is emphasised that this discussion addresses single-phase flow of *water*. The flow of hydrocarbons through low-permeability faults will be altered by capillary entry pressure effects that may allow the creation of true "impermeable" barriers to hydrocarbon flow.

Faults in the Central Graben may juxtapose two sections of thick, permeable Fulmar sandstones. In this case, fault-sealing may be related to cataclasis (Fowles & Burley, 1994). While significant for reservoir production in a human timeframe, such faults are likely to be inhomogeneous. They may contain zones of enhanced porosity and permeability that will allow fluid flow (Fowles & Burley, 1994). A detailed examination of the role of fault properties in controlling lateral seals within sandstones is beyond the scope of this project due to the absence of cored faults available to this project for study.

Of more significance is the juxtaposition of permeable sandstone against mudstone, as is implied to occur at fault block margins. This situation forms a major restriction to flow. However, mudstones buried to 5000m in other basins have a measurable lateral permeability in core (Coyner *et al.*, 1993). This may be reduced by deformation close to a fault (Gibson, 1994). It seems probable that over geological time, faults can allow fluid flow. Assumption of total hydraulic discontinuity across a fault is unjustified.

The argument presented above also applies to the lateral discontinuity of permeable Jurassic and Triassic sandstones in the region. Lateral grading of the Fulmar Fm. into silts of the Heather Fm. and depositional onlap onto sandy-siltstones of the Pentland Fm. (Donovan *et al.*, 1993) will form a restriction, but not an absolute barrier, to lateral fluid flow between cells.

Thus this study concurs with the view of Bredehoeft *et al.*, (1994), founded on physical hydrogeological principles, that "every rock material in the subsurface is permeable" and that the subsurface may be viewed as a hydraulically-continuous system for the wetting-phase fluid.

3.6.4 Pressure Seals in the Dynamic Model

The dynamic model of fluid flow presented above also allows insight into the detailed morphology of pressure-depth profiles. It was identified that rapid rises in formation pressure occur in the Kimmeridge Clay Fm, or at the top of the permeable sub-seal sandstone. The pattern of inter-cell and intra-cell fluid flow advanced in Section 3.6.2 allows a pattern to be imposed on the complex, small-scale pressure distribution.

Permeable Jurassic sandstones in structurally-elevated positions have been suggested to possess a hydraulic connection to deeper regions. Fluid flow from deep to shallow regions in the permeable sandstones increases pressure in the sandstones on the shallow structures. Thus pressure in the sandstone will be increased to levels in excess of the pressure in the overlying mudstones. Accordingly, wells on the crest of fault blocks in the Central Graben exhibit rapid rises in pressure at the top of the permeable sandstone. This situation is exhibited by wells 22/30a-1 (Fig 3.11), 29/10-2 (Fig 3.13), 22/27a-1 (Fig 3.15) and 30/1c-2 (Fig 3.19).

In contrast, sandstones in deep terraces that have the potential to "leak" fluid laterally up-dip exhibit lowered pressures in the sandstone. Wells drilled in this position encounter high pressure within the Kimmeridge Clay Fm (wells 29/5b-4, Fig 3.12; 29/5a-3, Fig 3.14; and 23/26a-7, Fig 3.17). Jurassic sandstones are at similar pressure to the overlying mudstones. Overpressures in the Kimmeridge Clay Fm. may be higher than overpressures in the underlying sandstone (e.g. well 29/5b-4, Fig 3.12). This distribution of fluid pressure suggests that vertical flow through the Kimmeridge Clay seal will be inhibited, and that lateral flow beneath the Kimmeridge Clay pressure seal is significant. High pressures within the Kimmeridge Clay Fm. may be attributed to the generation of gas (Cornford, 1994). This produces a large fluid volume increase (Ungerer *et al.*, 1981) and has been suggested to cause overpressuring in many basins world-wide (Hunt *et al.*, 1994; Spencer, 1987).

Thus the model of structurally-controlled flow in a hydraulically-continuous medium allows explanation of both the distribution of overpressure on a basin-scale (describing magnitude of pressure in pressure cells) and on a reservoir-scale (describing the distribution of pressure seals).

3.6.4 Pressure Seals in the Dynamic Model

The dynamic model of fluid flow presented above also allows insight into the detailed morphology of pressure-depth profiles. It was identified that rapid rises in formation pressure occur in the Kimmeridge Clay Fm, or at the top of the permeable sub-seal sandstone. The pattern of inter-cell and intra-cell fluid flow advanced in Section 3.6.2 allows a pattern to be imposed on the complex, small-scale pressure distribution.

Permeable Jurassic sandstones in structurally-elevated positions have been suggested to possess a hydraulic connection to deeper regions. Fluid flow from deep to shallow regions in the permeable sandstones increases pressure in the sandstones on the shallow structures. Thus pressure in the sandstone will be increased to levels in excess of the pressure in the overlying mudstones. Accordingly, wells on the crest of fault blocks in the Central Graben exhibit rapid rises in pressure at the top of the permeable sandstone. This situation is exhibited by wells 22/30a-1 (Fig 3.11), 29/10-2 (Fig 3.13), 22/27a-1 (Fig 3.15) and 30/1c-2 (Fig 3.19).

In contrast, sandstones in deep terraces that have the potential to "leak" fluid laterally up-dip exhibit lowered pressures in the sandstone. Wells drilled in this position encounter high pressure within the Kimmeridge Clay Fm (wells 29/5b-4, Fig 3.12; 29/5a-3, Fig 3.14; and 23/26a-7, Fig 3.17). Jurassic sandstones are at similar pressure to the overlying mudstones. Overpressures in the Kimmeridge Clay Fm. may be higher than overpressures in the underlying sandstone (e.g. well 29/5b-4, Fig 3.12). This distribution of fluid pressure suggests that vertical flow through the Kimmeridge Clay seal will be inhibited, and that lateral flow beneath the Kimmeridge Clay pressure seal is significant. High pressures within the Kimmeridge Clay Fm. may be attributed to the generation of gas (Cornford, 1994). This produces a large fluid volume increase (Ungerer *et al.*, 1981) and has been suggested to cause overpressuring in many basins world-wide (Hunt *et al.*, 1994; Spencer, 1987).

Thus the model of structurally-controlled flow in a hydraulically-continuous medium allows explanation of both the distribution of overpressure on a basin-scale (describing magnitude of pressure in pressure cells) and on a reservoir-scale (describing the distribution of pressure seals).

overlying shales. In addition to this pressure distribution, vertical fluid flow through the pressure seal is enhanced at this point due to the reduced seal thickness. Flow through the pressure seal due to hydraulic fracturing is implied. Thus it is suggested that this well has penetrated the leak point for the deepest, highly-overpressured region of the Graben.

(ii) 22/27a-1: a dynamically leaking seal

Well 22/27a-1 is drilled on the crest of a fault block on the southwest margin of the Central Graben. The well exhibits a similar pressure profile to well 22/30a-1. Pressures rise sharply in the permeable sub-seal Fulmar Fm (Fig. 3.15), and formation pressure approaches the LOT pressure. A short gas column is retained at the top of the Fulmar Fm. A longer gas column, evidenced by gas shows, is also found in the Flounder Fm. immediately above the pressure seal.

The structural position and high fluid pressure in the sandstone in this well suggests that it forms the Leak Point to a pressure cell on the western margin of the Graben. It is suggested that this distribution of hydrocarbons demonstrates dynamic migration through the pressure seal. The high pressures in the permeable Fulmar Fm., increased beyond the pressure of the surrounding shales due to lateral transmission of pressure from deeper in the Graben, enable the migrating hydrocarbons to exceed the entry pressure of the overlying Kimmeridge Clay.

(iii) 30/1c-2: a regional inter-cell Leak Point

The potentiometric map (Fig 3.26) of the region demonstrates the significance of the axial horst block penetrated by well 30/1c-2. The relatively shallow depth of the 30/1c-2 cell allows the cell to form a zone of low potential energy. The pressure in the permeable sandstone is elevated considerably above the pressure of the overlying pressure seal (Fig 3.19), and fluid pressures are close to LOT pressures. Despite the comparable depth to well 22/27a-1, this leak point is water-bearing and fluid pressure is close to the rock fracture point. Permeable zones in the Hod and Tor Fms demonstrate hydrocarbon shows.

By these criteria, this well is interpreted as a leak point. The potentiometric gradients have the potential to induce lateral fluid flow from the adjacent, deeper cells in the East Forties Basin and Central Graben. Vertical fluid flow through the pressure seal in this cell is favoured by the absence of Jurassic and Lower Cretaceous shales,

suggesting a higher permeability in the pressure seal. Unlike well 22/30a-1, pressure communication with deeper wells cannot be shown (Fig 3.20); adjacent terraces in the East Forties Basin are separated by a barrier supporting 2MPa of differential pressure (see Section 3.4.3). It is hypothesised that the seal between these pressure cells is essentially a transient restriction to fluid flow. Pressures in the sandstone are close to the minimum stress due to the proximity of the HPHT deep Graben cells.

3.6.7 Additional supportive evidence for the Dynamic Model

The observed distribution of pressure is elegantly interpreted by the "Leak Point" model. However, a consideration of pressure distribution can only describe the potential for fluid flow. It does not imply automatically that this fluid flow does occur. As discussed above, lateral permeability restrictions may mitigate against flow. Other facets of the basin hydrogeology can be examined for supporting evidence.

(i) Temperature

Movement of fluid in a sedimentary basin may alter the distribution of heat in the region (Garven & Freeze, 1984). The temperature pattern in the Central Graben has been examined by Andrews-Speed *et al* (1984) and Fleming (in prep.). Both these studies, summarised in Fig 3.28, have detected temperature and heat-flow anomalies in the Cretaceous Chalk above the axial horsts. Heat flow is calculated from the measured thermal conductivity of the sediments (measured from core chips), the sediment porosity (measured in conventional cores or estimated from empirical porosity-depth relationships), and borehole temperature measurements. Temperature measurements are subject to considerable errors due to the cooling effect of circulating mud, and so have been corrected. Andrews-Speed *et al* (1984) identified variation of heat flow with depth in the Central Graben; the authors suggested that this variation could not be attributed to high sedimentation rates or refraction by the structure of the Graben. Instead, the anomalous heat flow was attributed to advection by fluid movement at the present day or in the geologically-recent past. Andrews-Speed *et al* (1984) discounted compaction-driven flow due to the extremely low fluid velocities normally inferred for this fluid-flow mechanism, and preferred advection due to topographic drive or thermal convection.

The analysis of the overpressure distribution presented above provides a third mechanism for this fluid flow. Vertical fluid flow through the pressure seal above the Forties-Montrose High has been suggested by the distribution of overpressure. The dynamic, episodic nature of pressure-driven fluid flow (where large volumes of fluid may be expelled rapidly along pressure-induced fractures) may account for the magnitude of the temperature anomalies. The distribution of heat flow with depth in well 30/2-1 on the central section of the axial horst (Andrews-Speed *et al.*, 1984), where the horst is adjacent to highly overpressured regions of the Graben is strongly suggestive of vertical fluid flow. The anomalies are absent in areas where the underlying strata are less overpressured, in the south of the study area.

(ii) Gas Chimneys

The distribution of hydrocarbons is an indicator of basinal fluid flow processes, as the secondary migration of hydrocarbons will be affected by the potentiometric gradients of overpressure. Vertical migration through the pressure seal is suggested by hydrocarbon shows in wells 22/27a-1 and 30/1c-2. Gas chimneys have been observed on seismic in the Chalk over eroded, structurally-elevated Jurassic fault blocks in the Western Central Graben, and over the "Puffin" Horst in Block 29/10 (Cayley, 1987; Cayley *et al.*, in press; Symington *et al.*, 1994). This is interpreted as being indicative of dynamic vertical leakage of hydrocarbons from Leak Points.

3.6.8 The role of Zechstein Salt

The discussion of vertical and lateral flow presented above has identified the pre-Cretaceous rift structure of the Central Graben as a major control on the distribution of overpressure. The role of the Zechstein salt that underlies much of the Central Graben is inextricably linked to the role of structure. Halokinesis has controlled the deposition and preservation of Jurassic and Triassic sands (Roberts *et al* 1990). A halokinetic control is implied for the morphology of the fault blocks in the region (Roberts *et al* 1990). Salt diapirism has maintained Jurassic sandstones (and thus pressure cells) in structurally-elevated positions. Fracturing on the flanks and crests of diapirs in the East Forties Basin has been identified as a control on fluid flow (Cornford 1994). Accordingly, halokinesis is suggested to exert a control on the fluid flow patterns in the Central Graben. By controlling the structural position of pressure cells and the geometry of the Jurassic sandstones, salt may influence the siting of leak points.

3.7 Implications for Hydrocarbon Migration and Entrapment

The Fulmar Fm. in Leak Point wells 22/30a-1 and 29/10-2 is water-bearing at the present day. The presence of bitumen (up to 20% of the rock volume) in the reservoirs suggests that these wells were hydrocarbon-bearing in the past (see Section 6.3). Hydrocarbon distribution in wells 30/1c-2 and 22/27a-1 is described in Section 3.6.6; these were interpreted as dynamically-leaking traps. Wells 29/5b-4 (the Franklin field) 29/5a-3 (the Puffin field), 23/26a-3, 23/26a-7 (the Erskine-Machar fields) and 22/24a-1 (the Marnock field) contain gas condensate. It is hypothesised that the pressure regime of the Graben influences the entrapment of hydrocarbons.

When hydrocarbon distribution is plotted on a pressure-depth plot of the study wells (Fig 3.29), it can be seen that Leak Points are water-bearing, or contain short gas columns which are implied to be dynamically leaking. Sandstones with the potential to transfer pressure laterally towards a neighbouring leak point are hydrocarbon-bearing. Leak Points, with higher pressures in the sub-seal sandstones than in the seal itself, form an unfavourable trapping configuration. Additionally, seal failure by hydraulic fracturing, which is implied to preferentially occur at Leak Points, will also mitigate against retention of hydrocarbons.

In contrast, it is suggested that the high pressures in the Kimmeridge Clay Formation overlying the Fulmar Fm in lateral-flow cells forms a highly efficient seal to vertical leakage of hydrocarbons. The low permeability of the caprocks to hydrocarbon accumulations requires that migrating hydrocarbons must overcome a capillary entry pressure (a positive pressure differential between reservoir and seal) to flow through the caprock. If pressures in the Kimmeridge Clay Fm are greater than pressures in the reservoir, as occurs in lateral-flow cells, flow cannot occur. The composite model for hydrocarbon entrapment in an HPHT cell is shown in Fig 3.30.

The buoyant pressure of a long gas column trapped in a laterally-leaking cell may complicate the model presented above. Pressures in the Kimmeridge Clay Fm. are in excess of water-leg pressures in the reservoir by 5-7 MPa (well 29/5b-4, Fig 3.12). If the additional buoyancy pressure of gas can increase pressures at top reservoir to beyond this pressure differential, the seal will fail. Some hydrocarbons will escape vertically, lowering the buoyancy pressure of the gas column and allowing re-

establishment of seal integrity (Fig 3.31). If the reservoir can be replenished by continued migration of gas from source rocks, the system will oscillate around a dynamic equilibrium (Holm, in press).

The buoyancy pressure of hydrocarbons is of additional importance if the Kimmeridge Clay Fm. is locally absent from the crests of fault blocks (Roberts *et al* 1990). If there is no pressure impedance to vertical flow by the Kimmeridge Clay, buoyancy effects may lead to remigration of hydrocarbons *despite* the possibility of lateral leakage of pressure to higher positions in the pressure cell.

3.8 Summary

Overpressure in the Central North Sea is primarily controlled by structure. The influence of the structure of the region extends from the basin-scale to the scale of individual reservoirs. It controls the magnitude and distribution of overpressure, and the location of pressure seals (Fig 3.32).

A regional aquitard is formed by Cretaceous chinks and Cretaceous-Jurassic shales. In the north of the study area, the basin-wide permeable sheet of the Palaeocene sandstones overlying the aquitard drains the basin, remaining hydro pressured and allowing the Cretaceous Chalk to dewater freely. To the south of the region, this aquifer becomes thin and over pressured, leading to overpressure in the upper Chalk.

Below the regional aquitard, extremely high over pressures are developed in deep Jurassic and Triassic sandstones. These strata are divided into pressure cells.. Pressure cells on the crests of the axial horsts exhibit extreme over pressures in permeable sandstones. The magnitude of fluid pressure is close to the minimum stress. The sandstones are at much higher overpressure than the overlying mudstones. In contrast, sandstones in deeper cells, on the flanks of the axial horsts, exhibit sandstone fluid over pressures significantly less than the minimum stress. Sandstone pressures in these cells are less than or equal to over pressures in overlying mudstones.

High pressures in sandstones in structurally-elevated positions can be attributed to hydraulic communication with deeper regions. Fluid flow between deep regions and elevated regions has increased pressure in the shallow structures. In contrast, the deeper cells have lowered pressures in the permeable sandstones due to lateral leakage. These cells exhibit high pressures in the Kimmeridge Clay Fm., which

forms the upper pressure seal to the deep pressure cells. The highly overpressured horsts are termed "Leak Points", as vertical fluid flow at these points is facilitated by the relative thinness of the regional aquitard and the possibility of hydraulic fracturing of the aquitard. The recent existence of such vertical flow is independently evidenced by temperature anomalies.

The hydrogeology of the Central Graben is a dynamic system; the basin seeks to re-equilibrate at a stable low-energy state. Re-equilibration occurs by fluid flow. This dynamic model of fluid flow accounts for overpressure and hydrocarbon distribution in the region (Fig 3.32).

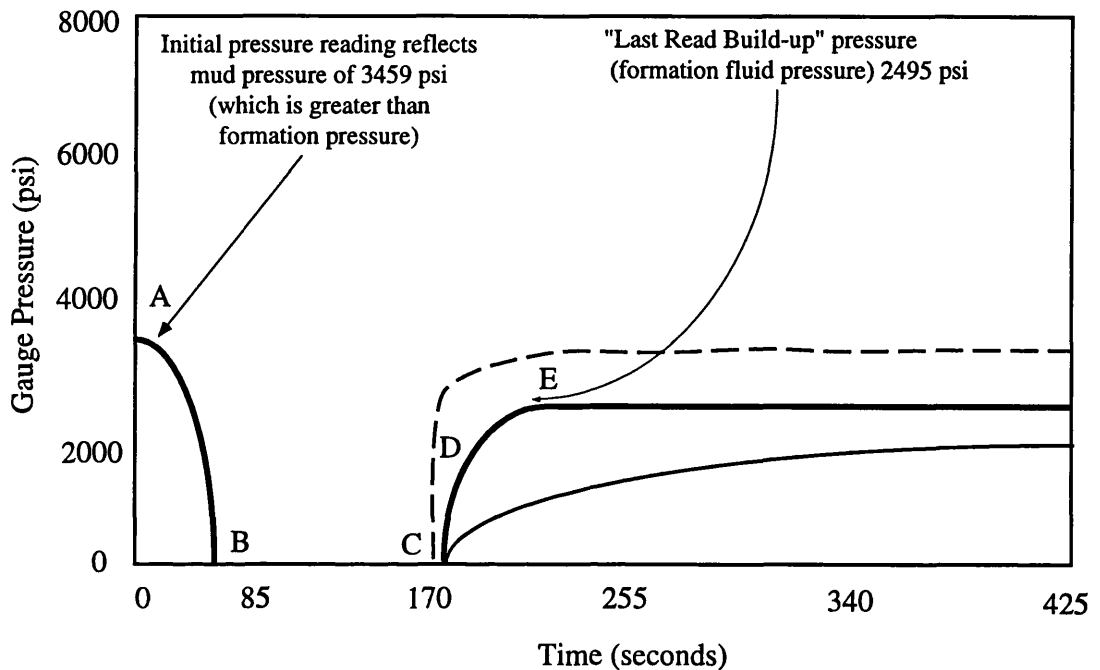


Figure 3.1 Example Repeat-Formation Test Logs

The **bold line** demonstrates a typical log for a valid RFT. The initial pressure recorded as the RFT chamber is opened (A) reflects the pressure of the drilling mud, which may be considerably greater than the formation pressure. The chamber is voided (B) by being forced against the formation, and then re-opened and fluid from the formation is allowed to fill the chamber (C). This results in a build-up of pressure in the chamber (D), which is considered complete when a steady-state is achieved (E).

Problems can occur if drilling mud is not completely voided from the chamber (dotted line) due to an imperfect contact between chamber and formation. This results in an artificially high formation pressure, and is termed "supercharging".

A second problem occurs in low-permeability formations where the rate of flow from the formation into the chamber is very slow, and the test is stopped before the pressure in the chamber reflects the true formation pressure (thin line). This is indicated by the failure of the log to show a steady-state.

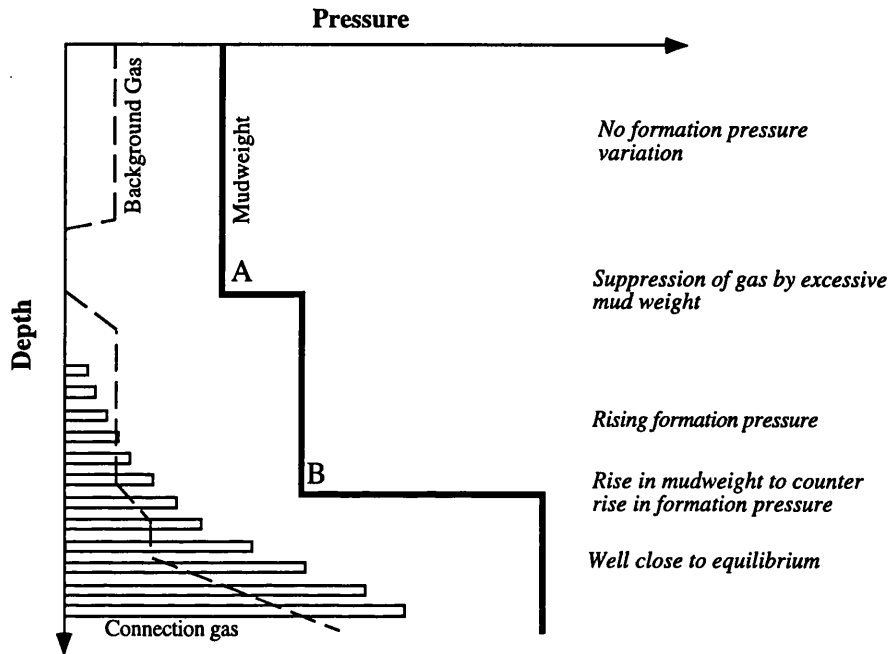


Figure 3.2 Use of gas levels and mudweight as qualitative pressure interpretation

Mudweight is always in excess of formation pressure, except when a kick or blow-out occurs. Thus the well should have a positive pressure differential between the borehole and the formation being drilled. The levels of gas present in the borehole reflect this pressure differential: where mudweight is greatly in excess of formation pressure, all gas is suppressed and retained in the formation; as formation pressure increases, gas levels may increase.

This allows recognition of conditions where mudweight has been raised as a pre-emptive precaution (A) and where mudweight has been raised to counter rising gas levels (B).

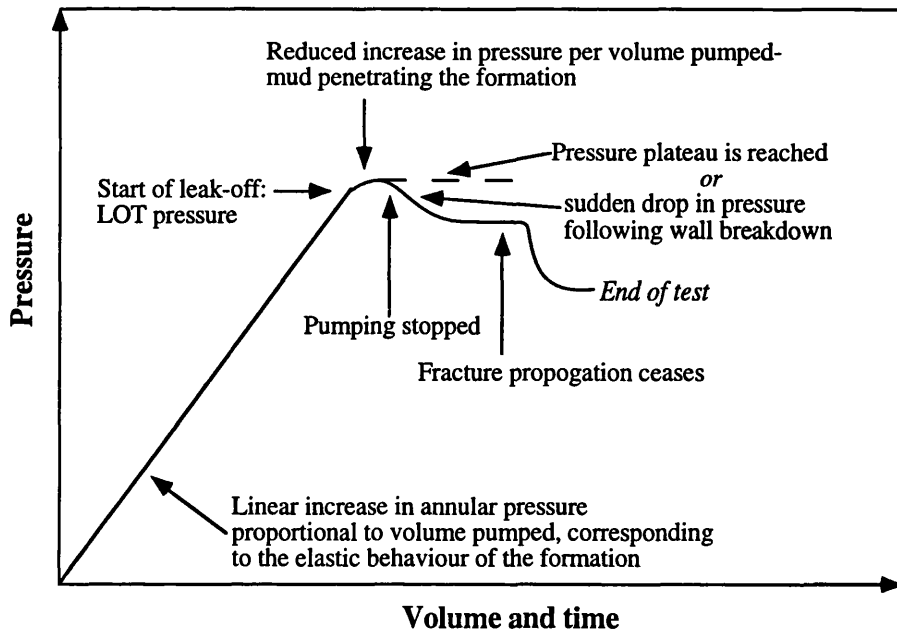


Figure 3.3a Typical Leak Off Test profile (after Mouchet & Mitchell 1989)

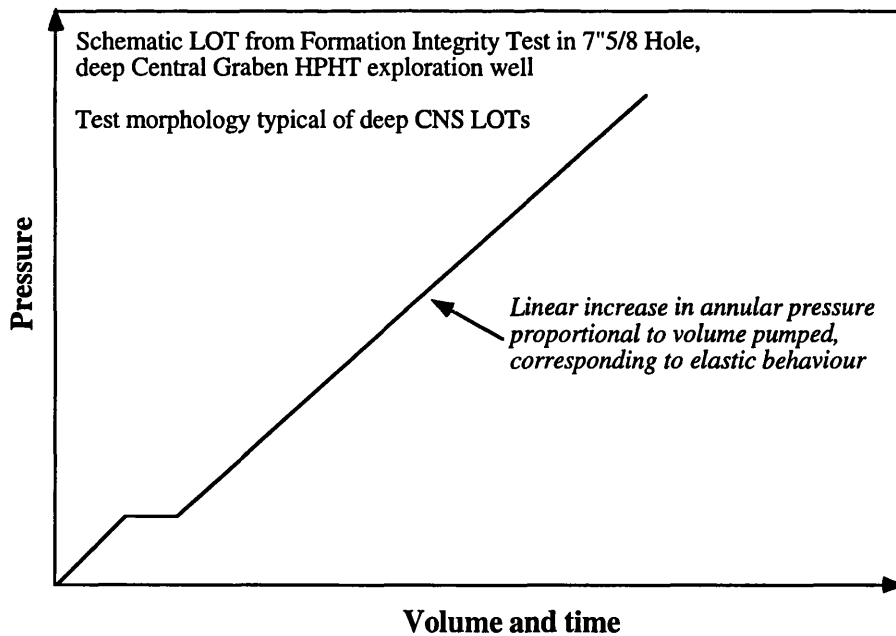


Figure 3.3b Central North Sea LOTs in Lower Cretaceous and Jurassic shales show a non-standard test profile, without any clear pressure plateau. The formation being tested may be undergoing elastic deformation without loss of mud to the formation.

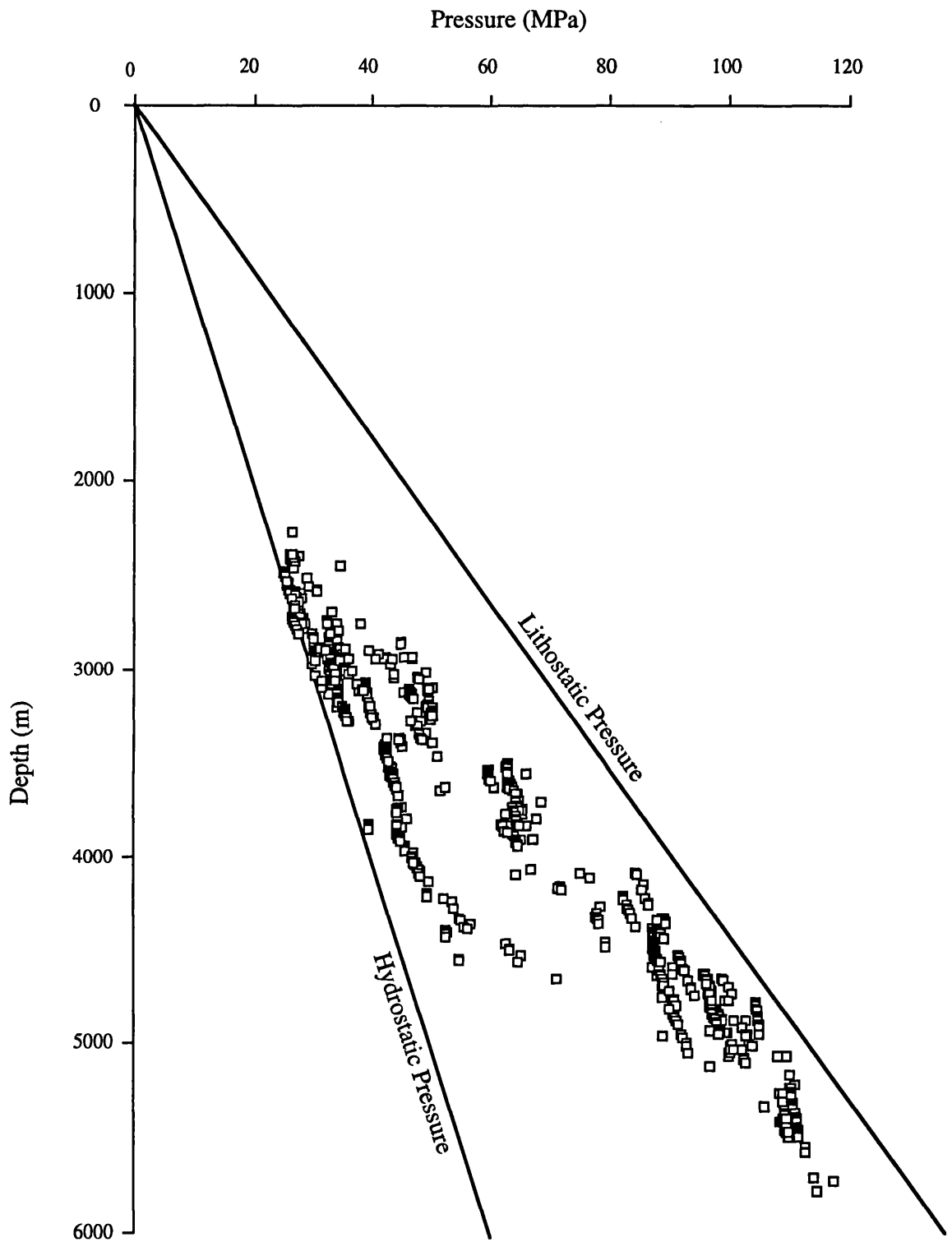


Figure 3.4 Regional RFT pressure-depth plot

Overpressure is recorded from 2500-3000m to a maximum drilled depth of 6000m. However, there is no simple relationship between magnitude of overpressure and depth: at 4500m depth, formation pressure may be close to hydrostatic pressure or close to lithostatic pressure. Numerous pressure gradients parallel to the hydrostatic pressure gradient can be defined, suggesting the presence of pressure cells and the compartmentalisation of the basin fluids.

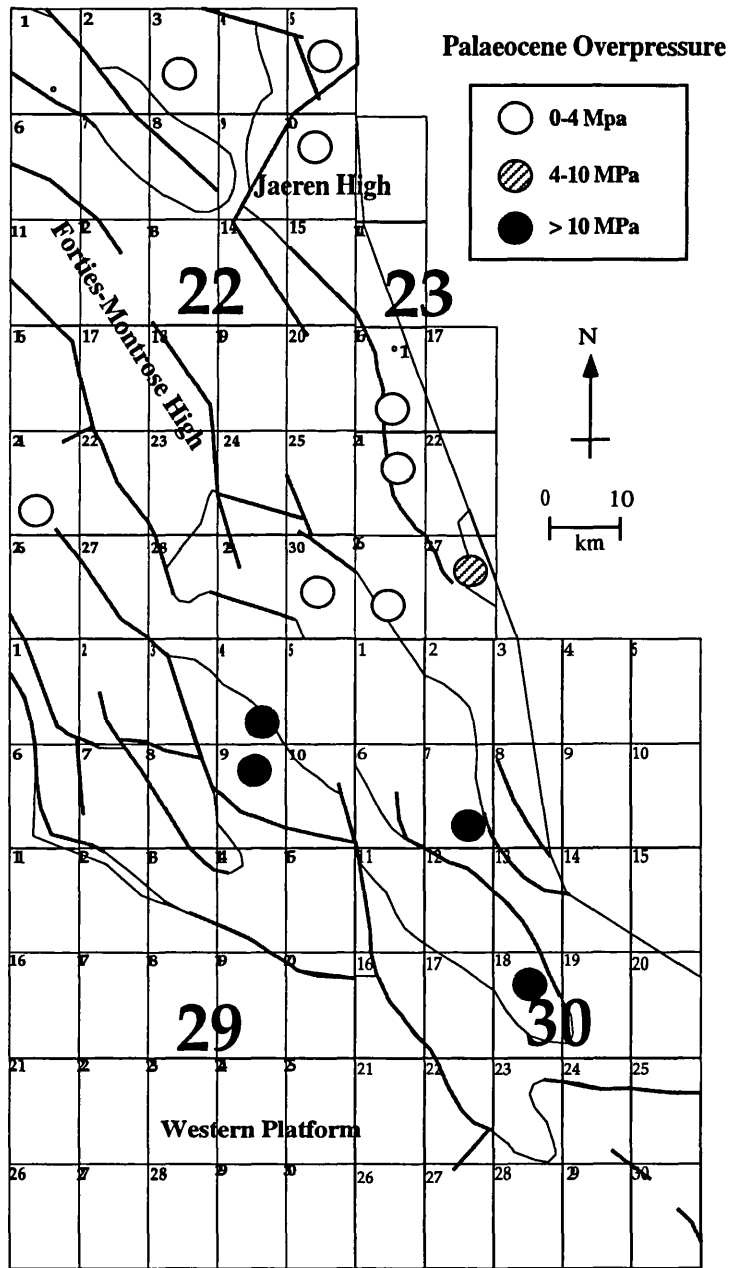


Figure 3.5 Map of distribution of pressure in Palaeocene sandstones in the Central Graben. Overpressure increases southwards and eastwards as the Palaeocene submarine fan sandstones become thinner and discontinuous.

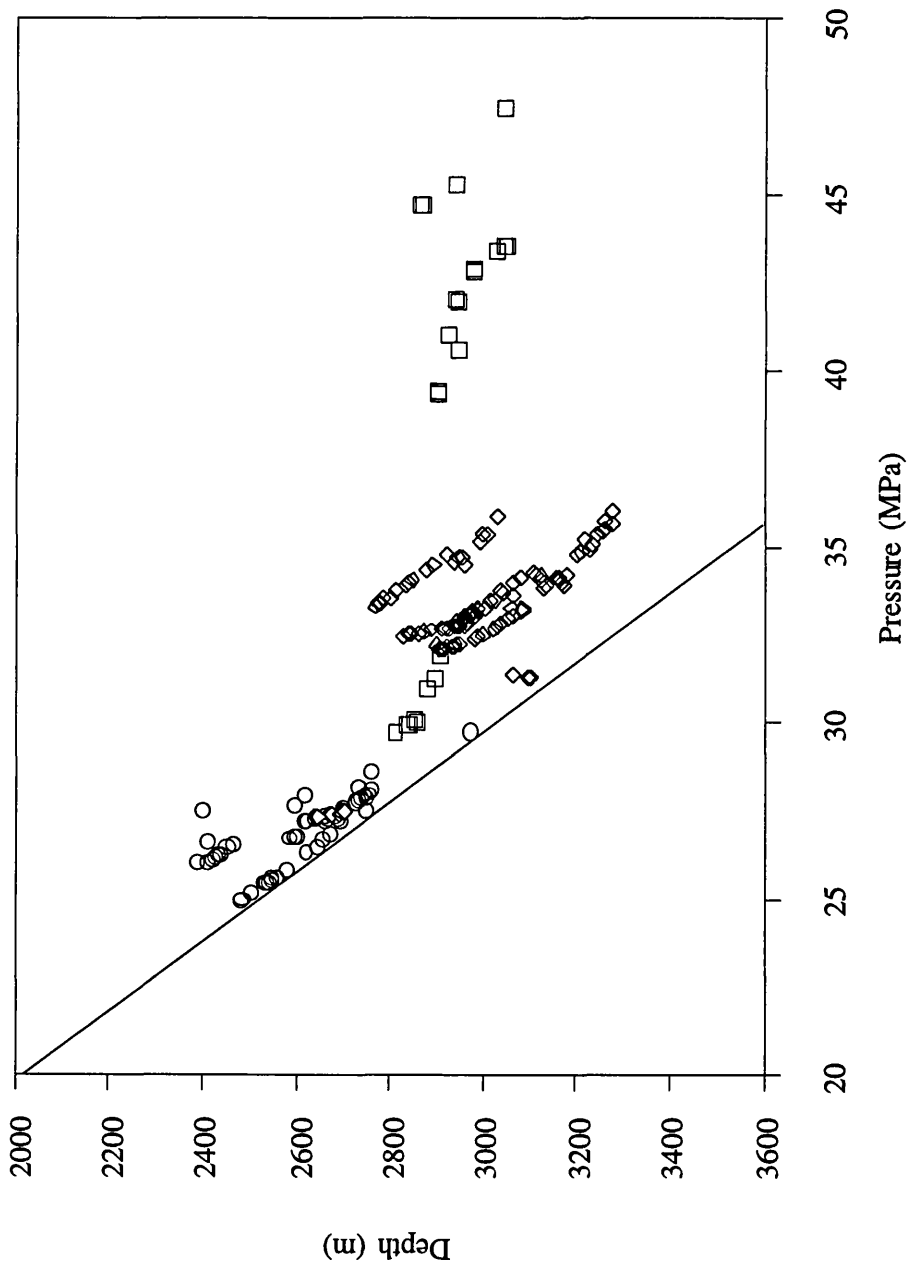


Figure 3.6 Palaeocene RFT pressure-depth plot. Pressures in Palaeocene sandstones are close to hydrostatic pressure in the north of the study area, but become increasingly overpressured in the south and east as the Palaeocene submarine fans become thinner and discontinuous.

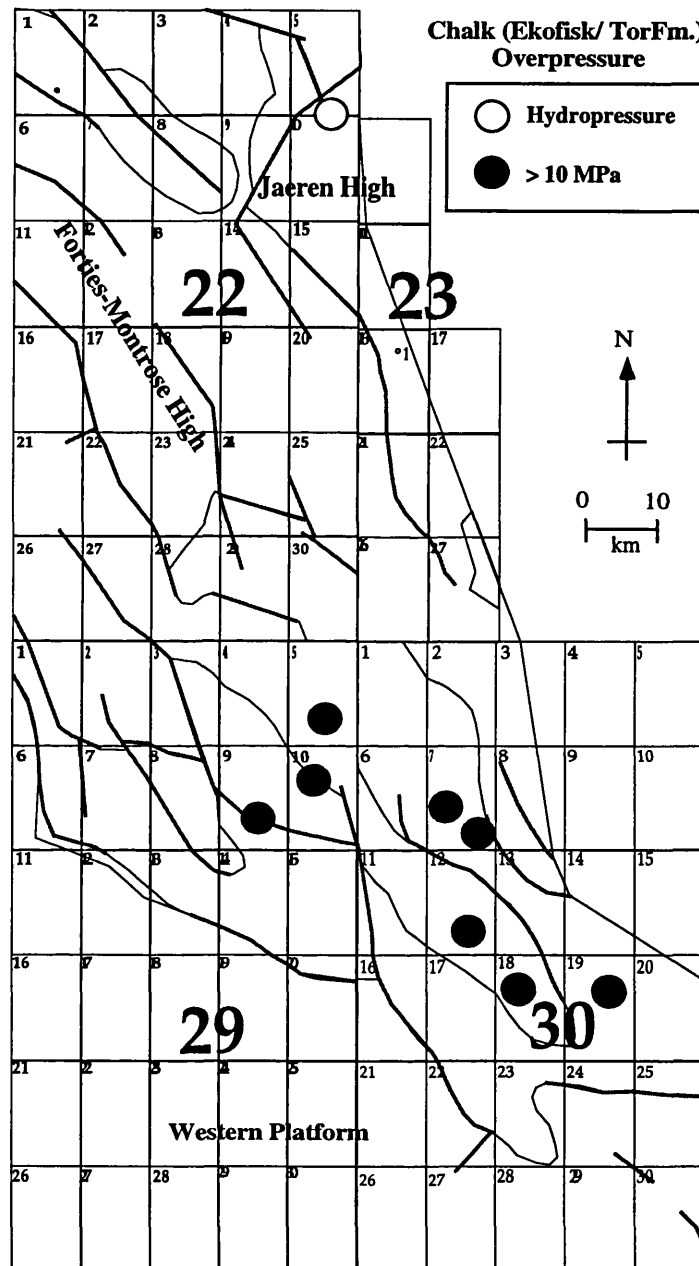


Figure 3.7 Map of distribution of pressure in the Cretaceous Chalk. Although data is scarce, a trend of increasing overpressure towards the south of the study area may be noted. This relates to the distribution of the overlying Palaeocene sandstones, which drain the upper Chalk Group. Where the sandstones are thin, discontinuous and overpressured, fluid flow is restricted in the upper Chalk, which becomes overpressured.

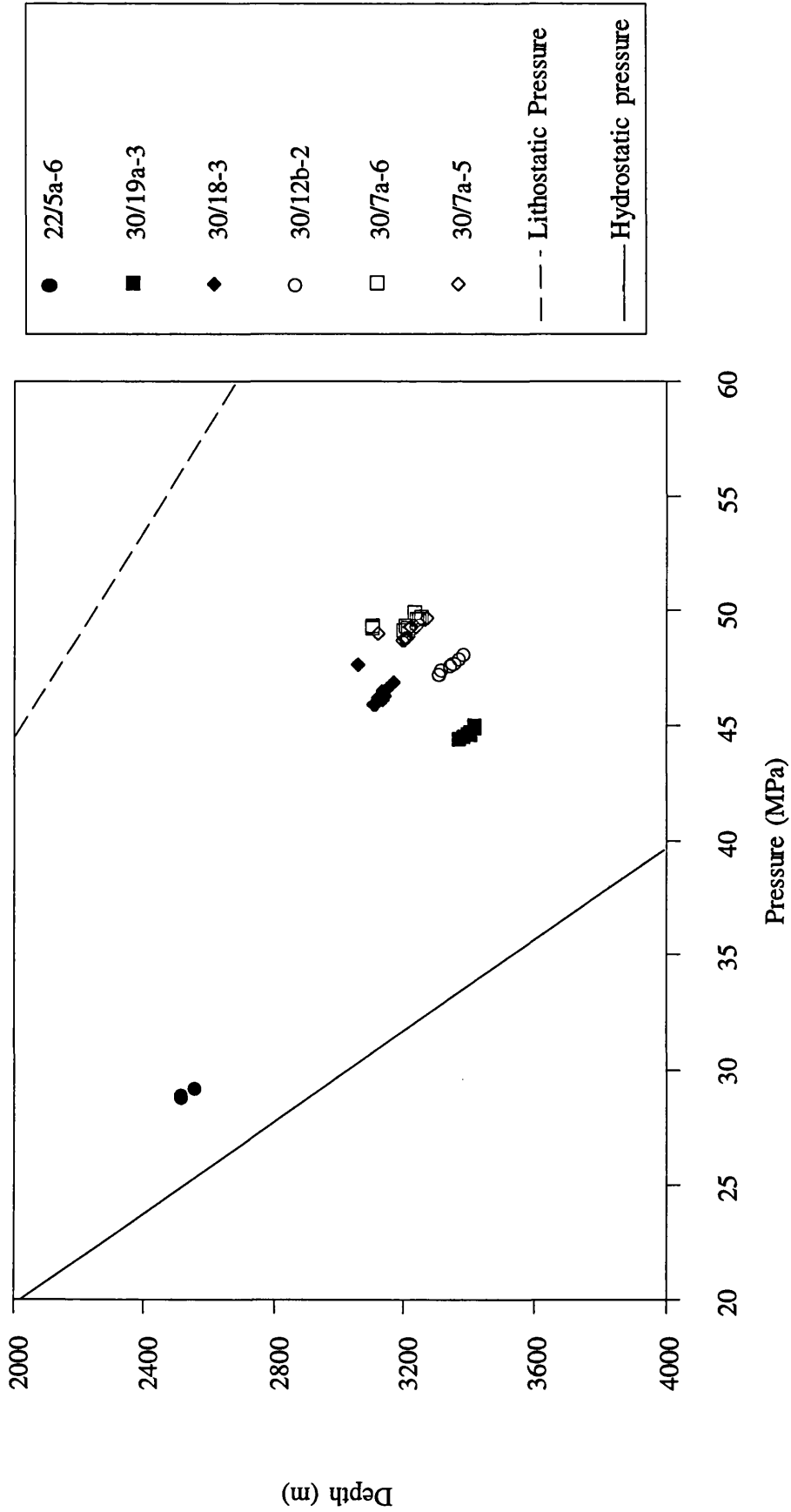


Figure 3.8 Cretaceous Chalk RFT pressure-depth plot

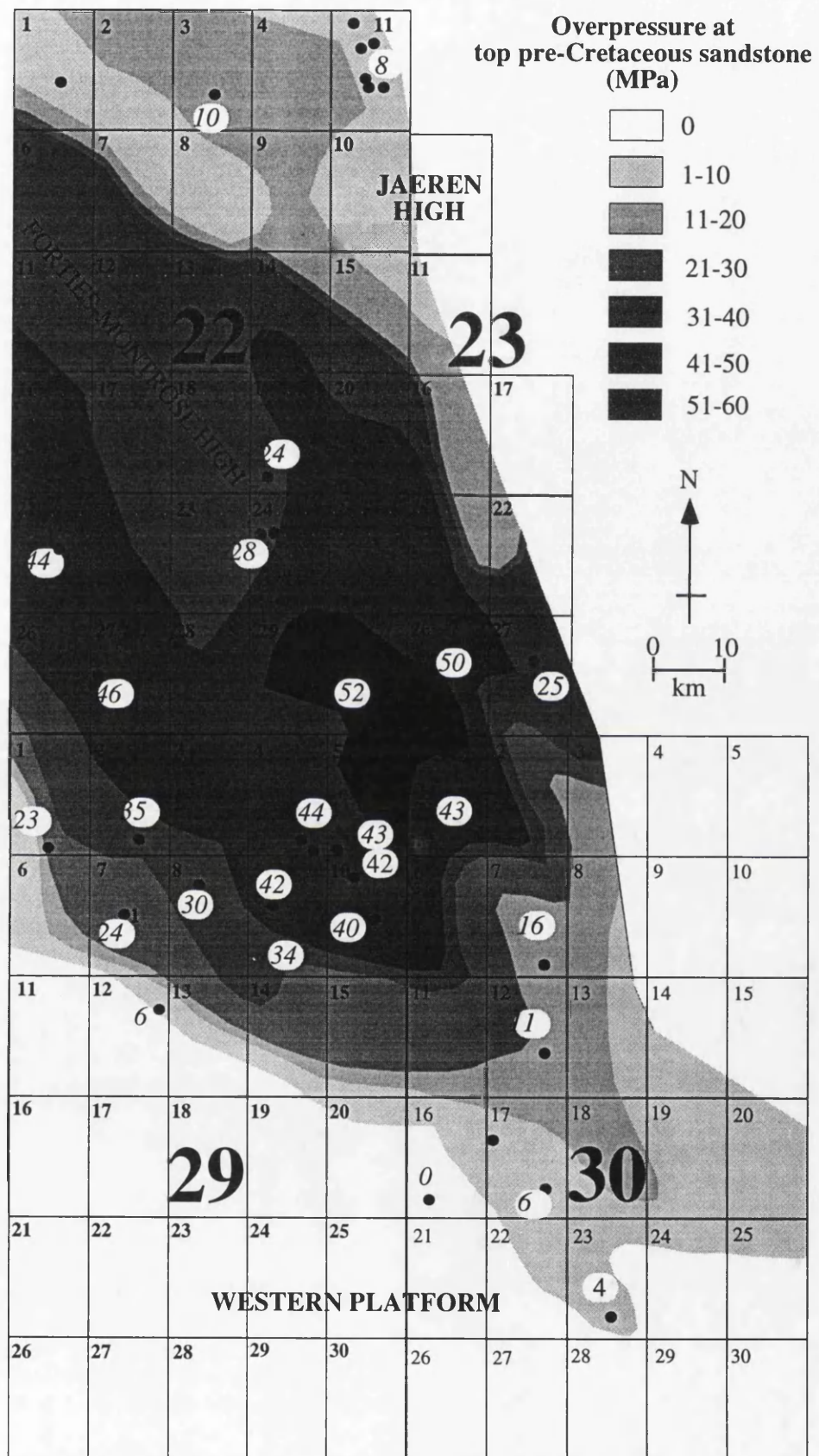


Figure 3.9 Overpressure in Jurassic and Triassic sandstones in the Central Graben. Overpressure shows a concentric pattern, following the Graben structure. Block number is noted; italic numbers denote magnitude of overpressure in adjacent wells.

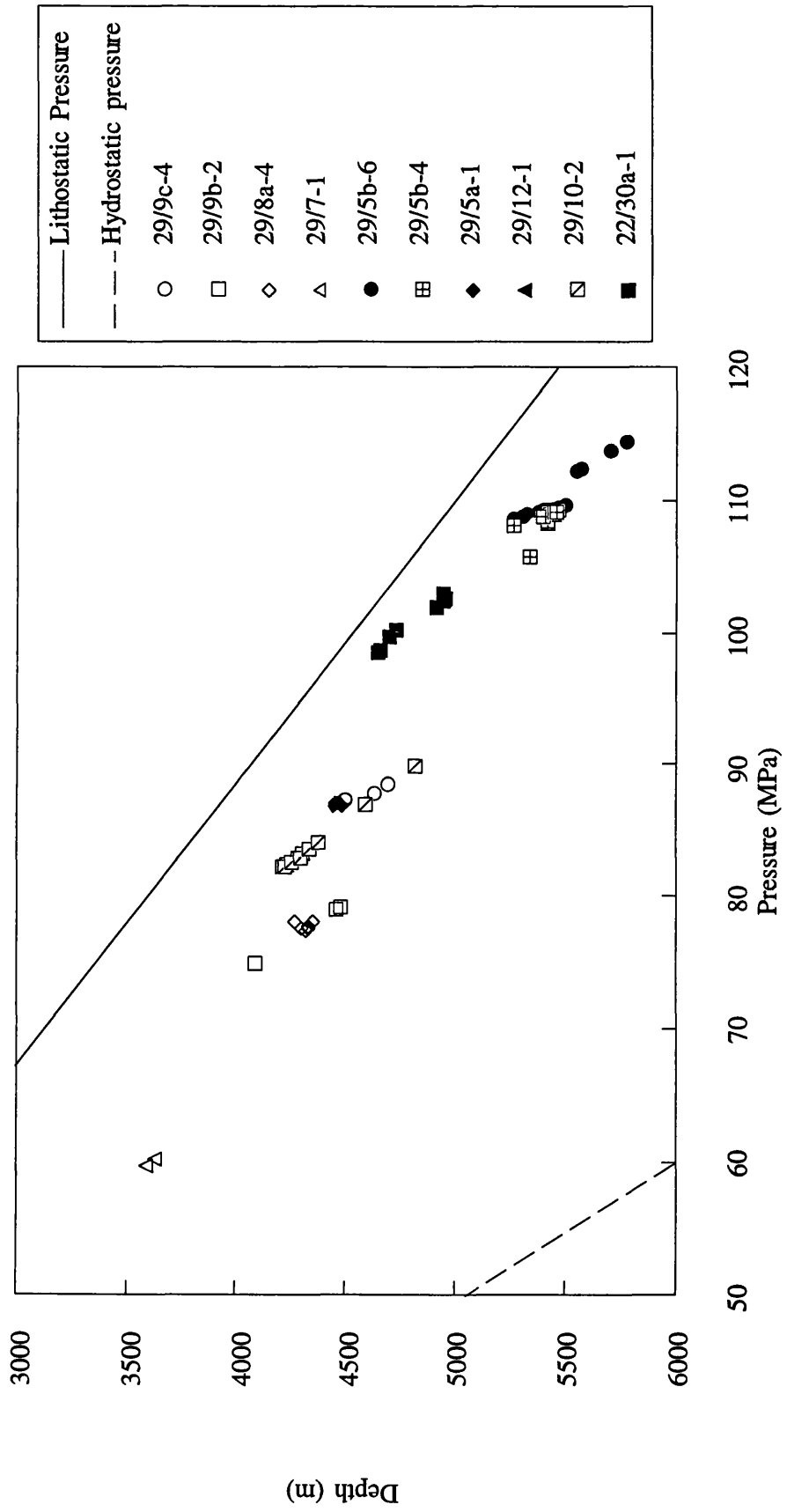


Figure 3.10 Overpressure in Jurassic and Triassic sandstones in the Central Graben. The presence of distinct pressure gradients that parallel the hydrostatic pressure gradient suggest the compartmentalisation of the region into pressure cells.

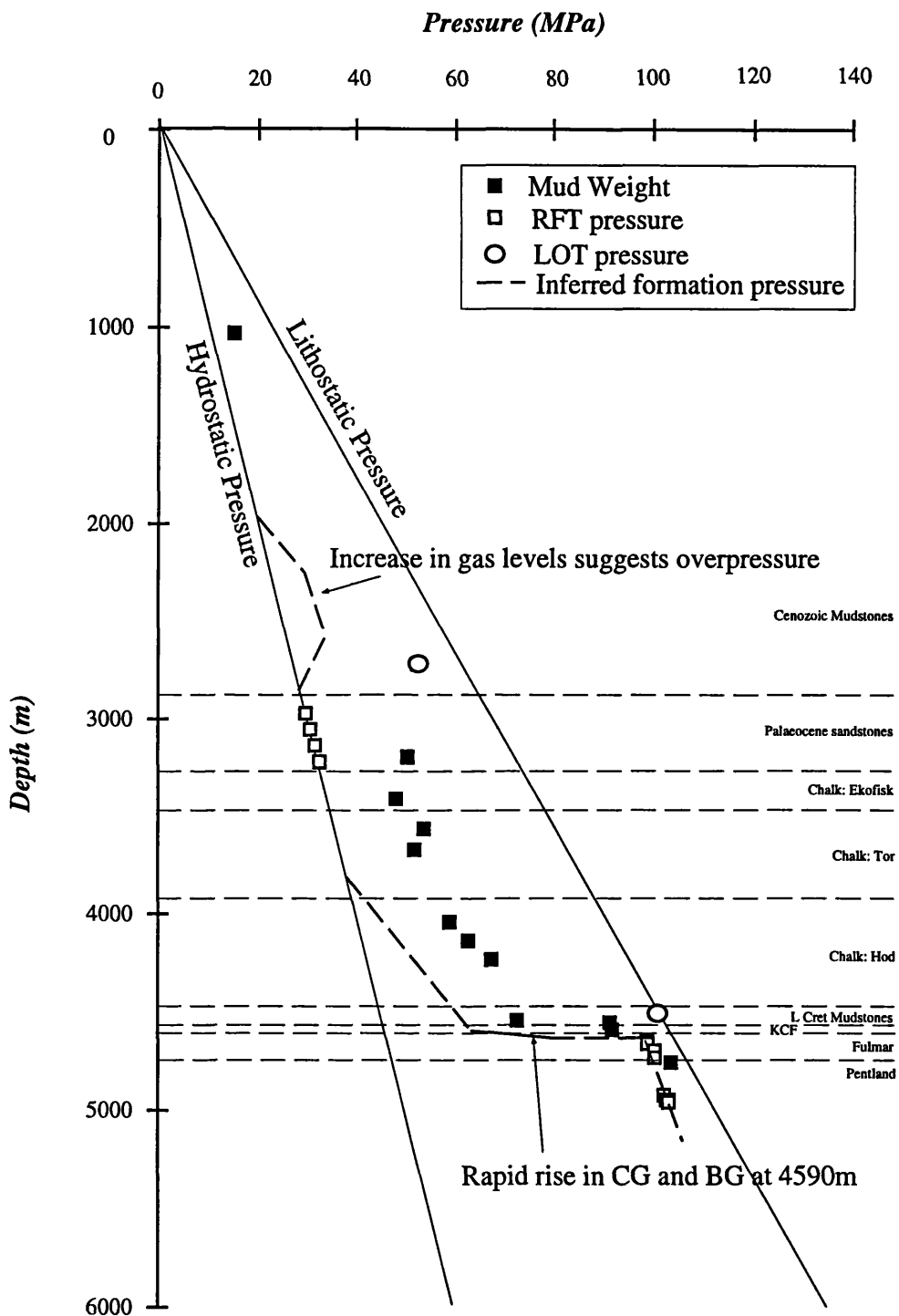


Figure 3.11 Pressures in well 22/30a-1. Gas levels suggest overpressure in the base of the Cenozoic mudstones and in the argillaceous base of the Cretaceous Chalk Group. A sharp rise in pressure occurs at the top of the Fulmar sandstone. In the pre-Cretaceous sandstones a constant pressure gradient is observed.

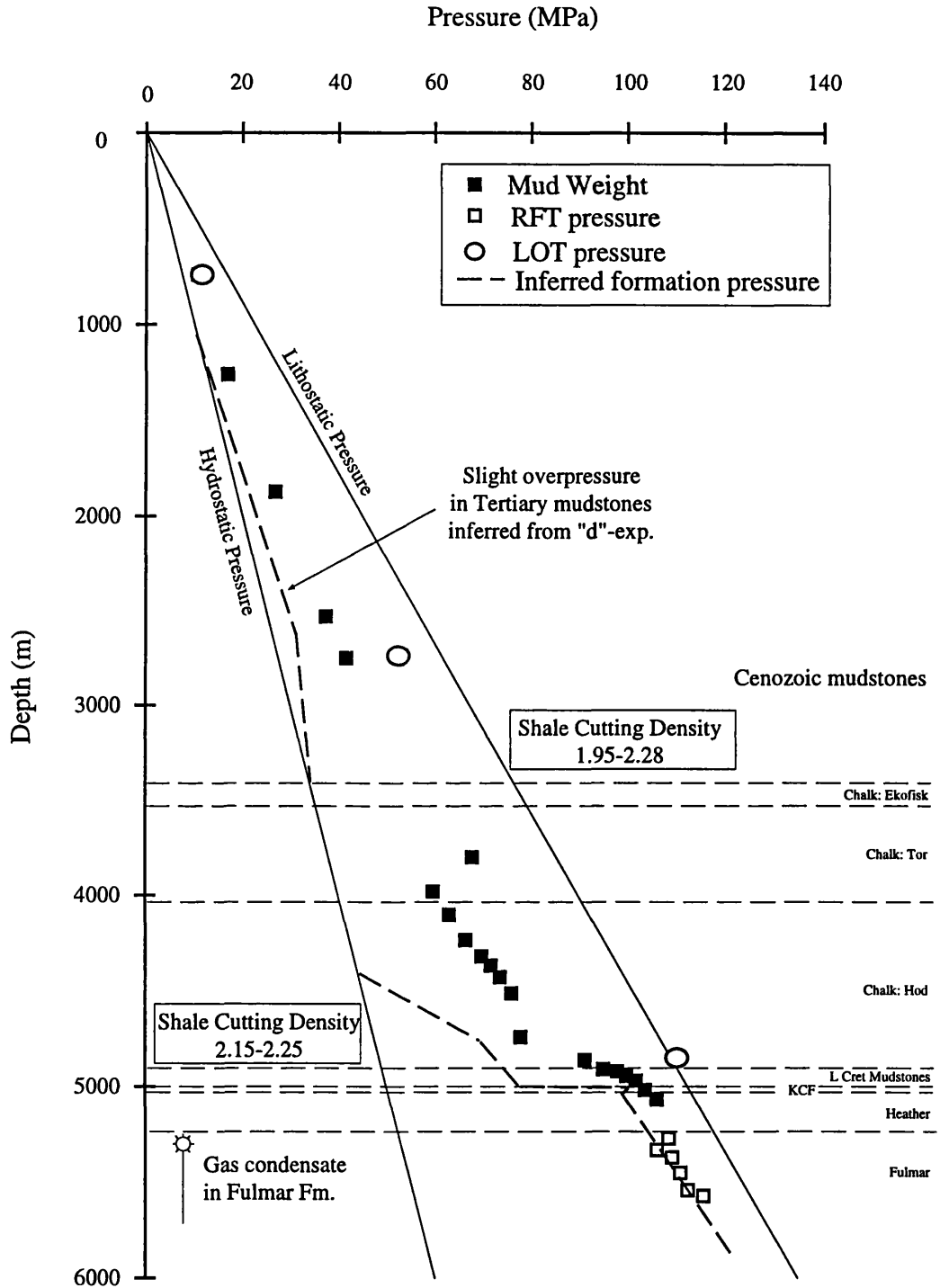


Figure 3.12 Pressures in well 29/5b-4. Pressure increases through base Chalk and L. Cret. mudstones, and reaches a maximum at top KCF. Pressure decreases slightly at base KCF, and is constant throughout the Jurassic pressure cell. Pressure is inferred from gas levels and drilling reports.

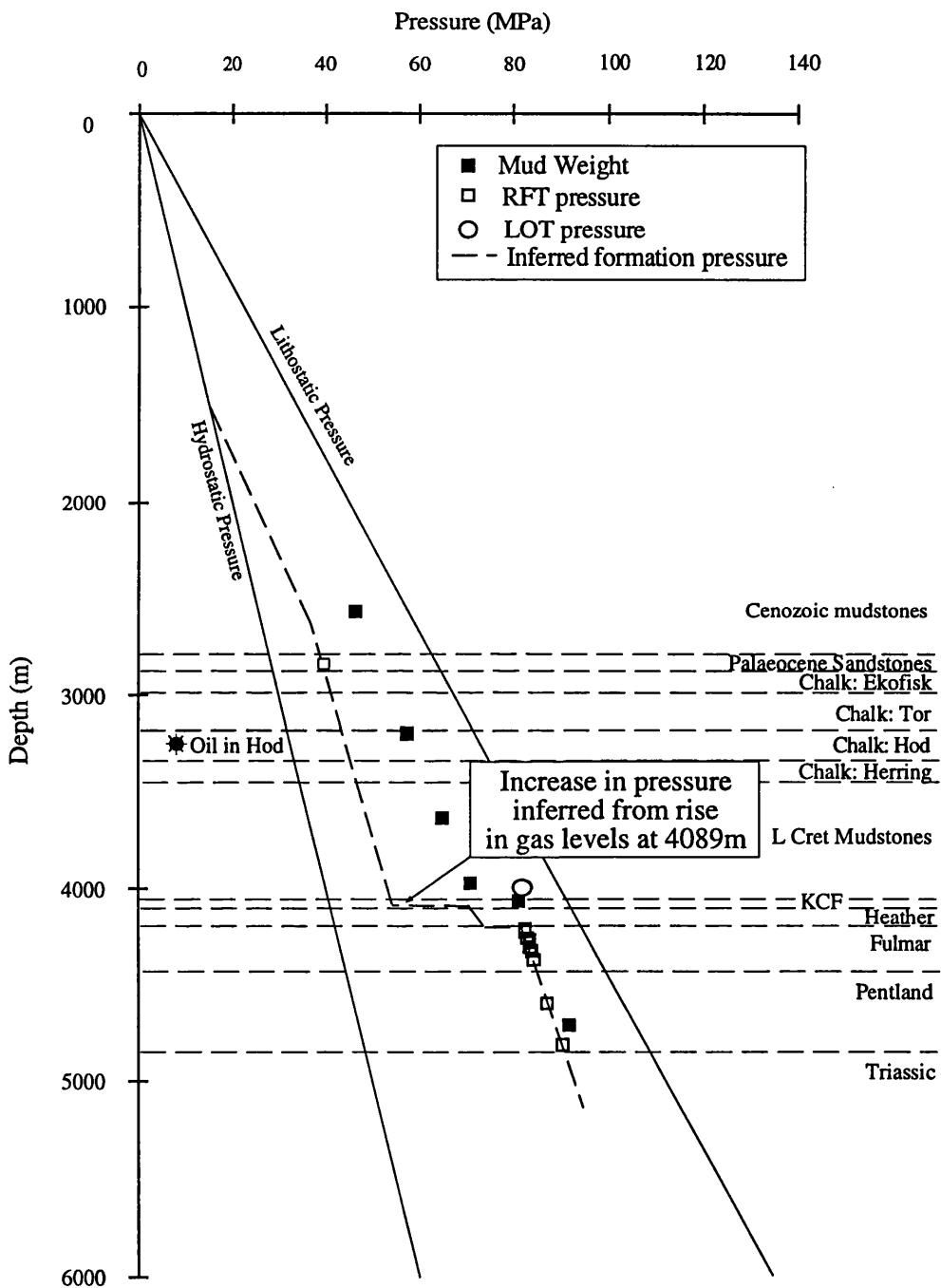


Figure 3.13

Pressures in well 29/10-2.

The thin Palaeocene sandstones in this well are overpressured, and overpressure is inferred from gas levels in the Chalk Group. A sharp increase in pressure occurs in the KCF and at the top of the Fulmar Fm. Pressure is constant through the Jurassic and Triassic sandstones.

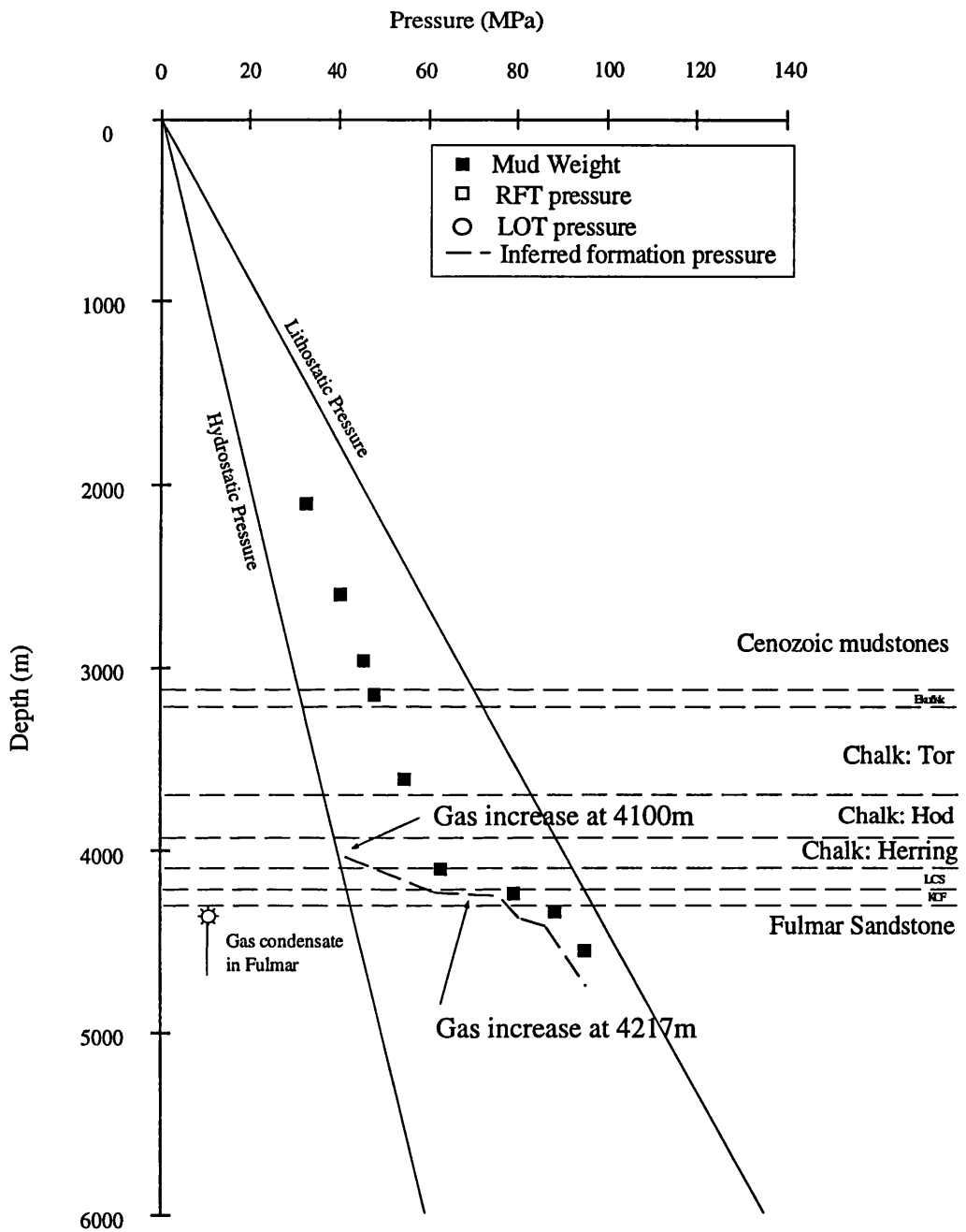


Figure 3.14 Pressures in well 29/5a-3. Pressures demonstrate a sharp increase in the KCF. The upper Fulmar sandstone is at approximately the same overpressure as the KCF. However, the Fulmar Fm. contains intraformational seals which give rise to rapid rises in pressure in the gas-condensate reservoir.

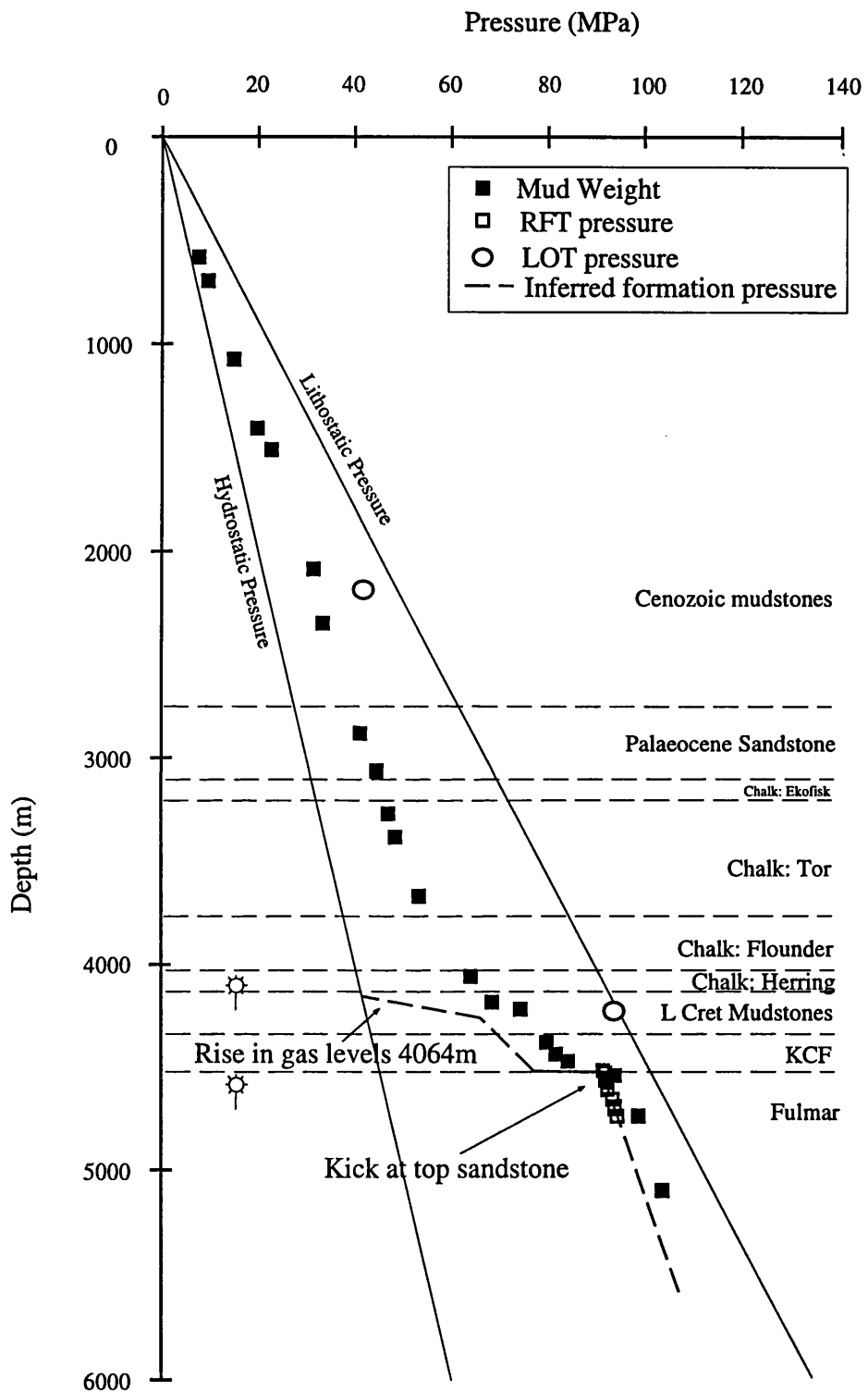


Figure 3.15 Pressures in well 22/27a-1. This well is sited on the crest of a fault block in the western arm of the Graben. Pressure begins to rise in the muddy base of the Chalk Group. The well demonstrates a sharp rise in pressure at the top of the Fulmar Fm. The Jurassic sandstones are highly overpressured and pressures approach the minimum stress. The Jurassic sandstones are at higher pressure than the overlying mudstones.

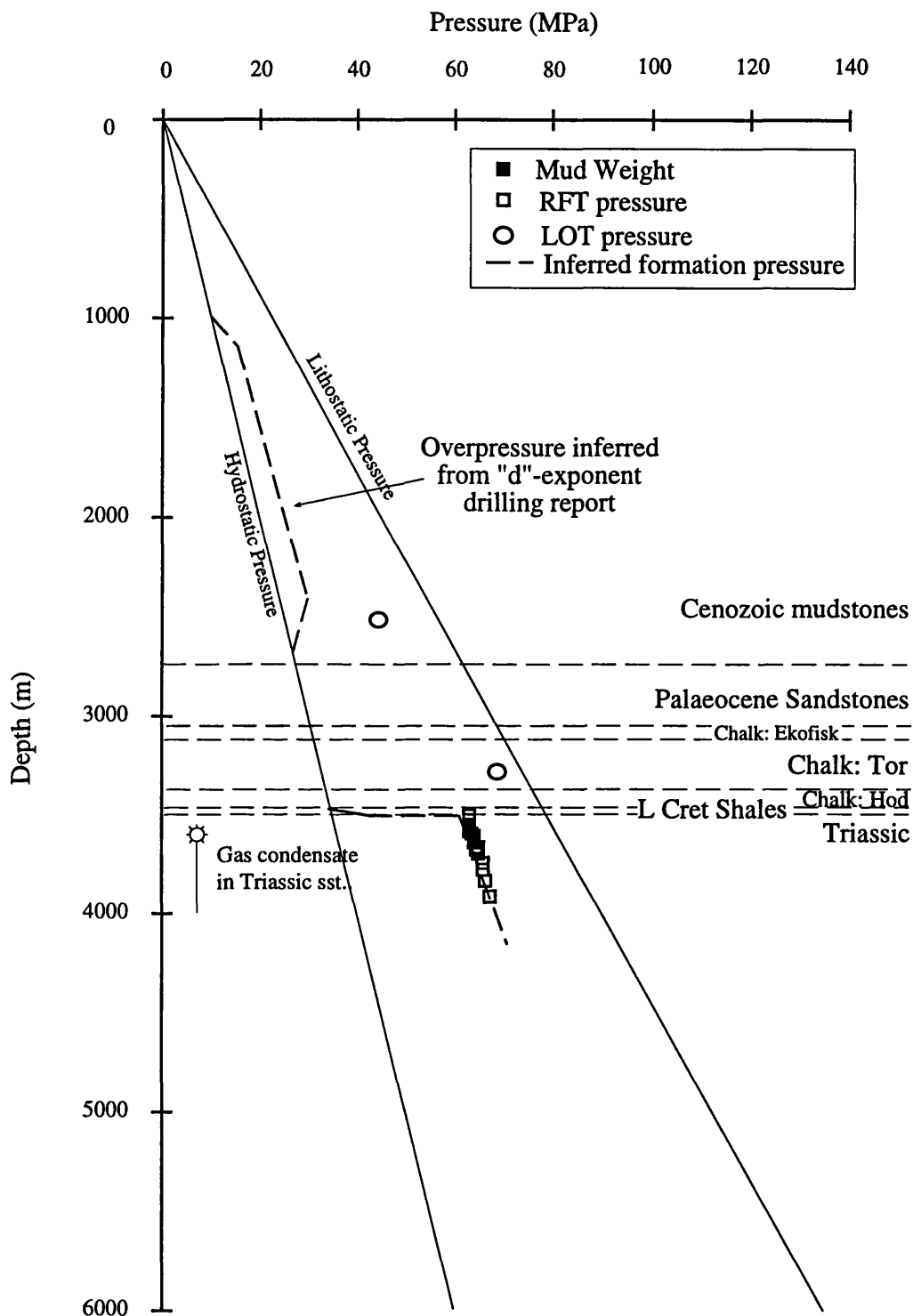


Figure 3.16 Pressures in well 22/24a-1
 Slight overpressure is inferred for the base of the Tertiary shales. The Chalk Group and the Lower Cretaceous are extremely thin in this well on the Forties-Montrose High due to erosion (Roberts *et al* 1990); nevertheless high overpressures are observed in the Triassic sandstone.

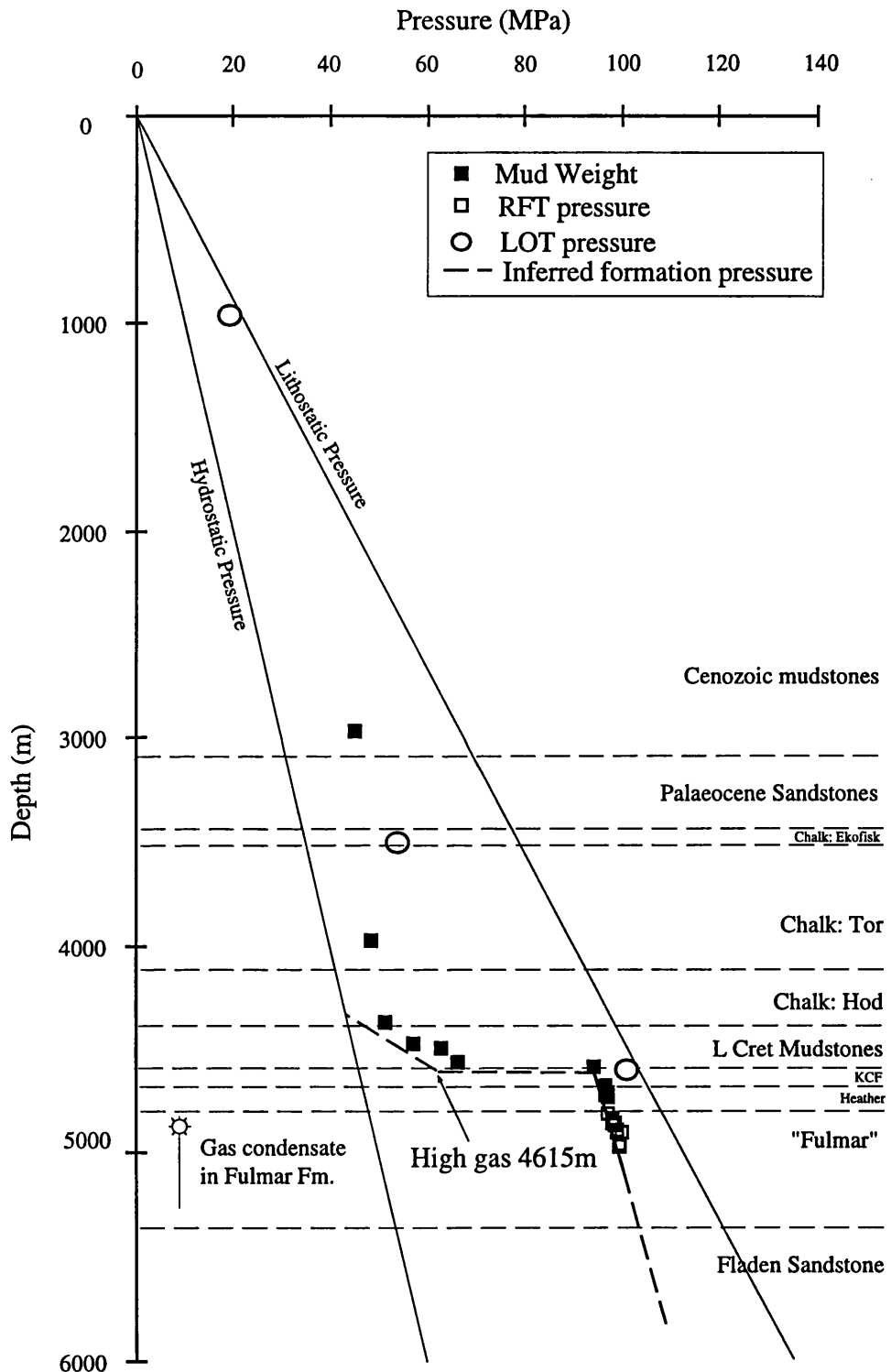


Figure 3.17

Pressures in well 23/26a-7.

A sharp rise in pressure is recorded in the KCF, with the well close to equilibrium and mudweight near to the fracture pressure, leading to a hazardous and difficult drilling situation. Overpressure remains constant through the Jurassic sandstones. Pressure inferred from drilling report and gas levels.

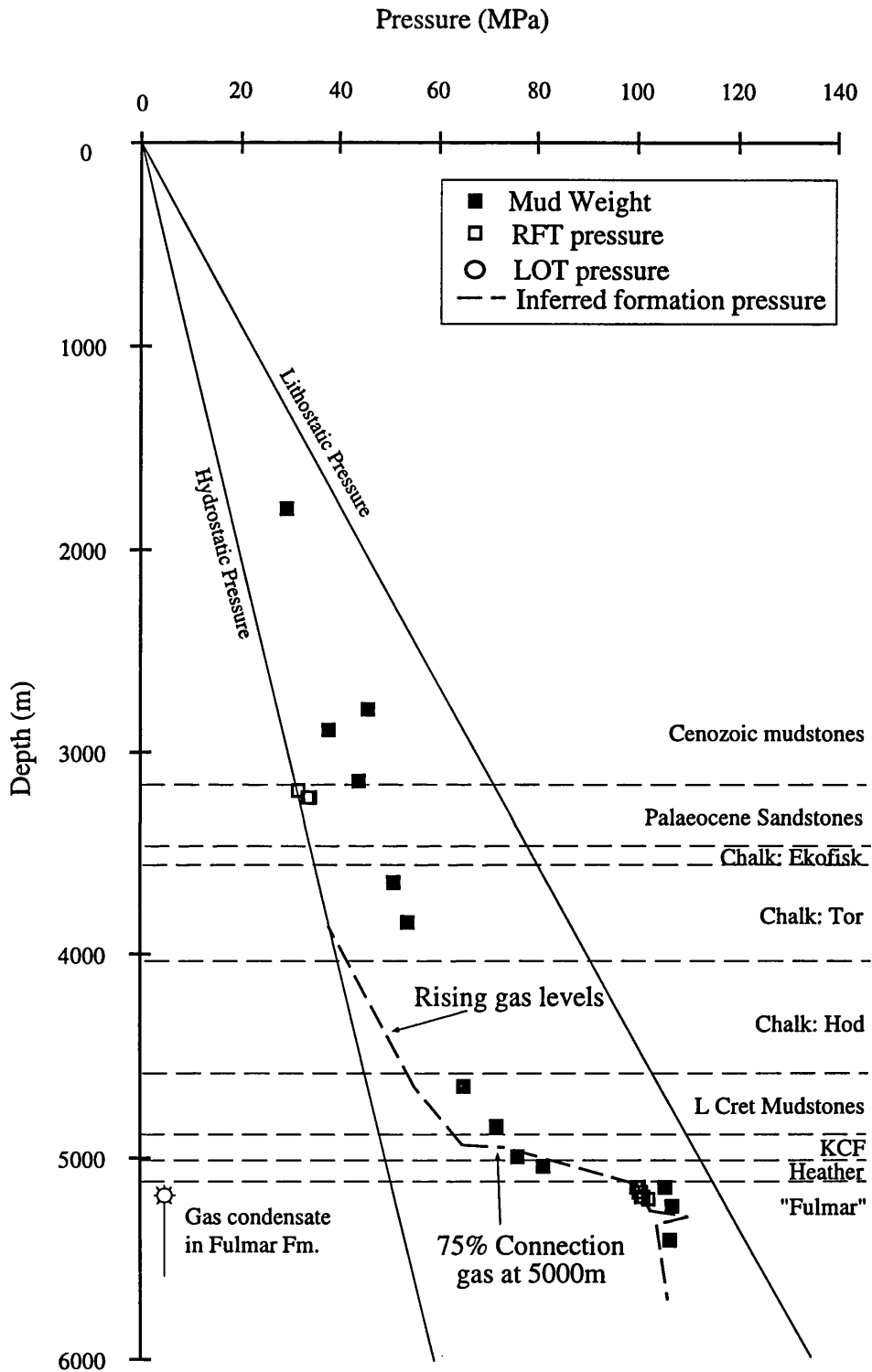


Figure 3.18

Pressures in well 23/26a-2.

Overpressure is inferred from gas levels for the argillaceous base of the Chalk Group. A rise in pressure in the KCF leads to probable negative pressure differential in the Jurassic mudstones. The Fulmar Fm. demonstrates intraformational pressure seals which caused kicks.

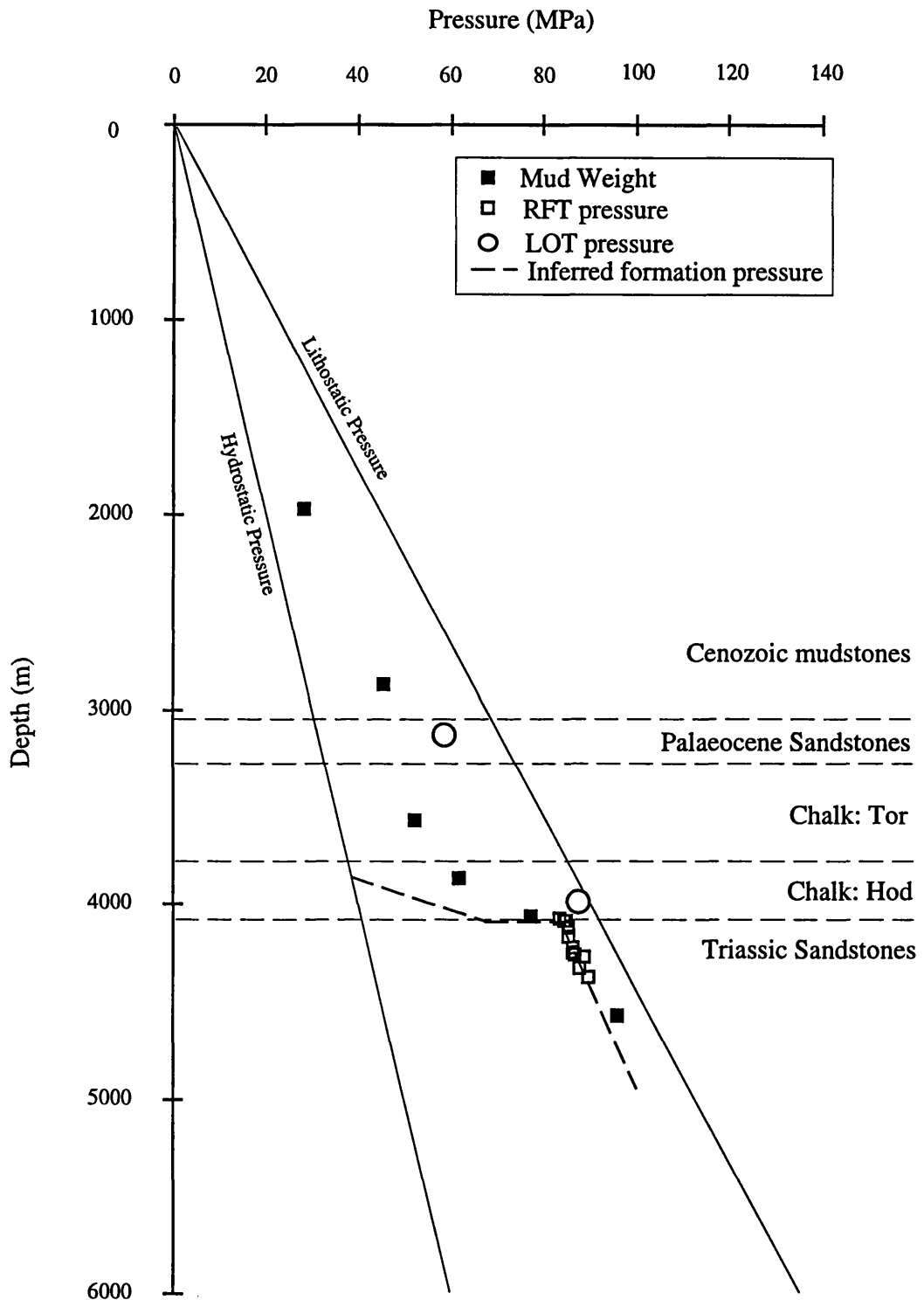


Figure 3.19 Pressures in well 30/1c-2. The Lower Cretaceous is absent due to erosion in this well on the axial Forties-Montrose High (Roberts et al 1990); nevertheless extremely high overpressures are observed in the Jurassic sandstones, with a sharp increase in pressure noted as the sandstones are drilled. Overpressure in Hod is inferred from drilling reports.

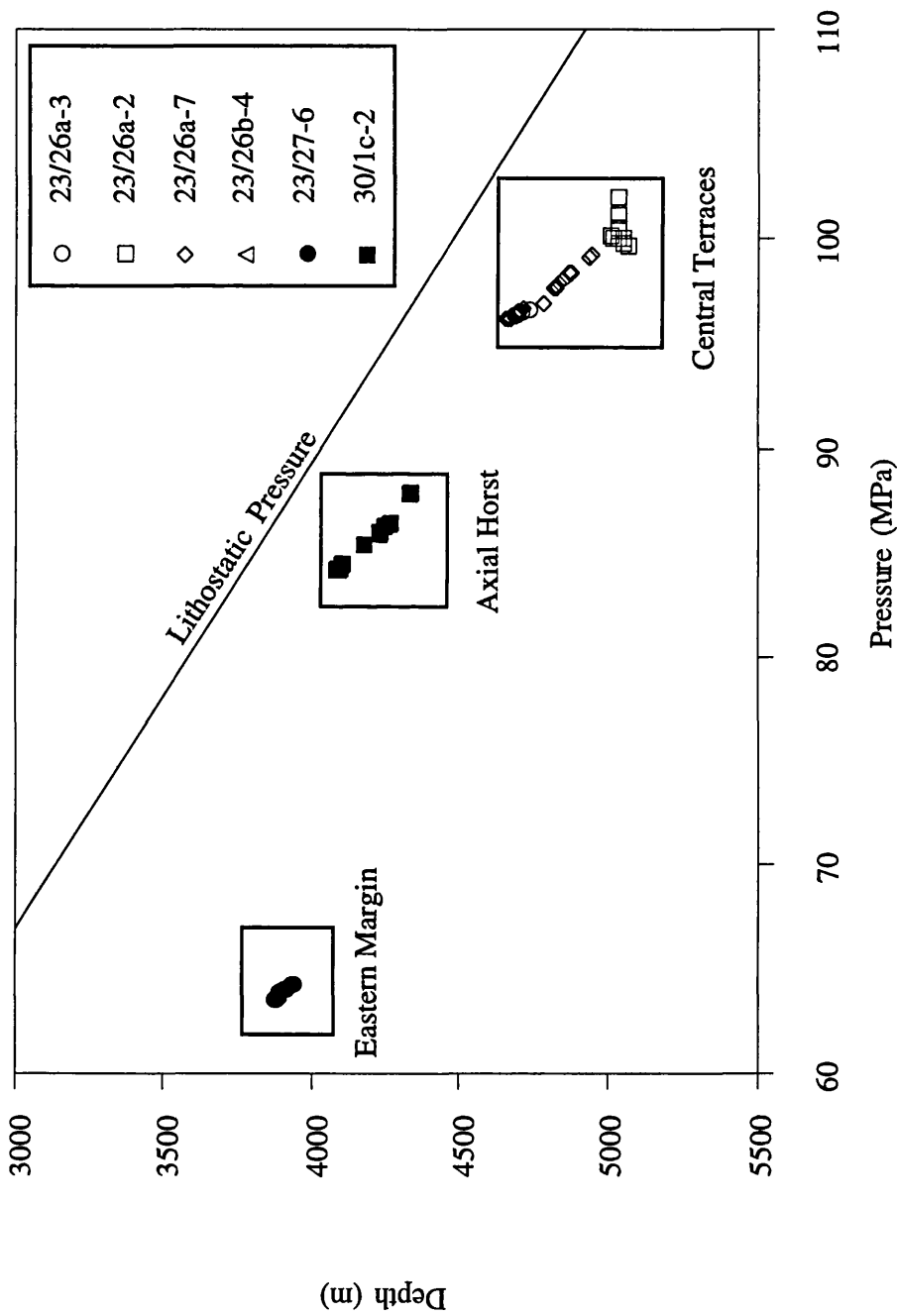


Figure 3.20 Pressure Cells in Jurassic sandstones in the East Forties Basin. Three distinct pressure cells can be recognised on the basis of pressure gradients. The cell penetrated by well 30/1c-2 is separated by only 2 MPa from the cell penetrated by wells 23/26a-2, 23/26a-3, 23/26a-7 and 23/26b-4. Well 23/27-6 penetrates a cell on the Graben margin that is clearly distinct and at a lower level of overpressure, although it is only 200m shallower.

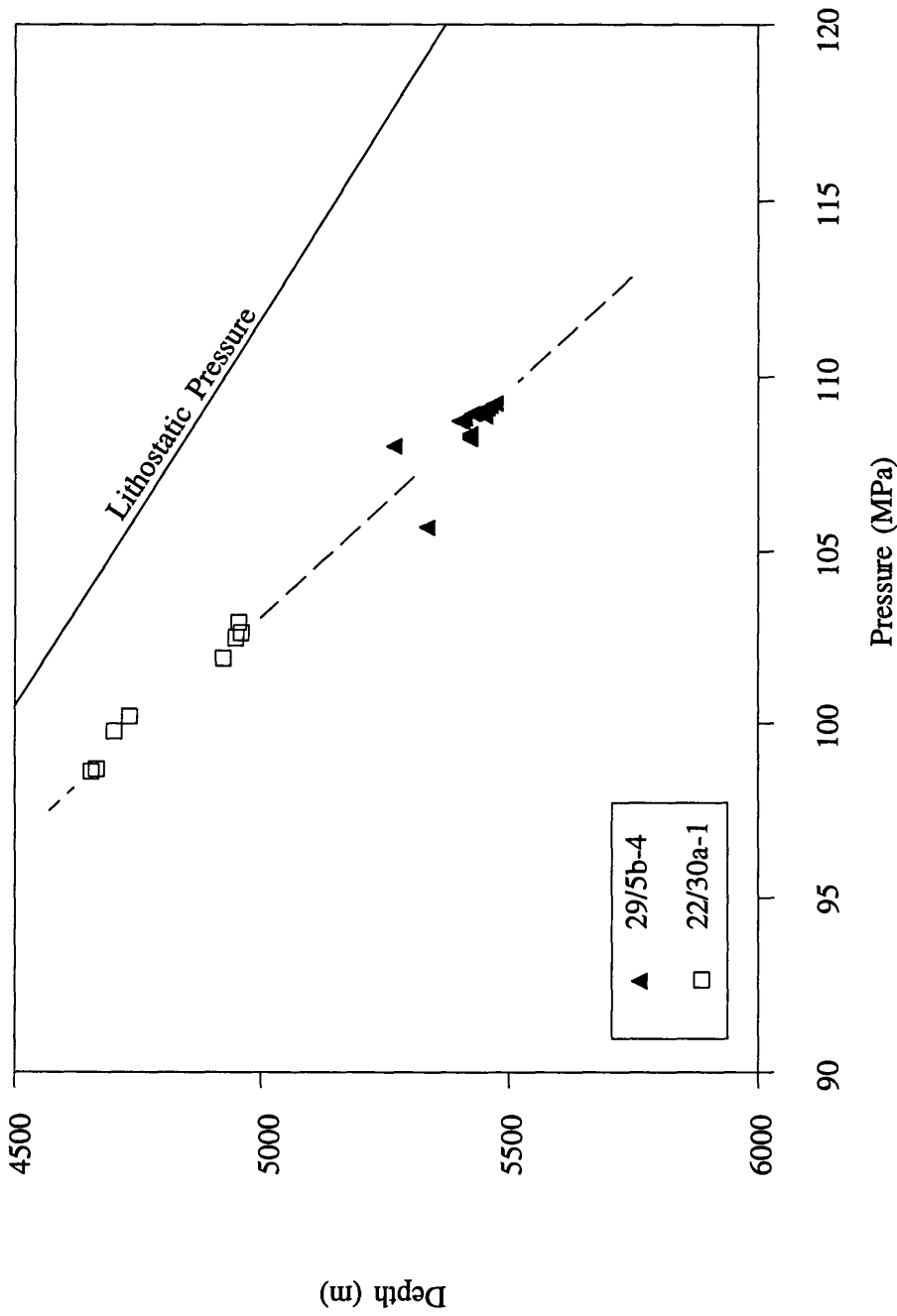


Figure 3.21 Detail plot of cell relationships in the Block 22/30-29/5 region. Wells 22/30a-1 and 29/5b-4 demonstrate identical pressure gradients, and so are suggested to penetrate the same pressure cell.

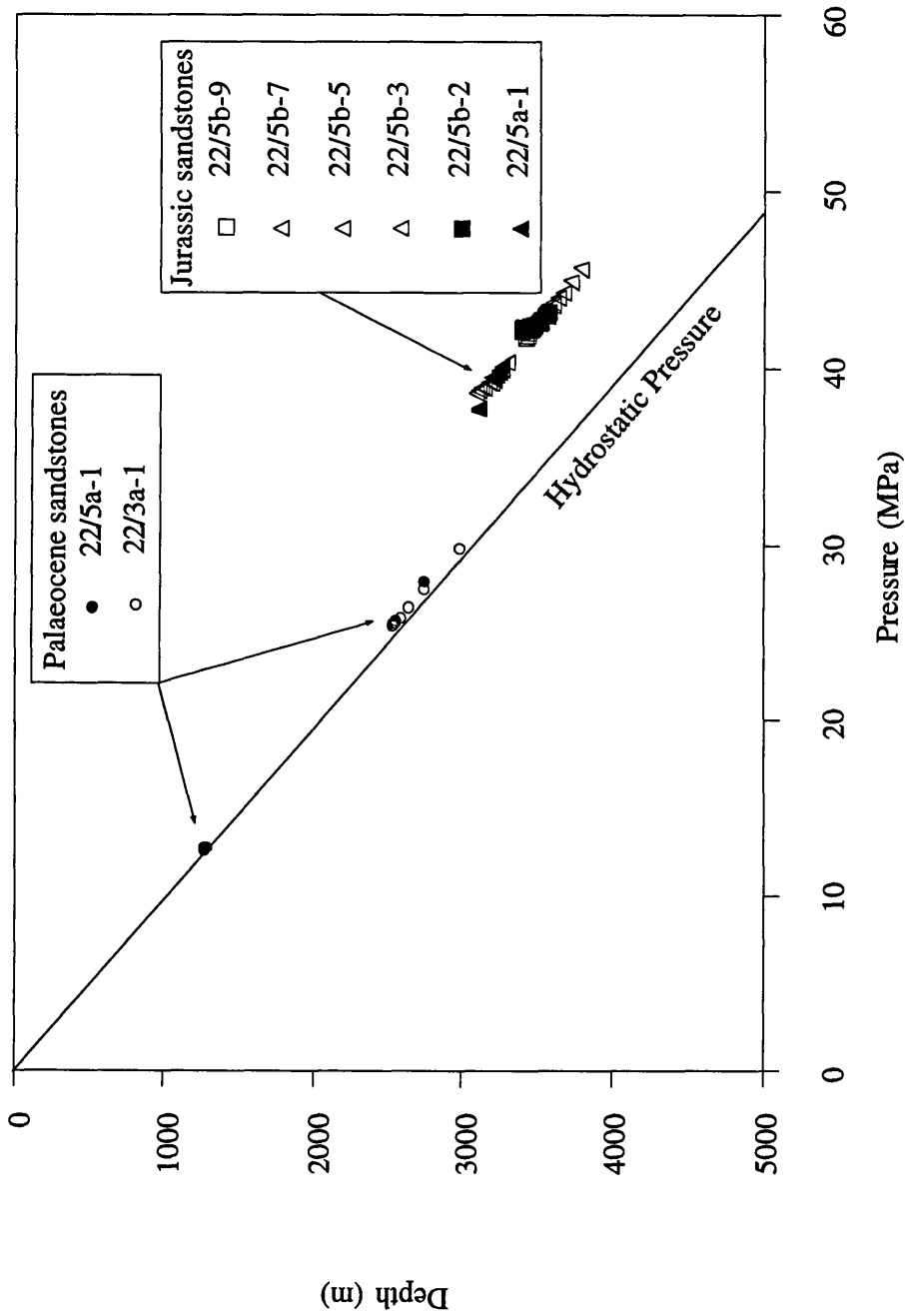


Figure 3.22 A Pressure Cell on the Jaeren High Terrace. Shallow Palaeocene sandstones in the north of the study area demonstrate normal hydrostatic pressure; however a series of wells penetrate Jurassic sandstones that have a common gradient of overpressure and which form a shallow pressure cell.

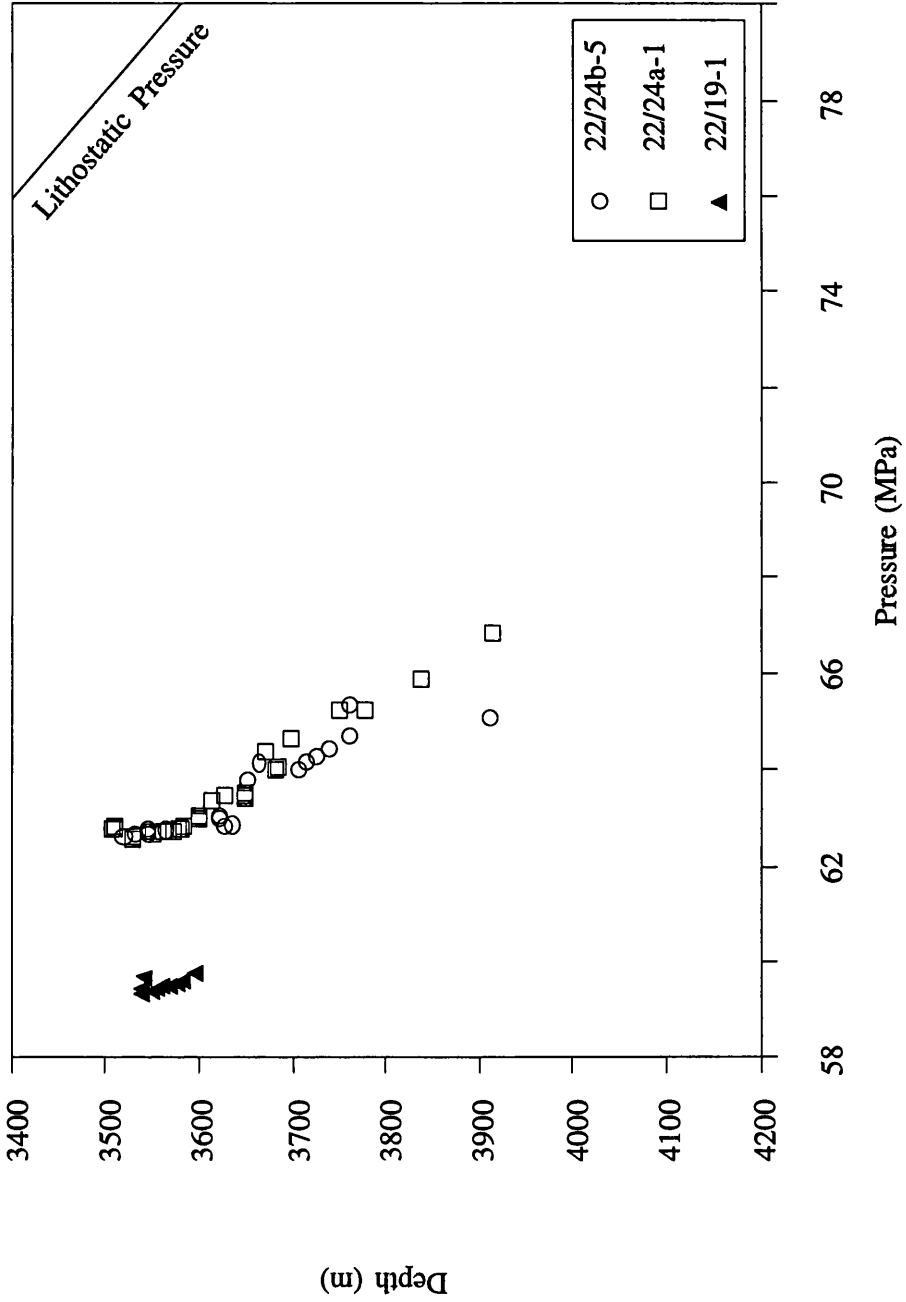


Figure 3.23 Pressure Cells on the Forties-Montrose High Terraces in Quadrant 22. Wells 22/24a-1 and 22/24b-5 penetrate the same pressure cell on one fault terrace; well 22/19-1, on an adjacent fault terrace, penetrates a separate cell.

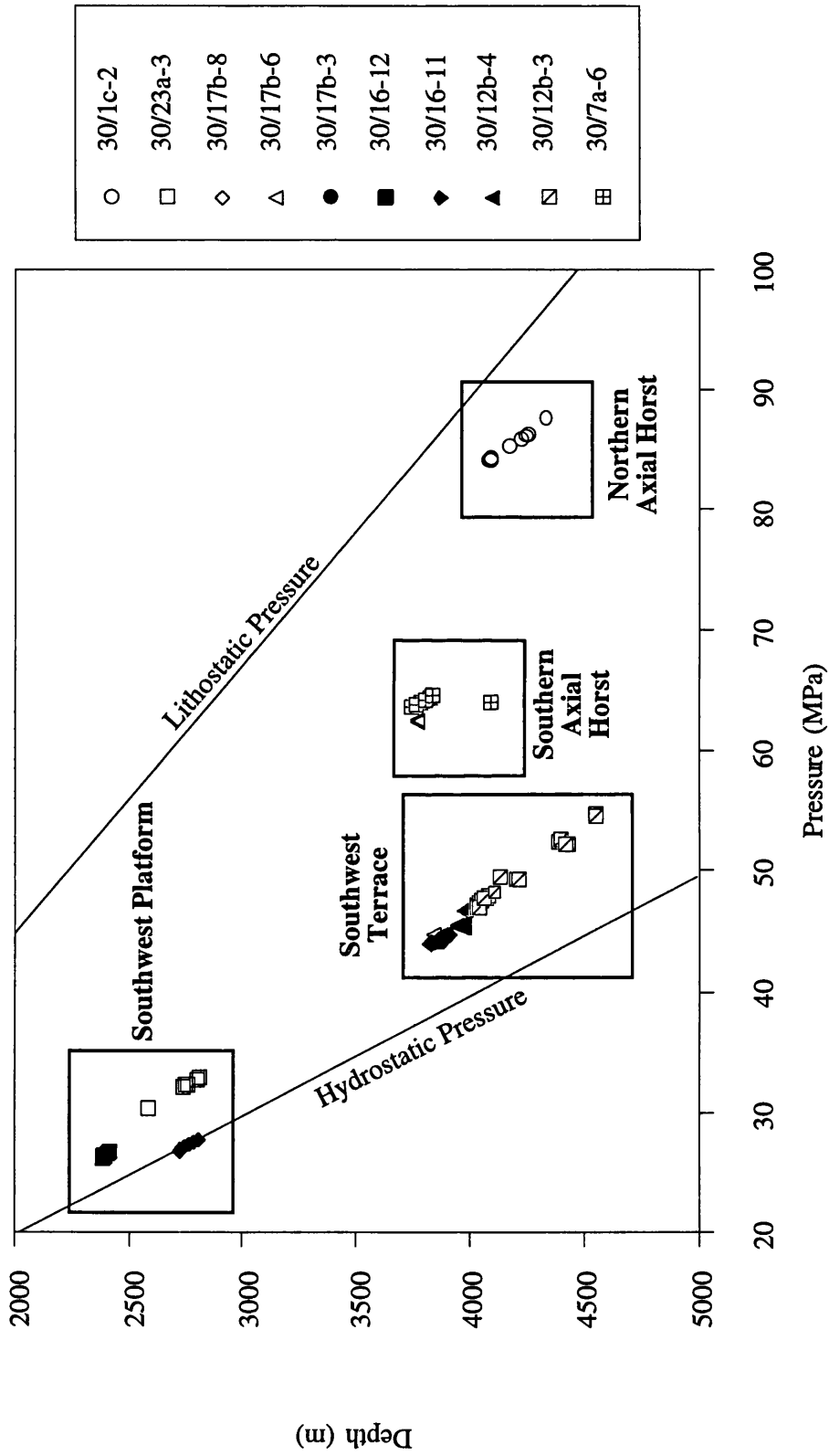


Figure 3.24 Pressure Cells in Jurassic sandstones in Quadrant 30. A series of pressure cells can be defined on the basis of pressure gradients. The magnitude of overpressure in each cell varies according to structural position and location in the Graben, and not according to depth.

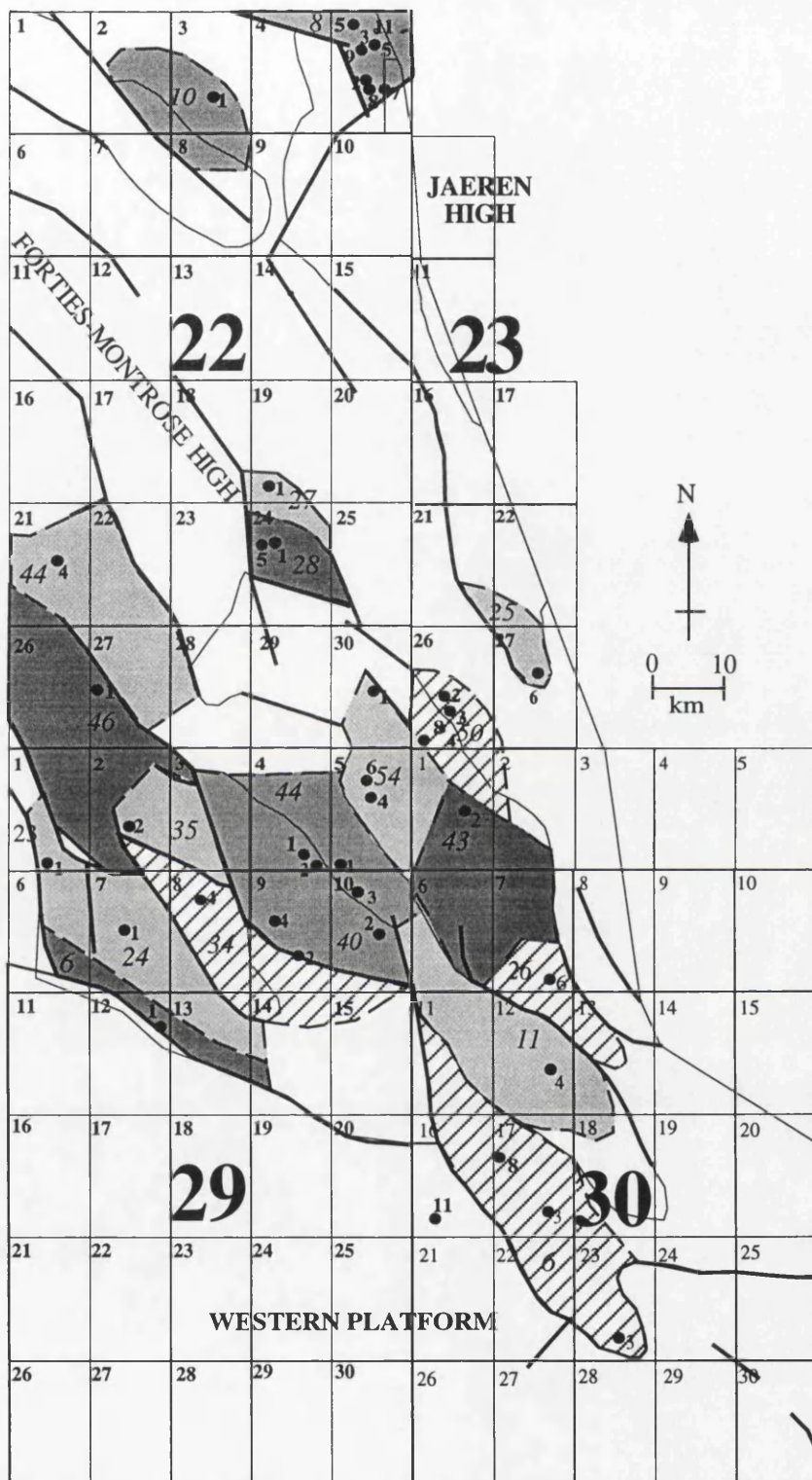


Figure 3.25 Map of pressure cells in the Central Graben in sub-Cretaceous stratigraphy. Italic numbers denote magnitude of overpressure in each cell. Solid numbers denote well number and block number. Well locations are those data points from which pressure information has been derived. On the basis of available data, 18 cells can be delineated. The NW-SE trending boundaries to cells are inferred to be faults. NE-SW trending boundaries are poorly defined, and are hypothesised to be formed by lateral sedimentary discontinuity as the sandstones pass laterally into mudstones of the Heather Fm. The compartmentalisation of the Graben's hydrogeology reflects the complexity of the basin's syn-rift structure.

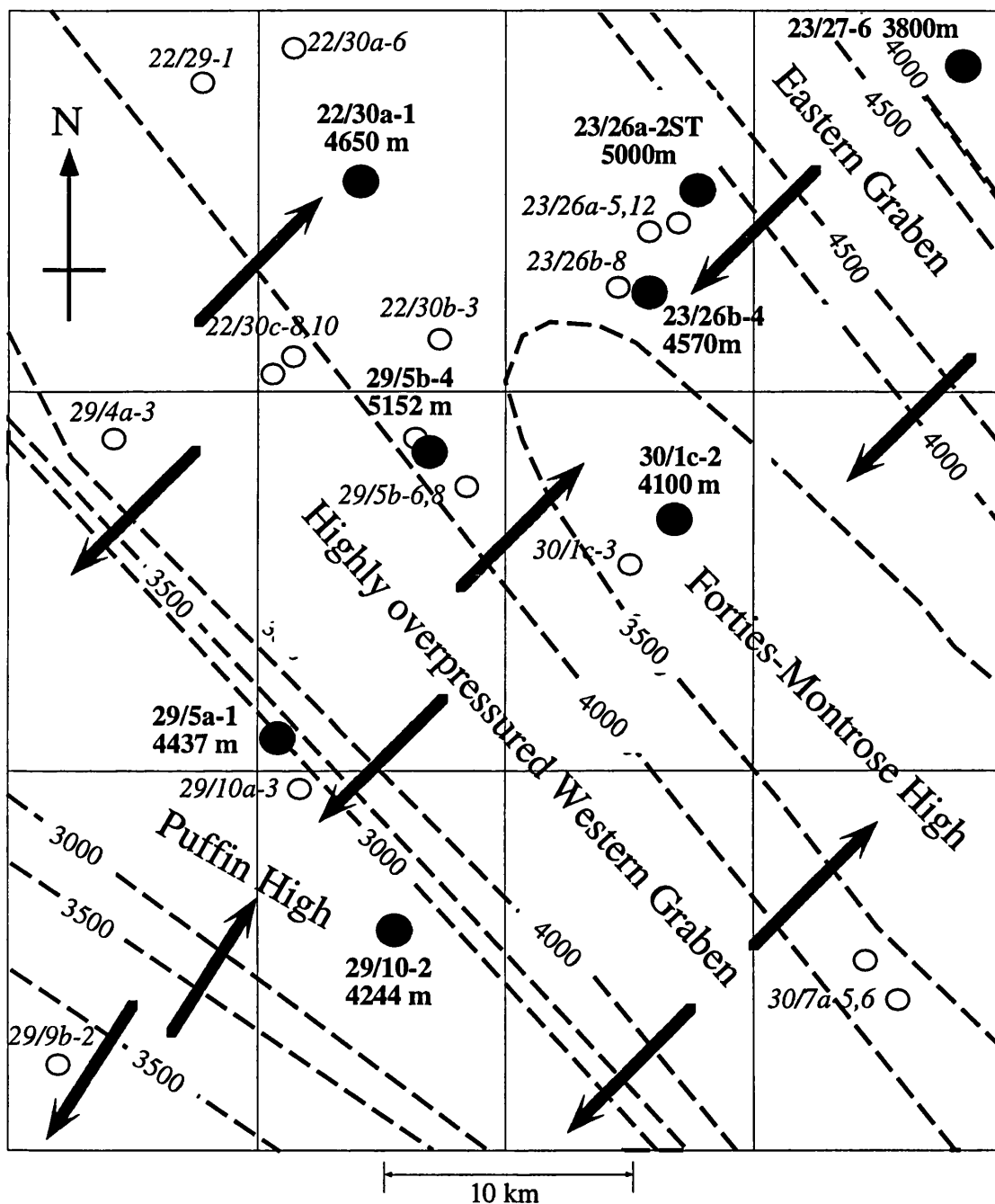


Figure 3.26 Potentiometric map of central study area.

Released wells used in construction of the map are shown as a large solid circle, and are marked with well number and depth to Jurassic sandstone. Confidential wells are shown as a small open circle with well number. Data from confidential wells used in the construction of this map cannot be presented in this study; they are shown for corroboration only. Contours show hydraulic head in metres at top sandstone. Contours are drawn on the basis of data from released wells and contour position is interpretative. Gradients in SW and NE are inferred from the presence of low overpressures on the shelf regions (Fig 3.9). Datum is sea level. Flow may occur perpendicular to contours (heavy arrows). For reference, hydraulic head due to hydrostatic pressure would be 0m. Flow may be directed towards the margins of the Graben or towards the axial horsts.

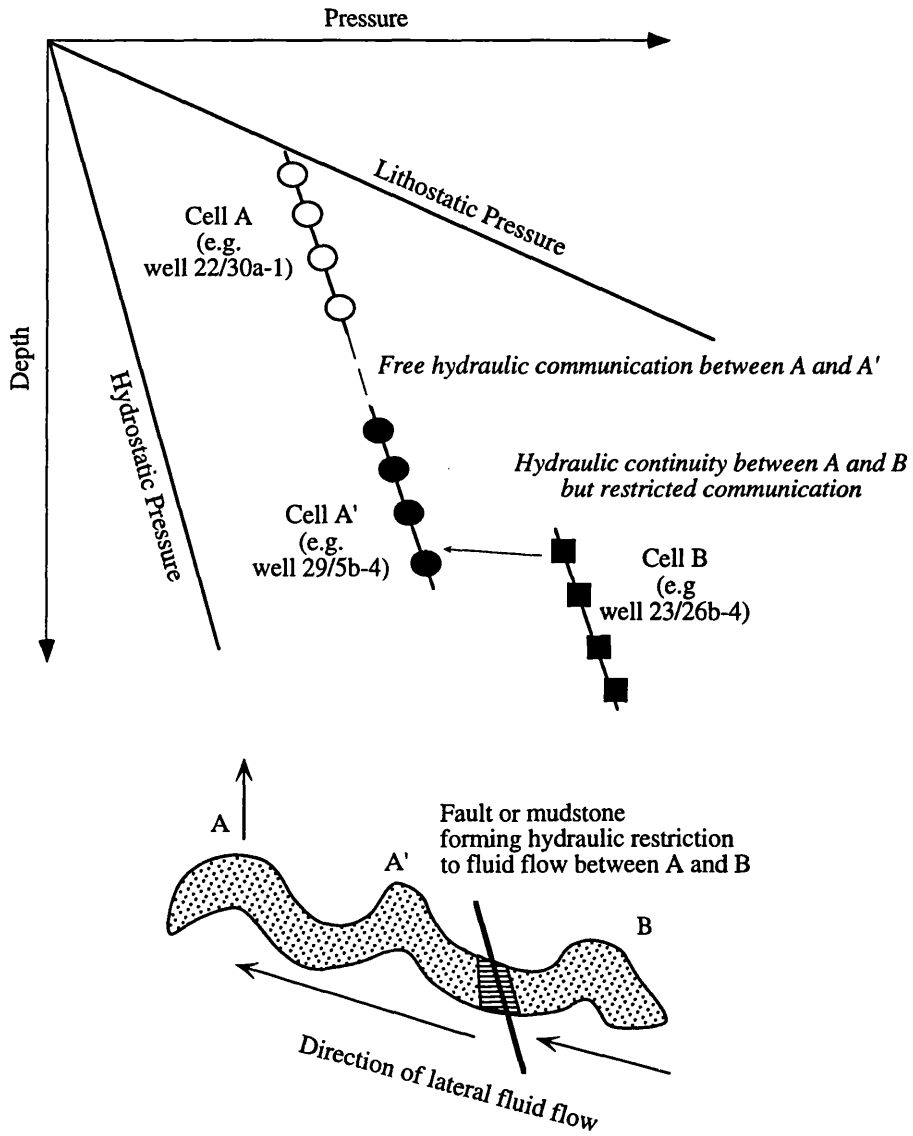


Figure 3.27 Cartoon of hydraulic connectivity and resulting pressure-depth relationships in the Central Graben. Fluid flow from structure A' to A will increase pressure in A.

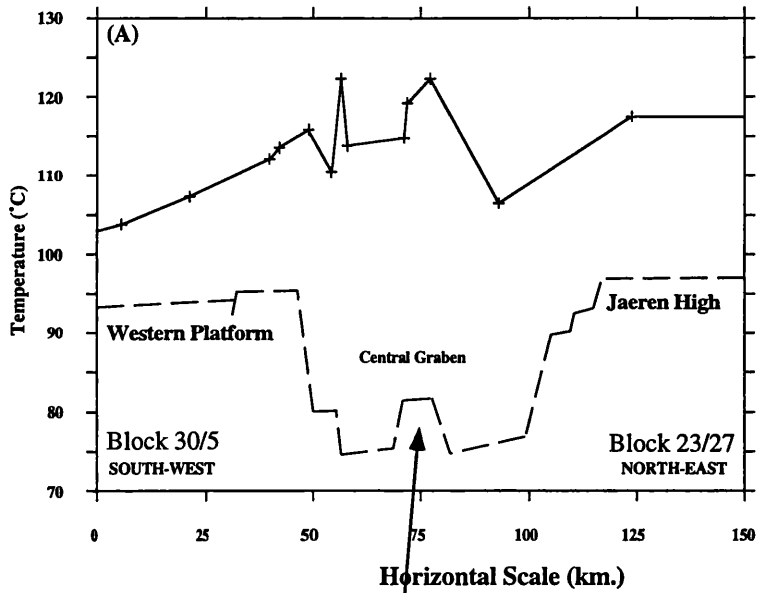


Figure 3.28a Temperature profile from 3000 m across the Central Graben shown as solid line. Simplified structure shown as dashed line. After Fleming (1995, in prep). High temperatures are noted for the axial horst. Vertical fluid flow can explain this anomaly, while variations in thermal conductivity cannot.

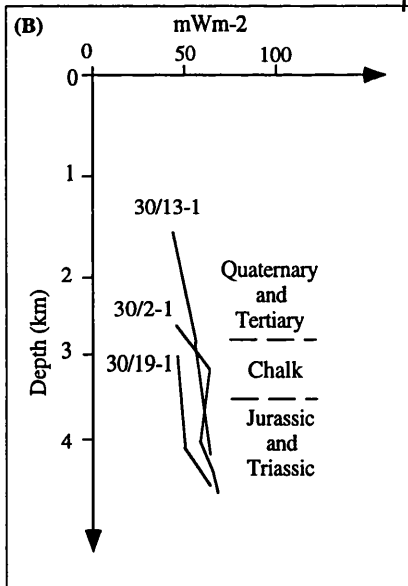


Figure 3.28b Variation of heat flow with depth for three wells in the Central Graben (from Andrews-Speed et al 1984). Well 30/2-1, located on the central section of the axial horst, shows a heat flow anomaly which the authors related to vertical fluid flow. Figure 3.19 has shown that this region of the horst is highly overpressured, and forms a Leak Point; thus it is suggested that vertical pressure-driven fluid flow may explain the heat flow anomaly.

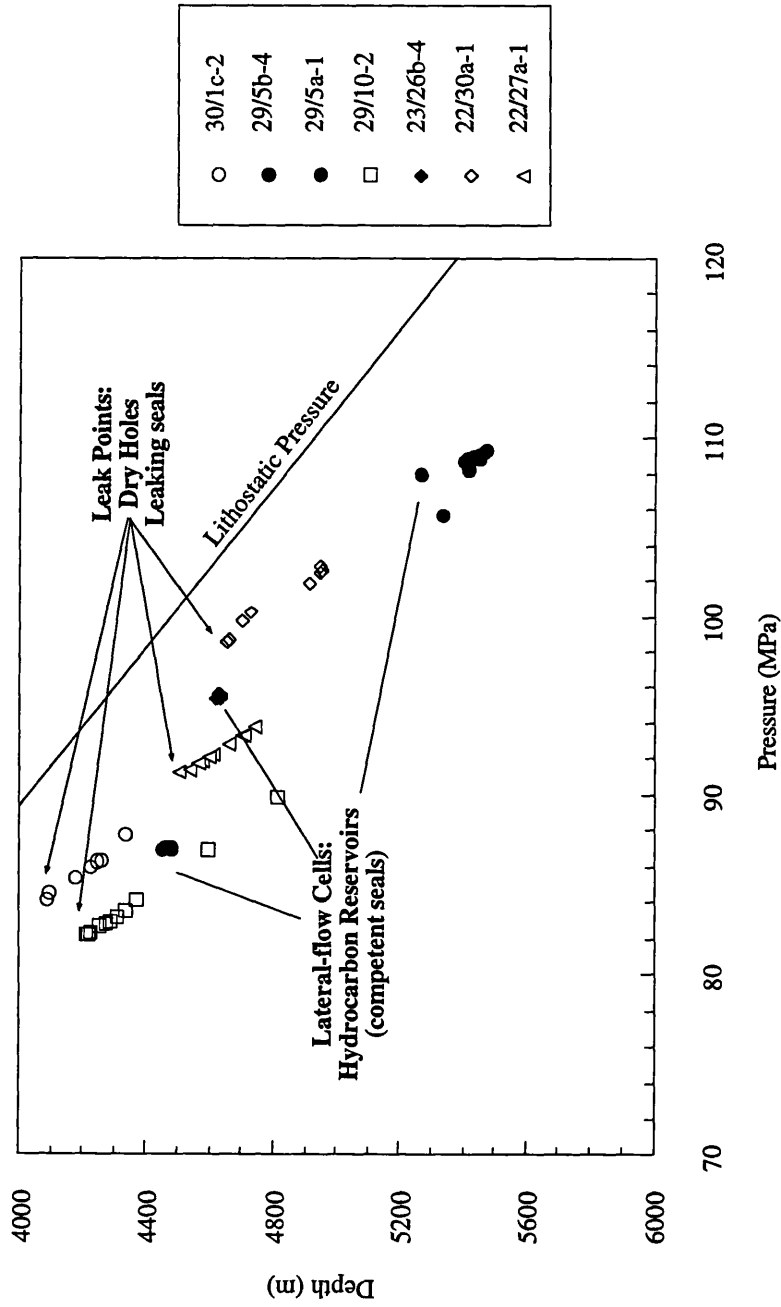


Figure 3.29 Hydrocarbon reservoirs and the dynamic model. Leak Points have high pressures in sandstones and are currently water-wet (although bitumen residues suggest hydrocarbon entrapment in the past); adjacent lateral-flow cells have lowered pressures in the sandstone and highest pressures in the overlying mudrocks, which forms a favourable configuration for retaining hydrocarbons.

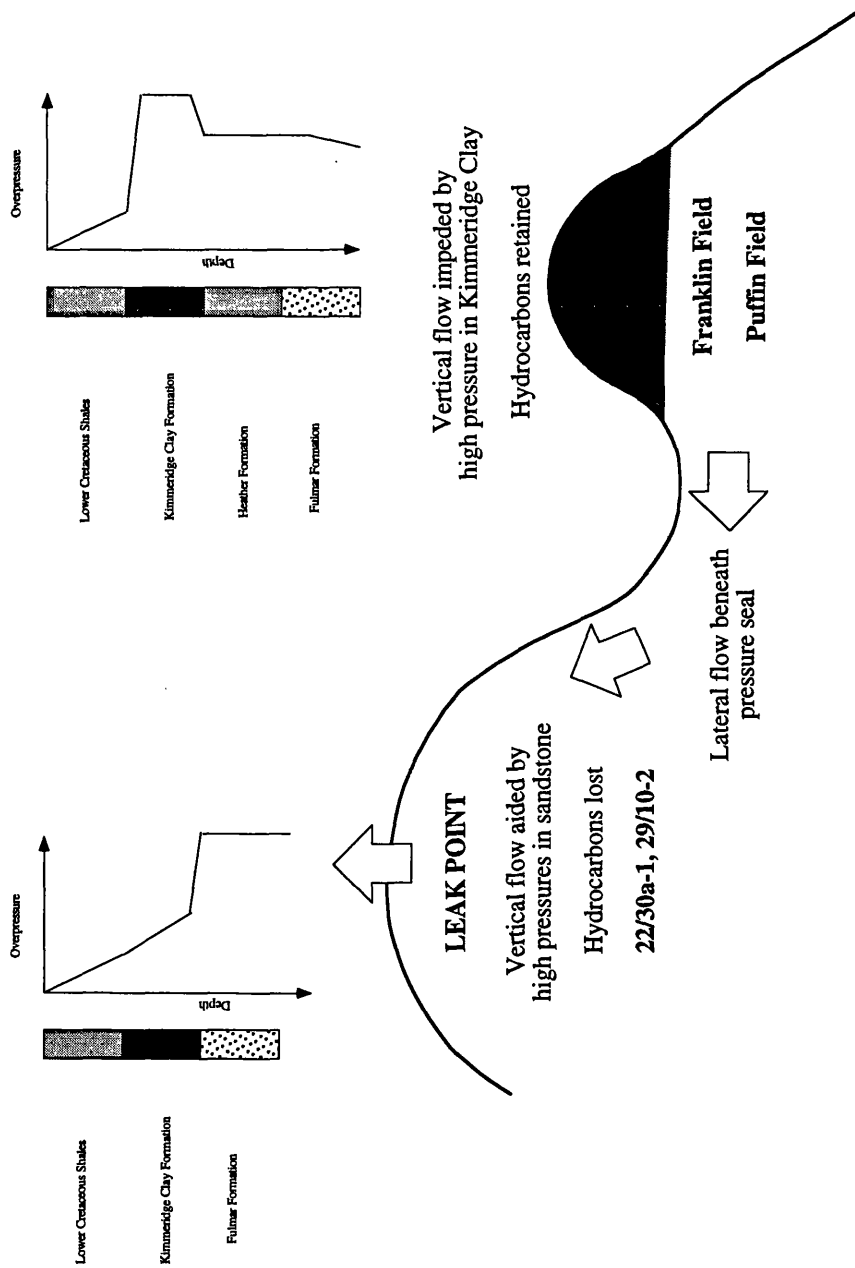


Figure 3.30

Hydrocarbon entrapment and retention in HPHT regions. High overpressure in the Kimmeridge Clay Fm. in deeply-buried sandstones which have a hydraulic connection to shallower structures forms a favourable pressure configuration for retaining hydrocarbons. The Puffin, Franklin and Erskine gas-condensate fields are in this pressure configuration. Leak Points (shallow structures where the Jurassic sandstone is at higher overpressure than the overlying mudstones) are water-wet, suggesting that this pressure configuration is unfavourable for retaining hydrocarbons.

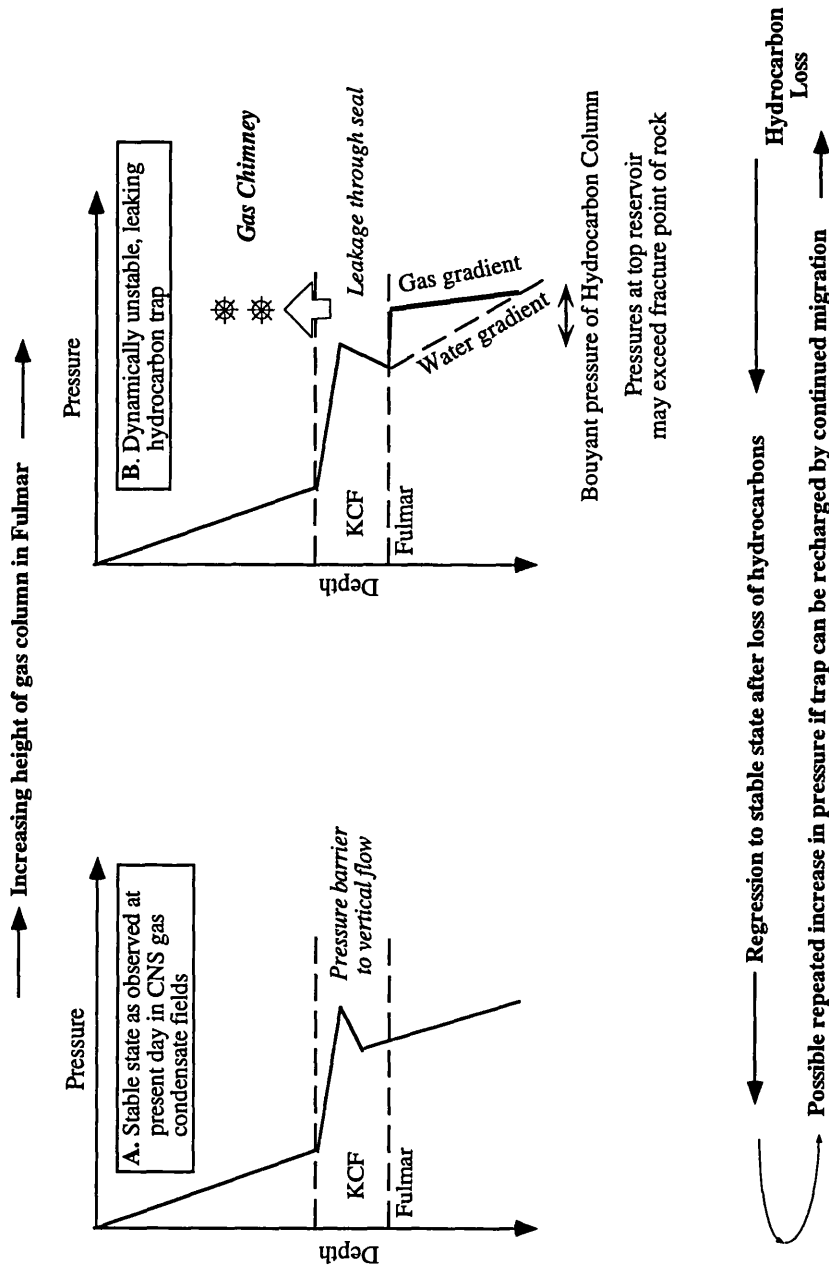


Figure 3.31 The dynamic nature of hydrocarbon entrapment in HPHT reservoirs (with thanks to G. Holm). If the buoyant pressure of a long hydrocarbon column allows pressure at top reservoir to exceed pressure in the Kimmeridge Clay Fm., leakage through the seal may occur. This leakage will occur by hydraulic fracturing of the seal, and will continue until the hydrocarbon column is depleted and the pressure in the reservoir falls to a stable state. If continued migration can occur, this process will be cyclical.

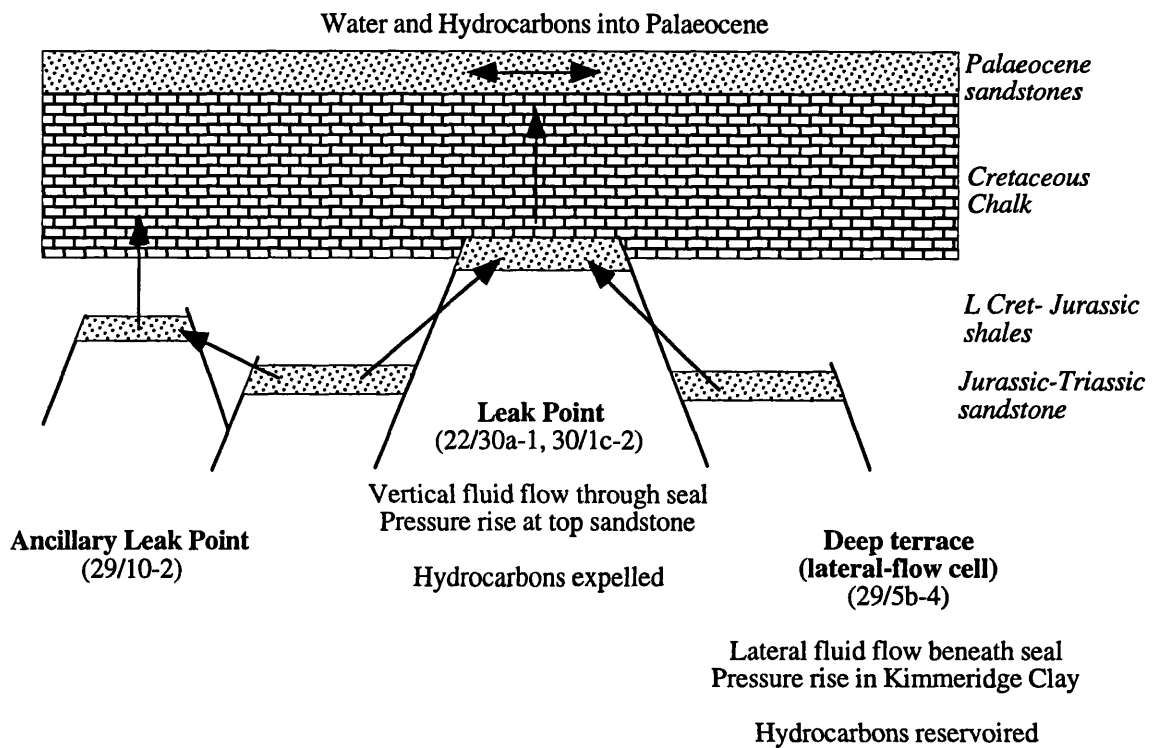


Figure 3.32 Summary cartoon of Central North Sea overpressure. Fluid flow between deep sandstones and sandstones on shallow structures increases pressure in the shallow structures. Pressures in these structures may approach the minimum stress. High pressures, possible hydraulic fracturing, and thin Cretaceous-Jurassic mudstones on the axial horst combine to favour vertical fluid flow through the pressure seal at these points. Such structures are termed "Leak Points".

Chapter Four

Causes of overpressure in the Central Graben

- 4.1 Introduction**

- 4.2 Disequilibrium compaction**
 - 4.2.1 Sonic log measurements of porosity*
 - 4.2.2 Density measurements*
 - 4.2.3 Caliper Logs*
 - 4.2.4 The sub-seal porosity anomaly: primary or secondary*
 - 4.2.5 Assumptions of this approach*

- 4.3 Hydrocarbon generation**
 - 4.3.1 Pressure distribution*
 - 4.3.2 Magnitude of minimum stress*
 - 4.3.3 Pressure sealing and pressure generation in the Kimmeridge Clay*
 - 4.3.4 Hydrocarbon generation in HPHT regions*

- 4.4 Aquathermal pressuring**

- 4.5 Clay mineral dehydration**

- 4.6 A synthetic model for the origin of Central North Sea overpressure**

- 4.7 Conclusions**

4.1 Introduction

Chapter 3 demonstrated that the Central North Sea today forms a dynamic hydrogeological system. The system is out of equilibrium. Fluid flow may be induced by fluid energy gradients as the basin seeks to re-equilibrate at a stable, low-energy state. This model of dynamic overpressure implies that an identification of the mechanisms that have caused this disequilibrium is required to describe the system fully (Deming, 1994). The purpose of this chapter is to identify the "driving force" of the dynamic model presented in Chapter 3.

The chapter comprises:

- A detailed critique of possible processes and mechanisms that could cause overpressure in the Central North Sea. Observational data from well logs and well tests are used to refute or support hypotheses of causal mechanisms.
- The development of a synthetic model for the generation of abnormal fluid pressure in the region.

Studies of the processes which act as causal mechanisms of overpressure have formed a main branch of overpressure research over the past 40 years. Numerous mechanisms have been identified in basins (Section 2.7); however there is no consensus on a dominant worldwide mechanism, and indeed it is possible that there is no one mechanism for generating overpressure.

The Central North Sea (Fig 1.2) is typical of hydrocarbon basins worldwide, in that it is affected by several overlapping processes, each of which could cause overpressure. This is to be expected for a complex, dynamic system resulting from the interaction of numerous variables. Gaarenstroom *et al.*, 1993) outlined the processes in the Central Graben that may theoretically contribute to overpressuring. The region has experienced *rapid subsidence* during the Tertiary, and has undergone 1km of burial in the past 5 Ma. The Jurassic depocentres contain up to 1km of *gas-mature source rock* (Cornford, 1994). Early-emplaced oil in Jurassic traps may have been *cracked* to gas. The presence of thick, regionally-extensive aquitards implies the possibility of *aquathermal pressuring*. The mudstone-dominated sedimentary section contains the possibility of *clay-mineral dehydration*. Thus the Central Graben may be affected by both external and internal causes of overpressure (Section 2.7).

The contribution of each of these mechanisms to the magnitude of overpressure in the Central North Sea will be discussed below. The number of overpressuring mechanisms that can be advanced theoretically for the Central Graben means that the first stage in identifying the cause of overpressure in the region must be the construction of data-driven hypotheses. Such hypotheses can be constructed from the examination of pressure and ancillary geological data. In this section, pressure and porosity data is presented and discussed, leading to presentation of data-driven hypotheses of overpressuring mechanisms in the region.

4.2 Disequilibrium Compaction

As sediment thickness increases due to basin subsidence and loading, increasing vertical stress tends to cause a reduction in the porosity of the sediments. This porosity reduction requires porewater expulsion. During normal "equilibrium" compaction, porosity decreases in response to loading and fluid will be expelled. However, if the rate of fluid escape is low due to low permeability, the sediment cannot change porosity freely; stress is transferred in part to the fluid, which becomes overpressured (Rieke & Chilingarian, 1974). This mechanism for causing overpressure is termed disequilibrium compaction (Section 2.7). If overpressure in a basin is caused by disequilibrium compaction, there is an expectation that higher porosity will be observed in overpressured sediments than in normally-pressured sediments.

Disequilibrium compaction requires the presence of low-permeability restrictions to fluid flow. Mudstones have low permeability and thus commonly exhibit anomalous porosity in overpressured basins. High overpressure is noted for pressure cells adjacent to Jurassic depocentres (Section 3.3.1). These overpressures may be related to restricted compaction of the thick mudstone sequences in the depocentres, and greater restriction of fluid flow by the thick mudstones. However, direct measurements of mudstone porosity are rarely made. Direct measurements of porosity are made from conventional cores, which are expensive and rarely taken outwith reservoir intervals of a well. Thus mudstone porosities must be inferred from wireline logs. Sonic and density logs give allow semi-quantitative analysis of mudstone porosity. Wireline logs allow examination of the porosity of mudstones in the Central Graben for an association of high porosity and overpressure. This will allow testing of the hypothesis that disequilibrium compaction has caused the overpressure in the basin.

4.2.1 Sonic Log measurements of porosity

Wireline sonic logging is widely used to measure mudstone porosity, and thus identify undercompacted zones (Wyllie, 1956; Wyllie, 1958). Sonic velocity depends on the bulk modulus and density of the rock. The relationship between velocity and porosity (Wyllie, 1956) is

$$\Delta t = \phi \Delta t_L + (1 - \phi) \Delta t_{ma}$$

where Δt is the interval transit time measured by sonic log, Δt_L is the transit time of interstitial fluid, Δt_{ma} is the transit time of matrix material and ϕ is the porosity. Sonic velocity is higher in undercompacted shales assuming bulk modulus is identical. This assumes that fluid type is identical, matrix material is identical and the formation has a uniform distribution of pores. Transit time may be related to matrix porosity (Magara, 1968), or to the presence of microfractures (Engelder, 1993). In the Central Graben, sonic logs are run throughout most wells, allowing establishment of normal trends for mudstone sonic velocities (Magara, 1968).

Figs 4.1, 4.2, 4.3 and 4.4 present sonic logs from several Central North Sea wells. A sonic velocity anomaly occurs within the L Cretaceous- Jurassic mudstones in all wells examined. Where sonic logs are available throughout the well, a sonic velocity anomaly can also be noted in the Cenozoic mudstones. The anomalies correspond to overpressured zones. The correspondence between low sonic velocities and overpressure in the Central Graben suggests that overpressure in the region is related to high mudstone porosity. The association of high porosity and overpressure suggests that disequilibrium compaction may be contributing to overpressure in the Central Graben.

However, the interpretation of wireline log data is often complicated by additional factors. The sonic velocity within the overpressured rocks is ubiquitously highest in the Kimmeridge Clay Fm (KCF). This stratigraphic bias is evident in all wells in the region. The sonic response of the KCF may be related to organic content (Meyer & Nederlof, 1984) or hydrocarbon saturation of pores. An additional factor in the low sonic velocity in the KCF in the Central Graben may be a high density of open microfractures related to active hydrocarbon generation (Duppenbecker *et al.*, 1991; Lindgreen, 1987).

Additionally, sonic velocity in rocks has been suggested to show a relationship to the effective stress acting on the rock, and not directly to porosity (Bowers, 1994;

anomalies in overpressured zones are not coincident with density anomalies, and so do not reflect porosity change (Fig 4.5; Wensaas *et al.*, 1994). A similar relationship may hold for the "d"-exponent (Section 3.2). If sonic velocity relates to effective stress and not directly to porosity, the presence of a sonic velocity anomaly in overpressured rocks in the Central Graben does not carry any information about the cause of the anomaly. Assuming that low effective stress relates to high porosity makes an *a priori* assumption that overpressure is caused by disequilibrium compaction. This assumption is not automatically valid for the Central Graben. A sonic log may not be a suitable tool for testing the association of overpressure and porosity.

In the Central Graben, sonic log profiles appear to follow the effective stress profile (Fig 4.6). Effective stress is lowest at the upper boundary to a pressure cell, that is, the pressure seal. This is where lowest sonic velocities are observed. Accordingly, the interpretation of sonic logs in the Central Graben in terms of porosity is complicated by the lithological overprint of the KCF, and by a possible relationship to the effective stress acting on the rock. Sonic logs suggest that anomalously high porosity may exist beneath the pressure seal in Central Graben wells, but the data is ambiguous. Corroborating data is required. This can be provided by other methods of determining porosity.

4.2.2 Density Measurements

Formation density can be measured by the wireline neutron density logging tool. Measured formation density is related to porosity and lithology. Low density measurements suggest high porosity, assuming mineral density is identical. Density measurements are also affected by fluid type in the porosity, and measurements are sensitive to borehole rugosity (Mouchet & Mitchell, 1989). Insights into the porosity of mudstones in the aquitard are also hampered by the rarity of density measurements outwith reservoir intervals in the region. Density log measurements are presented in Figs 4.1, 4.2, 4.3 and 4.4.

These figures show that mudstone formation density in decreases from 2.65 g/cm³ above the pressure seal to 2.5-2.4 g/cm³ in the pressure cell, and density decreases with increasing depth.

Quality-control of the density log is problematic, and can only be exercised where problems have been noted on the log (such as "tool sticking" in sticky Lower

Cretaceous marls), or where a caliper log suggests borehole instability. Density and sonic logs are consistent. The low density anomaly noted in the Herring and top Fulmar formations in well 22/27a-1 (Fig 4.2) may be related in part to gas saturation. However, the sonic log does not show a decrease in sonic travel time. In the Kimmeridge Clay Fm. of wells 29/10-2 and 22/27a-1, the density and sonic logs are sub-parallel, a typical log response for this formation in the North Sea (Pepper, 1991). The low density of the Kimmeridge Clay Fm. may be due to high organic richness (Meyer & Nederlof, 1984) or hydrocarbons in the pores.

Formation density can also be measured from mudstone cuttings by water displacement. This is used as an on-site method of detecting and predicting overpressure during drilling, and recorded in pressure evaluation reports. In well 29/5b-4 (Fig 2.18), mudstone densities decrease in the overpressured Lower Cretaceous from 2.25 g/cm³ to 2.15 g/cm³.

Thus density measurements suggest that mudstones below the pressure seal are of anomalously low density. The overpressured mudstones are thus inferred to have anomalously high porosity.

4.2.3 Caliper Logs

Caliper logs use sensitive, flexible arms to measure the width of the borehole. In hard, compacted rocks, borehole width is close to the width of the drill bit used to drill the borehole. In porous, poorly-consolidated rocks, recorded borehole size tends to be greater than bit size as the porous rocks slough off into the borehole. Hole size that is recorded as being smaller than the drill bit reflects the build-up of residues of drilling mud on the walls of the borehole (a "mud cake"). Thus caliper logs allow identification of porous, unconsolidated zones that are sloughing into the borehole.

The caliper logs of wells 29/10-2 and 23/26a-2 (Figs 4.7 and 4.8), suggest that L. Cretaceous and Upper Jurassic mudstones are undercompacted and sloughing. These borehole conditions are characteristic of undercompacted zones. The Heather Fm. does not show high rugosity in well 29/10-2. This is indicative of compacted rocks. The compaction of the Heather Fm is attributed to the coarser nature of the formation which can support freer fluid flow (Symington *et al.*, 1994). The caliper log of well 22/30a-1 (not shown) indicates a low rugosity borehole except in the one thick intra-Fulmar mudstone encountered by the well. This is in agreement with the

distribution of overpressure in this well, where the top of the Fulmar Fm. marks the upper boundary of the overpressured cell.

The available caliper logs of Central Graben wells provide additional, qualitative evidence for the presence of undercompacted, anomalously porous mudstones in the overpressured regions of the Graben.

4.2.4 *The sub-seal porosity anomaly: primary or secondary?*

Density, sonic and caliper logs, together with mudstone cutting density measurements, demonstrate the presence of anomalously high mudstone porosities beneath the pressure seal. The presence of a porosity anomaly could be attributed to undercompacted, overpressured sediments. However, this anomaly must be examined before attributing its causes to disequilibrium compaction. As discussed for sandstones in section 5.4, high porosities do not automatically imply arrestation of the compaction of primary porosity. High porosities may also be secondary in origin, and may give no insight into the causes of overpressure. Anomalous mudstone porosity can be a cause of overpressure, or a symptom.

If mudstone porosity is secondary, export of solutes from the mudstone is required. This can be difficult due to the low permeability and low fluid fluxes generally inferred for mudstones (Coyner *et al.*, 1993; de Caritat *et al.*, 1994). However, a Leak Point such as 22/27a-1 may enhance export of solutes from mudstones due to hydrofracturing and high fluid flux through the pressure seal. Enhanced solute export should be recorded in the geochemistry of sub-seal sandstones, which can be directly observed. Mudstones and associated sandstones do not necessarily show the same diagenetic patterns (Jansa & Urrea, 1992). Solute export related to fluid flow through hydrofractures should follow similar patterns in adjacent formations over 100m (as observed in Central North Sea Jurassic sandstones and mudstones by Greenwood *et al.*, (1994) . Thus secondary porosity developed in a mudstone should be accompanied by secondary porosity in the adjacent sandstones.

The porosity of the Fulmar sandstones in well 22/27a-1 shows enhanced secondary porosity (Section 6.4). The mudstone overlying the sandstone in this well also exhibits high porosity. Thus the high porosity in the mudstone could be attributed to secondary porosity, with solute export enhanced by vertical fluid flux (Section 6.4). However, well 29/10-2 does not exhibit enhanced sandstone porosity, implying limited removal of solutes from the sandstone. This well *does* exhibit porosity

anomalies in the mudstones overlying the sandstone. There is no evidence in this well for fluid flux allowing secondary porosity to develop. Additionally, the caliper log response is more characteristic of preserved primary porosity in undercompacted rocks than secondary porosity in competent, compacted rocks. Accordingly, mudstone porosity in well 29/10-2 must be primary. It is hypothesised that measured mudstone porosity does reflect disequilibrium compaction. The presence of undercompacted primary porosity indicates that disequilibrium compaction is one cause of the overpressures observed in the region.

4.2.5 Assumptions of this approach

Mudstones have a central role in fluid flow in sedimentary basins. They act as the engine for driving fluid flow through changes in porosity, and act as a barrier to fluid flow due to their low permeability. Despite the quantity of mudstones in the Central Graben, (which form two-thirds of the thickness of the sedimentary section) and their inferred hydrogeological role, mudstones are rarely directly observed. They are rarely cored, and their physical characteristics make measurement of hydrogeological properties difficult. The hydrogeological behaviour of mudstones is inferred from log interpretations (which are subject to interpretation error), rare measurements of petrophysical properties (such as Coyner *et al.*, (1993), based on intra-reservoir mudstone bands), and mechanical and numerical models of sediment compaction. Laboratory mechanical models (e.g. Rieke & Chilingarian, 1974) can be criticised for neglecting geological time. Numerical models (e.g. Audet & Fowler, 1992; Bredehoeft & Hanshaw, 1968) have been extrapolated from sandstones and do not take into account the mineral shape and geochemistry of mudstones.

The dearth of knowledge about fluid flow in mudstones forces assumptions on a hydrogeological investigation. The data-driven model of overpressuring due to disequilibrium compaction detailed in this section makes several assumptions about the nature of fluid flow in mudstones:

- It is assumed that the porosity profile derived for the Central Graben represents a disequilibrium situation, and that fluid flow will lead to the restoration of porosity to a stable equilibrium. The restriction of this re-equilibrating fluid flow leads to overpressure (Rieke & Chilingarian, 1974). This view has also been applied to the Gulf of Mexico (Dickinson, 1953). It has been challenged by Hunt *et al.* (1994), who have used a unique database of direct measurements of

mudstone porosity to demonstrate that porosity profiles derived from overpressured and hydro pressured regions are identical. This shows that the porosities in overpressured regions are not out of equilibrium. Instead, it is the assumption of a "normal" compaction which is at fault. Compaction is not related to overpressure in the deep Gulf of Mexico, and so overpressure in that basin cannot be the result of disequilibrium compaction. This hypothesis cannot be examined in the Central Graben, as no wells exist that show hydro pressure at similar depths to overpressured wells.

- Direct measurements of mudstone porosity in a region of the Gulf Coast (Hunt *et al.*, 1994) have shown that anomalous porosities within mudstones in overpressured wells are the result of mineral dissolution and are thus secondary in origin. Section 4.2.4 above demonstrates that this effect is unlikely to be ubiquitous in the Central North Sea, but is based on the assumption of diagenetic similarity between adjacent mudstones and sandstones.
- Re-equilibration of porosity by fluid flow in mudstones assumes that Darcy's Law applies to deep, highly-compacted mudrocks. This has not been demonstrated (Hermanrud 1994; see Section 7.4).

In conclusion, it is convenient to assume that fluid flow in mudstones is governed by Darcy's Law, and that mudstones compact in a non-linear process that can be arrested by restricted fluid flow. These assumptions allow the construction of quantitative models of fluid flow in sedimentary basins (e.g. Burrus *et al.*, 1991; Garven, 1989; see also Chapter 5) that adequately describe the observed hydrogeology of the basins investigated. This does not imply uniqueness in the description of the geological system, as the assumptions do not describe the data of Hunt *et al.* (1994). A paradigm shift in the understanding of fluid flow in sedimentary basins may be imminent.

4.3 Hydrocarbon Generation

The fluid volume increase that occurs as solid kerogen is transformed into liquid oil and gas has been advanced as an internal overpressuring mechanism by many authors (e.g. Meissner, 1988; see Section 1.8). A fluid volume increase and a consequent increase in pressure during hydrocarbon generation has been theoretically advanced by Barker, (1990), Duppenbecker *et al.*, (1991) and Ungerer *et al.*, (1981). These theoretical studies are supported by empirical observations. An

association of overpressure with mature source rocks has been noted by Spencer, (1987) and Hunt *et al.*, (1994), amongst others. Additionally, overpressure due to hydrocarbon generation has been postulated to increase the magnitude of minimum stress in an overpressured basin (Engelder & Fischer, 1994). Thus there is an expectation that overpressures should be spatially associated with source rocks and increased minimum stress if hydrocarbon generation contributes to the overpressure in a basin. These hypotheses are tested below.

4.3.1 Pressure distribution

In the Central Graben, high overpressures are spatially associated with Jurassic depocentres (Fig 3.9). These depocentres contain great thicknesses of the Kimmeridge Clay Fm. (KCF), the source rock for much of the North Sea's hydrocarbons (Cayley, 1987; Cornford, 1994); see Fig 1.7). However, as discussed above, the great thickness of the Jurassic mudstones in the depocentres forms an aquitard, which may have restricted fluid flow and thus restricted compaction. The spatial association of overpressure and Jurassic depocentres is insufficient to demonstrate a causal link to hydrocarbon generation.

A strong implication of the role of hydrocarbon generation is revealed by the small-scale distribution of pressure *within* the mudstone aquitard (Section 3.3.5). High pressures are observed in the KCF, which forms a pressure seal for many pressure cells in the region (e.g. Fig 3.12). The KCF. is mature for gas generation below 4000m (Cayley, 1987; Cornford, 1994). Overpressure is highest in this formation in the deepest well available to this study (well 29/5b-4, Fig 3.12). In this well, pressure is 5MPa in excess of the formation pressure in the underlying Heather Fm. and the water-leg pressure in the underlying sandstones. Drilling problems occur in the KCF, in well 23/26a-2(Fig 3.18): mud gas levels fluctuate rapidly within the formation. This suggests that the wellbore is close to balance, and that open fractures within a generally low-permeability matrix may be present (Grauls & Cassagnol, 1993).

Hydrocarbon generation is also believed to be occurring in the Heather Fm., which contains 1-3% TOC Type III kerogen (Cornford, 1994; see Fig 1.7). As a poor-quality gas-prone source rock, it can be hypothesised that this formation will also play a role in overpressure generation. However, pressure data shows that pressure in the Heather Fm. is slightly lower than the overlying KCF. This suggests that even

though the Heather Fm. may contribute to overpressure, it is less significant than the KCF.

The sharp transition zones observed in the KCF. are untypical of transition zones in homogenous mudstone sequences. In the Northern North Sea, the transition zone from hydropressure to overpressure is smoother and more gradual (Fig 4.5) than that observed in the Central Graben (Wensaas *et al.*, 1994). Transition zones in the Northern North Sea are related to gradual reductions of mudstone porosity and permeability reductions with increasing depth (Mello *et al.*, 1994) and see Section 5.4.6). An additional mechanism must be advanced for the sharp transition zones in the KCF of the Central Graben. Fluid generation within the KCF is a probable mechanism.

Thus a spatial association exists between high overpressures and mature source rocks in the Central Graben. High overpressures and sharp transition zones in the KCF. suggest that hydrocarbon generation plays a role in Central North Sea overpressures.

4.3.2 *Magnitude of minimum stress in the Central Graben*

An increase in pore fluid pressure will increase the total stress exerted on a rock due to the poroelastic behaviour of porous, fluid-filled bodies (Biot, 1941). This increase in stress will occur if the rock is constrained by rigid boundaries. Poroelastic behaviour in rocks has been observed to occur over ten years: reduction in pore pressure in producing oilfields has caused a decrease in minimum stress (Engelder & Fischer, 1994). Thus, the driving of poroelasticity over geological time, when changes in vertical stress and horizontal strain are likely, requires continued fluid generation (Engelder & Fischer, 1994). An increase in the magnitude of minimum stress may be indicative of poroelasticity, caused by an increase in pore pressure driven by fluid generation.

Minimum stress may be approximated by the pressure recorded in a Leak-Off Test (LOT). A non-linear increase of minimum stress (as measured by LOT) with depth has been observed in the Central North Sea (Fig 4.9). This has been attributed to poroelastic behaviour of the sediments due to overpressuring (Engelder & Fischer, 1994). This has been specifically attributed to hydrocarbon generation in the Kimmeridge Clay source rock. Overpressuring due to disequilibrium compaction, with its implication of limited fluid volumes, could not drive poroelastic response. A

similar mechanism for the stress distribution in the Beaufort Basin of Western Canada has been noted by Yassir & Bell, (1994). The data of Spencer, (1987) for the Piceance Basin of the Rocky Mountains, USA, shows a similar non-linearity in stress magnitudes in gas-generating source rocks (Fig 4.10). The distribution of stress can be taken as evidence of overpressuring due to hydrocarbon generation in the Central Graben, the Beaufort Basin, and the Piceance Basin (Engelder & Fischer, 1994).

The detailed examination of pressure distribution presented in Chapter 3 reveals a complexity in the hypothesis of Engelder & Fisher (1994). The minimum stress measured by LOT increases to higher values 300-500m *above* the top of overpressure in wells such as 22/30a-1 (e.g. Fig. 3.11). The increase in minimum stress is *not* coincident with highly-overpressured formations in these wells. LOT pressures in deeper wells such as 29/5b-4 and 23/26a-7 record similar high values, and are in highly-overpressured rocks, as suggested by Engelder & Fischer (1994).

An analogous situation has been noted for the Beaufort Basin (Yassir & Bell 1994). Minimum stress increased 200-300m above the top of the overpressured rocks. The authors attributed the difference in depth between the pressure seal and the increase in minimum stress to episodic upward expulsion of overpressured fluids. Wells that exhibit increases in minimum stress above the overpressured rocks (e.g. well 22/30a-1) have been advanced as Leak Points (zones of vertical expulsion of overpressured fluids). However, as poroelastic relaxation can occur over ten years (Engelder & Fisher 1994), these fluid expulsion events must occur almost continuously and decay immediately. This rapid movement of fluid could not be supported by the low matrix porosity of the aquitard; fluid flow in fractures is the only valid mechanism. A present-day example of this nature and timescale of dynamic fluid ejection from overpressured zones has been recognised in the Louisiana Gulf Coast (Whelan *et al.*, in press). Episodic expulsion of hydrocarbons from highly-overpressured deep reservoirs to shallow, normally-pressured reservoirs occurs up a fault system on a yearly basis.

Thus the magnitude of minimum stress in the Central Graben can be taken as additional evidence that suggests that overpressure in the Central North Sea is due to hydrocarbon generation. The magnitude of minimum stress can also be considered to support the model of vertical fluid flow at Leak Points.

However, two lines of argument can be taken against this evidence. Firstly, there is a strong element of data bias in the above hypothesis. A continuous record of stress

magnitude cannot be taken in a well, and so comparing LOT pressures taken in deep, highly compacted Jurassic mudstones to trends derived from shallow Cenozoic mudstones may be invalid. It is also impossible to evaluate whether minimum stress may increase above the pressure seal in wells 29/5b-4 and 23/26a-7, as they do in Leak Points, as LOTs have not been run. Secondly, LOTs in the sub-Chalk strata show a non-standard profile (Section 3.2.4). No clear leak-off value (which normally forms a plateau on the LOT graph) can be discerned. The formations may be undergoing continued elastic deformation. The measurement may not reflect the magnitude of minimum stress.

If methodology and data quality are adequate, LOT measurements of minimum stress suggest that overpressure in the region is due to hydrocarbon generation. Additionally, they support the pattern of fluid flow advanced in Chapter 2.

4.3.3 Pressure Sealing and Pressure Generation in the Kimmeridge Clay.

The spatial association of pressure seals and high overpressure to the KCF source rock is significant. The association suggests that the geochemical process of hydrocarbon generation exerts an important control on the physical processes of fluid flow in sedimentary basins. The nature of this relationship is elucidated in this section.

The link between source rocks and overpressuring is thought to be related to the fluid volume increase that occurs as kerogen is converted to hydrocarbon (Law & Dickinson, 1985; Meissner, 1980; Spencer, 1987). However, the process of kerogen transformation is complex and the relationship of the maturation process to overpressure bears a detailed discussion. It is hypothesised that the hydrocarbon-overpressure system will follow a three-stage evolution (Fig 4.11):

(a) Generation and expulsion of oil (Fig 4.11a)

The volume balance for kerogen maturation presented by Ungerer et al (1981) is reproduced as Fig 4.12. The balance suggests that in a partly closed system (selective escape of the most reactive gases, CO₂ and H₂S, through diffusion or water solution), a Type II kerogen (such as that contained within the KCF) will undergo a *total* volume loss of 3-4% when mature for oil generation (Ro= 0.65-0.9).

Porosity increase upon maturation of oil is greater than the fluid volume increase. Clearly, a volume loss will not directly lead to overpressuring.

However, expulsion of the oil from the source rock is a complex mechanism. An review of primary migration mechanisms is presented by (Mann, 1993). Expulsion may depend on source rock permeability and interbedding with permeable conduits (Burrus et al 1993, Duppenbecker *et al* 1991), thickness (Leythauser *et al.*, 1984) or kerogen type (Pepper, 1991).

Overpressured, oil-mature source rocks are documented, and can be used for comparison to the KCF in the Central Graben. A suitable case is the Bakken Shale Fm. of the Williston Basin of Western Canada. The Bakken Fm. is a thick, overpressured source rock within a normally-pressured basin (Fig 3.13). Overpressures are confined to the Bakken Fm. which consists of mudstones and discontinuous interbedded sandstones (Meissner 1988). Fluid type is oil, with no associated water produced (Meissner 1988). The Bakken Fm. is highly overpressured (15 MPa at a depth of 2800m). The Bakken Fm. contains 3.8% TOC, with a maximum of 10% TOC (Meissner 1988), but has retained its hydrocarbons. It has not expelled petroleum outwith of the formation (Osadetz *et al.*, 1992) despite its thinness (44m maximum, Spencer 1987). This may be due to low permeability (as suggested by Burrus et al, 1993 and Spencer 1987). Well instabilities such as kicks and rapidly fluctuating gas levels (Spencer 1987) suggest open fractures, as suggested for the Kimmeridge Clay Fm. in Section 4.3.1.

Why should an oil-mature source rock become highly overpressured, if the conversion of solid kerogen matrix to hydrocarbon fluid leads to a total volume decrease? The answer may lie in the dynamic geohistory of the Williston Basin. Subsidence has continued during oil generation (Meissner 1988). Accordingly, vertical stress on the Bakken Fm. will have increased. If a rock experiencing increasing stress cannot expel fluid, either due to low permeability or adsorption of hydrocarbon onto kerogen surfaces (Pepper 1991), stresses will transfer to the interstitial fluid. The pore fluid will rapidly become highly overpressured. Thus a source rock will become overpressured if it cannot expel its hydrocarbons. The overpressure is not due to a fluid volume increase.

This model of the pressure behaviour of a source rock during oil generation is useful for interpreting the hydrogeological evolution of the KCF. The KCF encountered above 5000m depth in wells in the Central Graben is thin (10-30m). It is a high-quality source rock (Pepper 1991) and the adsorption of hydrocarbon onto kerogen

surfaces will not retard fluid expulsion upon continued compaction of the source rock. Expulsion from the KCF can be implied to be efficient (Mackenzie *et al.*, 1987). The KCF has expelled oil that may have migrated tens of kilometres from the source rock (Cayley 1987). These characteristics are the opposite of the Bakken Fm. The geochemical restriction to fluid expulsion from a source rock- and the restriction of vertical dewatering of underlying formations- will not apply to on-structure and shelf regions of the Graben. Oil generation will not affect the sealing characteristics of the KCF. The hydrogeological characteristics of the KCF will be entirely mediated by its physical permeability (Fig 4.11a).

As migration efficiencies also depend on the physical properties of the source rock (Burrus et al 1993), the greater thickness (up to 1km, Cornford 1994) of the KCF nearer to the Graben depocentres suggests that expulsion efficiency will be lower. Cornford (1994) noted that the efficiency of the petroleum system in the Central Graben is extremely low (1-2%). Oil will not be completely expelled and will remain to be cracked to gas in the source rock. The deeper, thicker sections of the KCF may show analogous behaviour to the Bakken Fm.

(b) Generation and expulsion of gas (Fig 4.11b)

Most of the wells discussed in this project penetrate Kimmeridge Clay that is currently mature for gas generation (Cayley 1987). During the conversion of Type II kerogen to gas, a major volume increase occurs (a volume increase of 57% from $R_o = 0.9$ to $R_o = 2.0$ in a partially closed system (Ungerer et al 1981)). It is noteworthy that this large volume increase at the metagenesis stage occurs only if the hydrocarbons are transformed to dry gas *without expulsion at previous stages* (Ungerer et al 1981). This situation is characteristic of poor source rocks or thick sequences of higher-quality source rocks. Thus in the Central Graben a large volume increase, and associated overpressuring, will occur within the very thick KCF. in the Graben depocentres during metagenesis (Fig 4.11b). The same process will lead to net expulsion of a single-phase gas condensate from the HPHT regions of the normally oil-prone KCF (Larter & Mills, 1991). Deep Jurassic reservoirs in the Central Graben contain single-phase gas condensate. This suggests that the process is occurring in the Central Graben.

This model of poor expulsion and gas overpressuring suggests that the thick, gas-mature KCF will be highly overpressured. The deepest wells available to this study,

such as 29/5b-4 (Fig 3.12) and 23/26a-2 (Fig 3.18), exhibit high overpressures in the KCF.

(c) Post-generative and post-expulsional role (Fig 4.11c)

The KCF is mature for gas generation in the deepest wells studied in the Central Graben. Consequently, the deeper regions of the East Forties Basin are likely to be post-mature for hydrocarbon generation. It is suggested that even in this post-mature period, the source rock will continue to exert a control on the basin hydrogeology. The KCF will have lost volume due to the conversion of rock to hydrocarbon fluid in addition to the conventional expulsion of water from a compacting mudrock. Thus the KCF will have lost more porosity than a corresponding non-petroliferous mudrock. The post-mature source rock will be more compacted, and so less porous and permeable than other mudrocks. It will form an important barrier to vertical fluid flow (Fig 4.11c).

The processes discussed above play an active role in increasing fluid pressure within source rocks. They also play a passive role in controlling the fluid flow- and thus the overpressure- in surrounding formations.

4.3.4 Hydrocarbon generation in HPHT regions

The increase in fluid volume upon the conversion of kerogen and oil to gas presented by Ungerer et al (1981) and Barker (1990) may cause high overpressures. However, the process may be affected by several important negative feedbacks:

- Cracking of oil to gas in reservoir or source rock may not lead to two-phase hydrocarbon columns, as presented by Barker (1990). Gas may dissolve in oil, and vice versa, leading to a reduced volume increase. Under Central Graben HPHT conditions, single-phase gas condensates will form (Larter & Mills 1991).
- Gas can dissolve in formation water (Fig 4.13). Gas solubility is strongly dependent on pressure (Magara, 1978). Thus gas generation in formations that are already highly overpressured will lead to the solution of over $5.3\text{m}^3/\text{m}^3$ of formation water.

- Diffusion of gas through the seal can lead to the reduction of a gas accumulation by 50% in 5 Ma (Montel *et al.*, 1993). Thus, as generation and cracking occur, gas diffusion is resulting in a volume loss from the system. Primary gas migration from source rocks is highly efficient. Thus the actual build up of overpressure is a function of generation rate and diffusion rate. Generation rate is variable and dependent on the subsidence and heating rate. Diffusion rate is variable and changes as seal porosity changes.

These three modifications to the volume balance of hydrocarbon generation and cracking demonstrate that the hydrogeology of the basin is not a fully closed system, as assumed by Barker (1990). The pressure increase resulting from the volume increase due to hydrocarbon generation will not be as great as predicted by Barker (1990). Diffusion losses ensure that overpressuring due to gas generation is dependent on a rapid rate of generation.

The physical and chemical processes operating during hydrocarbon generation are summarised in Fig 4.15.

4.4 Aquathermal Pressuring

Aquathermal pressuring has been re-evaluated in recent years (Luo & Vasseur 1992; see Section 2.7), and the conditions under which this overpressuring mechanism may operate have been more precisely identified.

A crucial consideration is the application of Darcy's Law to lithologies. If Darcyian flow is negligible, thermal expansion of water is extremely significant to overpressuring (Miller & Luk, 1993). Darcy's Law may be considered inapplicable to evaporite formations in the Central North Sea due to the absence of matrix permeability that could support Darcyian flow. Thus aquathermal pressuring may explain the extremely high pore pressures encountered in porous dolomite formations enclosed within Permian Zechstein salt in the region (e.g. well 29/27-1), where the pressure cannot be related to rapid subsidence or hydrocarbon generation. The Zechstein Salt itself is not highly overpressured.

A decrease in effective stress values is required for aquathermal pressuring to affect rocks supporting Darcyian flow. As stated in Luo and Vasseur (1993), such conditions are rarely met in natural systems, requiring very low permeabilities and inhibition of hydraulic fracturing. Reductions in effective stress may occur at the

crests of fault blocks in the Central Graben (Fig 4.15). However, this reduction in effective stress is a local effect. The crests of fault blocks are in hydraulic communication with deeper regions. In deeper, off-structure regions, effective stress will always increase during burial (as suggested by the one-dimensional analysis of Luo & Vasseur, 1993). Thus any aquathermal pressuring will be local and will be dissipated in the large volume of fluid in hydraulic communication with zones undergoing aquathermal pressuring.

Unloading upon uplift may cause reductions in the effective stress acting on a rock. However, uplift cannot result in aquathermal pressuring as the rocks are cooled (Luo & Vasseur, 1992). However, if uplift can occur without cooling, aquathermal pressuring may result. In the Central Graben, 100-200m of uplift has occurred in the early Tertiary as a result of transpression (Roberts *et al.*, 1990). Note that some salt domes have maintained geostatic equilibrium, but this is not uplift (Hodgson *et al.*, 1992) Tertiary uplift may have occurred in rising geothermal gradients (Burley, 1993), maintaining the temperature of the rocks. The "Tertiary hot fluid flush" is noted from anomalously hot fluid inclusions (Burley 1993), but it can be challenged by re-interpretation of the same data (Osborne & Haszeldine, 1992). Additionally, it is not supported by a pattern of declining heat flow since the Jurassic inferred from vitrinite reflectance data (Cornford 1994), which suggests lowered geothermal gradients in the early Tertiary. Finally, during the early Tertiary, the regional aquitard had not achieved deep burial and so was unlikely to be highly compacted and impermeable. Consequently Darcyian flow would have been high, and fluid escape would have been easy.

In summary, aquathermal pressuring is considered to be of minor relevance to the Central Graben of the North Sea, affecting only porous dolomite formations within the Zechstein salt.

4.5 Clay Mineral Dehydration

The smectite-illite transformation occurs at temperatures corresponding to between 2000-3000m in the North Sea (Burst, 1969; Pearson & Small, 1988). Although this reaction releases considerable quantities of water (section 2.7), the dehydration will have occurred prior to deep burial of the regional aquitard. Any perturbation of the formation fluid pressure above 3000m is likely to be geologically transient (Mello *et al.*, 1994). Unless the causal process is ongoing, the overpressure will be dissipated rapidly. The overpressuring will not be preserved to present-day burial depths as the

dehydration process will cease before the critical 3000m mudstone-compaction depth defined by Mello (1994). Clay mineral transformation cannot be the causative mechanism of sub-KCF overpressures in the Central North Sea.

The contribution of clay mineral dehydration to overpressures in the Tertiary mudstones is less clearly defined. The approximate depth to overpressure in the Tertiary mudstone sequence is coincident with smectite-illite dehydration depths. However, sonic log and "d"-exponent measurements suggest undercompaction in these formations. The magnitude and distribution of the overpressure is adequately described by quantitative models of sediment compaction being inhibited by the low permeability of the mudstones. Accordingly, the philosophical application of Occam's Razor suggests that clay mineral dehydration plays little role in the overpressuring in the Tertiary section.

4.6 A synthetic model for the origin of Central North Sea overpressure

The data presented and discussed above implies that (a) disequilibrium compaction of the Graben sediments has caused anomalously high mudstone porosities. This suggests that overpressuring is caused by restricted fluid flow in the sub-seal regions. The data also suggests that (b) fluid generation due to hydrocarbon generation in the Kimmeridge Clay source rock has led to high pressures in the formation, and overpressure in the region is maintained by continued hydrocarbon generation in off-structure regions at the present day (Fig 4.17). Thus the cause of the disequilibrium of fluid energy in the Central North Sea is demonstrated to be due to the combination of (a) the *external, physical* process of disequilibrium compaction, which has affected overpressure on the basin-scale; and (b) the *internal, chemical* process of hydrocarbon generation within the Kimmeridge Clay source rock, which has led directly to high pressures being generated in the Kimmeridge Clay Fm. and indirectly to a further restriction of fluid flow in the underlying strata. Aquathermal expansion and clay mineral transformations do not play an important role in causing Central North Sea overpressure.

It is impossible to differentiate the mechanisms of disequilibrium compaction and hydrocarbon generation in the Central North Sea on the basis of observed data. Hydrocarbon generation cannot adequately account for the high porosities of overpressured mudstones without the contribution of disequilibrium compaction. Disequilibrium compaction alone cannot account for the small-scale distribution of

overpressure within the mudstone aquitard, and cannot explain the increase in the magnitude of minimum stress in the overpressured rocks.

However, these two mechanisms are not incompatible. Both require restricted fluid flow. It would appear from observational data that both mechanisms are required. Hydrocarbon generation actively increases overpressure in source rocks; it also passively controls overpressure in adjacent formations. A synthetic model that combines both overpressuring mechanisms can be constructed. However, it is unclear whether hydrocarbon generation plays an active role in causing basin-scale overpressure outwith source rocks in the Central Graben. By analogy with other basins such as the Anadarko Basin of the USA (Ortoleva, 1993) and the Mahakam Delta of SE Asia (Burrus *et al.*, 1993), it can be shown that both hydrocarbon generation and disequilibrium compaction can actively cause basin-scale overpressure. It is unclear from the present study which mechanism plays the dominant role in Central North Sea overpressure. For insight into the relative importance of the two causal processes, and to quantify how much overpressure each process can contribute, we are forced to rely on theoretical models of the physical processes at work (see Section 5.2). Acquisition of additional observational data on mudstone porosity and experimental data on volume changes during hydrocarbon generation may allow the refinement of the models.

In the Jurassic depocentres of the Central Graben, more than 1km thickness of mudstones may be undercompacted and may be generating gas. Whichever overpressuring mechanism is dominant in the Central Graben, it is likely that the mechanism is acting in these depocentres. The pressure measured in exploration wells on relatively shallow structures will be controlled by processes occurring in these unobserved regions.

The synthetic model presented by this chapter, based on observational data, is that compaction disequilibrium of the thick mudstone sequences in the Graben combined with hydrocarbon generation in the Kimmeridge Clay Formation controls the magnitude and distribution of overpressure throughout the region. The synthetic model is shown in Figure 4.16.

4.7 Conclusion

Overpressure in the Central North Sea is caused by disequilibrium compaction of the mudstone-rich section, combined with fluid volume increase upon hydrocarbon generation in the gas-mature source rocks. These two dominant overpressuring mechanisms operate at different scales. Rapid subsidence of the basin during the Cenozoic has led to basin-wide overpressuring as the sediments seek to adjust to loading by expelling fluid. Generation of gas condensate has further elevated pressures within the Kimmeridge Clay Fm. This has led to a dynamic regulation of pressures and stresses in the basin.

The two overpressuring mechanisms affect each other in a series of feedbacks. Overpressure resulting from hydrocarbon generation restricts the compactional flow of water, and the effects of hydrocarbon generation are, in turn, modified by imposed elevated fluid pressure.

The disequilibrium in the system is caused by the response of rock pores to both external imposed stresses (ultimately caused by global-scale plate reorganisation, Van Balen & Cloetingh, 1994) and to internal pore volume changes that operate on a scale of microns. It is clear that pore-scale physico-geochemical processes control the characteristics of basin-scale pressure cells. This scaling-up of process is typical of complex dynamic systems (Waldrop, 1993). The dynamic perturbation of the equilibrium of basinal fluids by the internal and external mechanisms detailed in this chapter produce the energy imbalances that control fluid flow in the Central Graben today.

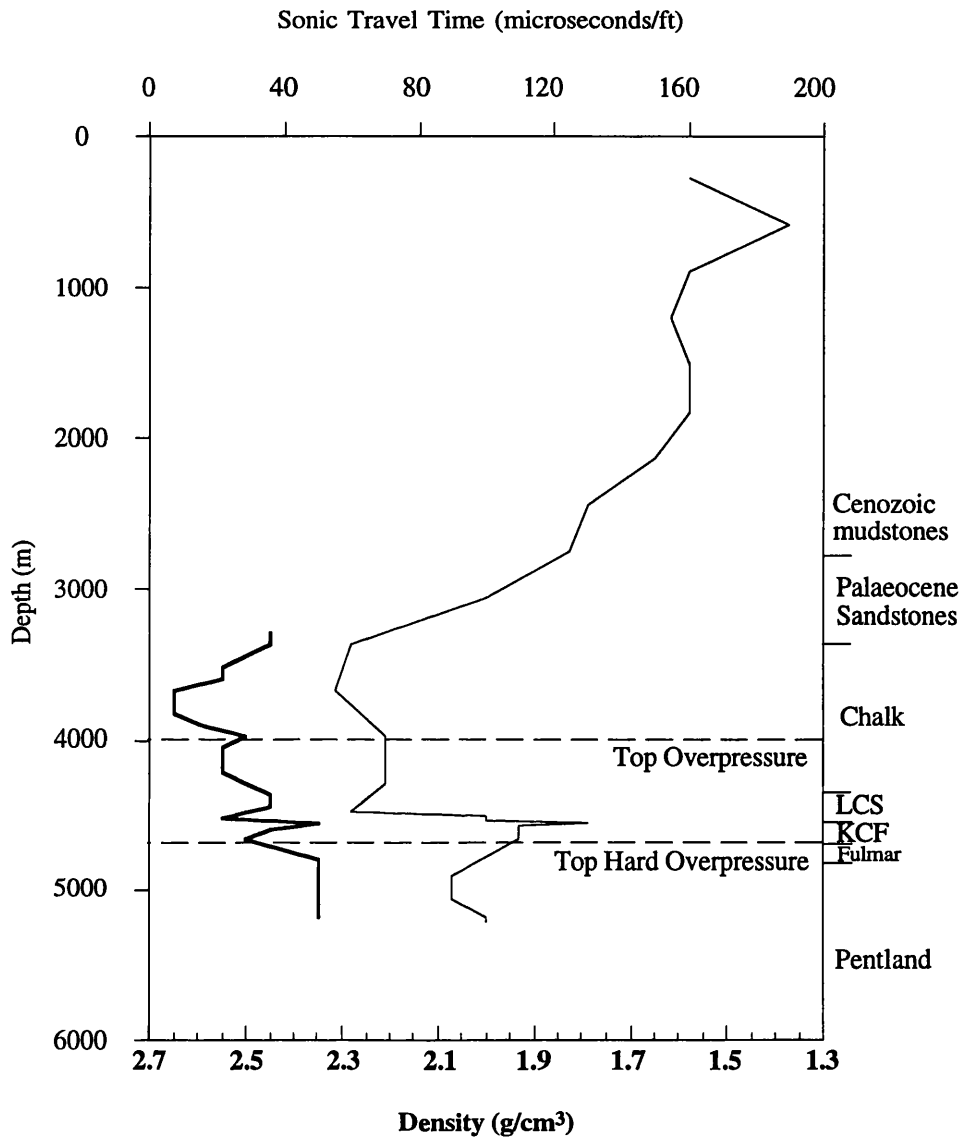


Figure 4.1 Sonic and density logs of well 22/30a-1. Density log is heavy line. LCS is Lower Cretaceous, KCF is Kimmeridge Clay Fm. Low sonic velocity and low density in overpressured rocks suggests that the overpressured regions have anomalously high porosity. This in turn suggests that overpressure may be caused by disequilibrium compaction of the sediments.

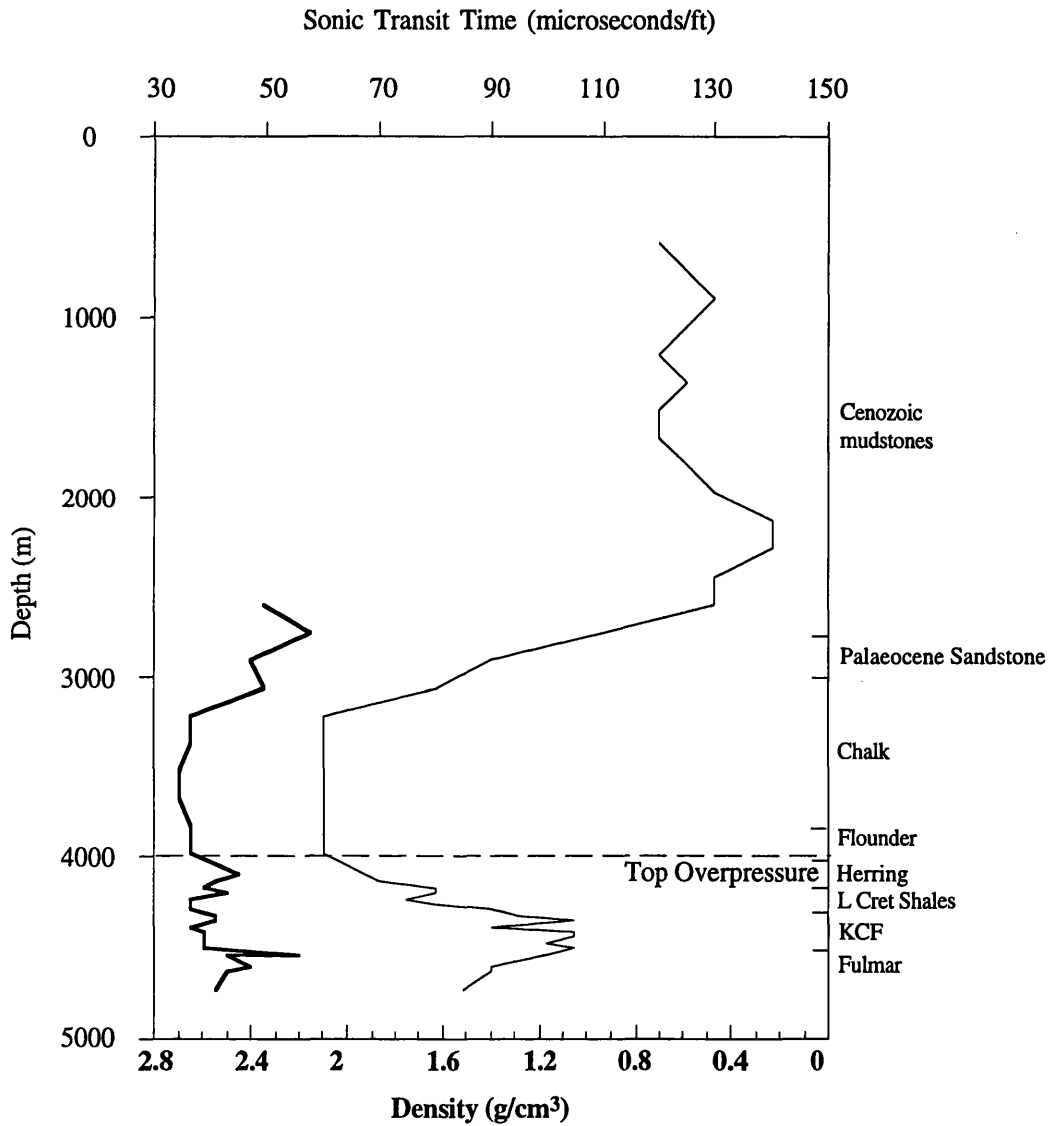


Figure 4.2 Sonic and density logs of well 22/27a-1. Density log is heavy line. Low sonic velocity and low density in overpressured rocks suggest that anomalously high porosity exists in the overpressured rocks.

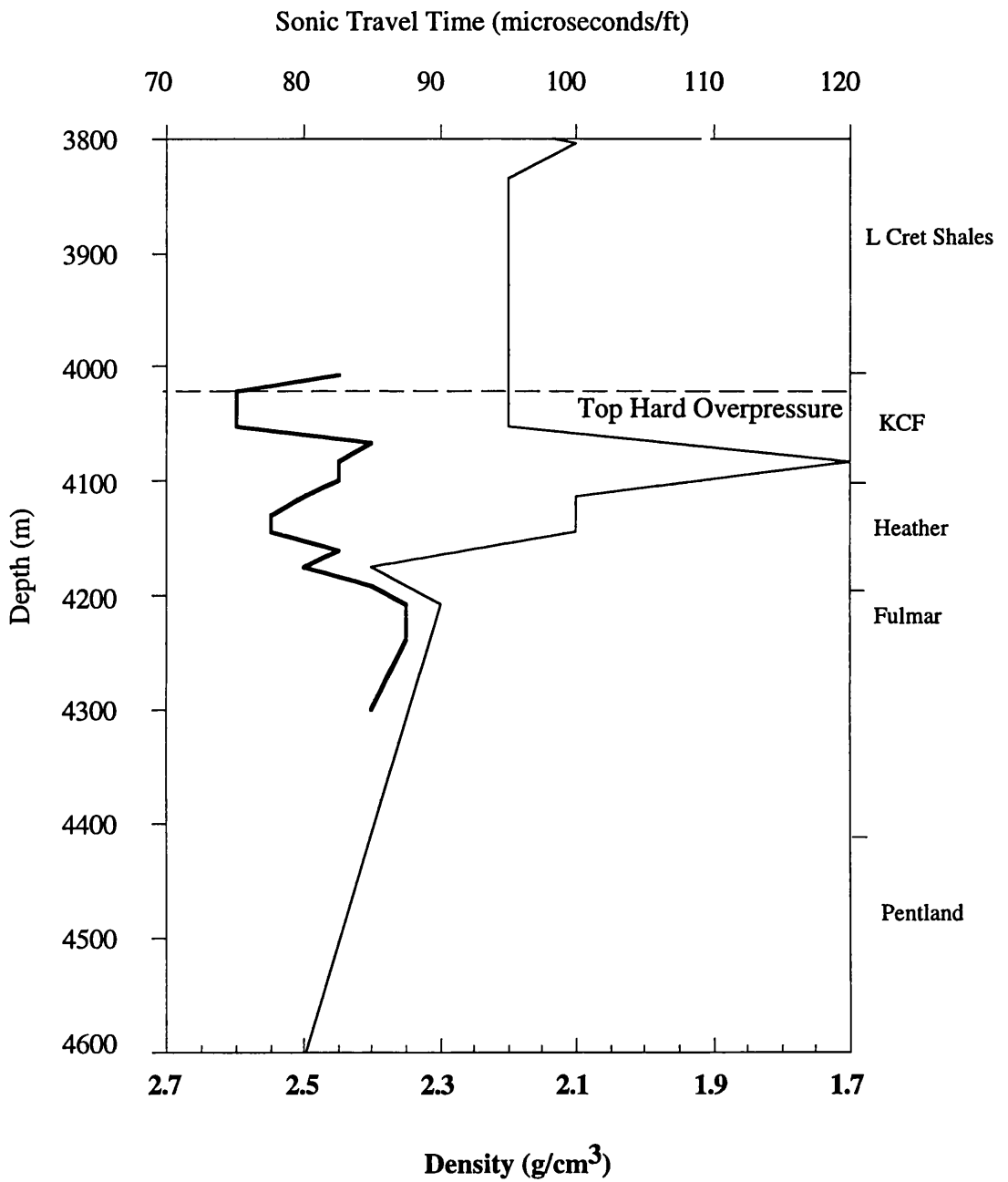


Figure 4.3 Sonic and density logs of well 29/10-2. Density log is heavy line. Low sonic velocity and low density in overpressured rocks suggest that anomalously high porosity exists in the overpressured region.

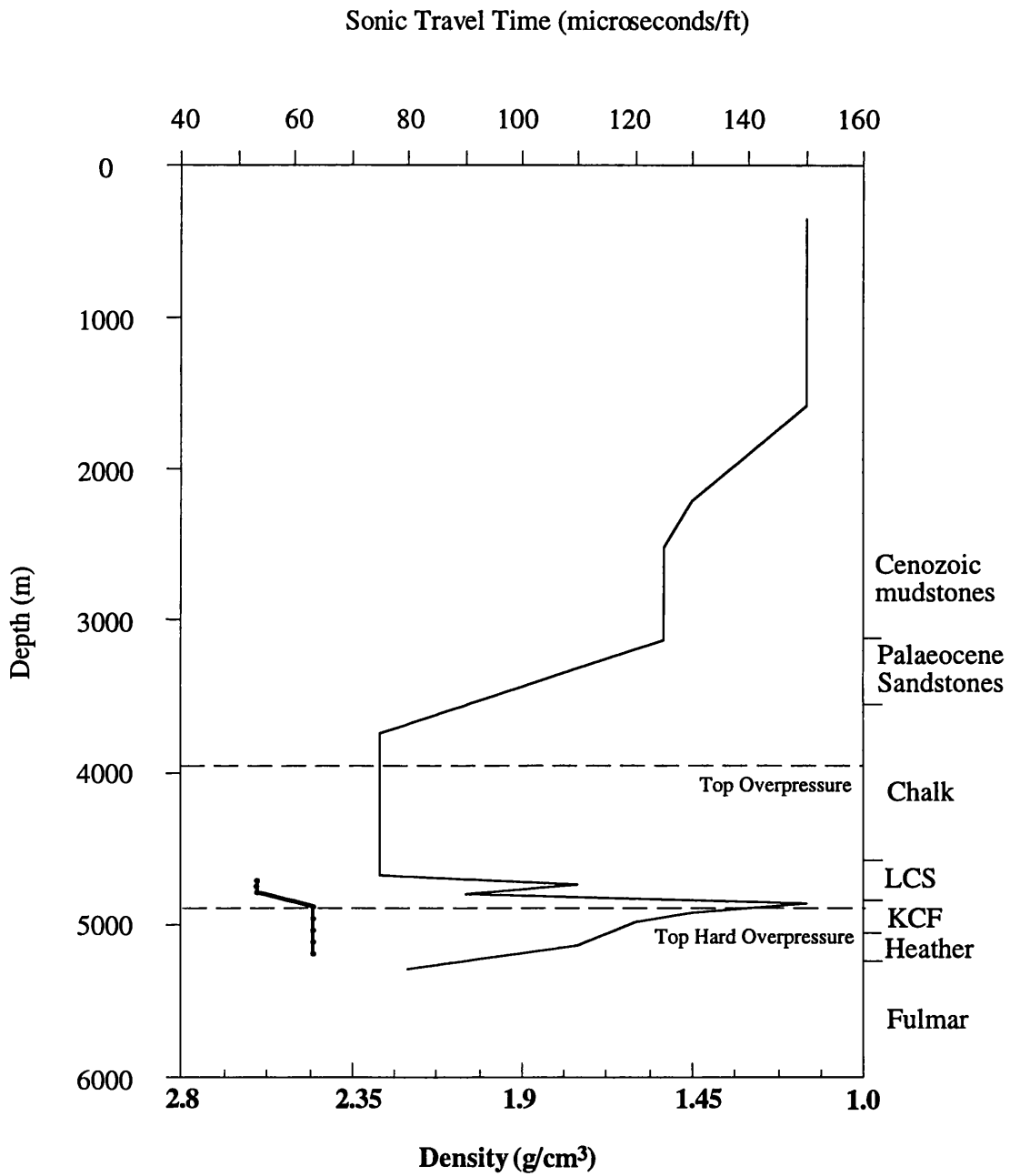


Figure 4.4 Sonic and density logs of well 23/26a-2ST. Density log is heavy line. Low sonic velocity and low density suggests high porosity in overpressured rocks.

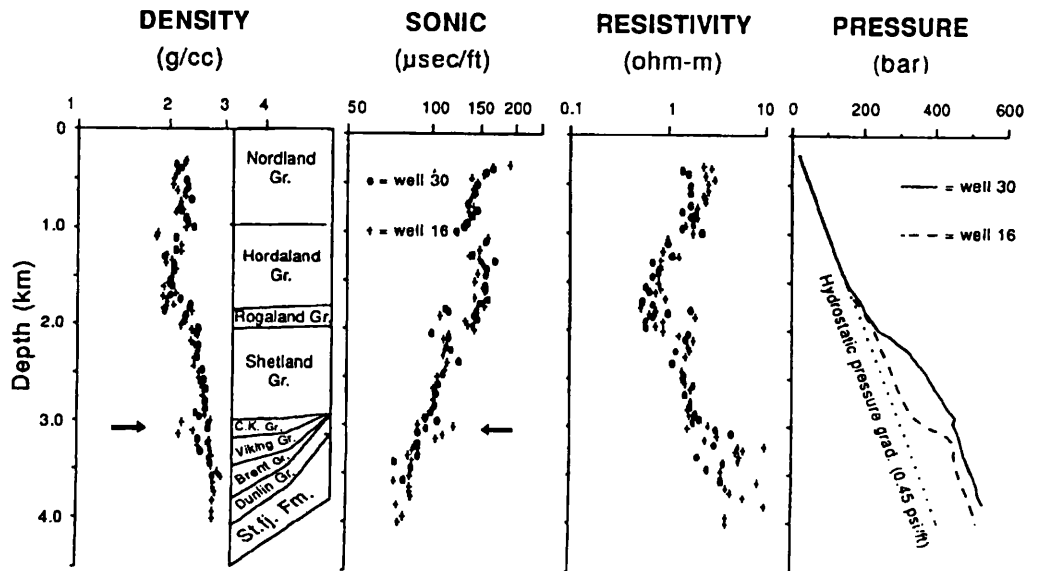


Figure 4.5 Pressure and wireline logs from the Gullfaks area, Northern North Sea (from Wensaas et al 1994).

Transition zones are smoother and more gradual than those noted for the Central Graben. This is suggested to be due to the contribution of hydrocarbon generation in the Kimmeridge Clay Fm. source rock in the Central Graben. A pressure difference of 100 bars in the Cretaceous section is not associated with any variations in sonic log response. Arrows point to deflections in sonic and density logs due to lithological effects. Sonic velocity reflects effective stress and not porosity in this region.

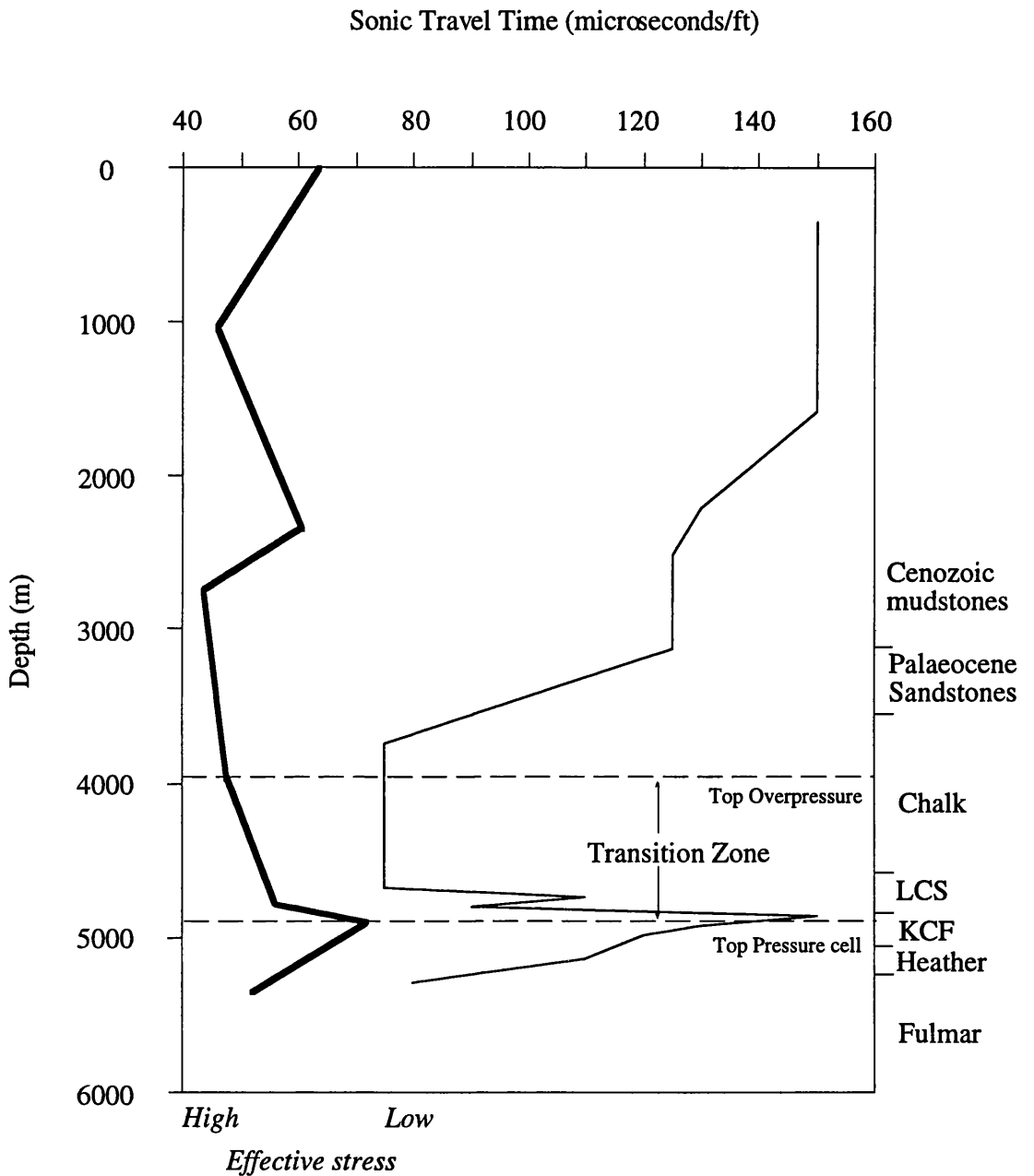


Figure 4.6 Sonic log and effective stress in well 23/26a-2ST. Effective stress is approximated by the heavy line. Effective stress will increase with depth as loading increases unless pore fluid is overpressured. Thus effective stress will decrease in the pressure seal and reach a minimum at the top of the pressure cell. Effective stress will increase with depth in the pressure cell. The sonic velocity appears to closely follow these variations in effective stress.

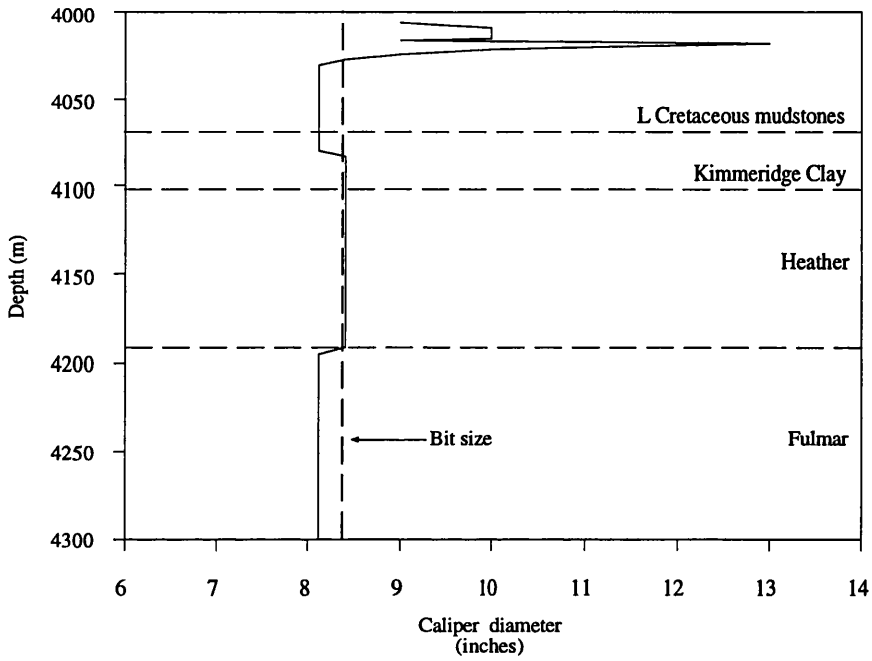


Figure 4.7 Caliper log of well 29/10-2. Undercompacted, sloughing mudstones are encountered in the L. Cretaceous leading to a hole size in excess of the bit size. A mud cake has reduced hole size in the Fulmar Fm.

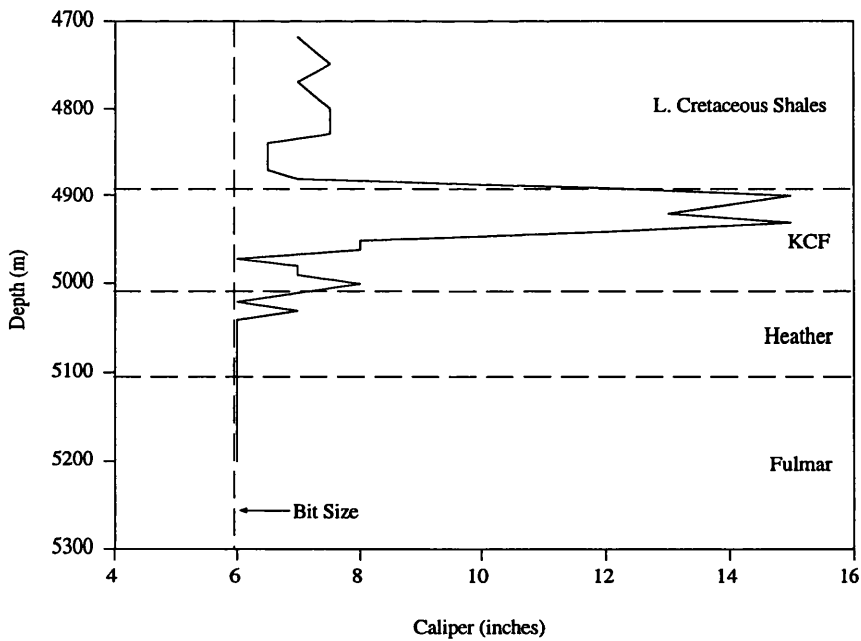


Figure 4.8 Caliper log of well 23/26a-2ST. Undercompacted, sloughing mudstones lead to a hole size greater than the bit size in the L. Cretaceous and KCF.

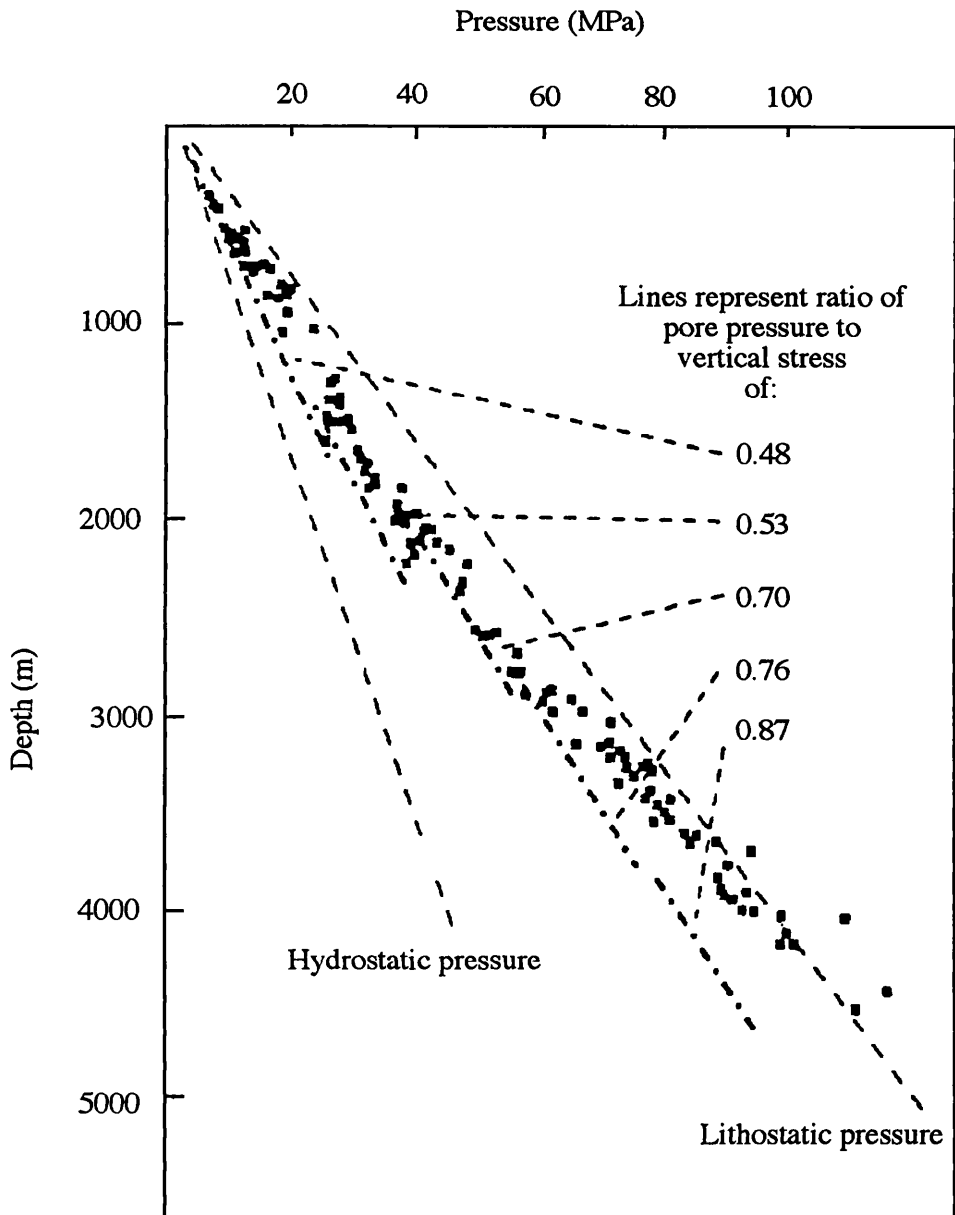


Figure 4.9 Graph of Leak-off Test pressures against depth from wells in the Central Graben (from Engelder & Fischer 1994). LOTs approximate the minimum stress acting in the basin. The minimum stress shows an increase with depth, which may correspond to poroelastic behaviour of the sediments.

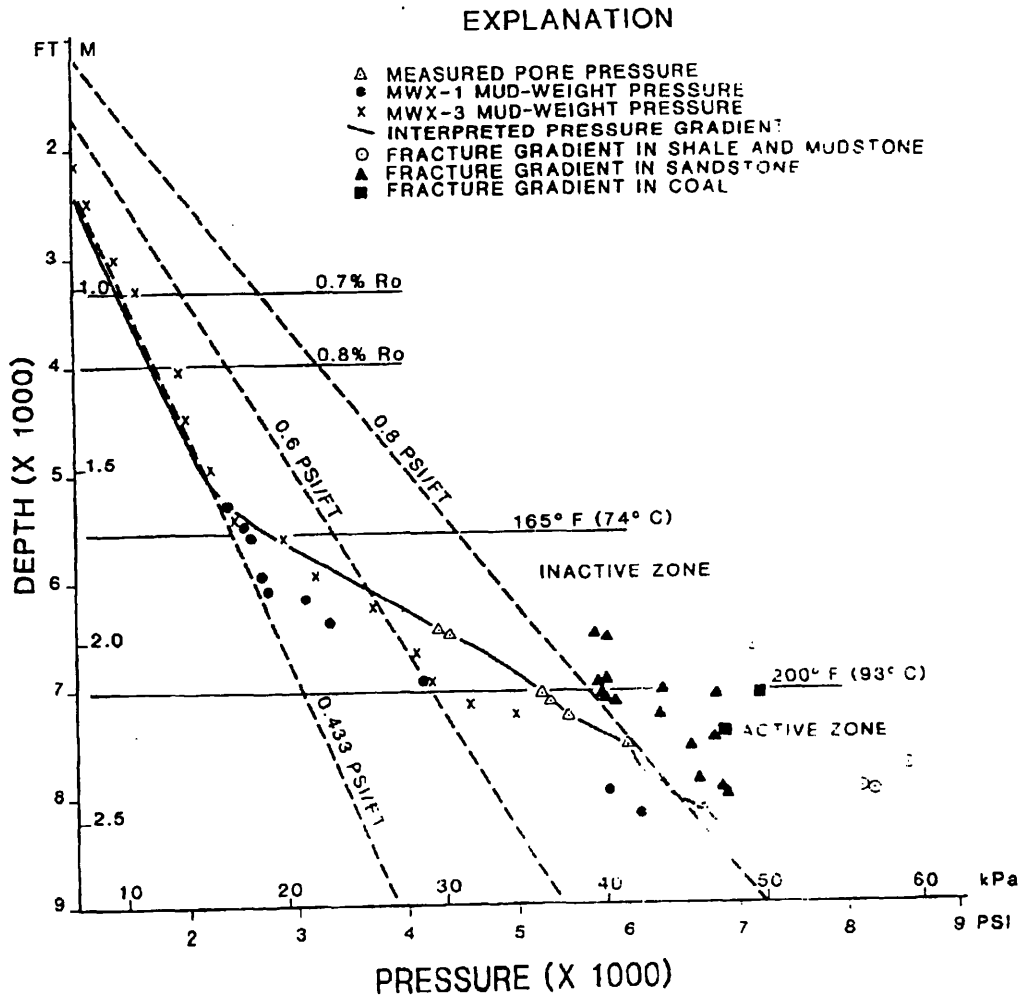


Figure 4.10 Pressures and stresses in the Piceance Basin, Rocky Mountains (from Spencer, 1987)

The fracture gradient (an approximation to the minimum stress) shows an increase in the overpressured zone. This is a similar pattern to that of the Central North Sea (Engelder & Fischer, 1994; Fig 4.9). The increase in stress may be attributed to poroelastic behaviour of the rock due to fluid generation at depth in source rocks. Note that Spencer (1987) attributes all overpressuring in the Piceance Basin to hydrocarbon generation.

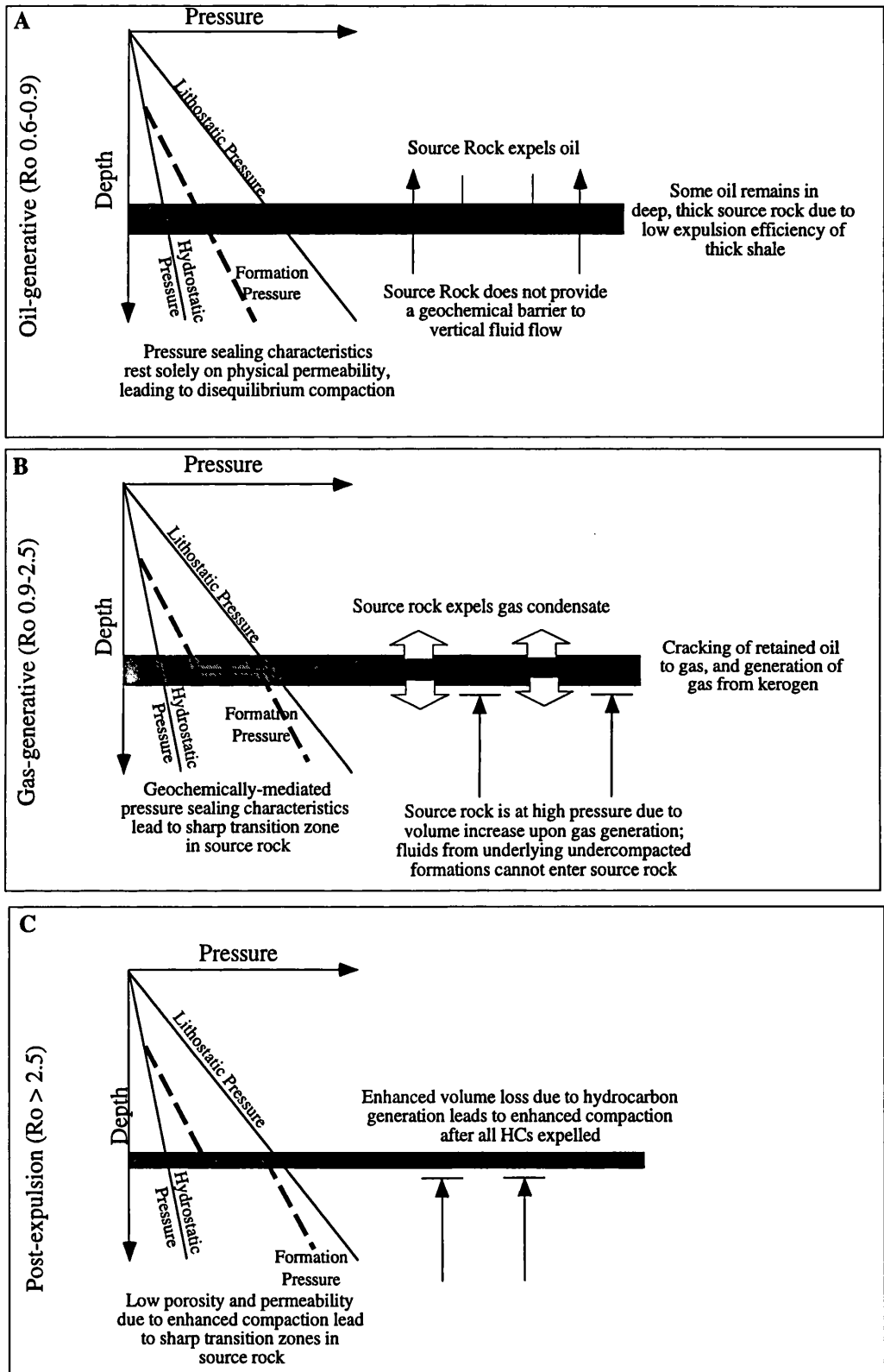


Figure 4.11 Three-stage evolution of Kimmeridge Clay Fm. overpressure. The pressure characteristics are mediated by the maturity and expulsion of hydrocarbons.

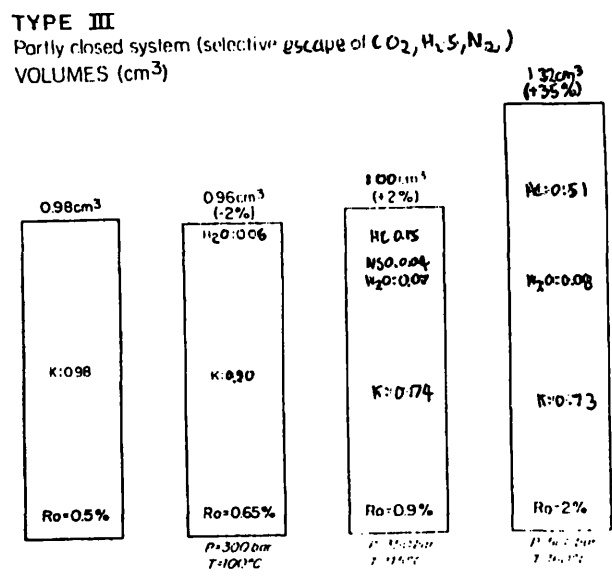
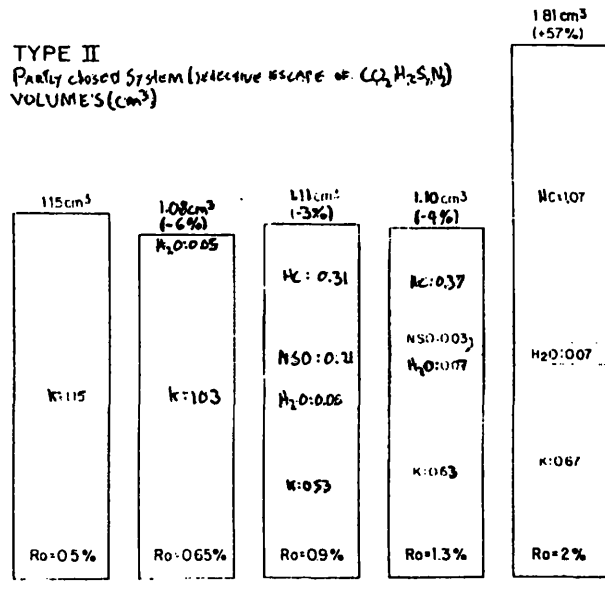


Figure 4.12 Volume changes during hydrocarbon generation (from Ungerer et al (1981)).

Source rocks containing Type II and Type III kerogens undergo a volume loss during generation. This assumes that the most volatile products (e.g. carbon dioxide) can escape. During gas generation, both systems undergo a major volume increase if no hydrocarbons have previously been expelled.

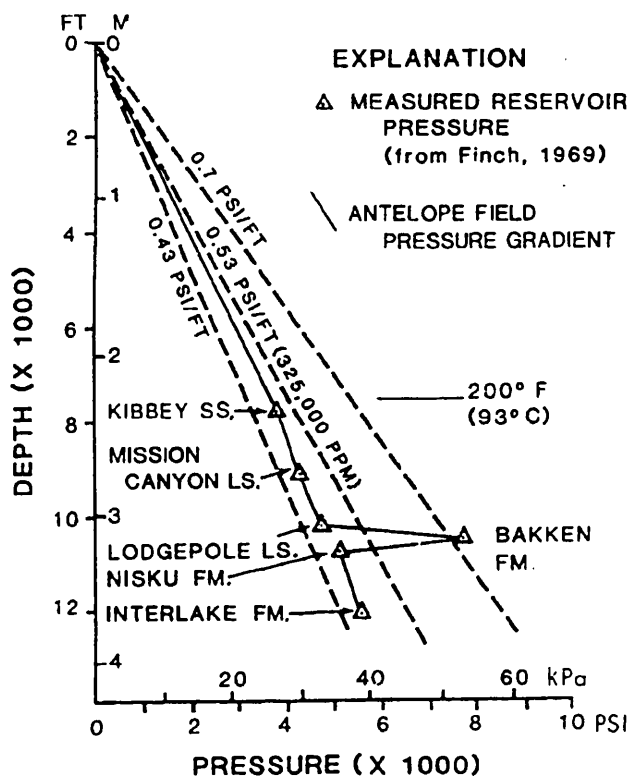


Figure 4.13 Formation pressures in the Williston Basin, from Meissner (1978)

The Williston Basin is generally normally pressured, but high overpressures are encountered within the Bakken Shale Fm. The Bakken Fm. is a mudstone source rock that has not expelled hydrocarbons. Restriction of fluid movement in this formation has led to high overpressure. This overpressured oil-mature source rock provides a useful comparison to the Kimmeridge Clay Fm. (KCF) in the Central Graben. Deep, thick regions of the KCF will behave analogously to the Bakken Fm. due to low expulsion efficiency. Thin, shallow regions of the KCF will not be overpressured due to high expulsion efficiencies.

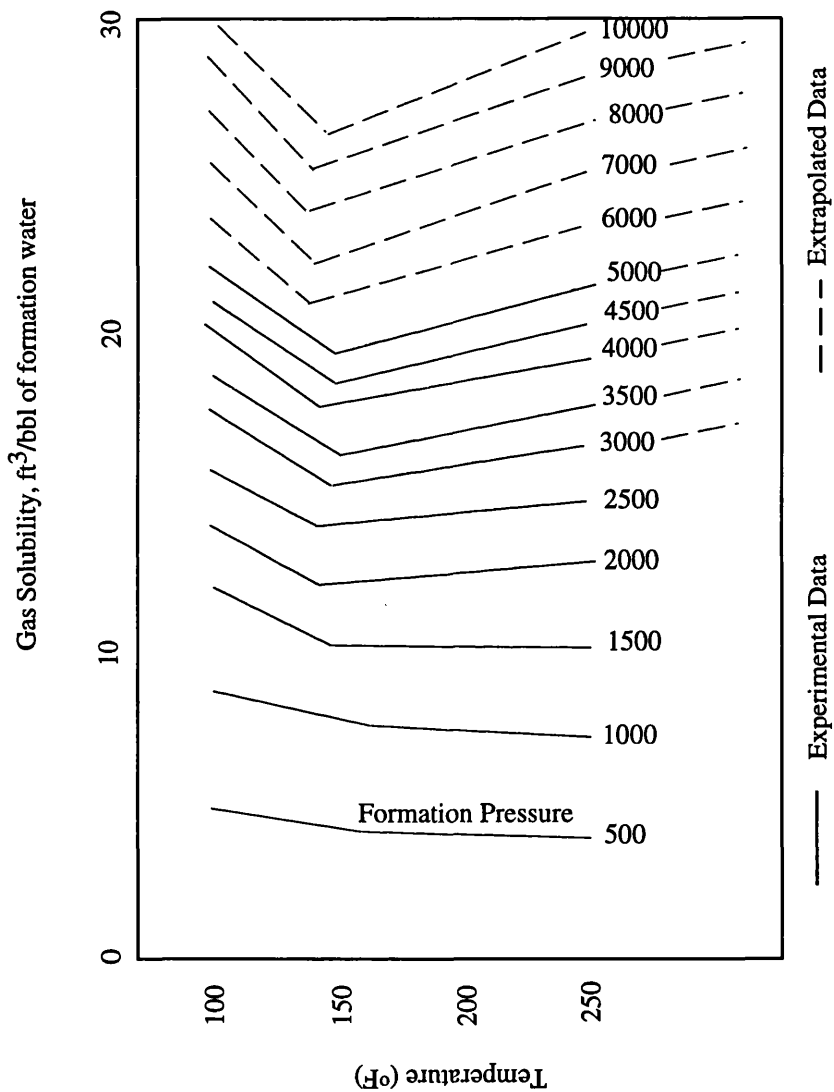


Figure 4.14 Solubility of natural gas in formation water (after Magara (1978)). Gas is extremely soluble in formation water at high pressures. Accordingly the pressure resulting from volume expansion due to gas generation will be reduced by this negative feedback.

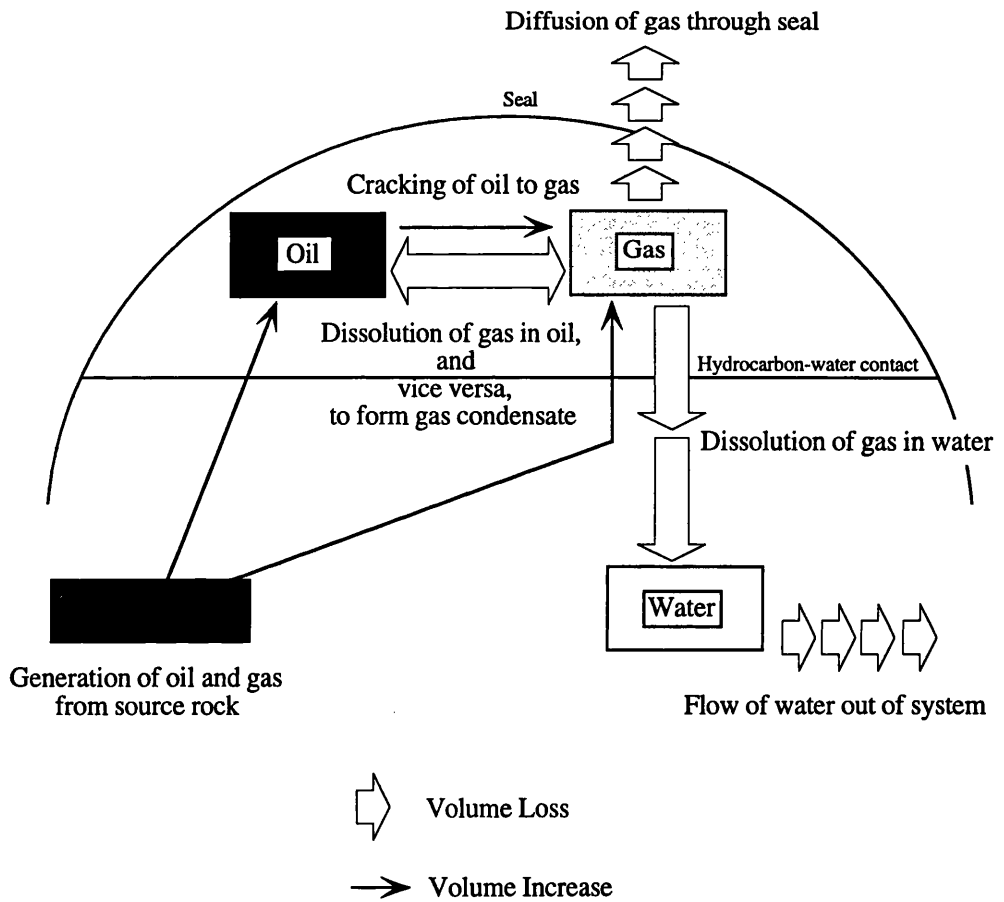


Figure 4.15 Volume changes affecting hydrocarbons in HPHT environments.

The complex processes of hydrocarbon generation can increase the fluid volume of the basin. However, the processes are subject to a series of negative feedbacks such as dissolution, diffusion and advective flow. The complexity of these inter-relationships makes quantification of the pressure caused by hydrocarbon generation extremely difficult.

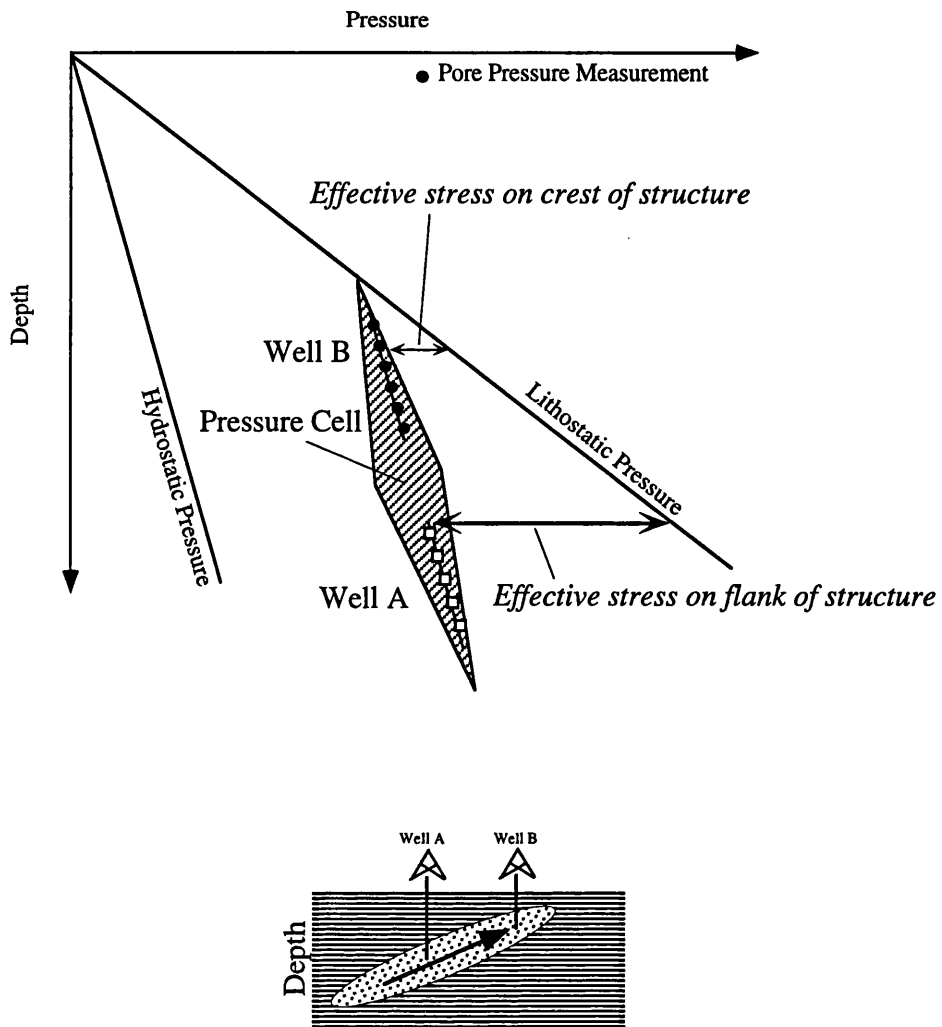


Figure 4.16 Effective stress in a dipping sandstone

If the crest of a dipping sandstone is in hydraulic communication with the deeper flanks, i.e. forms part of the same pressure cell, the effective stress will be low at the crest. This effective stress will have been reduced from higher levels prior to overpressuring. The pressure and effective stress experienced by the crest is dictated by processes occurring at greater depths. Thus crestal regions may locally satisfy conditions for aquathermal pressuring. Pressure can be dissipated in the large volume of water within the cell where aquathermal pressuring cannot occur.

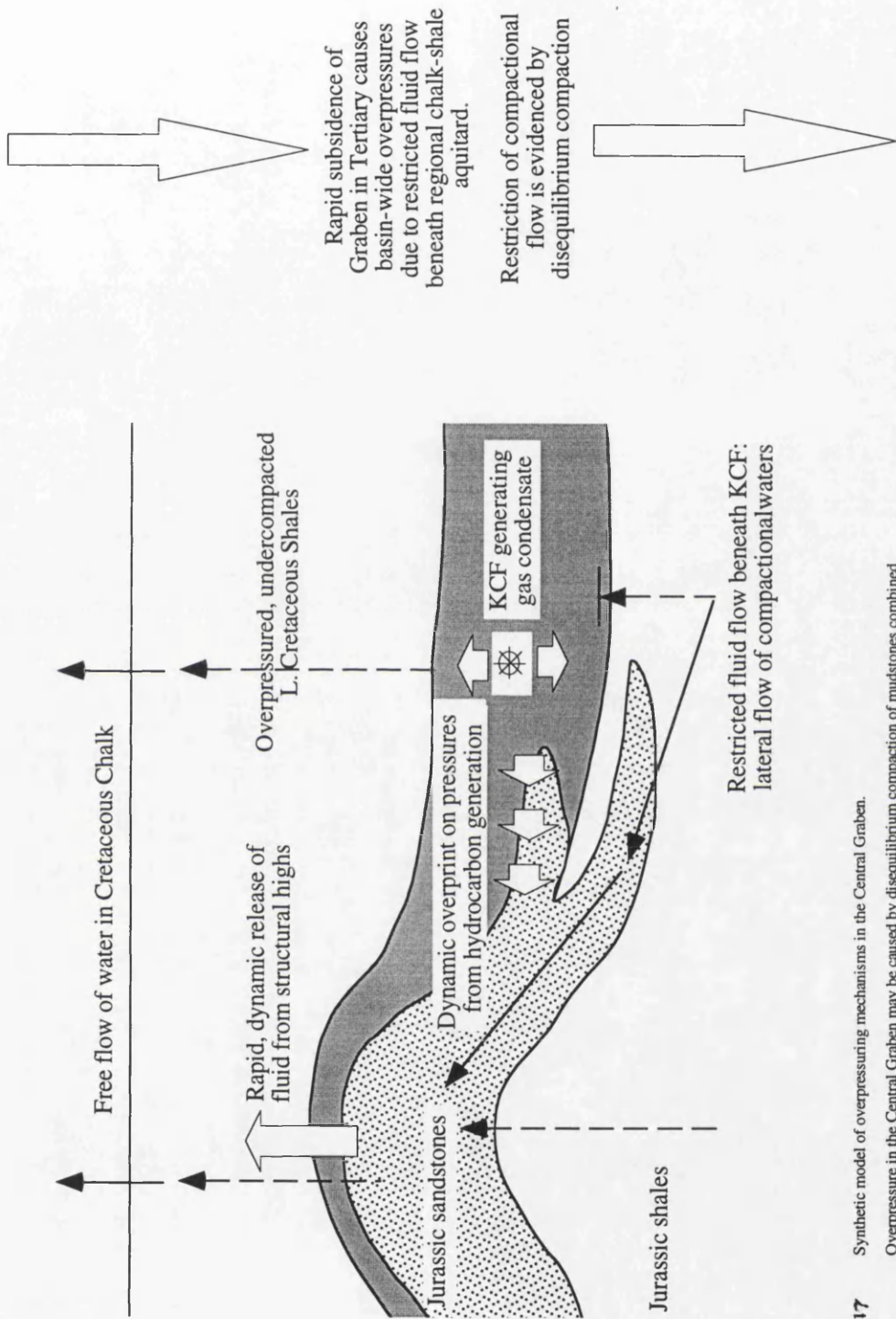


Figure 4.17 Synthetic model of overpressuring mechanisms in the Central Graben. Overpressure in the Central Graben may be caused by disequilibrium compaction of mudstones combined with gas generation in thick source rocks. Note that both these mechanisms are active in off-structure regions that are not yet penetrated by wells. It is impossible to differentiate the mechanisms of disequilibrium compaction and hydrocarbon generation in the Central North Sea on the basis of observed data. Hydrocarbon generation cannot adequately account for the high porosities of overpressured mudstones without the contribution of disequilibrium compaction. Disequilibrium compaction alone cannot account for the small-scale distribution of overpressure within the mudstone aquitard, and cannot explain the increase in the magnitude of minimum stress in the overpressured rocks.

Chapter Five

A Model Investigation of Central North Sea Overpressure

- 5.1 Introduction**
- 5.2 Review of existing model approaches**
- 5.3 Choice of methodology: the philosophy of modelling**
- 5.4 One-Dimensional Models**
 - 5.4.1 Aims of the one-dimensional model investigation*
 - 5.4.2 Data*
 - 5.4.3 One-dimensional model methodology*
 - 5.4.4 Evaluation of sensitivity to variations*
 - 5.4.5 One-dimensional model results*
 - 5.4.6 Discussion and conclusions*
- 5.5 Two-Dimensional models**
 - 5.5.1 Aims of two-dimensional model investigation*
 - 5.5.2 Data*
 - 5.5.3 Two-dimensional model methodology*
 - 5.5.4 Two-dimensional model results*
 - 5.5.5 Model hydrocarbon generation and migration*
 - 5.5.6 Evaluation of sensitivity to variations*
 - (a) Variation in lateral permeability and extent of sandstones*
 - (b) Variation in fault permeability*
 - (c) Variation in aquitard permeability*
 - (d) Sensitivity Summary*
 - 5.5.7 Discussion*
- 5.6 Conclusions**

5.1 Introduction

The previous chapters have demonstrated that overpressure in the Central North Sea is a facet of a dynamic hydrogeological system, and that this system is controlled by the complex interaction of structural, geochemical and fluid-flow components within the basin. The analysis of dynamic systems, where the characteristics of the system are determined by the interaction of numerous variables, has recently undergone a revolution. The advent of quantitative simulation of complex data using powerful computers has formed a new arm to scientific analysis, to be added to observational description and laboratory experiment. Computers allow the simulation of numerous interacting variables, and may reveal facets of the system that are invisible to simple descriptive investigations. Computer simulation is used in the analysis of many complex systems such as weather prediction, the global economy and even urban motor traffic flow (Waldrop, 1993).

Basin hydrogeology lends itself to investigation by computer simulation due to the complexity of the non-linear processes at work (Dewers & Ortoleva, 1994) and the extrapolation necessary due to the paucity of observational data. Computer simulation of basin processes is a rapidly-evolving field in geoscience. Computer-based hydrogeological models have been presented for many regions of the world (see Section 5.2), and computer modelling now forms a routine part of hydrocarbon exploration and prospect evaluation.

The aims of this chapter are:

- To use computer simulation of the dynamic processes of basin hydrogeology to arrive at a process-based understanding of the present-day pressure distribution in the Central Graben. One-dimensional models are used to investigate the interplay between subsidence rate and overpressuring and to formulate qualitative hypotheses that are fully explored and quantified by two-dimensional models. The methodology employed is discussed, and the results compared to observational data to test the models.
- To extrapolate these results from the present-day into the geological past, to gain insight into the palaeo-hydrogeology of the basin.
- To quantify the controls on the origin and distribution of overpressure by testing of the data-driven hypotheses developed in Chapters 2 and 3.

Computer simulation thus serves as a procedure for a *quantitative* assessment and critique of observational hypotheses, and as a *qualitative* theoretical framework for investigating the hydrogeological processes active in the Central Graben.

5.2 Review of existing model approaches

Hydrogeological models have developed along two main branches in the past ten years of research. One main branch of model is the "static" hydrogeological model that simulates flow by topographic drive through an unchanging, non-compacting basin geometry (e.g. Garven, 1989). The second branch of models is formed by those models that simulate the time-dependent change in basin geometry due to sediment loading, which are termed "basin models". This form of model may be further divided into two types. "Physical" models are based primarily on the physical description of compaction due to sediment loading (e.g. Audet & Fowler, 1992; Person & Garven, 1992; Ungerer *et al.*, 1990). These focus on organic geochemical processes to allow simulation of hydrocarbon maturation and migration. The second type of basin model are "physico-geochemical" models that are fully coupled to inorganic geochemistry, and whose methodology is based on time-dependent geochemical compaction (Dewers & Ortoleva 1994).

Basin models have been applied to numerous case studies in basins world-wide. Physical models are more widely used in applied studies than physico-geochemical models, due to their earlier development and lower hardware requirements; their use is also favoured by their clear application to economically-relevant phenomena such as hydrocarbon migration. Physical models are exemplified by the two-dimensional TEMISPACK code (Ungerer *et al.* 1990). The development, refinement and results of this code have driven much quantitative hydrogeological research in hydrocarbon basins during the past ten years. Indeed, the physical methodology and mathematical descriptions pioneered by TEMISPACK's developers have become standard to quantitative modelling methodology, and integral to basin hydrogeological description.

Physical models have been applied to the Mahakam Delta (Burrus *et al.*, 1993), the Viking Graben of the North Sea (Burrus *et al.*, 1991), the Gulf of Mexico (Bethke, 1986), the Central North Sea (Mudford *et al.*, 1991; Symington *et al.*, 1994), the Venture field of Eastern Canada (Forbes *et al.*, 1992), and the Bering Sea (Bour & Lerche, 1994), and many other regions. Physico-geochemical models such as CIRF.B (Ortoleva, 1993) have been primarily applied to the Anadarko Basin of the

central USA. Thus physical models have been developed and applied to young, actively subsiding and compacting basins, while physico-geochemical models have been developed in older, static basins with extensive diagenetically-cemented aquitards (Dewers & Ortoleva 1994). These differing geodynamic settings exhibit widely differing hydrogeologies. As the evolution of a model is based in part on the adequacy of its description of observational data, it is unsurprising that different models emphasise different aspects of hydrogeology. However, all modelling studies emphasise that aquitard permeability is the dominant control on overpressure.

Application of the two different forms of basin models to different geodynamic environments has only recently begun, with the study of the Williston Basin, onshore USA, using TEMISPACK (Burrus *et al.* 1993) and the study of the Viking Graben using CIRF.B (Payne & Park, 1995). Both types of models provide adequate representations of the observed hydrogeology.

Advances in computer hardware have allowed basin models to develop from initial one-dimensional studies into two dimensions. Three-dimensional simulations are now developing (Mudford, in press; Park *et al.*, 1995).

The application of basin models to the North Sea deserves full discussion in the context of the aims of this chapter. North Sea stratigraphy and structure is outlined in Section 1.4. A two-dimensional study of the Viking Graben (Burrus *et al.*, 1991) provided an accurate description of the observed hydrogeological phenomena. Undercompaction caused by rapid Cretaceous-Tertiary subsidence has caused overpressure, beginning in the late Cretaceous. Hydrocarbon generation plays little role in overpressuring. Sealed faults lead to basin compartmentalisation, and "the pressure-depth profiles correspond qualitatively to those presented by other authors (e.g. Chiarelli & Duffaud, 1980". England *et al.*, (1987) presented a one-dimensional model of sediment compaction using generalised North Sea RFT pressure data as calibration. Similarly, Mann & Mackenzie, (1990) presented a theoretical one-dimensional basin model for prediction of pore pressure, based on North Sea RFT pressures. Both of these one-dimensional studies attributed overpressuring to gravitational compaction, with observed divergence from model trends related to structural complexity. In a more detailed study, Mudford *et al.* (1991) presented a one-dimensional model of compaction-driven overpressuring and fluid flow for well 30/19-1 in the southern Central Graben; rapid Neogene sedimentation and the low-permeability, mudstone-dominated section leads to overpressure. Undercompacted porosity and the low overpressure developed within the model agree with observational data. Mello *et al.*, (1994) have presented a one-dimensional basin

model for the Northern North Sea that adequately explains the position and morphology of pressure transition zones, and the magnitude of sub-seal overpressures, using a physical model of sediment compaction. Symington *et al.* (1994) have applied a two-dimensional model to hydrocarbon migration in the Central Graben around wells 29/10-2 and 29/5a-1 on the "Puffin" Horst. Their analysis suggested that the silts of the Heather Fm. play an important role as lateral secondary migration conduits. In summary, previous investigations have attributed the magnitude of North Sea overpressuring, and the morphology of pressure transition zones, to disequilibrium compaction of sediments, linked to the presence of low-permeability aquitards.

5.3 Choice of methodology: the philosophy of modelling

Hydrogeological modelling faces an inverse problem (Oreskes *et al.*, 1994). The dependent variable in mathematical descriptions of fluid flow, the hydraulic head, is well known. The independent variable (porosity and permeability in the compacting basin under investigation) is poorly known. However, if the mathematical description of the hydrogeological system is adequate, it is possible to tune the porosity and permeability to the pressure to produce a "calibrated" model description of the present-day pressures. This porosity-permeability-pressure calibration methodology is followed by most basin modelling exercises (e.g. Mudford *et al.* 1991; Burrus *et al.* 1993). The model produced is *empirically adequate*; it is not demonstrating the *truth*. Models are thus essentially complex scientific hypotheses that are empirically adequate. Akin to all scientific hypotheses, they are subject to improvement or refutation in the light of new data.

Models presented in this chapter face problems of testing. Model predictions or retrodictions must be tested against observational data. However, data is restricted both geographically (to wells, and often to the reservoir section of wells) and in terms of time: observations are almost entirely made at the present day (Fig 5.1). Demonstrating the agreement between model pressures and present-day measured pressures is an insufficient test of the validity of a retrodictive model (Oreskes *et al.* 1994). The validity of the model must be discussed in terms of the underlying conceptualisation, the empirical adequacy of the governing equations, and the quality and quantity of model input parameters. These input parameters can be divided into those that are empirically-determined, those that are empirically constrained, and those that are empirically unconstrained (Oreskes & Belitz, 1994). It is necessary to make clear how much of any model is based on the observation and

measurement of accessible data, and how much is based on informed judgement. This framework for an evaluation of model validity is followed in Section 5.4.2 and 5.5.2.

With the preceding caveats of model use, it must be outlined why quantitative basin models were employed in this research. Models are used where there is a lack of full access to data in the subsurface; they are used to corroborate and challenge the hypotheses based on observational data presented in Chapters 2 and 3; and they are used for sensitivity analysis, to guide further study towards new regions of data acquisition.

5.4 One-dimensional models

5.4.1 Aims of the one-dimensional model investigation

Previous authors (Mudford *et al.* 1991; Mann & Mackenzie 1991) have emphasised the role of the interplay between vertical aquitard permeability and subsidence rate in controlling the magnitude of overpressure. Comparison with these earlier studies allows formulation of an initial hypothesis to be tested by the model investigation. The initial hypothesis to be tested is that the magnitude of overpressure developed in Jurassic and Triassic strata in the Central Graben is directly dependent on the thickness and permeability of the overlying aquitard, and the rate of subsidence of the basin. That is, the petrophysical properties of the aquitard will impede vertical fluid flow during rapid sedimentation and lead to compaction disequilibrium- and thus overpressure- in the deep Central Graben. Thus, in this section, quantitative models have been used in an attempt to refute the dynamic model presented in Chapter 2, which emphasised the importance of structure and lateral fluid flow.

An ancillary aim of the modelling is to identify the variables in the simulation that have the greatest impact on the modelled system, and to investigate the validity of the model for simulating the basin hydrogeological processes on the basis of available data.

This initial hypothesis has been tested using the BasinMod™ one-dimensional basin modelling code. BasinMod™ simulates the subsidence, compaction and fluid flow of the sediment column in the vertical dimension, and so is suitable for testing the initial hypothesis. This widely-used basin modelling code has been presented in

numerous publications for maturity modelling (e.g. Cornford, 1994) and stratigraphic reconstruction (e.g. Ziegler *et al.*, 1994). Pressure simulation using BasinMod™ has been presented by Williamson & Smyth, (1992) and Swarbrick, (1994). The mathematical basis of the model is presented in the Appendix, abstracted from the BasinMod™ User's Handbook (Platte River Associates 1995). These are similar to those employed by Bethke, (1985), Mudford *et al.* (1991) and Lerche, (1990). BasinMod™ can initially be considered to be an adequate model for simulating basin processes in this study due to this demonstrated applicability of its mathematical formulation to other basins.

5.4.2 Data

Following the extensive review of available data presented in Chapter 3, five released wells in the Central Graben have been selected for detailed examination: wells 22/24a-1, 22/30a-1, 23/27-6, 29/10-2 and 30/1c-2. The wells were chosen to examine the controls of pressure in the Jurassic sandstones at a range of depths and from a variety of structural settings.

Empirically-measured data used to construct the models includes the well stratigraphy for the early Tertiary-Triassic section, derived from composite well logs; the subsurface temperature from corrected Bottom-Hole Temperatures (Fig 5.2); the fracture gradient, derived from LOTs (in the model, hydrofractures are induced by model pore pressures equal to the model fracture gradient, and fractures close immediately upon a drop in pressure); and present-day surface temperature (assumed to be 5°C).

Empirically-constrained data used to construct the model includes lithological data (initial porosity, initial permeability, thermal conductivity, and heat capacity). This data is constrained within limits for each lithology, and is presented in Table 5.1. A plausible, standard model was used based on parameters from Bethke (1985) and Person & Garven (1992) for sand, siltstone, mudstone and chalk lithologies (see Table 5.1). Due to the paucity of sampling outwith reservoir intervals in the Central Graben, this data cannot be more accurately constrained. The rock density is constrained by density logs. It may be suggested that the well stratigraphy should also be considered to be empirically-constrained (albeit to a high accuracy) as it is not possible to examine the palaeontological data that has led to the construction of the stratigraphy. In particular, Quaternary mudstone stratigraphy is poorly constrained in several wells. An assumption of uniform Quaternary deposition across

the region has been made, constrained by seismic sections (Figure 1.5) and the subsidence analysis presented by Thorne & Watts, (1989). Additionally, the model assumes continuous sedimentation in the Cenozoic section, as well logs do not delineate unconformities.

5.4.3 *One-dimensional model methodology*

The model performs calculations on a one-dimensional node network on a 100-m depth spacing. Additional calculations are performed at the top and bottom of every stratigraphic division. Calculations are performed at 1 Ma increments as the sediment column compacts. Depth resolutions of 1000m, 200m, 100m and 50m were tested, and it was found that a 100-m resolution of gridding was necessary to assess rapid increases in pressure over 100-m depth intervals. Time increments of 10, 5 and 1 Ma were tested, and it was found that time increments of less than 5 Ma were necessary to reproduce the rapid variation Cenozoic subsidence of the basin. BasinMod™ is a forward model, in that porosity compacts from a high initial value as the basin subsides and time moves forward, arriving at present-day thicknesses after a series of iterations. The initial burial history of the model is constructed using the Sclater & Christie (1980) compaction algorithm, which has been empirically-derived from Central North Sea mudrocks. This initial porosity-depth curve is modified by iterative coupled simulation of fluid flow and compaction processes. Two iterations are normally sufficient for agreement to within 1% of observed input sediment thicknesses. Porosity is related to permeability by a power law relationship (Lerche 1990). Initial porosity and permeability are calibrated to present-day pressures as discussed in Section 5.3. Model temperature is calculated from a steady-state constant heat flow that provides a calculated best-fit to present-day temperatures (Fig 5.2).

5.4.4 *Evaluation of sensitivity to variations*

As is typical with a quantitative geoscientific investigation, much data is empirically-constrained but not accurately measured. Thus it is vital to evaluate the sensitivity of the model to the constrained variation in input. The fundamental importance of aquitard permeability has been presented in Section 5.2 and is further explored in Section 5.4.5.

Fig 5.3 shows a sensitivity analysis for heat flow, surface temperature, and thermal conductivity. It can be seen that the interplay between these thermally-controlling variables does not strongly affect resultant pressures in this 1-D compaction-driven physical model. A variation of +/- 60% in the values of the initial model input for

surface temperature, heat flow, thermal conductivity and fluid conductivity results in only a +/- 2% variation in resultant model pressures (a variation of +/- 2 MPa for a base-case model pressure of 96 MPa).

However, variation in thermal variables does strongly affect maturity of the Kimmeridge Clay source rock (and thus the timing of hydrocarbon generation). Fig 5.4 presents a sensitivity analysis for well 22/30a-1, and demonstrates that a 20% change in heat flow (from 40 mW m⁻² to 50 mW m⁻², for example, which is within the empirical constraints) results in a 45% change in modelled maturity. This could alter vitrinite reflectance from $R_o=1$ to $R_o=1.5$.

Fig 5.5 shows a sensitivity analysis for empirically-constrained petrophysical parameters. An effect on pressure is exerted by initial aquitard porosity, as shown by Figure 5.5. However, this effect can be partly circumvented as discussed in Section 5.3. The variation in aquitard porosity and permeability can be calibrated against measurements of pressure made in the borehole. Density also has an effect on model pressures, due to the dependence of porosity change on vertical stress. A variation of +/- 4% in model pressure is caused by a variation of +/- 10% in input density, equivalent to a variation of +/- 4 MPa for an empirically- constrained variation between 2.64-2.45 g/cm³. It is considered that this is acceptable for the required precision of the study.

This sensitivity analysis allows the ancillary aims of the one-dimensional study to be achieved. The input data is adequate for quantitative simulation of overpressure with a likely error of +/- 4% if the adequacy of the model conceptualisation and the governing equations are assumed. Input data is insufficient for quantitative simulation of hydrocarbon generation, as errors may be as much as 45%.

5.4.5 One-dimensional model results

Burial curves are often represented as observed data in reports of geological investigations. This is inappropriate, as choice of algorithm can make +/- 600m difference in the palaeodepths of formations in a 6km-deep section (Liu & Roaldset, 1994), due to the dependence of burial curves on porosity change. Porosity change can only be calibrated against present-day fluid pressure. In this present work, it is considered that as model pressures agree approximately with observed pressures, and the original geohistory is constructed using the Sclater-Christie algorithm (which is appropriate for Central North Sea mudrocks), then the model uncertainty in the

burial curves is acceptable. The accuracy desired by this project in modelling pressure transition zone morphology will not strongly affect burial curves. Examples of burial curves resulting from this modelling for wells 22/30a-1 and 29/10-2 are presented in Figs 5.6 and 5.7.

Modelled heat flow in study wells varies from 43 mW m⁻² to 46 mW m⁻², providing a fit to present-day temperatures measured downhole. Isotherms are shown on the burial plots for example wells (Fig 5.6 and 5.7). Isotherms are perturbed by the deposition of the Cretaceous Chalk, and isotherms do not recover to the present-day geothermal gradient until the Eocene.

Seal porosity-permeability variations are found to be critical to modelled overpressures. These are so fundamental to a model investigation of fluid flow that model results are presented for cases of "high" and "low" seal permeability values. There is a world-wide paucity of measured data on in-situ permeabilities of mudstones. Consequently, mudstone permeabilities are constrained by measurements on overpressured mudstones from similar depths in the Venture Basin of Eastern Canada (Coyner *et al.*, 1993). Permeabilities of 10⁻⁶ mD are documented, which may form a standard for comparison. As porosity and permeability dynamically evolve with the compacting basin and the changing fluid pressure, they are plotted against time (Fig 5.8, 5.9, 5.10 & 5.15).

The model results are constrained by fluid pressures measured by RFT in the Jurassic Fulmar sandstone reservoir. However, to attain the extremely high pressures measured in the Jurassic, it is found that extremely low mudstone permeabilities are required in all wells (Fig 5.8b, 5.9b and 5.10b). Unfortunately, these low permeabilities produce pressures that exceed the mudweight used during drilling in Lower Cretaceous mudstones above the pressure seal (Fig 5.11b, 5.12b, 5.13b), and so these simulations cannot be considered valid. If mudstone permeability is increased (Fig 5.8a, 5.9a, 5.10a) to ensure that the upper portion of the mudweight profile in the aquitard is honoured, calculated pressures in the Jurassic sandstones are too low (Fig 5.11a, 5.12a, 5.13a). This result suggests that it is essential to maximise the pressure information from wells by use of indirect pressure measurements such as mudweight. This forms a vital stage of model calibration. Neglect of this ancillary pressure data would lead to invalid porosity-permeability-pressure calibration.

The divergence between the maximum model pressure constrained by mudweight and observed reservoir pressures occurs across the Graben (Fig 5.14). The divergence is most marked at sites where the pressure seal is thin, mudstones are thin

or absent, and rapid increases in pore pressure occur. These conditions are typical of the axial Forties-Montrose High (Fig 1.5).

A special case is presented by wells 22/24a-1 and 30/1c-2, where the Jurassic Fulmar sandstone occurs at shallow depths on the axial Forties-Montrose High. This situation is illustrated by the pressure distribution in well 22/24a-1 (Fig 5.13), where the Triassic reservoir is sealed by Chalk and a thin band of L Cretaceous mudstone. Model pressures cannot match observed reservoir water-leg pressures despite maximum modelled variation in aquitard permeability, due to the thinness of the aquitard in this well.

Chalk permeabilities used in modelling these wells (Fig 5.15a, 5.16a) are constrained by measured permeabilities of 0.01-1 mD measured on unfractured chinks in the Central Graben (Trewin & Bramwell, 1991). However, even if Chalk permeabilities are modelled as four orders of magnitude lower than those measured (Fig 5.15b, 5.16b), sufficient vertical fluid flow occurs in the model so that the simulated overpressures are below observed overpressure.

5.4.6 Discussion and conclusions

One-dimensional models do not accurately reproduce the observed morphology of pressure-depth profiles in the Central Graben.

From this initial, one-dimensional investigation of Central Graben overpressure, it is concluded that observed overpressure is not related to seal thickness and permeability. Extremely high overpressures are encountered where the regional chalk-mudstone pressure seal is thin. Seal permeability is constrained by measured pressure in the aquitard, and so cannot be validly modelled as being of sufficiently low permeability to account for the magnitude of sub-seal overpressure. Modelled fluid flow through the pressure seal is too great to account for the high pressures beneath the seal.

It is clear from this result that the region of the Central Graben investigated is an unusual overpressured environment. The hydrogeological system expressed by the distribution of overpressure must be distinct from those of the Northern North Sea (England *et al.* 1989) or even adjacent regions of the Central Graben (Mudford *et al.* 1991), where 1D simulations seem to adequately account for the observations.

The one-dimensional model investigation suggests that Central Graben hydrogeology is a dynamic system. Leak-off through the pressure seal by Darcyian matrix flow will maintain sub-seal overpressure at levels below those observed, unless additional processes are maintaining pressure (Fig 5.39a). A feasible process is lateral communication with deep regions, as suggested in Section 3.6.

Reasons for the inadequacy of the one-dimensional model can be advanced, as per Section 5.3. It must be assumed that the mathematical formulation of the model is correct, as similar models have been used to adequately describe the hydrogeology of other regions. Quantity and quality of input data has been rigorously examined, and it has been demonstrated that it is impossible to achieve adequate calibration to observed pressures regardless of the variance in empirically-constrained input data. Accordingly, it must be concluded that the underlying conceptualisation is inadequate: a one-dimensional conceptualisation cannot adequately describe the multi-dimensional nature of Central Graben fluid flow. However, the conclusions drawn from this model remain valid: the initial hypothesis has been disproved. Overpressure is not solely dependent on aquitard thickness, permeability and subsidence rate. The data-driven hypotheses advanced in Chapter 3 are supported and reinforced by this model investigation.

5.5 Two-Dimensional Models

5.5.1 Aims of two-dimensional model investigation

If the underlying conceptualisation of the one-dimensional models presented above is inadequate, it is necessary to move to a multi-dimensional model to address the aims of this chapter. A two-dimensional model allows the simulation of lateral and vertical fluid flow. However, a more complex, two-dimensional model remains based on the same well-derived data as the one-dimensional models. It is necessary to carefully delineate the aims of the two-dimensional modelling, to deliver conclusions to these aims, and to examine the validity of these conclusions in the light of the available data.

A two-dimensional model allows direct testing of the role of lateral flow and geological structure in controlling fluid flow and overpressure, as indicated by the observational hypotheses of Section 3.5. The initial hypothesis to be tested is that

hydraulic communication with deep, off-structure regions controls the magnitude of overpressure observed in Central Graben wells. Testing of this hypothesis forms the **primary** aim of the two-dimensional model investigation. Ancillary hypotheses to be tested are that the structurally-mediated flow systems also control the reservoir-scale morphology of pressure transition zones (Section 3.6.4) and that overpressure is caused by disequilibrium compaction of the Graben sediments (see section 4.6). Testing of these ancillary hypotheses form the **secondary** aims of the modelling. The **tertiary** aims of the model investigation are to examine hydrogeological phenomena related to palaeo-fluid flow, including palaeo-overpressure and hydrocarbon migration.

BasinMod 2-D™ has been employed for two-dimensional simulation. The algorithms contained within the model are a two-dimensional extension of those of BasinMod 1-D™. Although portions of the gridding algorithms are commercially confidential, the geological algorithms are derived from the public domain. They are described in the Appendix.

5.5.2 Data

Model geometry has been digitised from the published seismic sections described by Roberts *et al.* (1990) and shown in Fig 1.5. The model section runs 30km west-east across the East Forties Basin (Fig 5.17), from the crest of the axial Forties-Montrose High (which in this region forms a large tilted fault block), eastwards into the depocentre of the basin (formed by the flanks of the fault block) and onto the western terraces of Jaeren High. Cretaceous and Cenozoic sediments form a drape across the section, deepening to the west, while the Jurassic sediments are modelled as a fault-bounded pod deepening eastward. Fulmar Fm. sandstones are simulated as discontinuous across the Graben, passing laterally into siltstones of the Heather Fm.

Model geometry is necessarily simplistic; three main faults are modelled, defining the axial fault block, a deep fault-bounded section of the Graben, and the eastern terrace. Similarly, the model section extends only to the base of the Middle Jurassic siltstones, to simplify calculations.

The section has been calibrated to two wells that lie close to the input cross-section. Well 22/30a-1 is at the crest of the Forties-Montrose High, while well 23/27-6 lies in the east of the section on the Jaeren High. These wells provide calibration of input data, including the stratigraphic ties to the seismic geometry, lithology, and

lithological parameters (Table 5.1). Model stratigraphic horizons are shown in Figure 5.18.

It was decided to investigate a basin-scale section, as Chapter 3 and Chapter 4 have shown that overpressure is a basin-scale phenomena. A shorter section was investigated, and found to be subject to dominance by the imposed boundary conditions (Cavanagh, 1995). It is assumed that the boundaries of the model do not permit flow out of the model section. This is an adequate assumption, as the presence of the western Central Graben and the Danish Basin (Fig 1.4) will mitigate against free lateral fluid flow. Equally, it is assumed that no fluid flows into the East Forties Basin from external sources, as it is the deepest region of the basin.

Salt diapirs have not been included in the model. Salt diapirs are limited in three-dimensional extent, and would exert too great an influence in a two-dimensional model designed to test lateral flow. Additionally, the model employed cannot model halokinesis.

Empirically-determined input data is naturally identical in quantity to that of the 1D model of Section 5.4.2. However, extrapolation of empirically-determined data from the location of wells to elsewhere in the section becomes undetermined.

Empirically-constrained input data includes lithological information for calibrating wells, which is identical in structure to that of section 5.4.2. Additional data includes lateral permeability of lithologies. A good match was achieved using a plausible, standard model based on Bethke (1985) and Person & Garven (1992) for sand, siltstone, mudstone and chalk lithologies (see Table 5.1). The actual geometry of the model is also empirically-constrained by seismic but is not absolutely known. The positions of faults and stratigraphic horizons are subject to variability, and the interpretation of the geometry by Roberts *et al.*, (1990) will be subject to unverifiable interpretative error.

Empirically-unconstrained input data is regrettably dominant in a 2-D model. Lateral variations may exist in lithology, lithological parameters, and heat flow. Of extreme significance is the role of faults. Faults may be barriers or conduits for fluid flow and may change character through time (see Section 3.5.3); accordingly they have unconstrained variability. For the initial base-case model faults are considered to be impermeable; the impact of variation in fault permeability is investigated in Section 5.5.6b.

5.5.3 *Two-dimensional model methodology*

The section was discretised into 2448 cells, in 51 rows and 48 columns, forming 71040 calculation nodes. Grid density is non-uniform (Fig 5.19). This is imposed by BasinMod's™ proprietary gridding algorithms, which require high density of calculation in zones of structural or sedimentological complexity. As BasinMod 2-D™ is a finite difference model, calculations are performed in the centre of each cell. Accordingly, high calculation density is also required in the thin region of the aquitard, where it is necessary to reproduce sharp pressure transition zones without mathematical grid artifacts. Lower grid density produces artificially wide transition zones due to large grid block size. Calculations are performed at ages of 5, 10, 15, 20, 30, 40, 50, 60, 70, 80, 100, 120, 140, 150 and 200 Ma, in addition to the ages of tops and bases of each lithostratigraphic unit, as the model compacts the sediment column. Calculation density in age-space has been specified to allow density of calculation in the Cenozoic, forcing maximum precision during rapid subsidence. Longer time increments are unsuitable for reproducing the rapid variation in Cenozoic subsidence. A total of 52 timestep calculations are performed. Calculation density is a compromise between hardware run-time limitations, required section complexity, and desired validity of output.

5.5.4 *Two-dimensional model results*

The magnitude of simulated overpressure is an adequate match to observed overpressure in both the calibration wells (Figs 5.20, 5.21). The distinctive two-cell profile of the Central Graben is reproduced, with an upper zone of overpressure in the Tertiary mudstones separated and isolated from a lower zone of extreme overpressure below the Cretaceous Chalk by the hydro pressured Palaeocene sandstones. The model overpressure is shown in cross-section in fig 5.22.

The simulated pattern of water flow induced by the model overpressure is shown in Fig 5.23. Water flows laterally in the sub-seal Jurassic sandstones towards the structurally-elevated crests of fault blocks. Significant lateral fluid flow is induced in the Heather Siltstone in the centre of the basin. Rapid lateral flow occurs in the Palaeocene sandstones. Water flows vertically in the low-permeability aquitards separating the aquifers.

The morphology of observed pressure-depth profiles is adequately reproduced by the model (Figures 5.20, 5.21). Sharp transition zones are simulated for the crestal

regions of the sub-seal section. In off-structure regions deeper in the section, lateral flow of fluid in the Fulmar sandstone leads to lowered overpressures in this formation (Fig 5.24); this simulation qualitatively replicates observed pressure-depth profiles in deep wells (e.g. Fig 3.12). However, the stratigraphic control exerted by the Kimmeridge Clay Fm. suggested by the detailed analysis of Section 3.3.5 is not clearly reproduced. Rapid rises in pressure are observed in the Kimmeridge Clay Fm. The model shows a homogenous increase in pressure through the Cretaceous-Jurassic mudstones.

Significant undercompaction at several depths is suggested by the model (Fig 5.25). Zones of anomalous model porosity occur in the overpressured Tertiary mudstones and in the sub-seal Jurassic-Cretaceous mudstones. Anomalous model porosity also is noted for the sandstones in on-structure well 22/30a-1, but the sandstones in off-structure regions have compacted to a greater extent due to the higher effective stress, and have consequently low porosities (see Section 6.4). Chalk and mudstone aquitard porosity and permeability evolution is detailed in Figure 5.26. The aquitard decreases to low permeability values during Cenozoic subsidence and compaction, forming a restriction to vertical fluid flow.

As the model presented in this section provides an adequate representation of the present-day overpressure systems observed in the Graben, the model can serve as a guide to the palaeo-pressure systems. The timing of overpressure development for well 22/30a-1 is shown in Fig 5.27; for well 23/27-6 in Fig 5.28; and for the Graben depocentre in Fig 5.29. The Fulmar sandstones in well 22/30a-1 are simulated as becoming overpressured at 40Ma, with rapid subsidence in the late Cenozoic elevating model pressures to the observed high levels. In contrast, well 23/27-6 does not become overpressured until 10 Ma. This is due to the shallower depth and lower thickness of the aquitard in this well, which allows freer fluid flow.

5.5.5 Model Hydrocarbon Generation and migration

A tertiary aim of this model investigation has been to investigate hydrocarbon migration. Simulated hydrocarbon generation and migration is subject to considerable uncertainty due to the variability of heat flow and thermal conductivity as discussed in Section 5.4.4. Section 5.5.6 has demonstrated the sensitivity of model results to unconstrained variations in fault and sandstone permeability. Thus the model presented in this chapter is non-unique and *qualitative* for hydrocarbon

generation and migration. However, within this limitation, the pattern of hydrocarbon generation and migration can be discussed.

The Kimmeridge Clay and Heather Fms are simulated as potential source rocks in the section. The model parameters relevant to hydrocarbon generation in these units are presented in Table 5.2. Kerogen maturity evolution and hydrocarbon generation timing for the Graben depocentre is presented in Fig 5.30. Oil and gas began to generate in the Kimmeridge Clay Fm. at 65 Ma. Oil began to accumulate in crestal positions in the Fulmar sandstone at 30 Ma (Fig 5.31). Oil then subsequently re-migrated vertically as overpressure developed in the Fulmar, accumulating in the Paleocene sandstones. This pattern was repeated at 10Ma. This model of oil migration is supported by petrographic observations of bitumen residues in the Fulmar sandstones of well 22/30a-1 (Section 6.4; Wilkinson *et al.* 1994a), which suggest that hydrocarbons have been reservoired in well 22/30a-1 but have been removed. The geochemical similarity between reservoired hydrocarbons in the Palaeocene and Jurassic (Symington *et al.* 1994) also supports this model of vertical remigration. The hydrogeological patterns of this accumulation -remigration cycle are shown in cross-section in Figure 5.32.

Gas began to accumulate in the crestal Fulmar sandstone at 25 Ma; however leakage through the seal continually removed gas 20 Ma- present (Figure 5.31), and gas accumulation is dependent on the rate of gas generation (Fig 5.30). The model suggests episodic filling and leaking of the crestal structure. The timing of this process is constrained by the model calculation steps to occur at 5 Ma intervals but is undoubtedly a rapid, dynamic process.

Simulation of the overpressures resulting from hydrocarbon generation suggests that generation pressures contribute 1 MPa to the basin overpressures during peak oil and gas generation at 20 Ma (Figure 5.30). However, this overpressure does not extend beyond the KCF and does not affect the adjacent Fulmar sandstones (Fig 5.27), as conditions for hydrocarbon overpressuring are not satisfied for the sandstones due to their higher porosity and permeability (Duppenbecker *et al.* 1991). Peak oil and gas generation is thus in the geological past for the Graben source rocks; this agrees with the study of Cornford (1994). The source rocks continue to generate gas at the present day, but at such low rates that model pressure is unaffected. Moreover, examination of the governing equations (see Appendix) demonstrates that gas generation is strongly affected by the compressibility of gas, which forms a negative feedback to the generation pressure. However, as the location of pressure transition

zones within the Kimmeridge Clay Fm. is not adequately simulated by the model, it is likely that the algorithms describing generation pressures are inaccurate.

5.5.6 Evaluation of sensitivity to variations

As with the one-dimensional model in Section 5.4, variability in empirically-constrained input parameters was assessed by sensitivity analysis. The sensitivity analysis for the 2D model built on the results of the 1D sensitivity analyses. Model aquitard porosity and permeability were calibrated to observed pressures, as per Section 5.3. Additional elements of variability in the 2D model include lateral permeability of lithologies, fault permeability, structural geometry, and lateral extent of sandstones. For the purposes of this investigation as detailed in Section 5.5.1, it is assumed that the structural geometry of the model is adequate. The sensitivity of the model to variations will be discussed with reference to the "base-case" model discussed above.

(a) Variation in lateral permeability and extent of sandstones

(i) Fulmar sandstones

Fulmar sandstones have been simulated in the basic model as extending 12km, or approximately half-way, into the centre of the East Forties Basin. Their true lateral extent is unknown. To assess the importance of this variability, a model was run with Fulmar sandstones extending only 5km to the east of the crest of the Forties-Montrose High and rapidly passing down-dip into siltstones.

Model pressures in the position of the calibration wells were unaffected by lateral variations in the extent of the Fulmar sandstones (Table 5.3). Thus the principal aims and results of this model investigation are unaffected by this variation. However, as siltstones are simulated as having a much lower lateral permeability than sandstones (Table 5.1), discontinuous Fulmar sandstones alter the fluid flow directions in the base of the section. Water flow becomes predominantly vertical in the Cretaceous-Jurassic section (Fig 5.33).

While overpressure remains unaffected by this variation, patterns of hydrocarbon migration are fundamentally altered. As hydrocarbons in the source kitchen are no longer underlain by a permeable migration conduit, all hydrocarbons move vertically under buoyancy pressures through the source rock and accumulate in the supra-seal

regions of the section, bypassing the Fulmar sandstones in well 22/30a-1. This results in early accumulation of oil in Palaeocene sandstones (at 30 Ma compared to 10 Ma, Fig 5.34). Thus simulation of hydrocarbon migration in the Central Graben is fundamentally affected by lateral variation in lithology and permeability. As these variables are empirically-unconstrained, these hydrocarbon migration models are non-quantitative.

(ii) Palaeocene sandstones

Free lateral flow of fluid occurs in the permeable Palaeocene sandstones. Section 3.4.2 suggested that this lateral flow provides an important control on the magnitude of pressures and the morphology of pressure transition zones within the aquitard. To quantitatively assess the impact of variation in the characteristics of this Palaeocene sandstone "drain", a model was constructed in which the Palaeocene sandstone formation of the original model was simulated as a low-permeability siltstone (Table 5.2).

Fig 5.35 demonstrates that the lithological characteristics of this unit have a major control on the pressures developed in the section. Fluid flow is greatly restricted in the upper regions of the aquitard, as rapid lateral flow of fluid in the original model is replaced by slow vertical flow. Overpressure develops in the base of the Tertiary, providing a better fit to observed pressures in well 23/27-6. This suggests increased restriction of fluid flow on the Jaeren High. The absence of a highly-permeable sandstone migration conduit, and the presence of a positive pressure differential between Tertiary and Chalk, leads to hydrocarbon entrapment in the Upper Chalk (Fig 5.36) and increased retention of hydrocarbons in the sub-seal Jurassic strata. This supports the model of fluid flow in the Upper Cretaceous-Tertiary section advanced in Section 3.6, which suggested that overpressure in Palaeocene sandstones forms a favourable situation for trapping hydrocarbons in the underlying Chalk.

(b) variations in fault permeability

The initial model has been run with faults acting as absolute barriers to fluid flow (Leak Fraction = 0, see Appendix). A contrasting model (Fig 5.37) has been run with faults acting as permeable conduits (Leak Fraction = 1). Values of fault permeability used are presented in Fig A.3. The high grid density required over faults by BasinMod's proprietary gridding algorithms ensures that faults do not enhance

vertical permeability due to grid artifacts. Fault permeability does not change the present-day model pressures in the calibrating wells (Table 5.3) and so this empirically-unconstrained variable does not affect the primary results and aims of this model investigation. This result is unusual for two-dimensional investigations of overpressure, as overpressures have been used by other workers to calibrate fault permeability in a similar way to vertical aquitard permeability (Ungerer *et al.*, 1990). It is hypothesised that in this Central Graben model, fault permeability is of low importance to the relatively shallow sub-seal regions of the modelled section because the faults do not completely penetrate the L Cretaceous and are not significantly more permeable than unfaulted aquitard (Fig A.3). Thus permeable faults do not significantly enhance the vertical permeability of the aquitard.

However, fault permeability has a fundamental effect on hydrocarbon migration. No hydrocarbons accumulate in the fault-bounded "trap" on the crest of the Forties-Montrose High if the fault is permeable. Hydrocarbons can migrate along the fault. The permeable fault allows buoyant pressure to push migrating hydrocarbons through the aquitard. Migration through the aquitard occurs preferentially at fault tips and hydrocarbons are emplaced at 30 Ma in the Palaeocene sandstones (Fig 5.37), earlier than 10 Ma suggested in the base-case model.

Fluid flow in faults may also be controlled by tectonic events. Rapid fault movement may lead to breaching of traps (Gaarenstroom *et al.* 1993) and catastrophic expulsion of water (Cartwright 1994). The influence of these tectonic events cannot be addressed by this model.

(c) Variation in aquitard permeability

Section 5.4.5 has shown that model pressures are extremely sensitive to variations in mudstone permeability, and so palaeo-overpressure timing is also extremely sensitive to variations in this unconstrained variable. Calibration of mudstone porosity and permeability to observed present-day pressures requires a mudstone vertical permeability of 0.0004 mD. However, calibration to present-day pressures is insufficient to demonstrate that mudstone permeability is in this range. The proximity of model pressures to the rock fracture gradient in calibration well 22/30a-1 makes calibration of mudstone petrophysical properties difficult, as it is possible that pressures in the Fulmar sandstone may have achieved this high value in the past. That is to say that present-day overpressure may not be the maximum pressures achieved in this well, as pressure-induced hydrofracturing may allow oscillation of

pressure around the rock fracture gradient (Dewers & Ortoleva 1994). Measured mudstone permeability in comparable basins is far lower than the modelled value of 0.0004 mD (Coyner *et al.* 1993). A low-permeability model (Table 5.2) was constructed using lower initial mudstone porosity and permeability.

This low-permeability model simulates overpressure in well 23/27-6 (Fig 5.38) as being in excess of the observed pressures in the Cenozoic mudstones and in the L. Cretaceous- U. Jurassic mudstones. The low-permeability mudstone model can be considered to be invalid. Maximising the information for model calibration by using multiple wells reduces in the uncertainty in empirically-constrained data.

(d) Sensitivity Summary

In conclusion, the sensitivity analyses performed suggest that overpressure in the Central Graben is unexpectedly unaffected by variations in fault permeability, or by lateral extent of Fulmar sandstone. The presence of high-permeability Palaeocene sandstones forms a control on the large-scale morphology of transition zones. The vertical permeability of mudstones- and the evolution of that permeability with time- remains the principal unconstrained variable affecting the model, but variation in this parameter can be constrained by use of multiple calibration wells if the empirical adequacy of the equations simulating mudstone compaction is assumed.

5.5.7 Discussion

The model presented above satisfies the primary aim of this project by providing a robust, adequate simulation of the observed distribution of overpressure. A quantitative model description of Central North Sea overpressure requires the simulation of both vertical and lateral flow.

The secondary aims of this model investigation have been achieved. Transition zone morphology is accurately represented. The vertical permeability of the seal rocks can be represented as 3 orders of magnitude greater than that estimated by the 1D model (Fig 5.8), as the recharge and leakage of overpressure removes the need for ultra-low seal permeability. The compaction of the mudstones in the aquitard in well 22/30a-1 has effectively ceased by 30Ma; this agrees qualitatively with the estimates of mudstone porosity deduced from sonic logs (Section 4.2.2). The model suggests that disequilibrium compaction of the thick, mudstone-dominated Jurassic depocentres of the Graben is the major cause of today's observed overpressures in the region.

Extrapolation of the model into the geological past to examine the tertiary aims of this investigation is satisfactory. Timing and distribution of overpressure in the geological past is crucially dependent on the simulated change in mudstone porosity; however, rigorous calibration of the model constrains the onset of overpressure to the Eocene in well 22/30a-1 (Figure 5.27) and the late Miocene in well 23/27-6. The model allows useful qualitative and quantitative insight into the palaeo-hydrogeology of the region.

The performance of the model in simulating hydrocarbon migration, a tertiary aim of this chapter, has been explored in Sections 5.5.5 and 5.5.6. The lack of empirically-determined data, and the extreme sensitivity of the results to small variation in measured input, greatly limits the efficacy of computer simulation of hydrocarbon generation and migration in this study. These tertiary aims of this model investigation cannot be fully quantified. However, the interpretation of the model in a qualitative mode to examine a "what-if" situation supports the dynamic model of hydrocarbon migration advanced in Section 3.6. Quantification of generation pressure is hampered by this variation in input parameters, and also by the lack of quality-control on the empirical adequacy of the equations governing the simulation of this process. However, within this limit it would appear that hydrocarbon generation pressures are strongly limited by feedback processes as suggested by Section 4.4, and contribute little to the basin-scale overpressuring. This improves the conclusions of Chapter Four, where no decision could be made between the relative contributions of compaction and hydrocarbon generation.

5.6 Conclusions

1. The magnitude and distribution of overpressure in the Central Graben is controlled by the inhibition of vertical dewatering by the presence of a low-permeability mudstone aquitard, and by lateral communication beneath this regional mudstone pressure seal. One-dimensional modelling of the region shows that the distribution of pressure in the region does not show a simple relationship to the thickness and permeability of the vertical seal. Two-dimensional modelling allows recognition that the pre-Cretaceous structure of the Graben controls the flow of pore fluids, leading to elevated pressures and sharp transition zones on axial fault blocks where the regional pressure seal is thin.
2. The models suggest that disequilibrium compaction of thick mudstone sequences in off-structure regions is the principal overpressuring mechanism in the Graben.

This disequilibrium compaction has arisen during the Cenozoic (40-0 Ma) due to restricted fluid flow in low-permeability lithologies, coupled to the high Cenozoic sedimentation rate. As experimental data for the pressure increase resulting from hydrocarbon generation is lacking, this aspect cannot be adequately quantified. Accordingly the model suggests that overpressures from hydrocarbon generation play a minor role in the Central Graben, due to the high compressibility of hydrocarbon gas and the probable 30 Ma timing of peak hydrocarbon generation.

3. Free lateral flow of porewater in the Palaeocene sandstones above the pressure seal leads to a layered hydrogeological regime in the Central Graben, with an upper Tertiary pressure cell being isolated from the highly overpressured pre-Cretaceous pressure cell by a hydro pressured zone. This decoupling of upper and lower cells has a major effect on the large-scale morphology of transition zones in the aquitard and the retention of hydrocarbons in the Cretaceous Chalk.

These quantitative conclusions support the dynamic model of Central North Sea overpressure advanced in Chapter 3. These conclusions are robust with respect to the underlying conceptualisation of the model, and are unaffected by variations in empirically-constrained and empirically-unconstrained data. The initial hypothesis of the model investigation is supported (Figure 5.39).

The model presented in this chapter also qualitatively supports the model of secondary hydrocarbon migration advanced in Section 3.6. The model of hydrocarbon generation-related overpressuring advanced in Section 4.3 is also qualitatively supported, but hydrocarbon generation is shown to be an insignificant cause of overpressure. However, the computer simulations presented above are not a suitable method for quantitatively addressing these hypotheses due to the *probable* inadequacy of input data and the *possible* inadequacy of the governing equations.

Basin models provide an invaluable tool in building and testing hypotheses regarding the complex dynamic interplay of the basin processes that control fluid flow. The detailed models resulting from computer simulation can be improved by additional porosity-permeability data acquisition and an improved understanding of the processes controlling mudstone petrophysical behaviour. Maximising the multi-source pressure data available in the Central North Sea has provided a robust calibration framework for this study. Maximising observational data in exploration wells will advance the understanding and simulation of the complex basinal hydrogeological system.

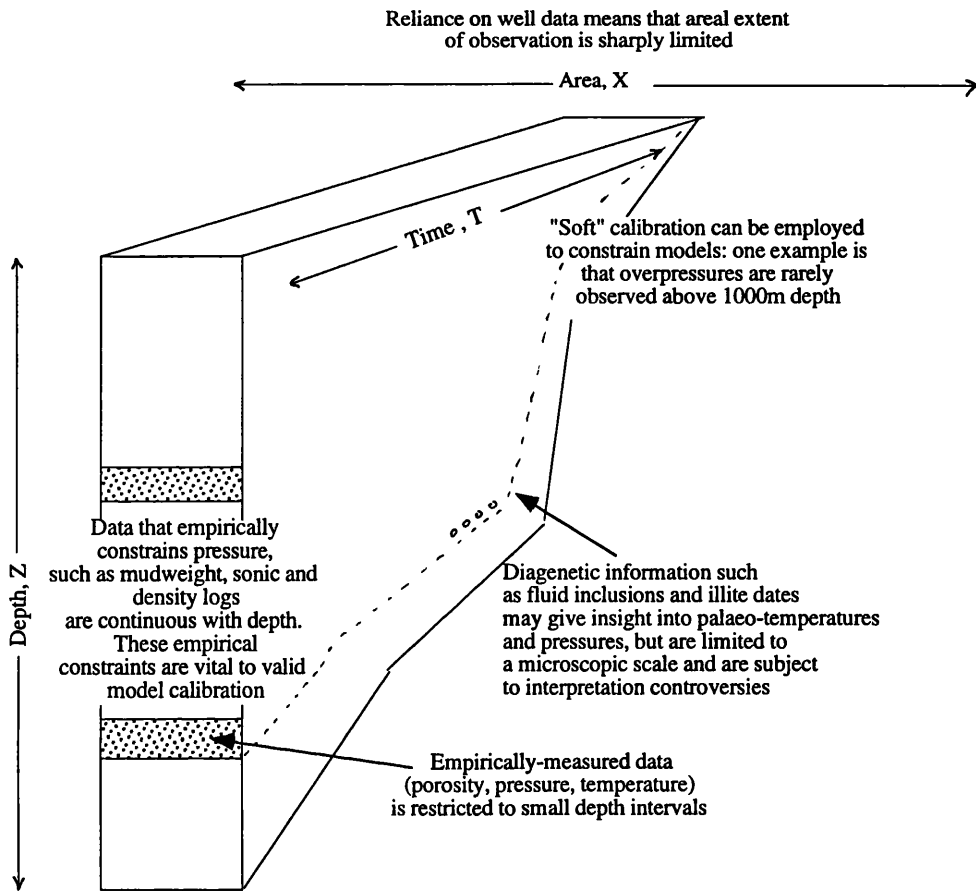


Figure 5.1 Data available for model calibration

Empirically-measured data is restricted in depth, space and time. Empirically-constrained data is restricted in space and time. These limitations enforce a non-uniqueness on a model investigation of a hydrogeological system.

22/30A-1

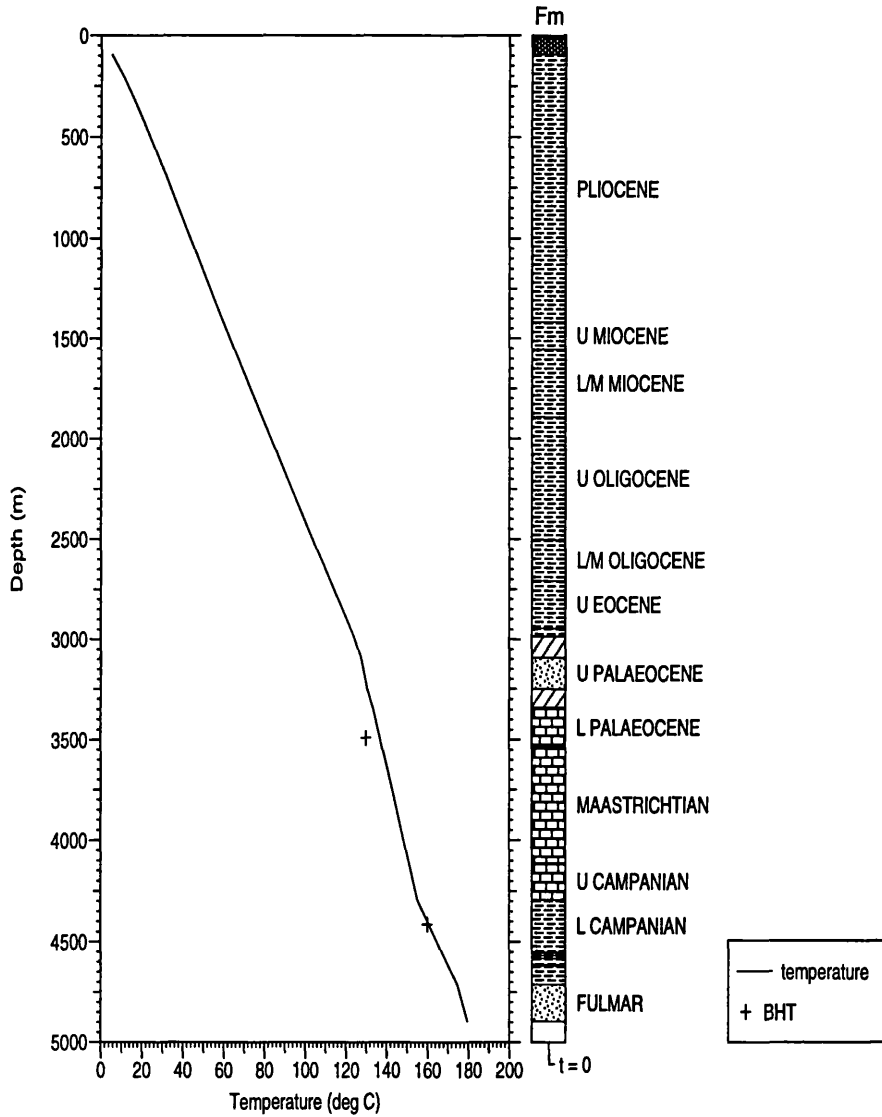


Figure 5.2 Modelled and observed temperatures in well 22/30a-1. BHT is Bottom-Hole Temperature. Solid line shows temperatures modelled from BasinMod.

22/30A-1

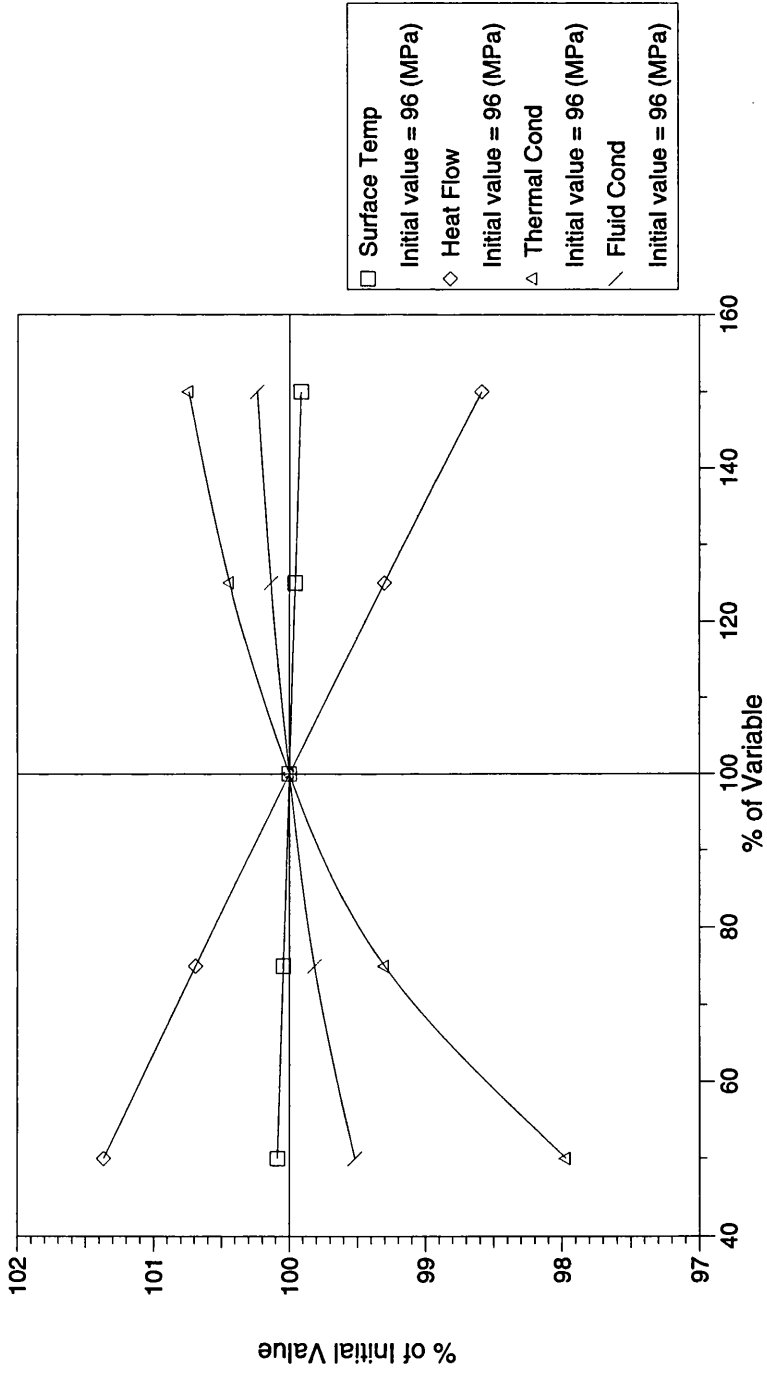


Figure 5.3 Sensitivity analysis of model pressure in Jurassic sandstone for thermal input variables. Variation of +/- 50% in surface temperature, heat flow, thermal conductivity and fluid conductivity (x-axis) result in only a +/- 2% variation in model pressures (y-axis).

22/30A-1

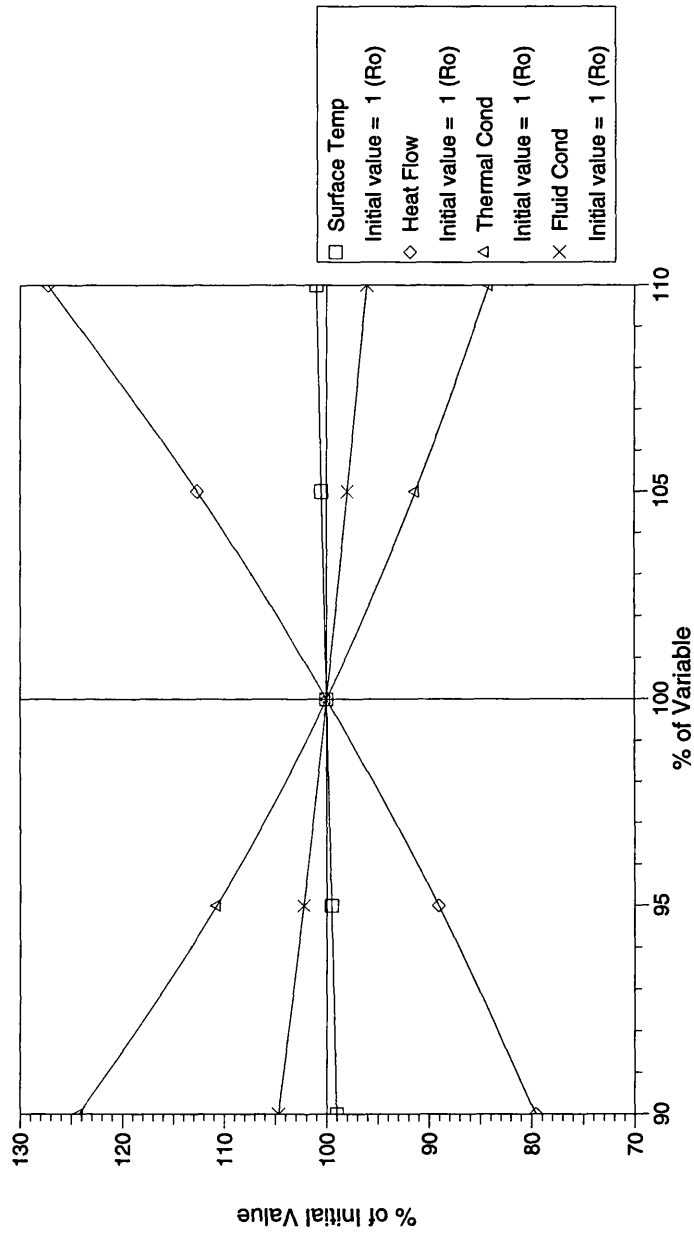


Figure 5.4 Sensitivity analysis of model maturity for thermal input variables. A variation of +/- 10% in initial input variables for surface temperature, heat flow, thermal conductivity and fluid conductivity (x-axis) results in a variation of +/- 20% in output modelled maturity (y-axis).

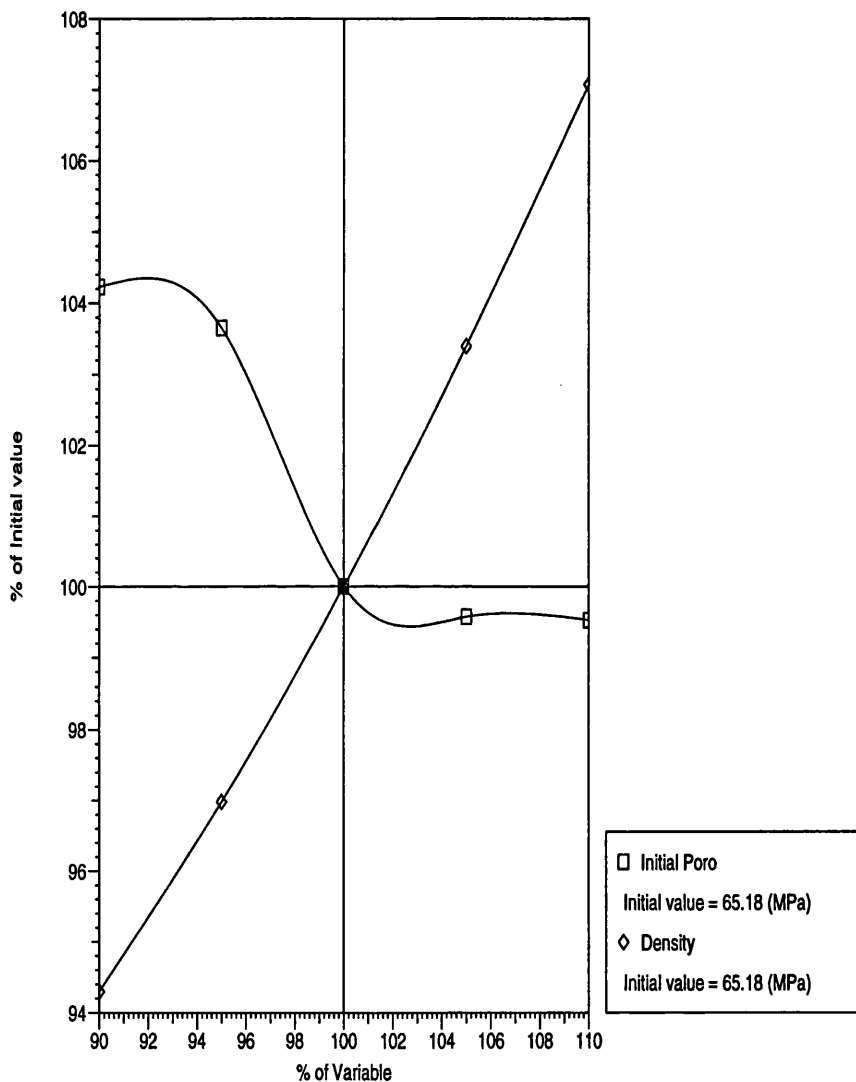


Figure 5.5 Sensitivity of pressure in aquitard to variation in sediment density and aquitard initial porosity. A change of +/- 10% in sediment density (x-axis) produces a change of +/- 4% in model output pressures.

22/30A-1

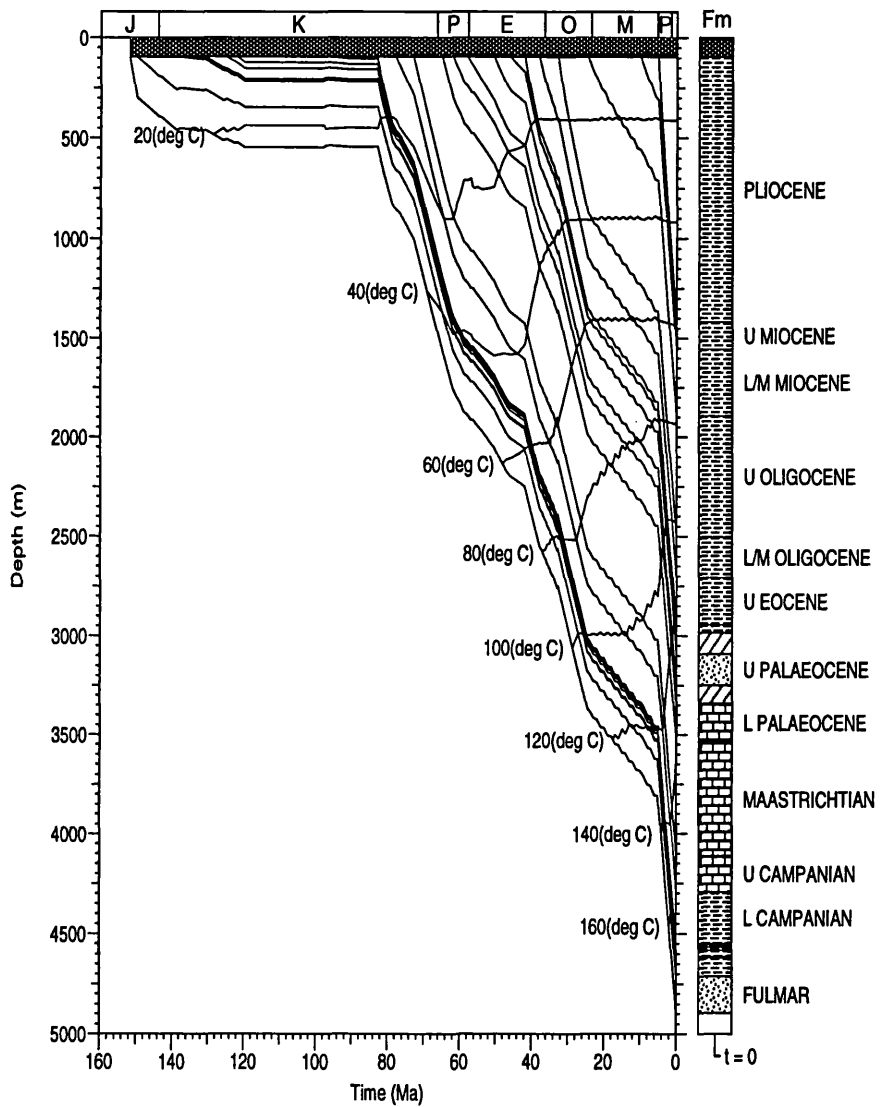


Figure 5.6 Subsidence curve of all formations in well 22/30a-1, with isotherms. Derived from BasinMod using coupled fluid-flow and compaction algorithms iterated to match present-day pressures in the Fulmar sandstone.

29/10-2

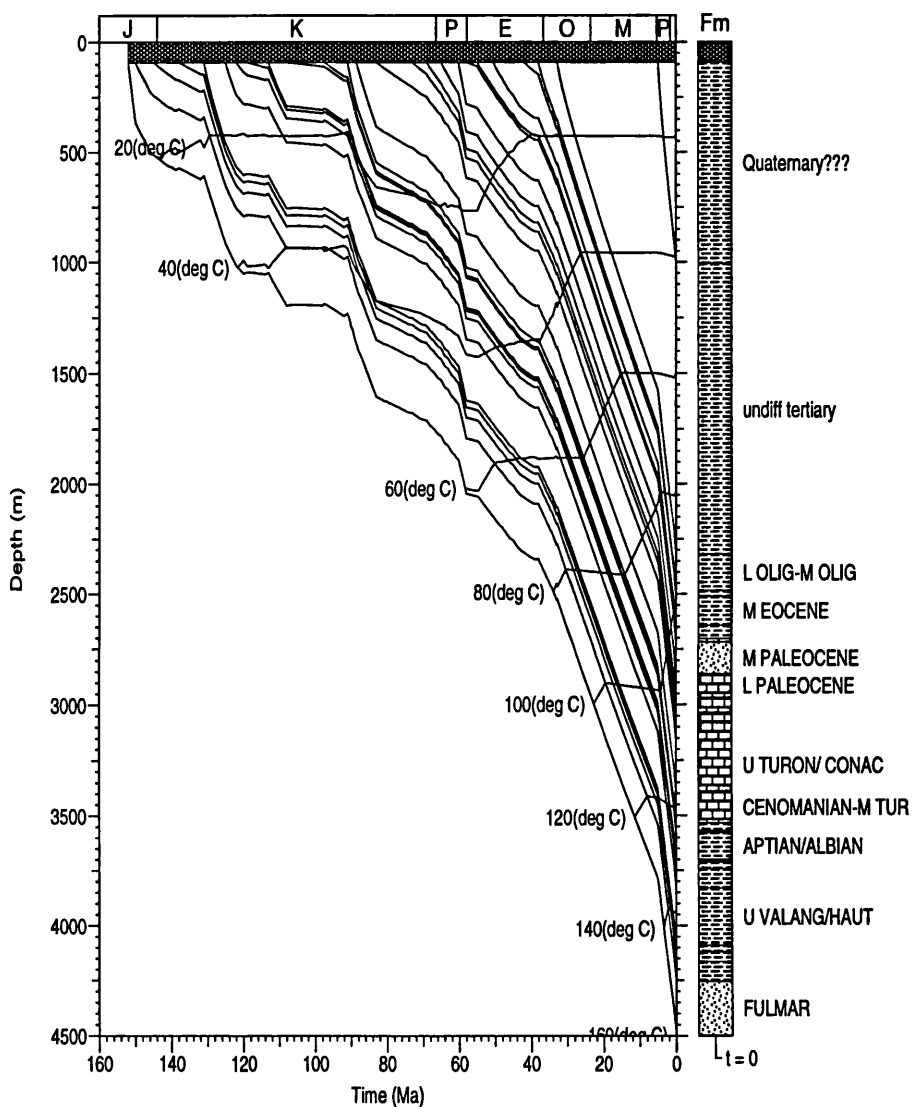
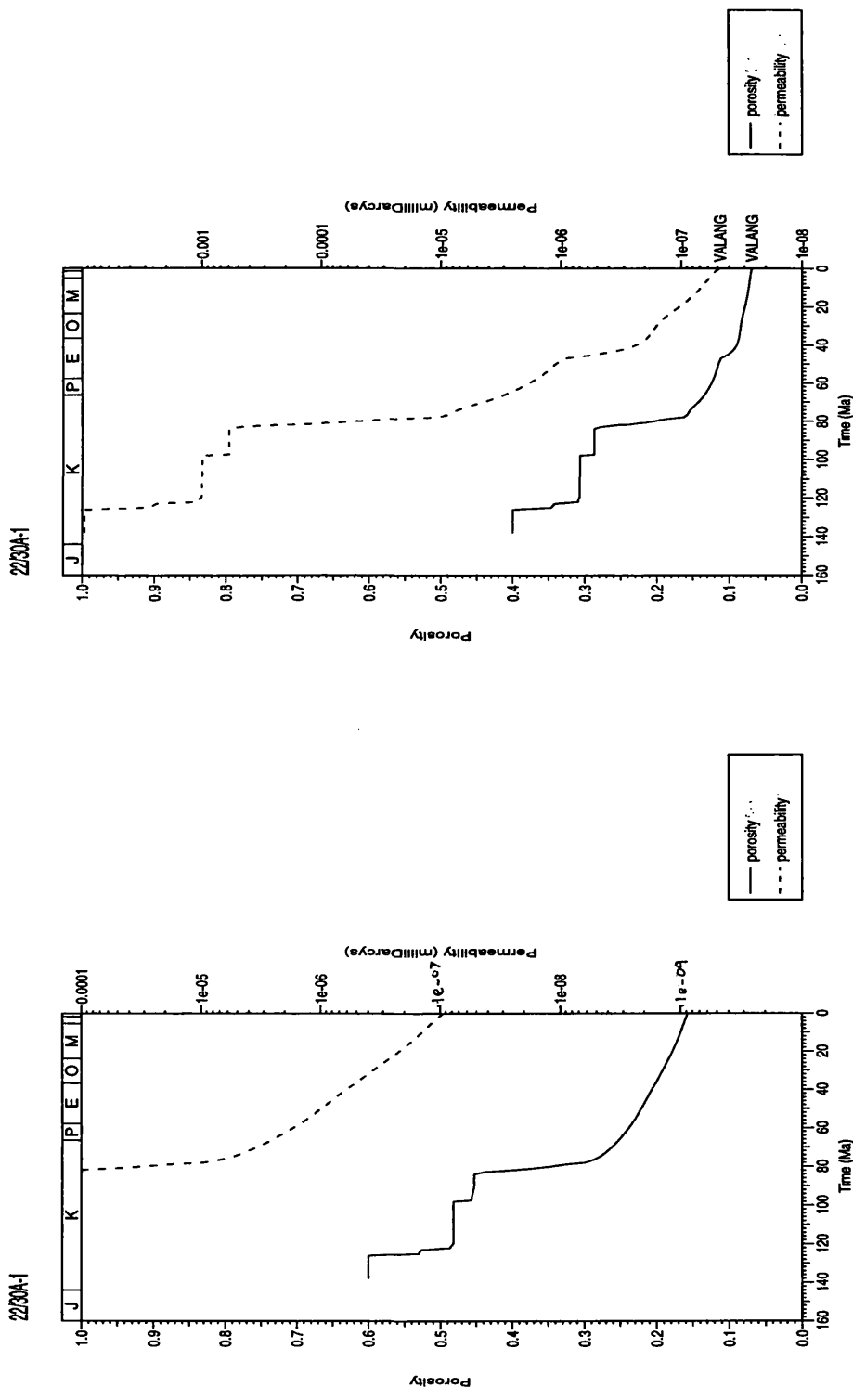


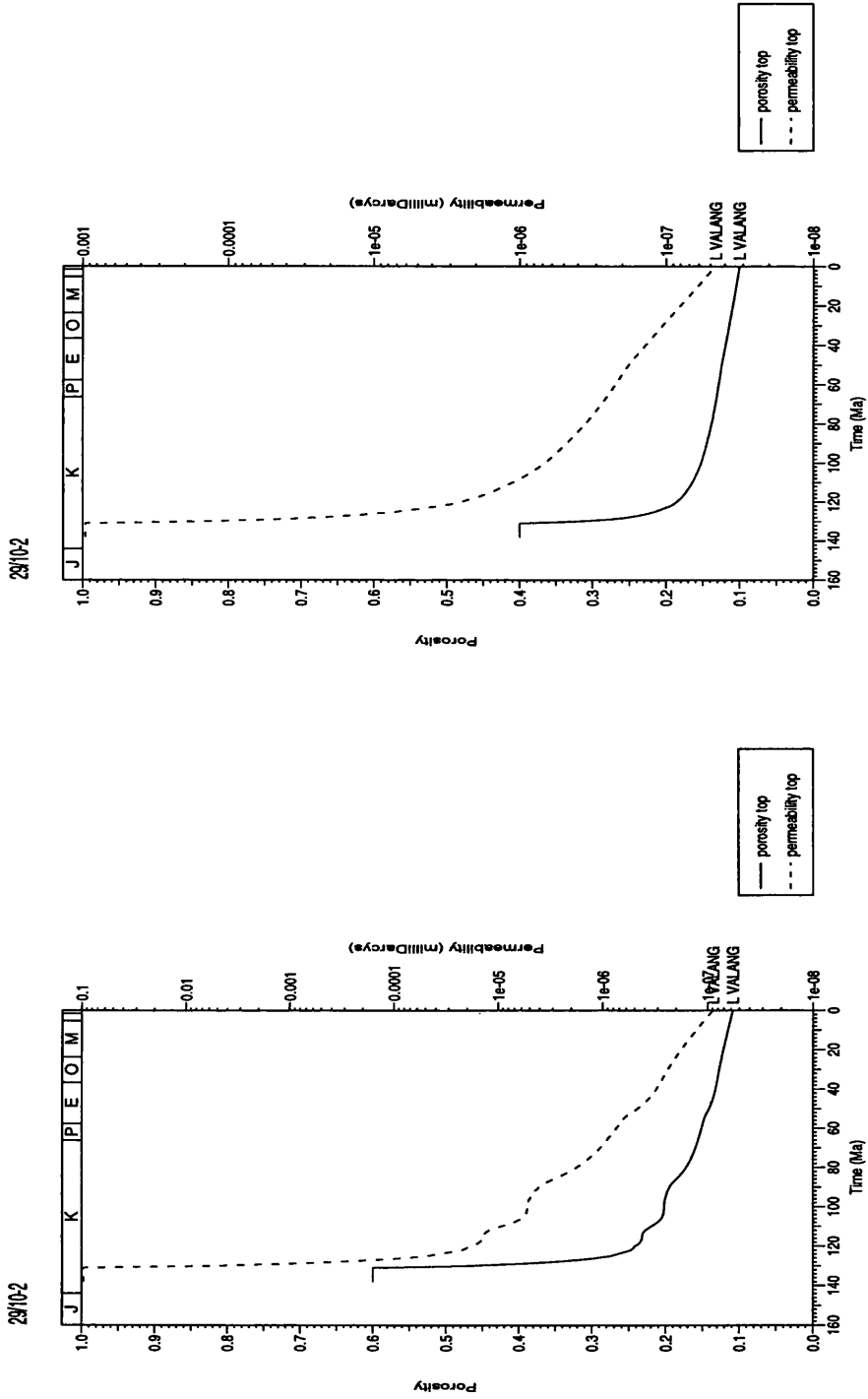
Figure 5.7 Subsidence curve of all formations in well 29/10-2, with isotherms. Derived from BasinMod using coupled fluid-flow and compaction algorithms iterated to match present-day pressures in the Fulmar sandstone.



(a) High-permeability case

(b) Low-permeability case

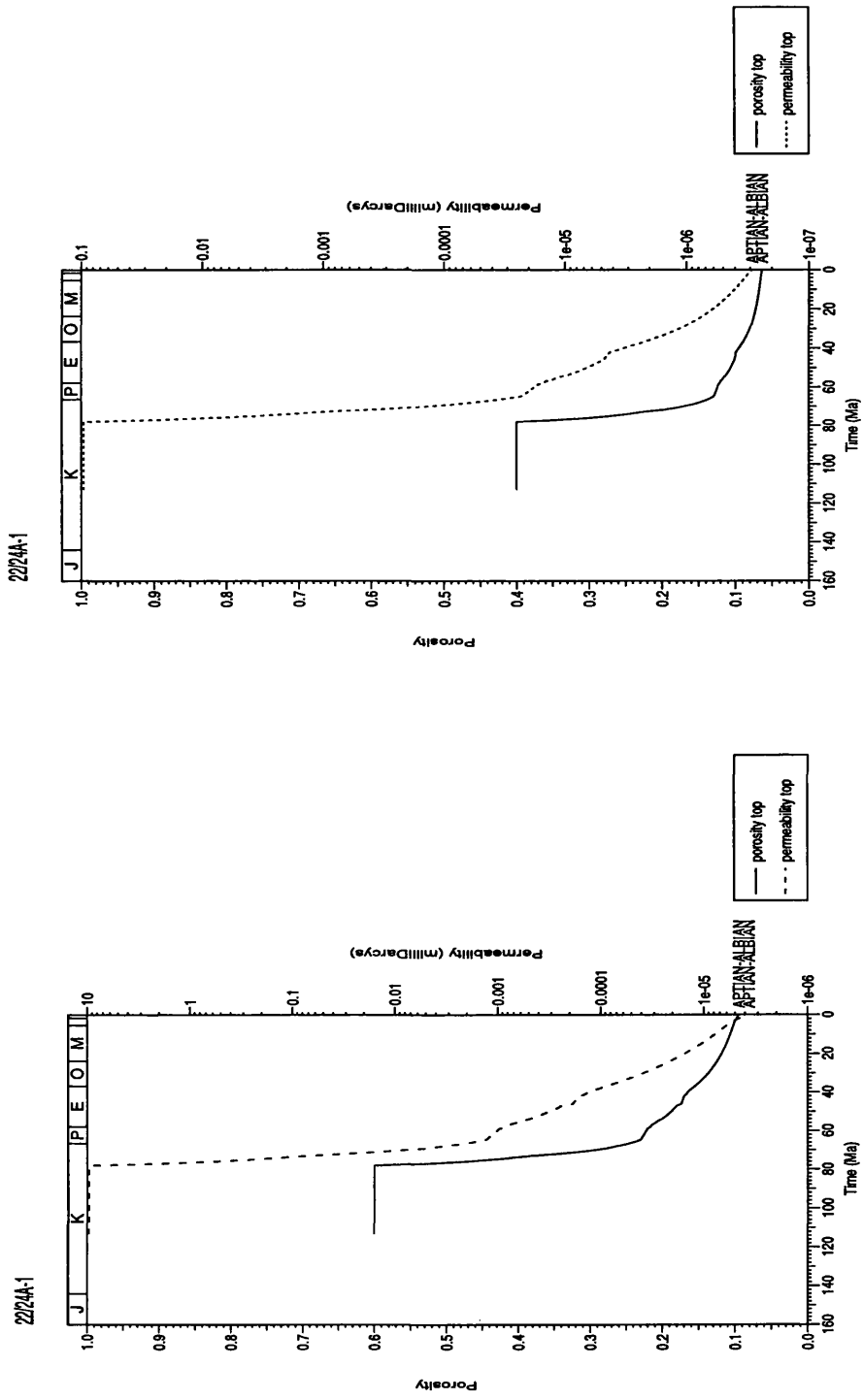
Figure 5.8 Model porosity and permeability for Valangian shales in well 22/30a-1



(a) High-permeability case

(b) Low-permeability case

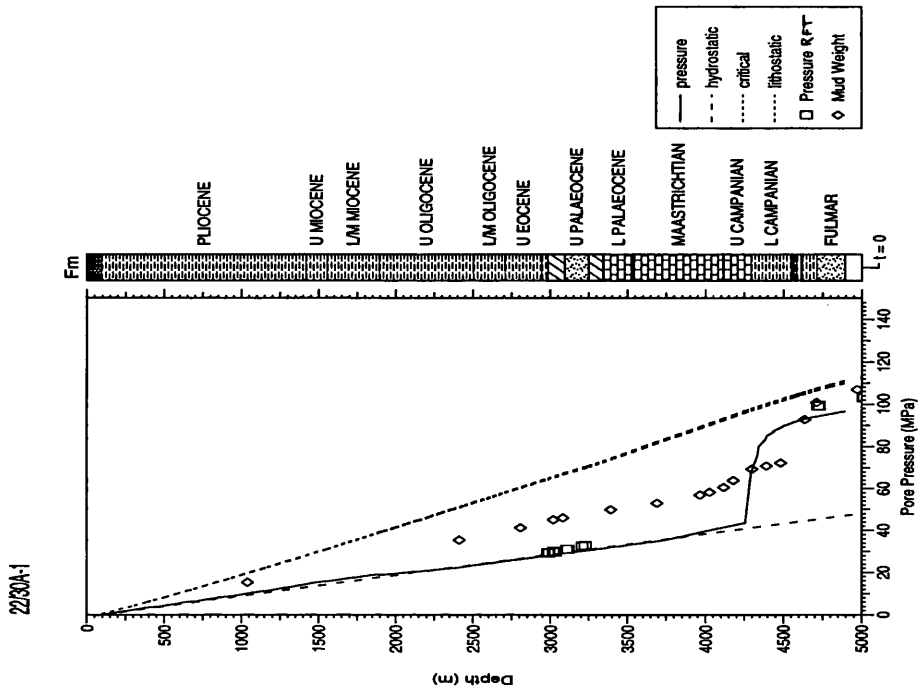
Figure 5.9 Model porosity and permeability for Valangian shales in well 29/10-2



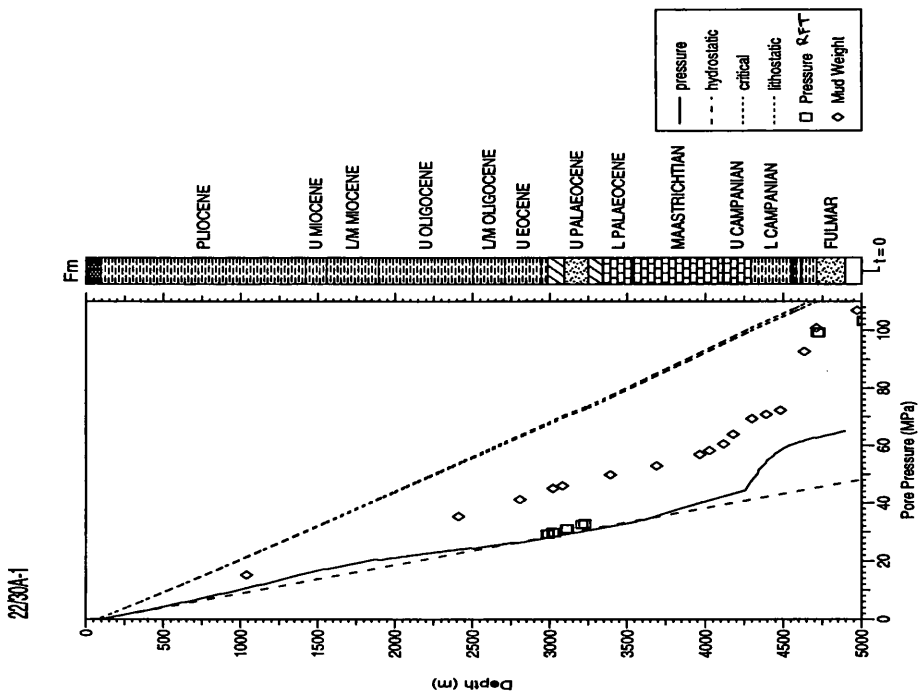
(a) High-permeability case

(b) Low-permeability case

Figure 5.10 Model porosity and permeability for Aptian-Albian Shale in well 22/24a-1



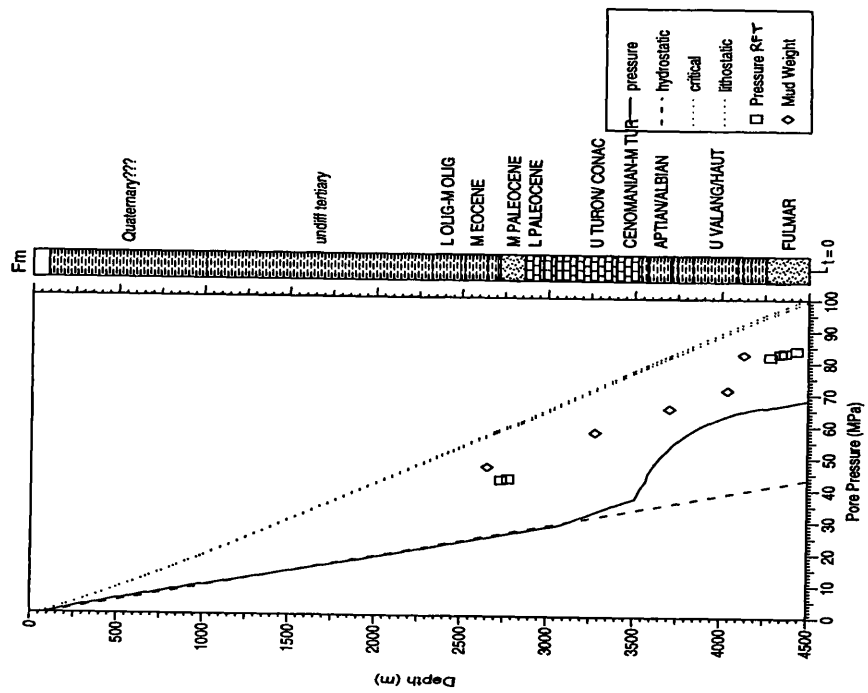
(b) Low-permeability case



(a) High-permeability case

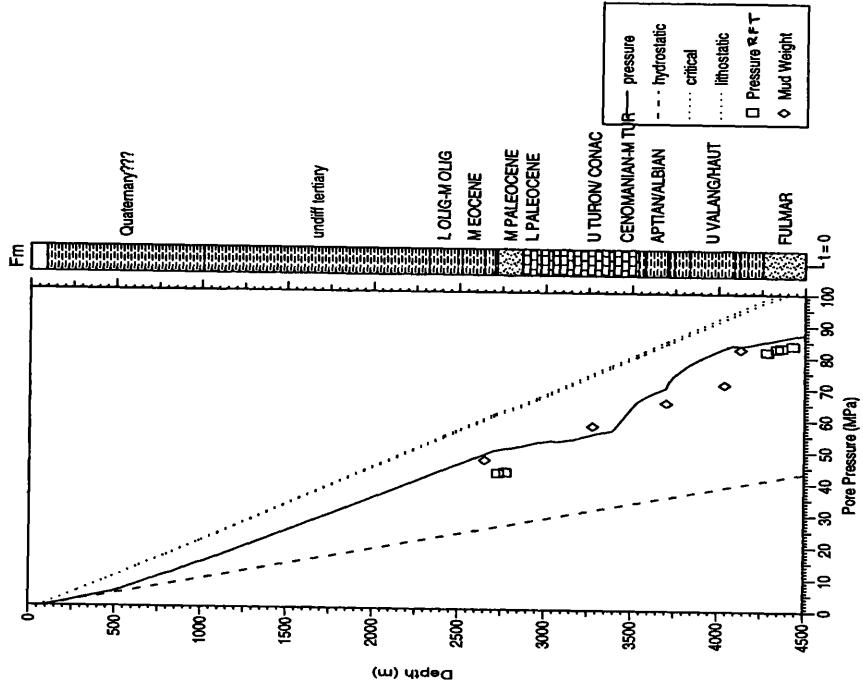
Figure 5.11 Model pressure-depth profiles for well 22/30a-1

29/10-2



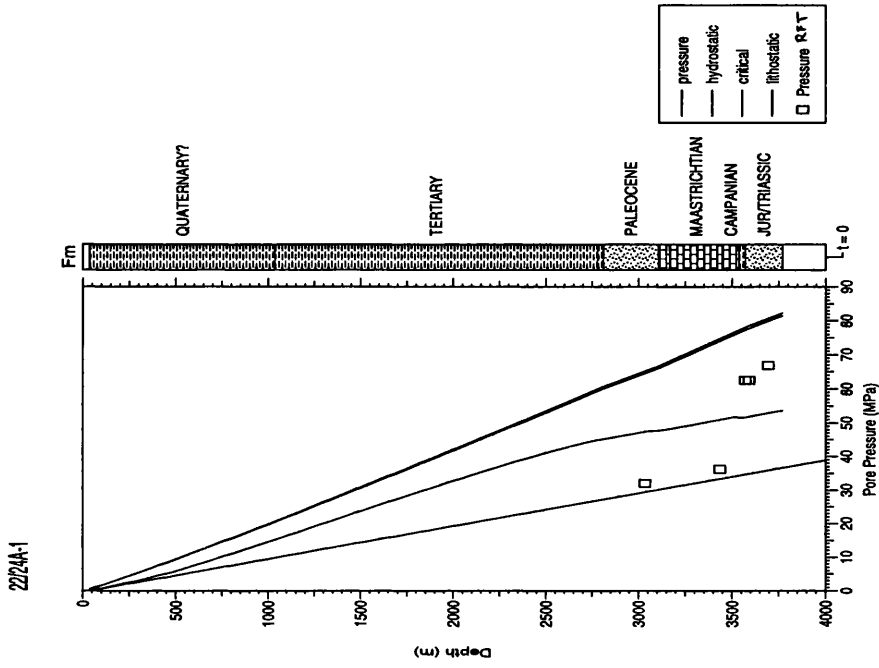
(a) High-permeability case

29/10-2

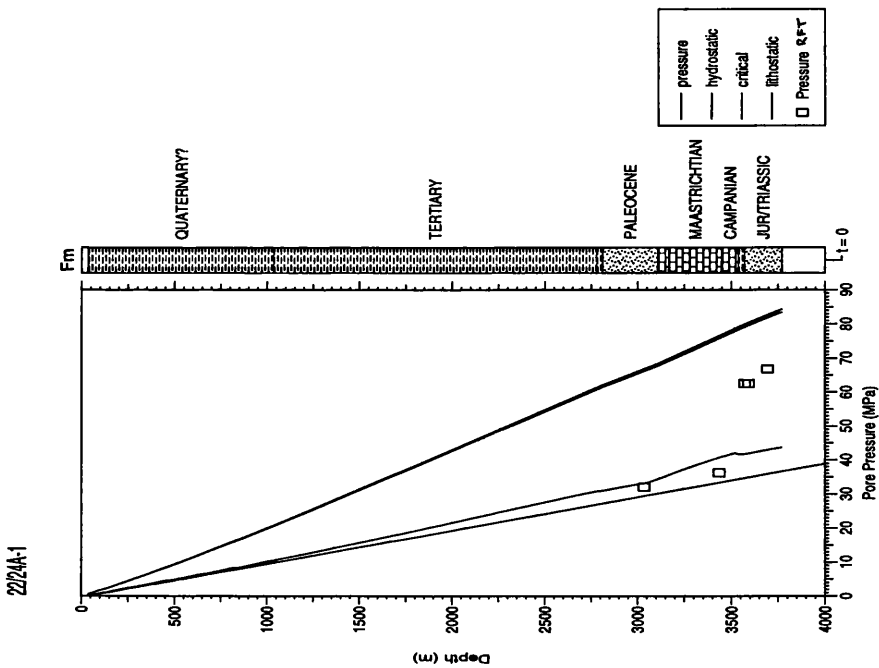


(b) Low-permeability case

Figure 5.12 Model pressure-depth profiles for well 29/10-2



(a) High-permeability case



(b) Low-permeability case

Figure 5.13 Model pressure-depth profile for well 22/24a-1

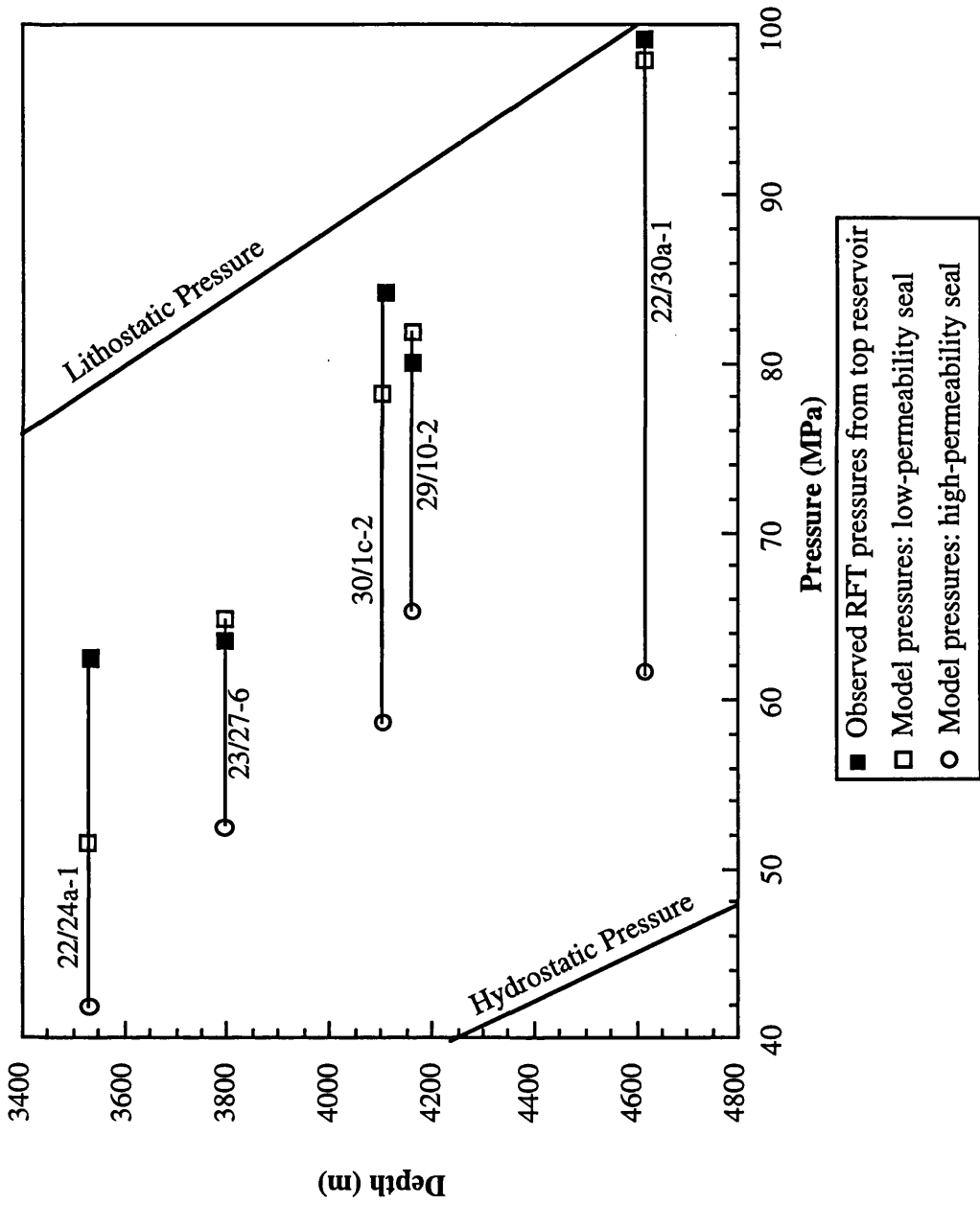
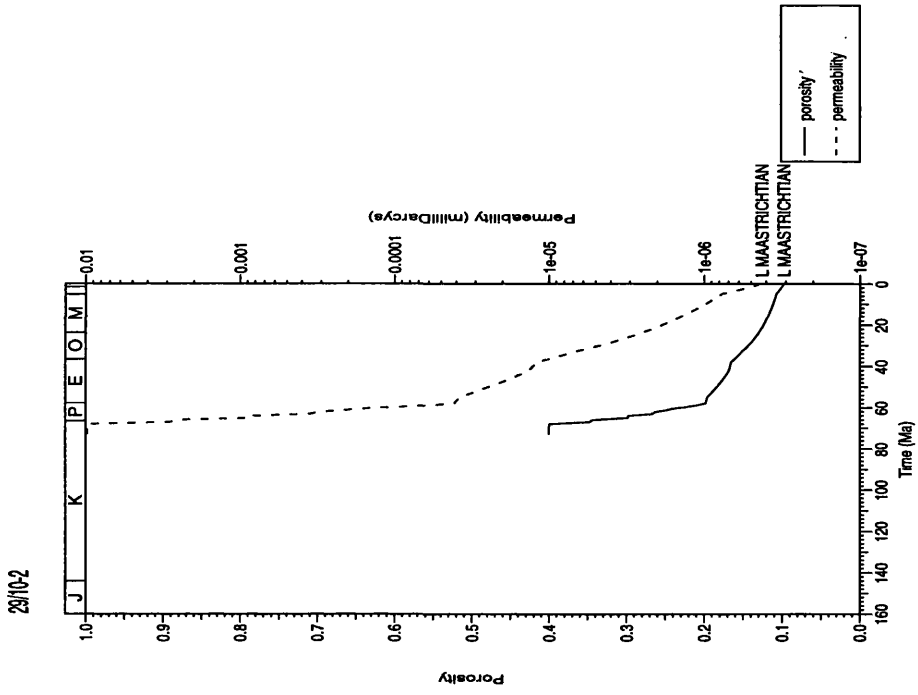
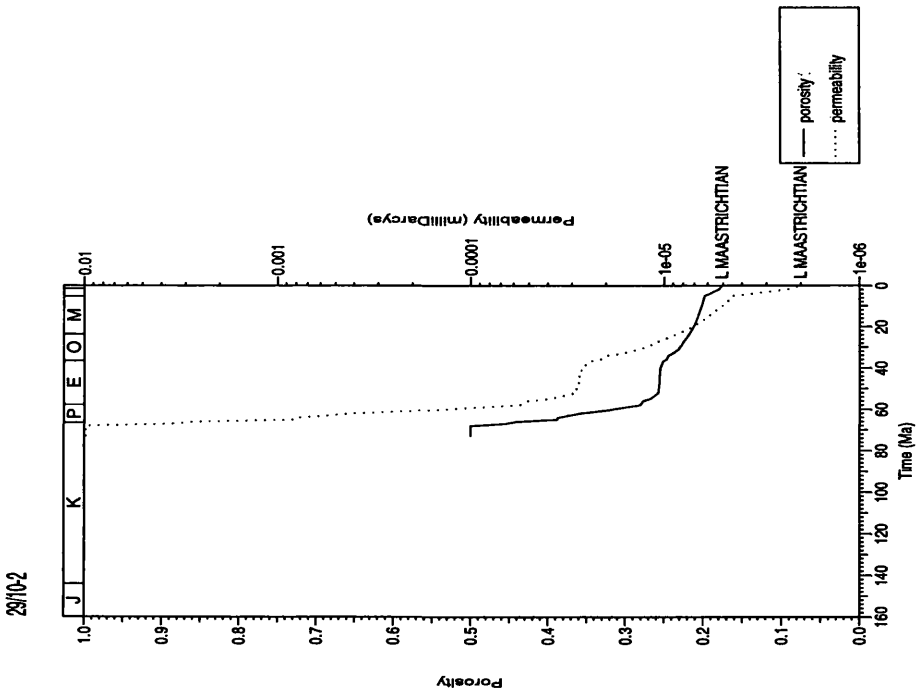


Figure 5.14 High-permeability models are valid for supra-seal pressures but underestimate the magnitude of overpressure in the sub-seal Jurassic sandstones across the region. Low-permeability models replicate sub-seal pressures but overestimate supra-seal pressures and thus are not valid. Wells 22/24a-1 and 30/1c-2, with high pressures and thin seals, cannot be matched in low-permeability model

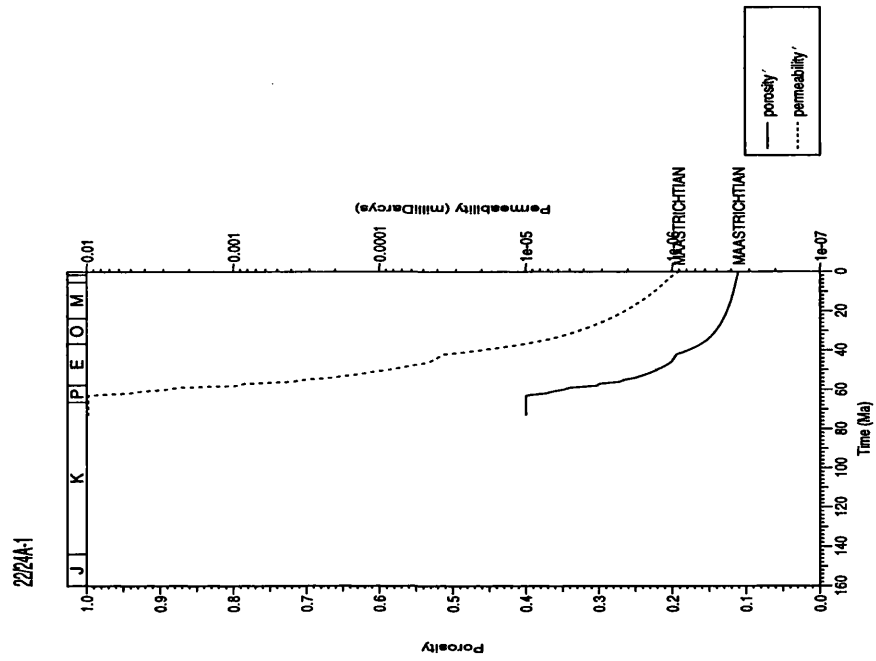


(a) High-permeability case

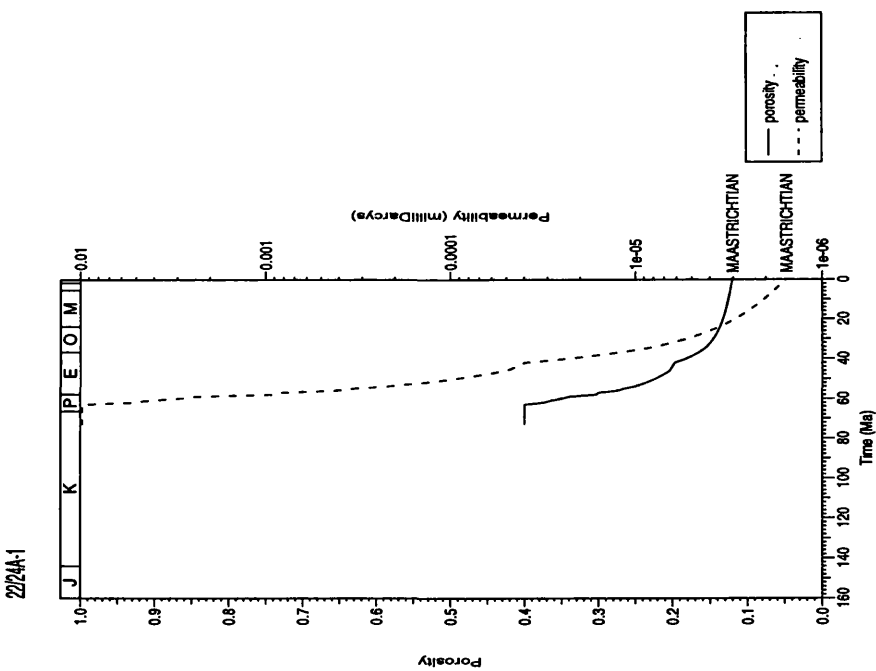


(b) Low-permeability case

Figure 5.15 Model porosity and permeability for Maastrichtian Chalk in well 29/10-2



(a) High-permeability case



(b) Low-permeability case

Figure 5.16 Model porosity and permeability for Maastrichtian Chalk in well 22/24a-1

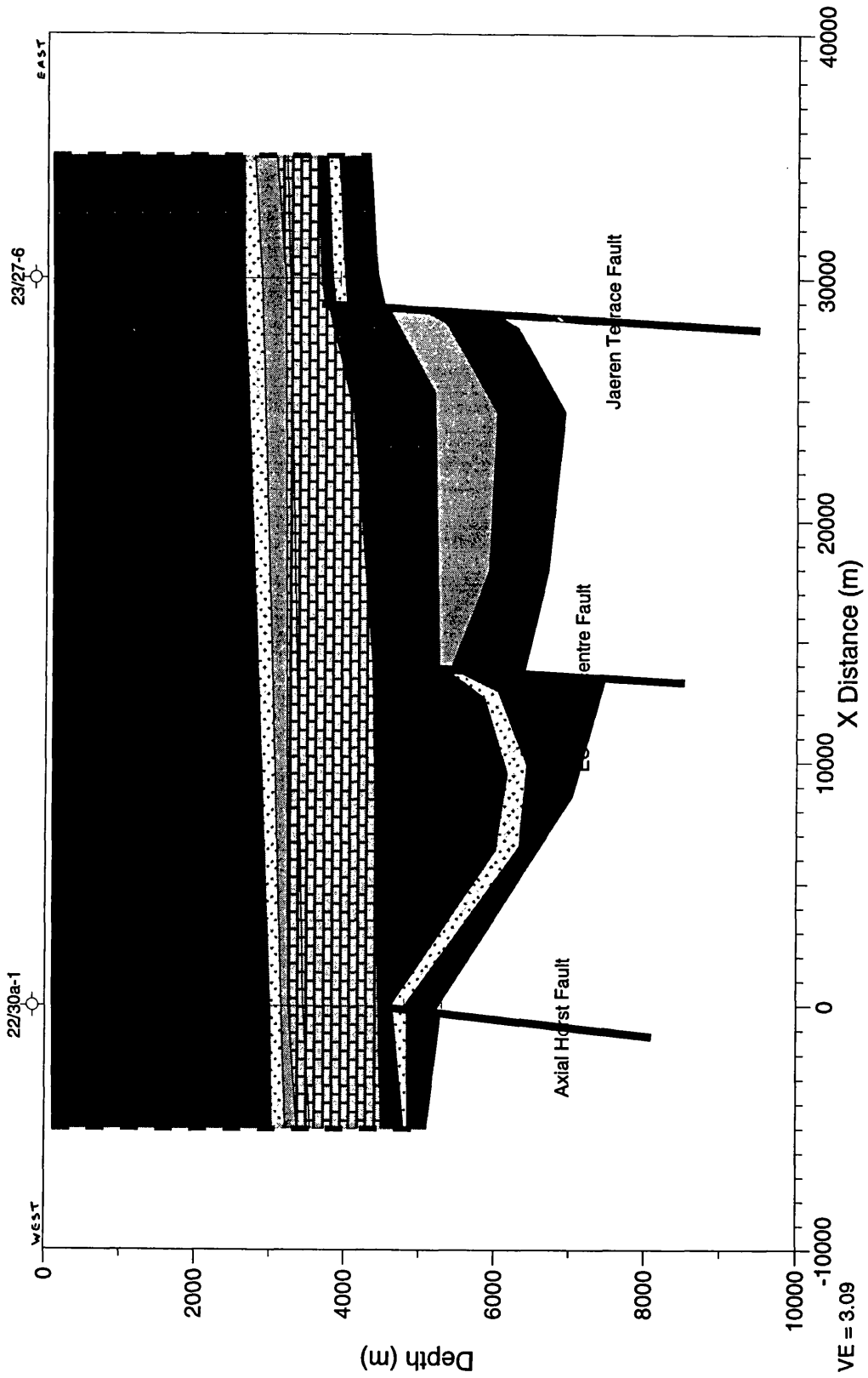


Figure 5.17 Initial input cross-section for two-dimensional model (after Roberts et al 1990)

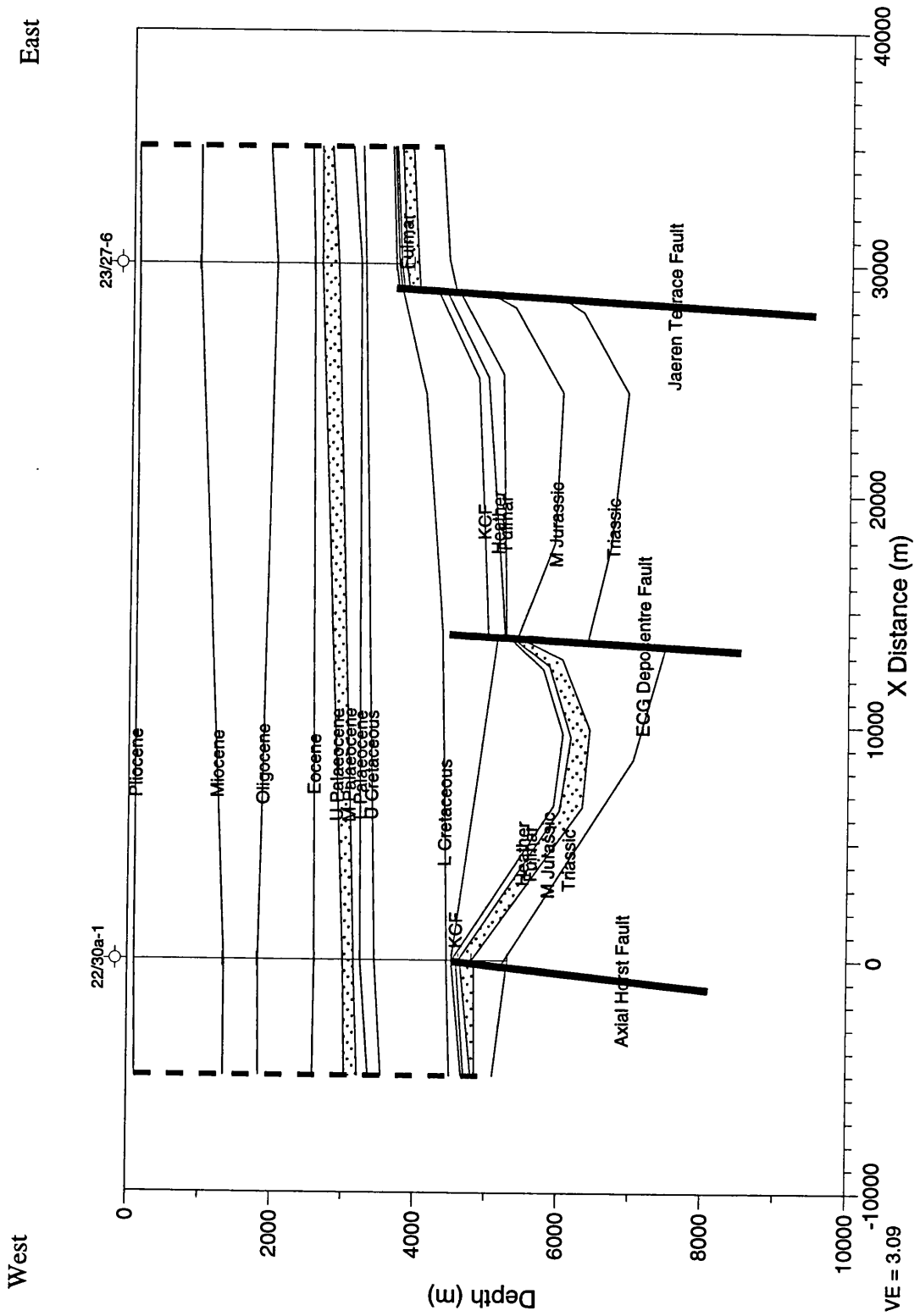


Figure 5.18 Initial input cross-section of East Forties Basin showing lithostratigraphic horizons and formation tops

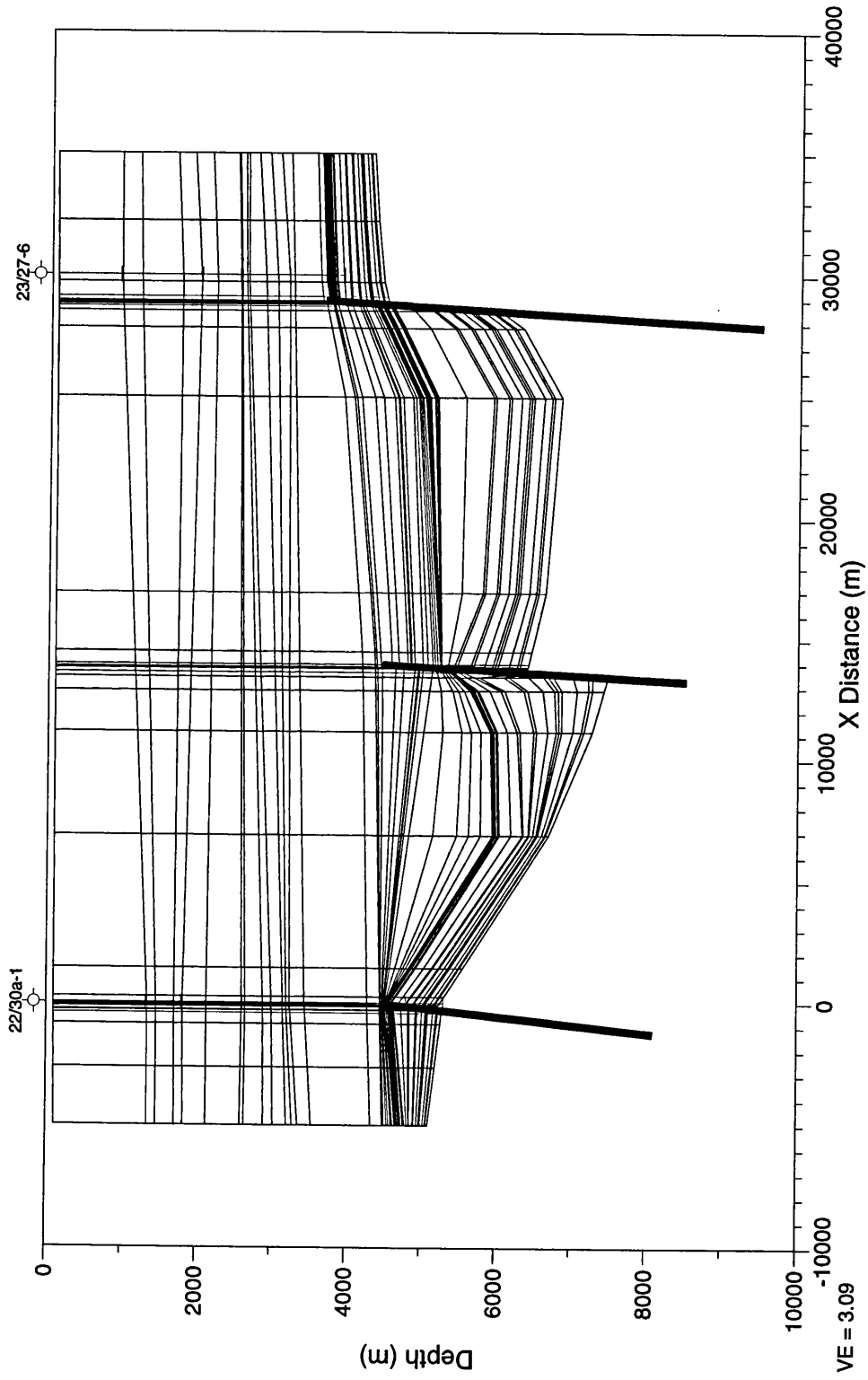


Figure 5.19 Cross-section calculation grid for two-dimensional model

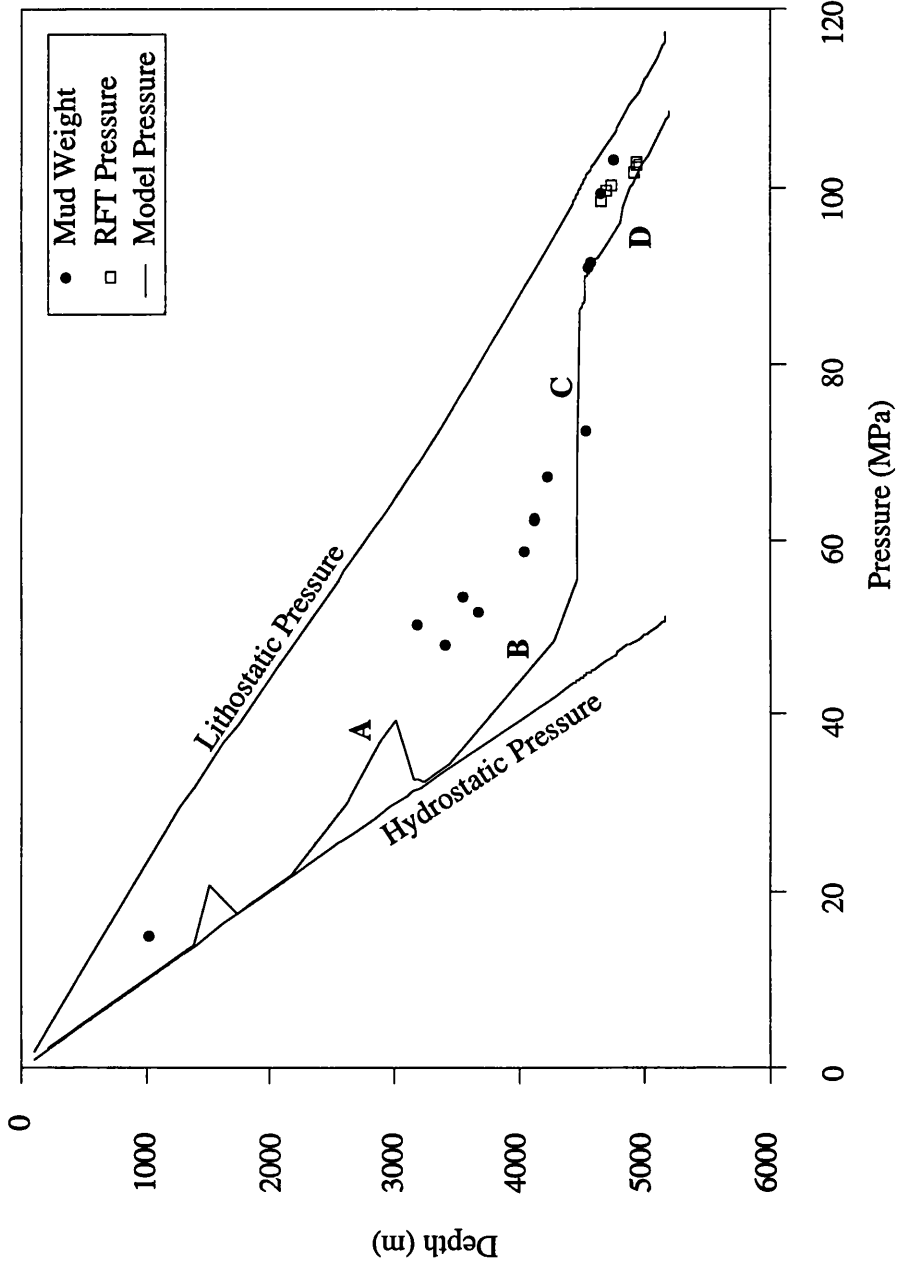


Figure 5.20 Modelled and observed pressure-depth profiles in well 22/30a-1. Stratigraphy shown in Figure 5.11. This well is situated on the crest of the Forties-Montrose High. The model reproduces overpressure in the Tertiary mudstones (A); rising pressures in the Chalk (B); a sharp rise in pressure in the Jurassic (C); and adequately simulates the high pressure in the Jurassic sandstones (D).

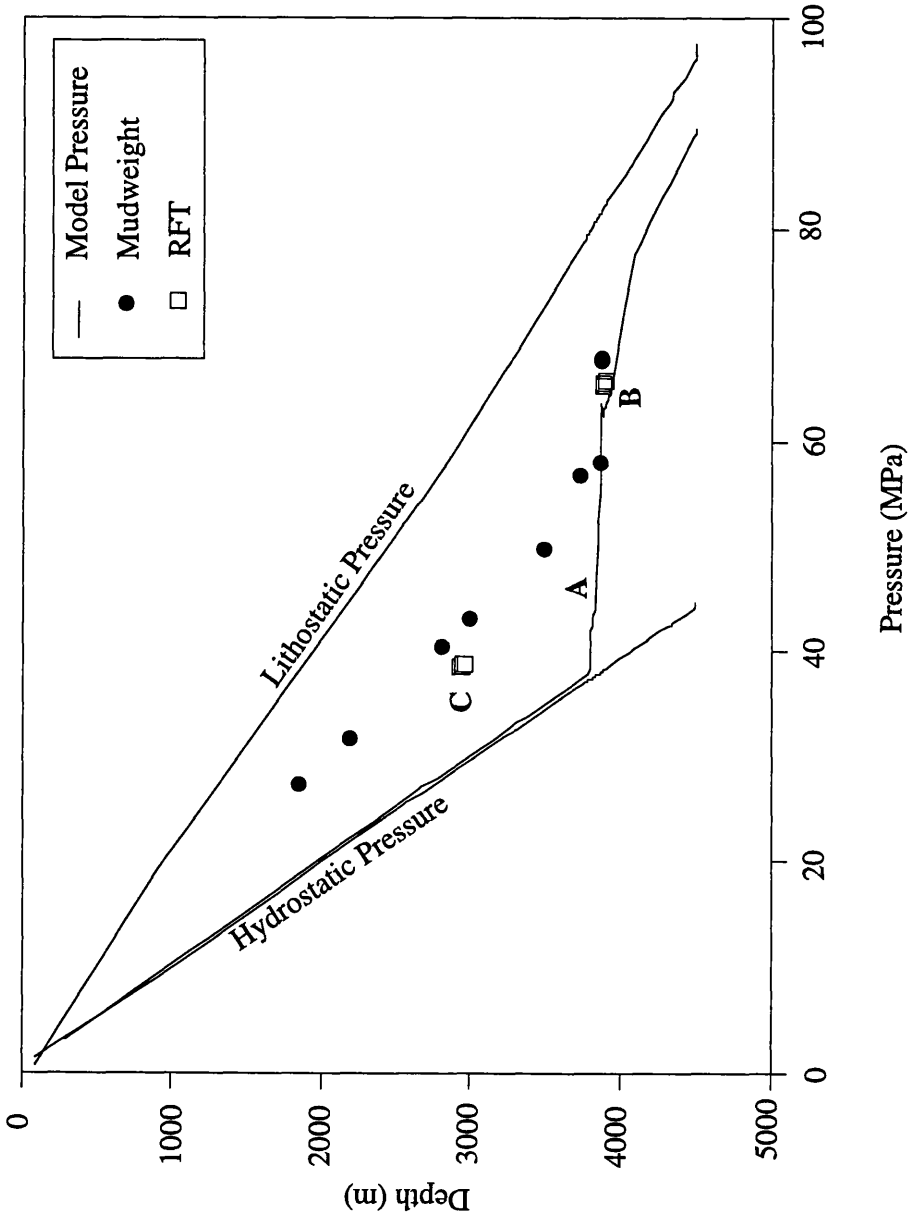


Figure 5.21 Modelled and observed pressure-depth profiles in well 23/27-6. This well is situated on the eastern margin of the Graben. The model reproduces a sharp rise in pressure in the Jurassic (A); and adequately simulates the high pressure in the Jurassic sandstones (B). It does not reproduce overpressure in the Palaeocene sandstones (C) due to high permeability in this unit. See Figure 5.32 for comparison.

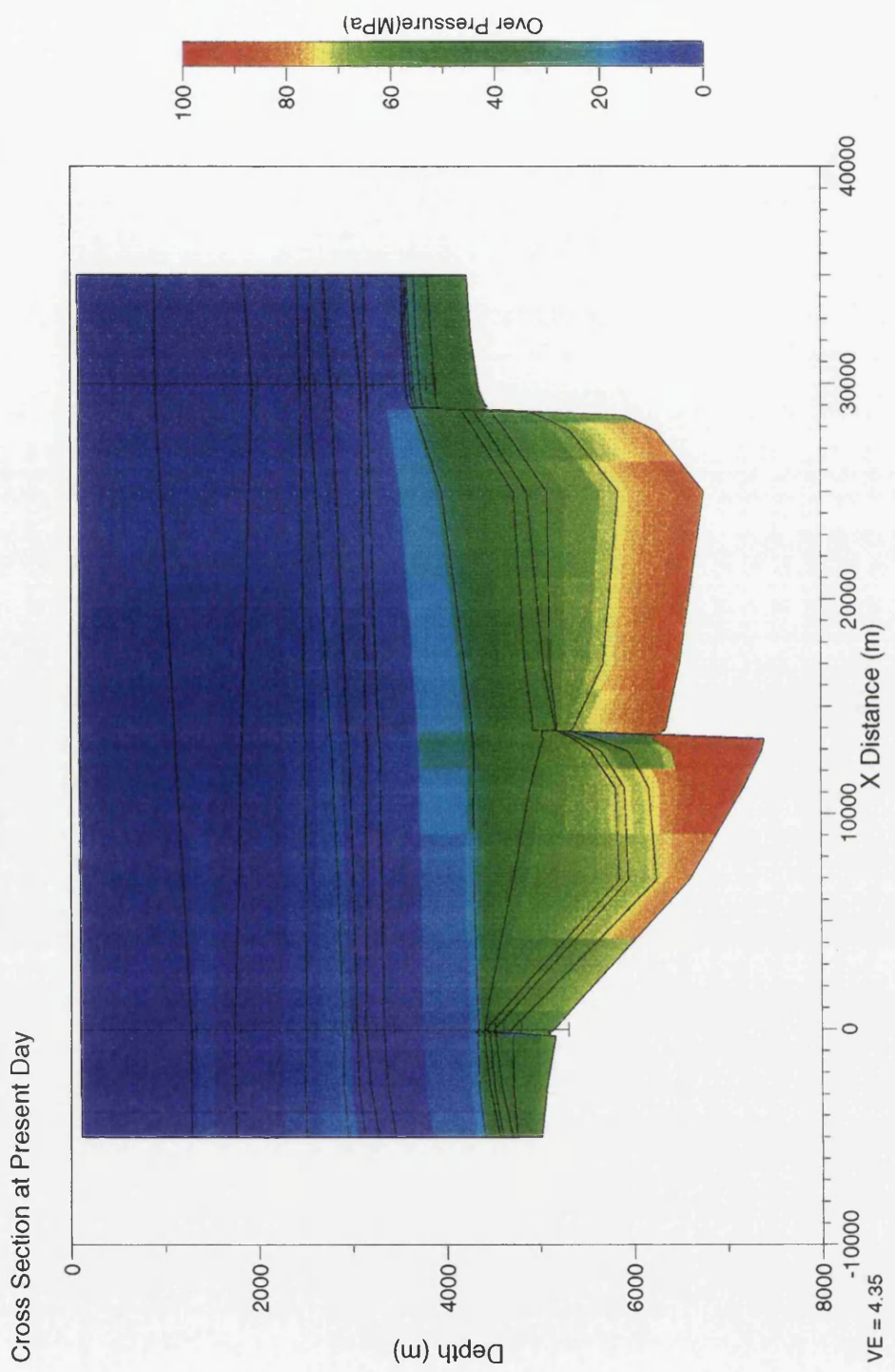


Figure 5.22 Cross-section of modelled overpressure

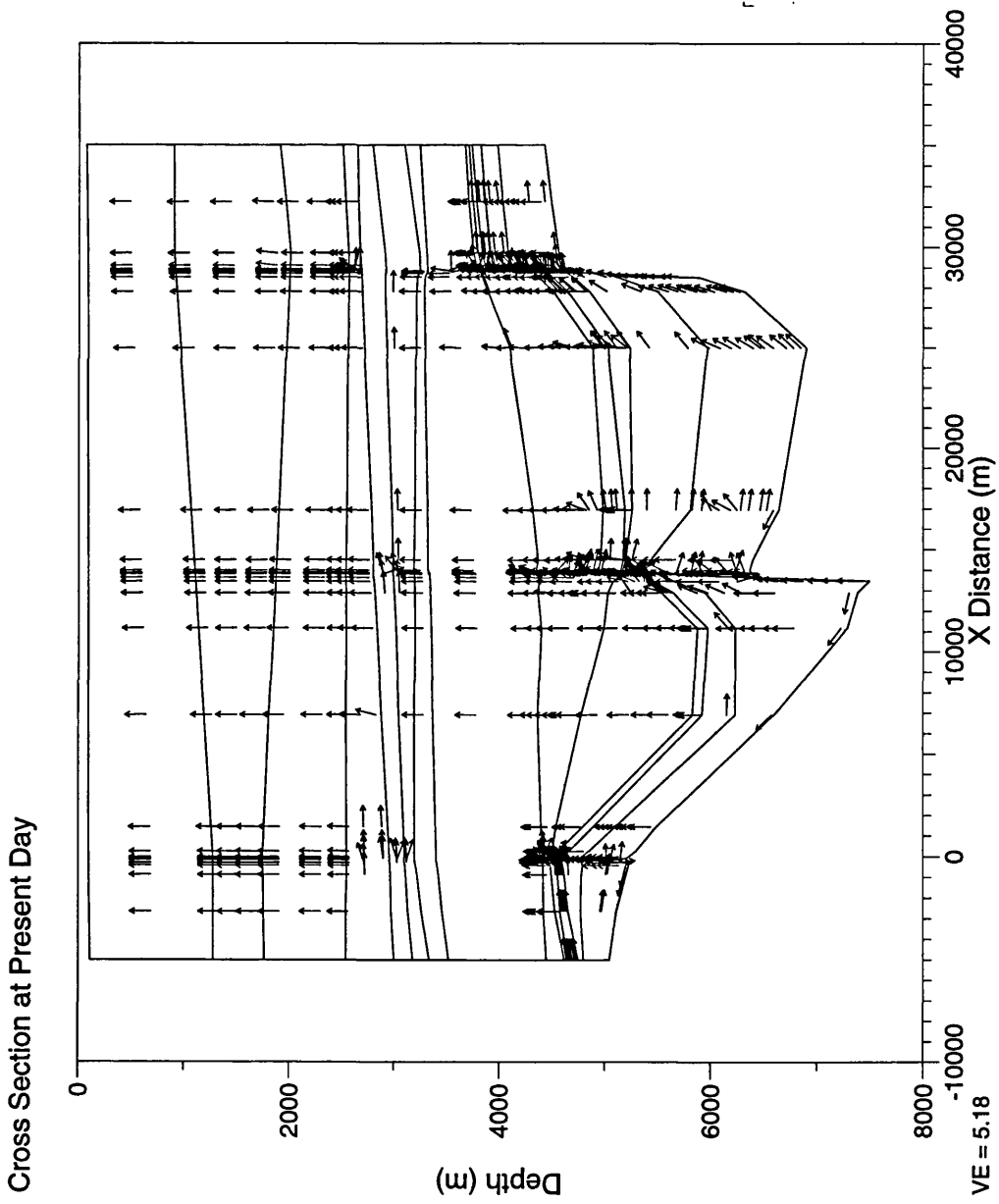


Figure 5.23 Simulated water flow directions in the model cross-section. Arrows are not scaled, and show flow direction at their point. Stratigraphy from Fig 5.18.

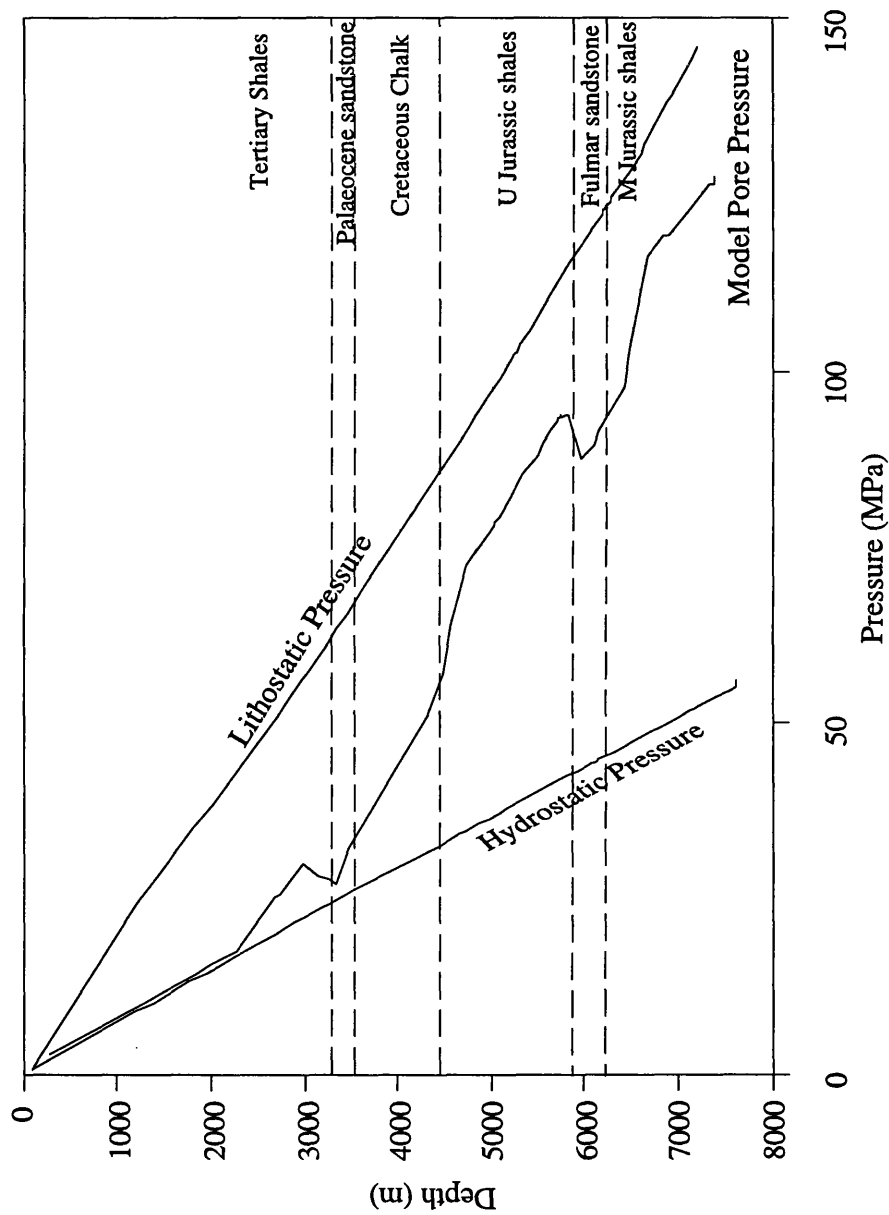


Figure 5.24 Model pressure-depth profile for off-structure pseudowell in deep E Forties Basin (located at $x=10000\text{m}$). Lowered pressures in Fulmar sandstone due to lateral flow are indicated. However, deep wells are observed to exhibit rapid rises in pressure in the Kimmeridge Clay Fm. This phenomena is poorly replicated by the model, which shows a homogenous increase in pressure through the Jurassic shale section.

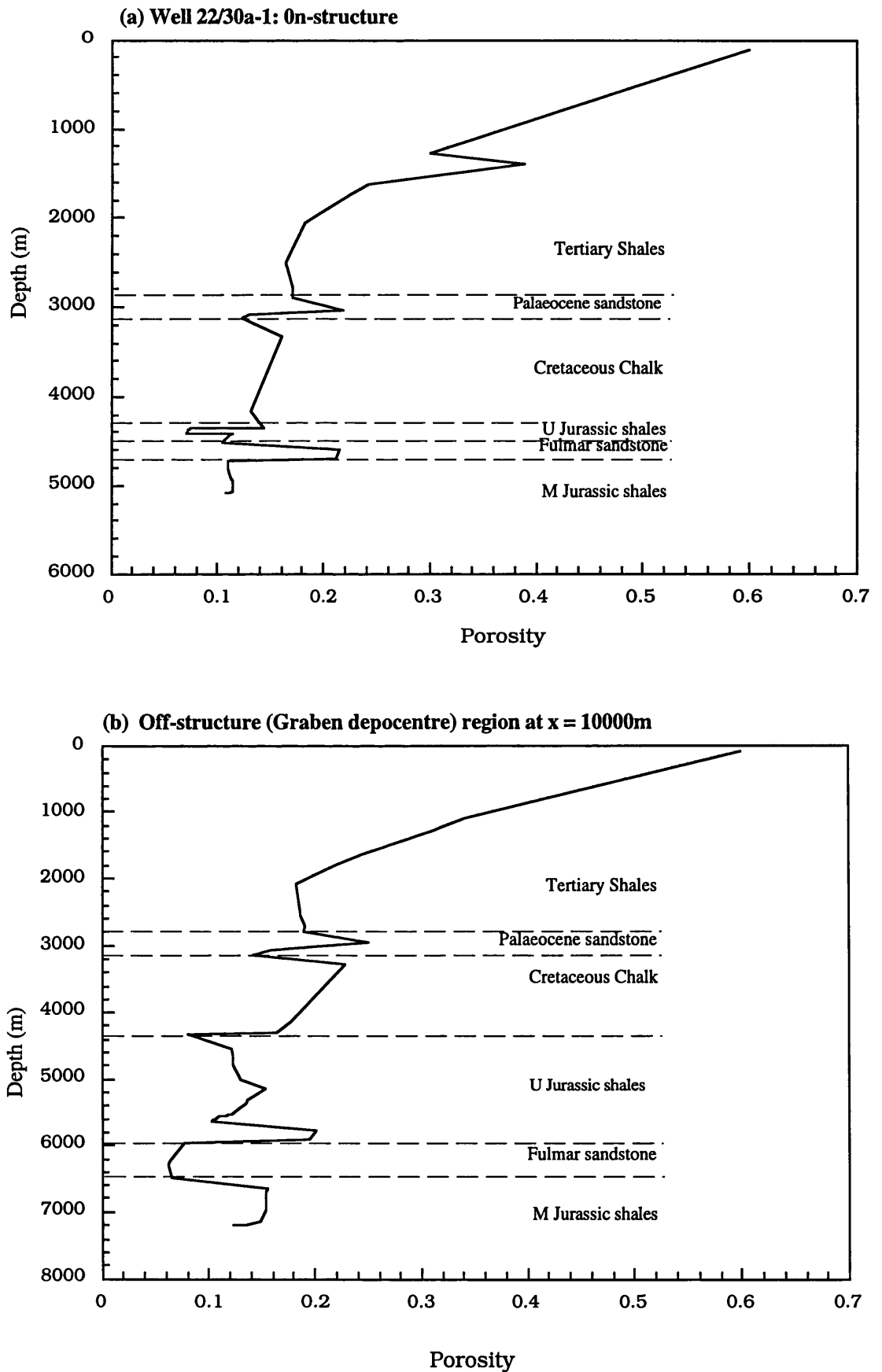


Figure 5.25 Porosity-depth profiles for well 22/30a-1 and an off-structure region. Undercompaction is exhibited in the thick shale sections and in the Fulmar sandstone in well 22/30a-1.

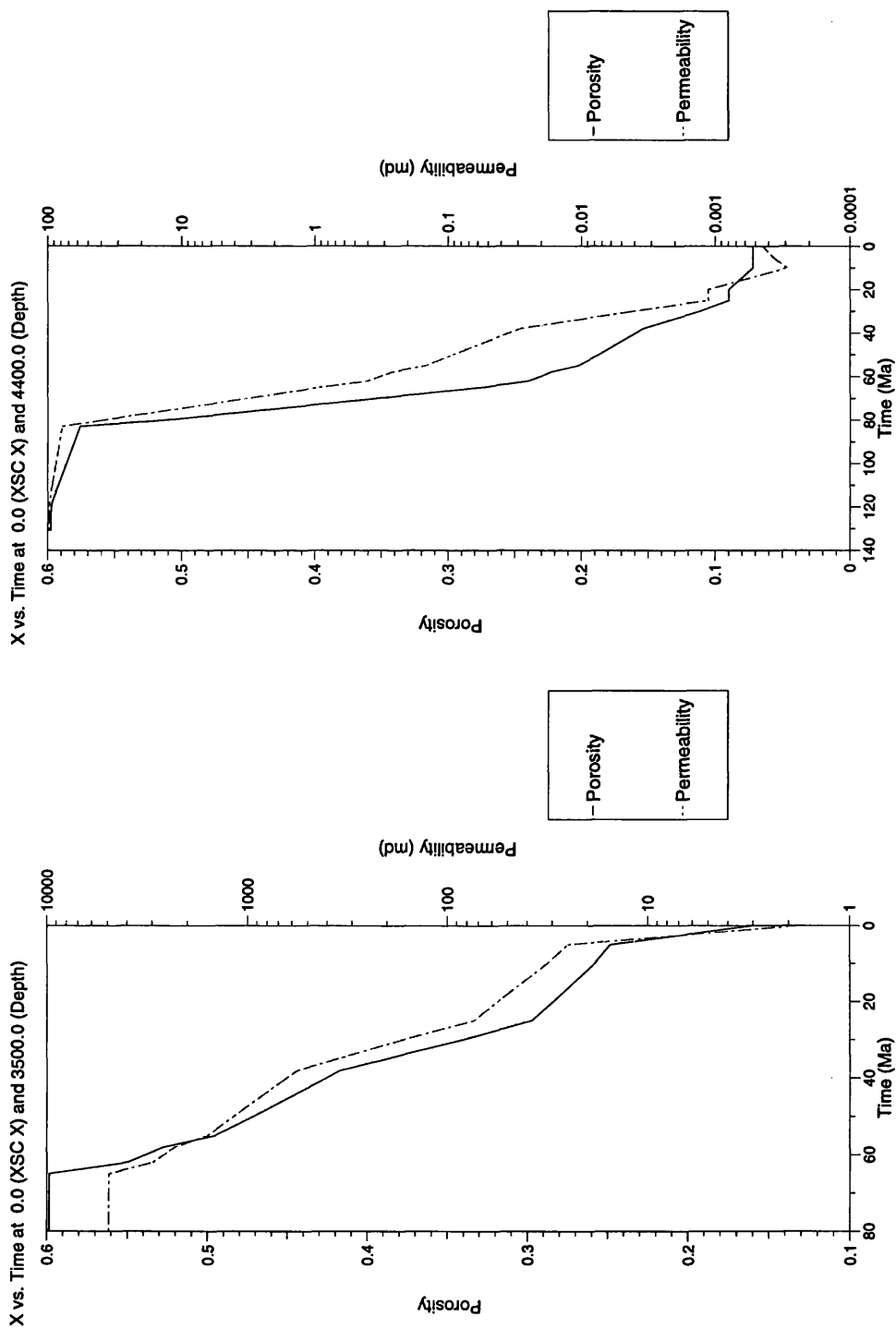


Figure 5.26 Evolution of model aquitard porosity and permeability for model well 22/30a-1, producing model pressure shown in Fig 5.20

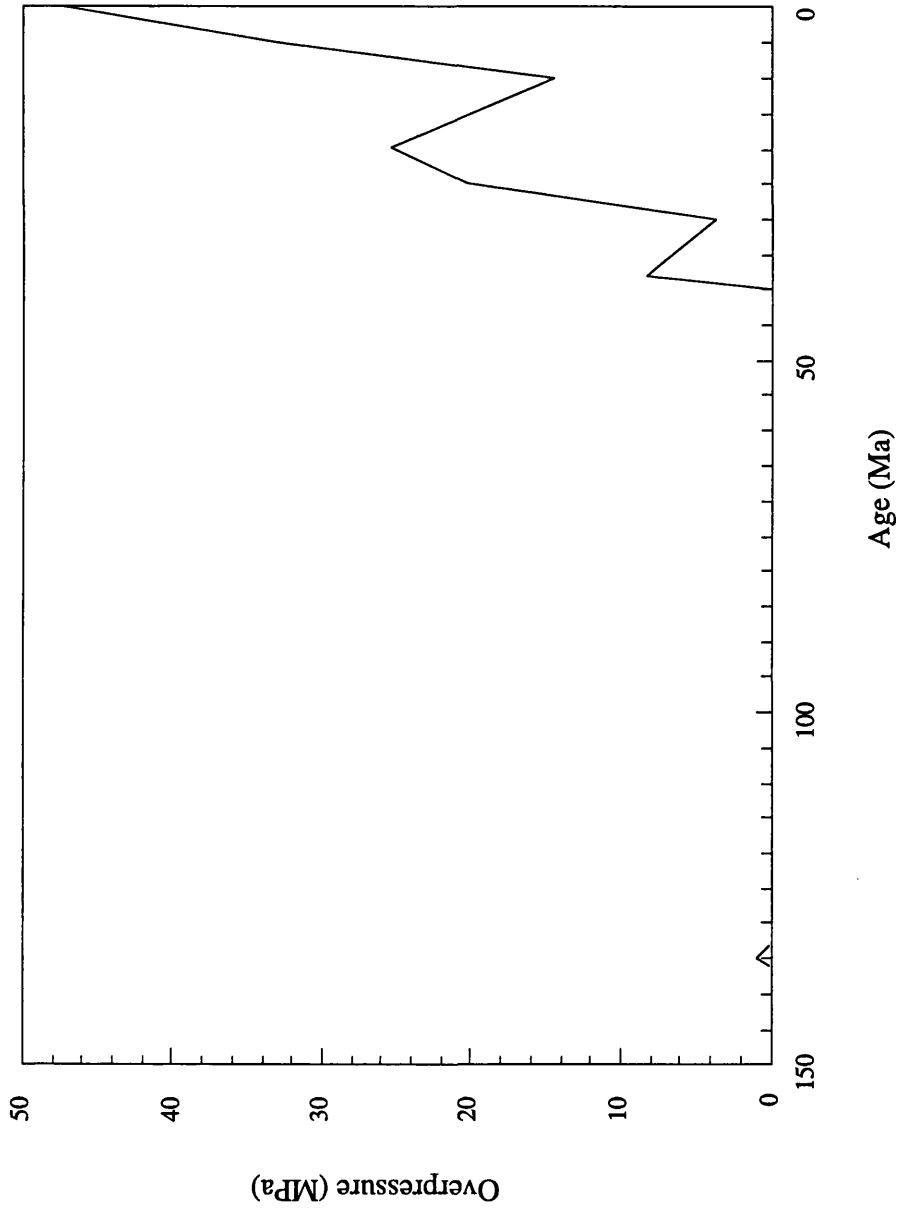


Figure 5.27 Modelled timing of overpressure development for Jurassic Fulmar sandstone in well 22/30a-1

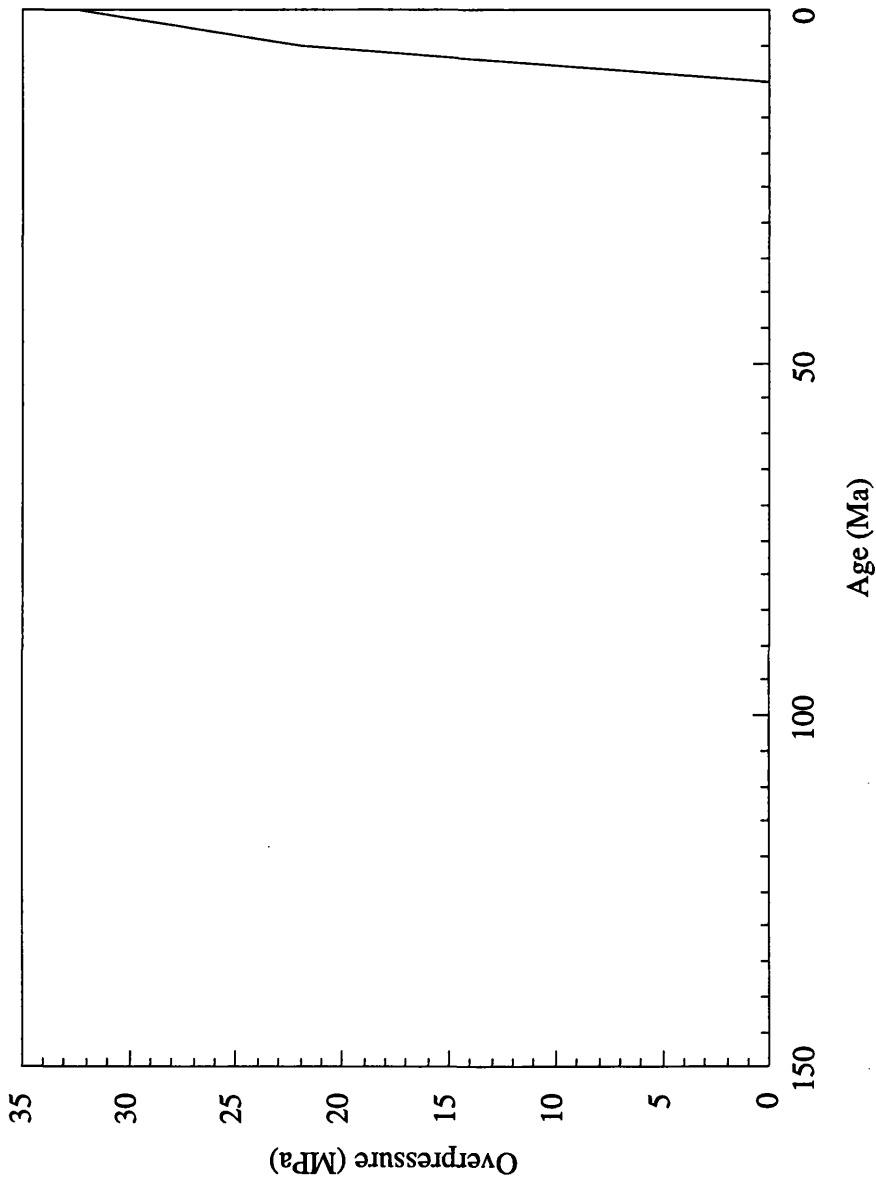


Figure 5.28 Modelled timing of overpressure development for Jurassic Fulmar sandstone in well 23/27-6. The sandstone remains hydropressured until the Plio-Pleistocene due to shallower burial and thinner seals than in well 22/30a-1 (Fig 5.27).

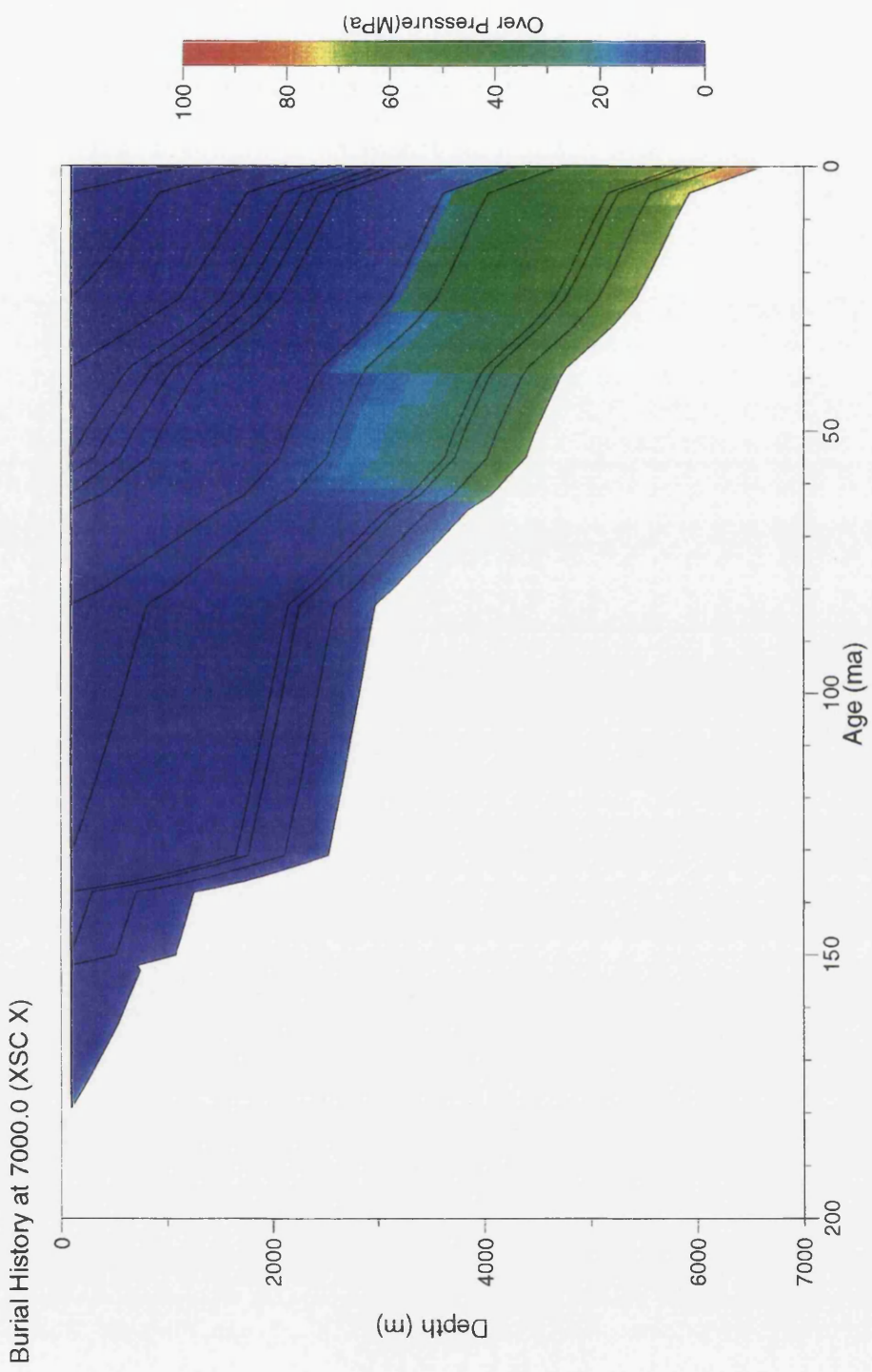
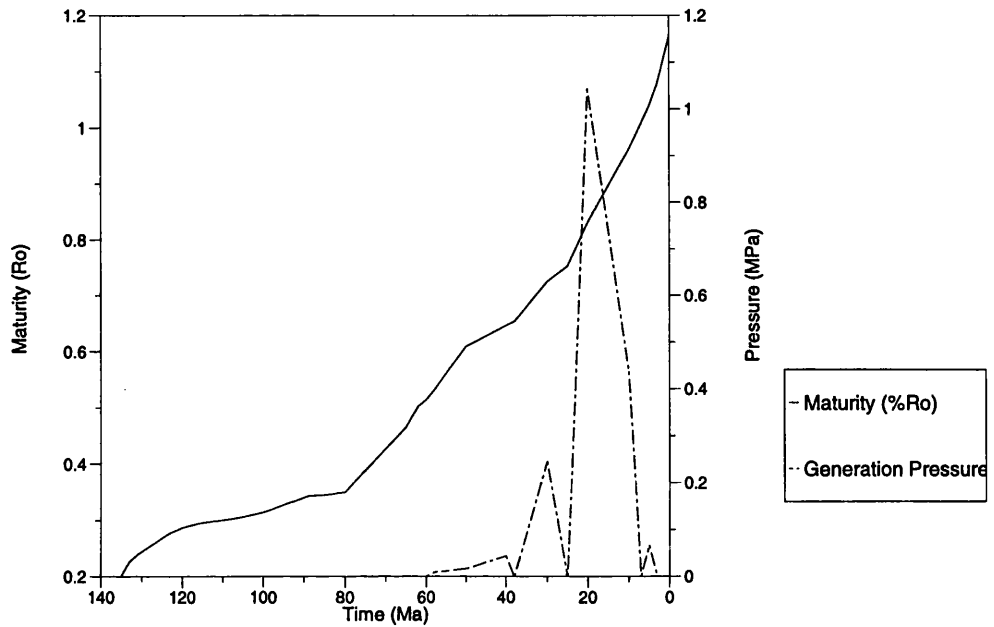


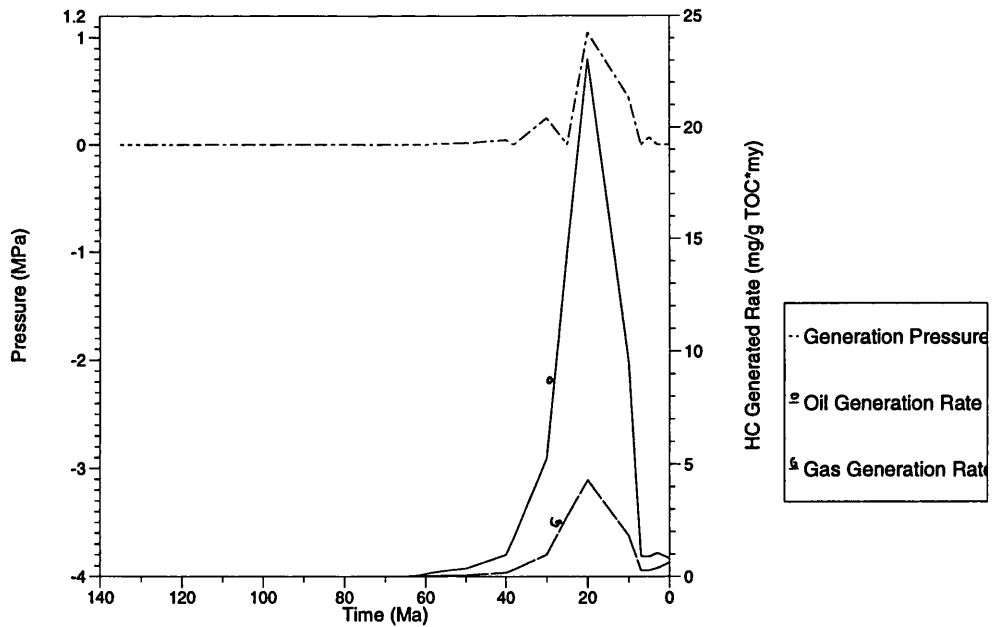
Figure 5.29 Evolution of modelled overpressure with time and burial history for off-structure region at $x=6000\text{m}$

X vs. Time at 7000.0 (XSC X) and 5500.0 (Depth)



(a) Simulated evolution of maturity and generation pressure

X vs. Time at 7000.0 (XSC X) and 5500.0 (Depth)



(b) Simulated hydrocarbon generation rates and generation pressure

Figure 5.30 Modelled timing of hydrocarbon generation and associated overpressuring in the Kimmeridge Clay Fm. in the source kitchen (at x=8000m on x-section)

X vs. Time at 0.0 (XSC X) and 4700.0 (Depth)

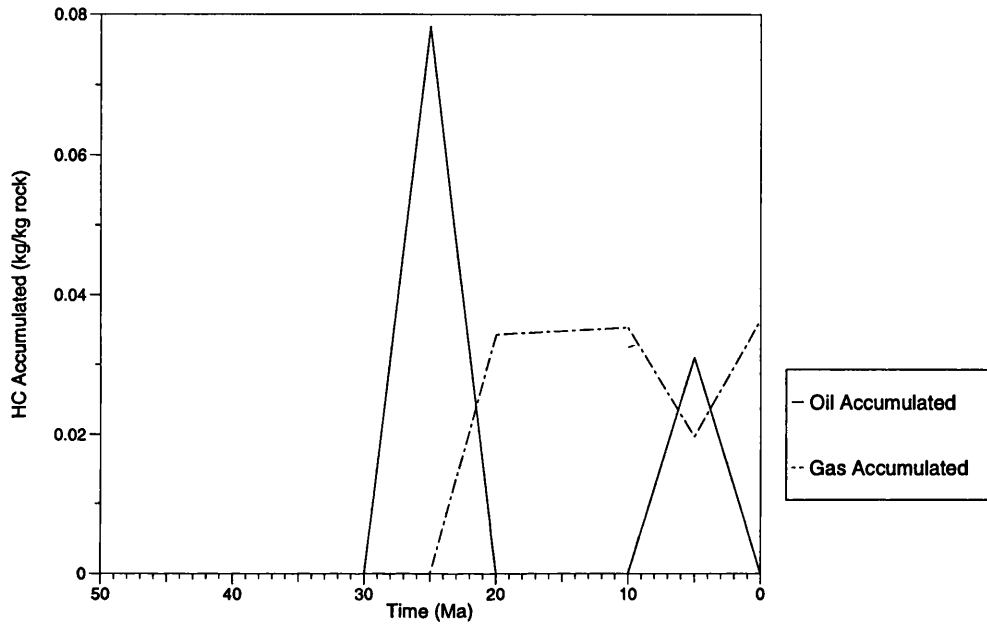
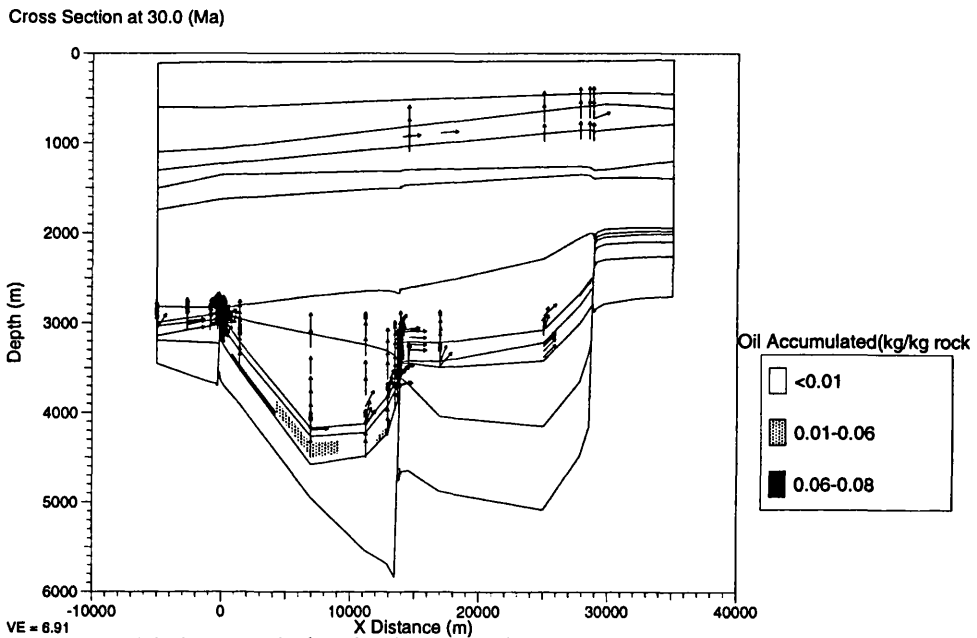
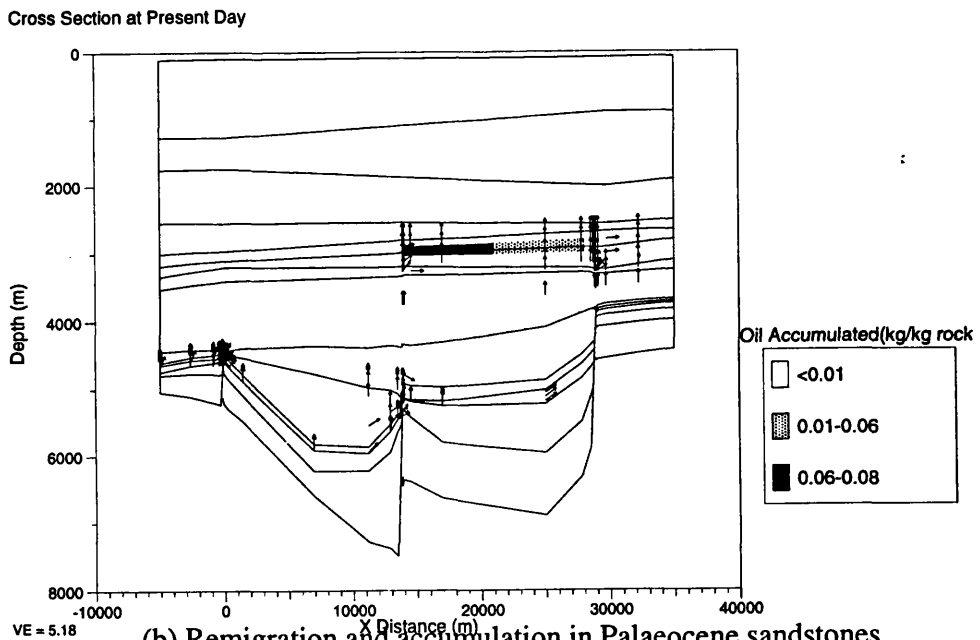


Figure 5.31 Modelled hydrocarbon accumulation through time in the Fulmar Jurassic sandstones in well 22/30a-1



(a) Accumulation in the Jurassic sandstones in the Oligocene



(b) Remigration and accumulation in Palaeocene sandstones

Figure 5.32 Simulated hydrocarbon migration and accumulation. Arrows represent direction of oil flow

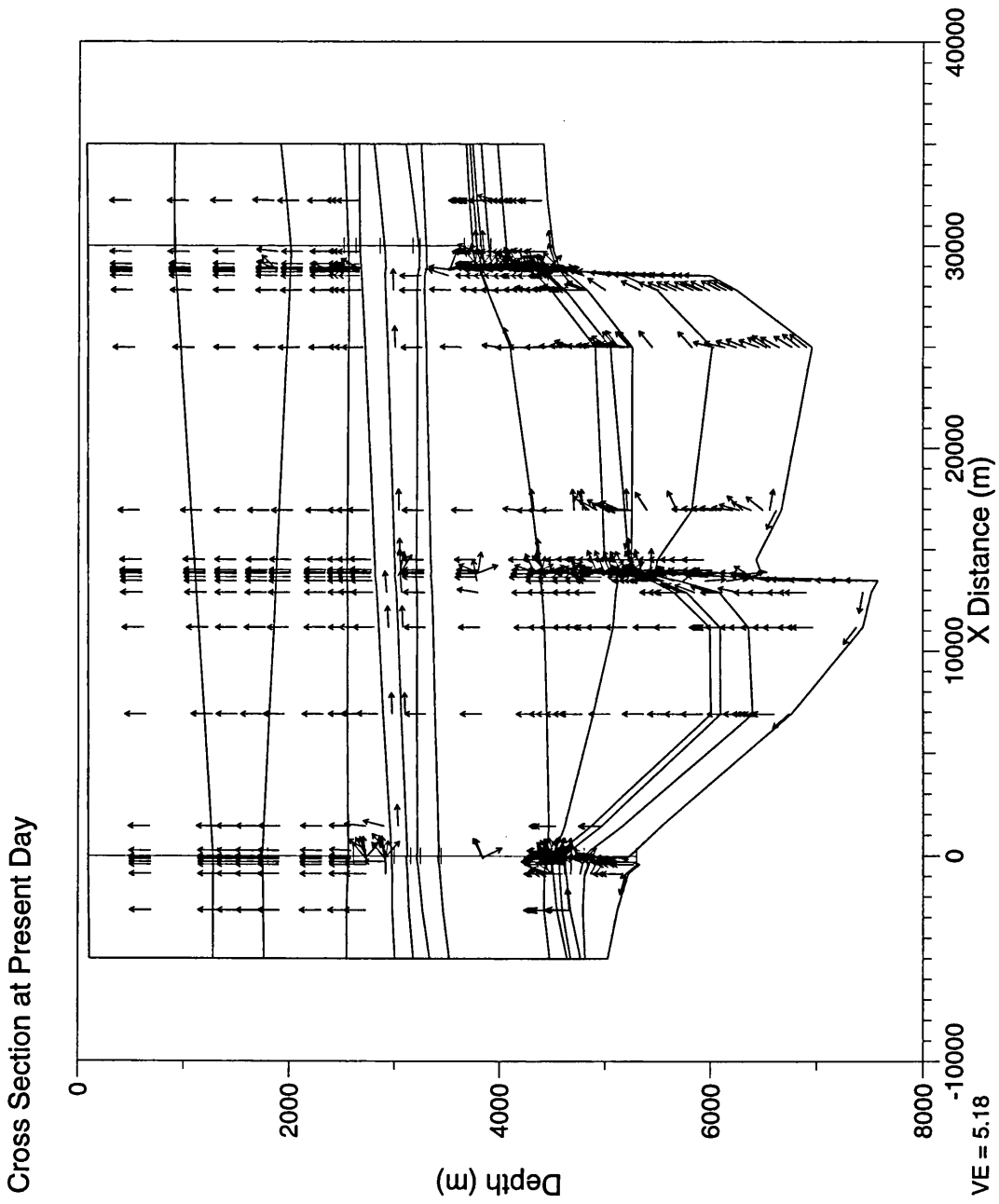


Figure 5.33 Water flow directions in simulation representing lateral shale-out of Fulmar sandstones

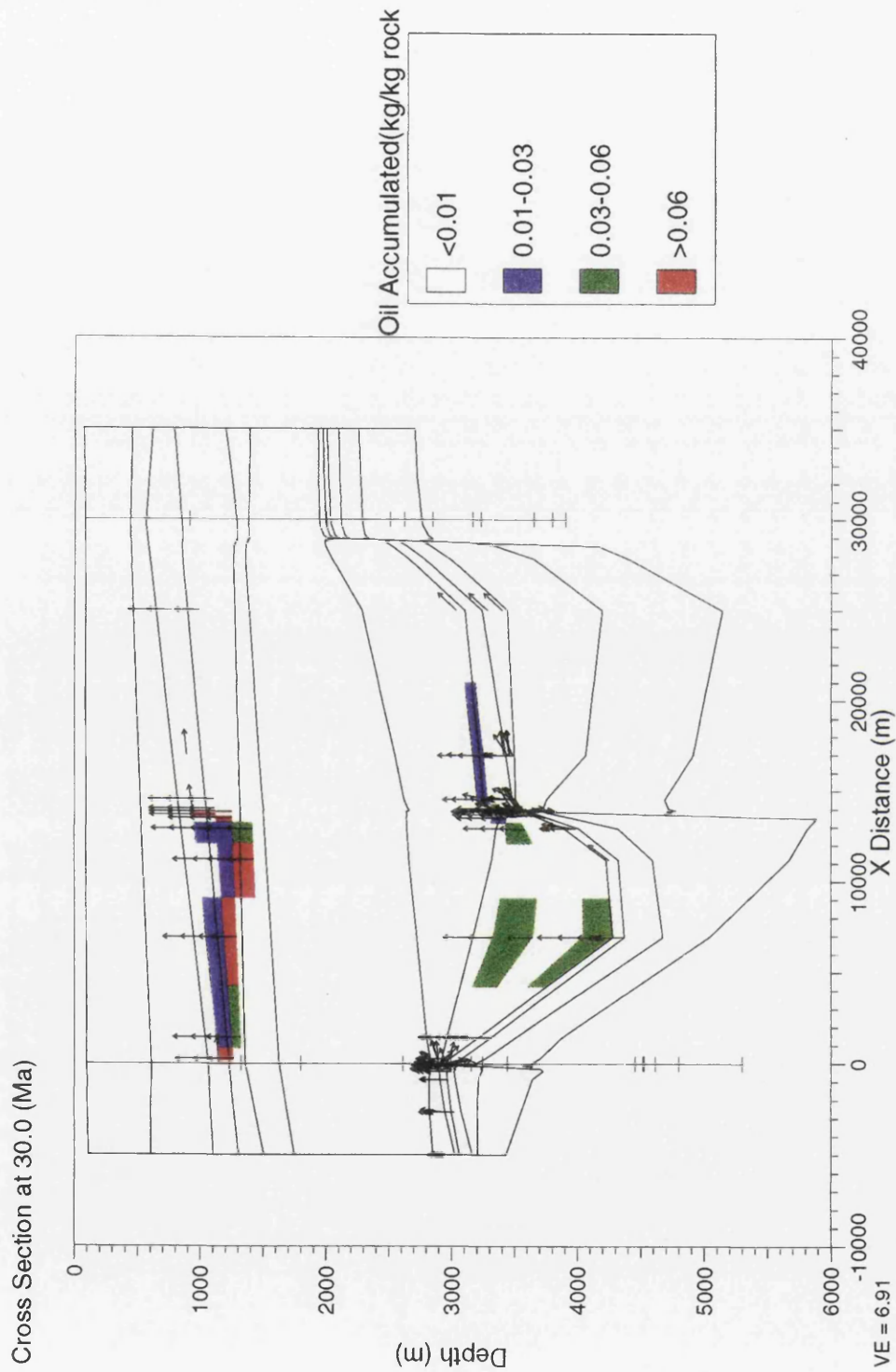


Figure 5.34 Oil accumulations and flow paths at 30 Ma in Fulmar Fm. lateral-shale-out model. Predominance of vertical flow leads to earlier emplacement of oil in Palaeocene sandstones than in continuous Fulmar Fm model (Fig 5.32)

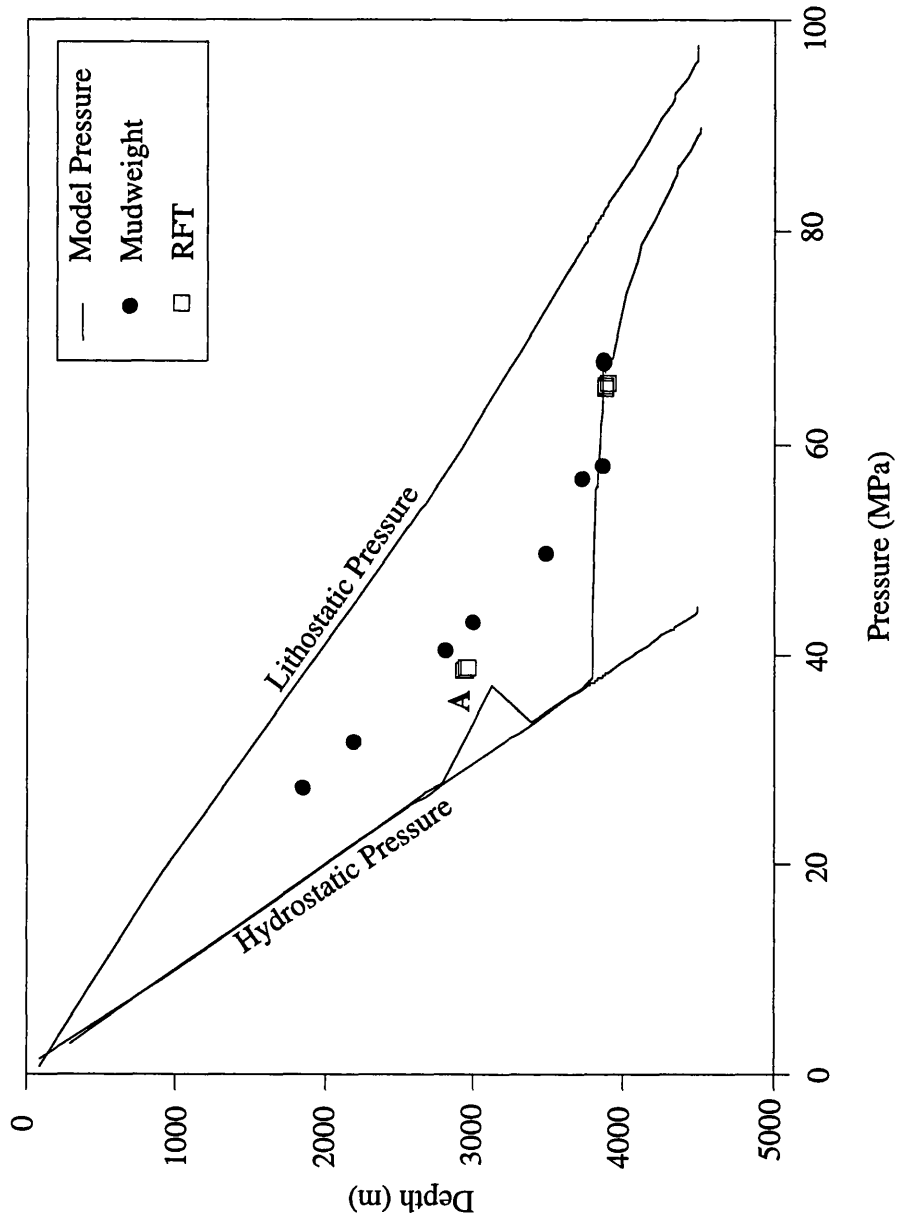


Figure 5.35

Modelled and observed pressure-depth profiles in well 23/27-6 with discontinuous Palaeocene sandstones. Overpressure is produced in the low-permeability Palaeocene sandstones (A), due to restricted fluid flow. This provides an approximate match to measured pressures. The pressure-depth profile is an improved fit to observed pressures than that of Figure 5.21, suggesting restricted lateral flow in the thin Palaeocene sandstones on the Jaeren High is more realistic.

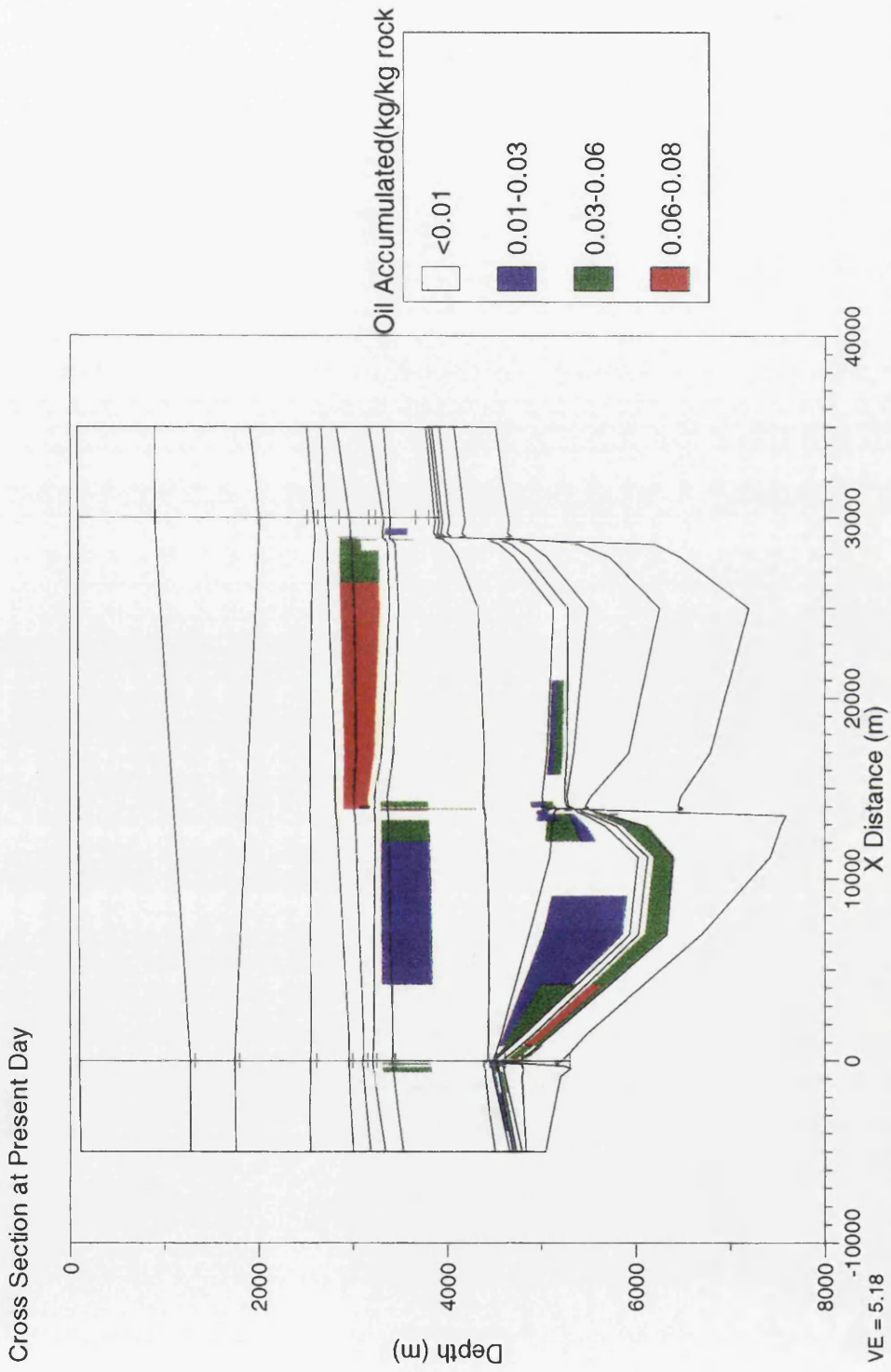


Figure 5.36 Modelled oil accumulations in the Palaeocene-siltstone model at present -day. Model assumes low-permeability Palaeocene (Fig 5.34) Oil is trapped in the Upper Chalk due to the pressure differential between the overpressured Palaeocene "siltstones" and the underlying hydropressured Chalk. Compare to Figure 5.34, where hydrocarbons are not trapped in the Chalk due to the presence of the hydropressured, permeable Palaeocene sandstone "drain".

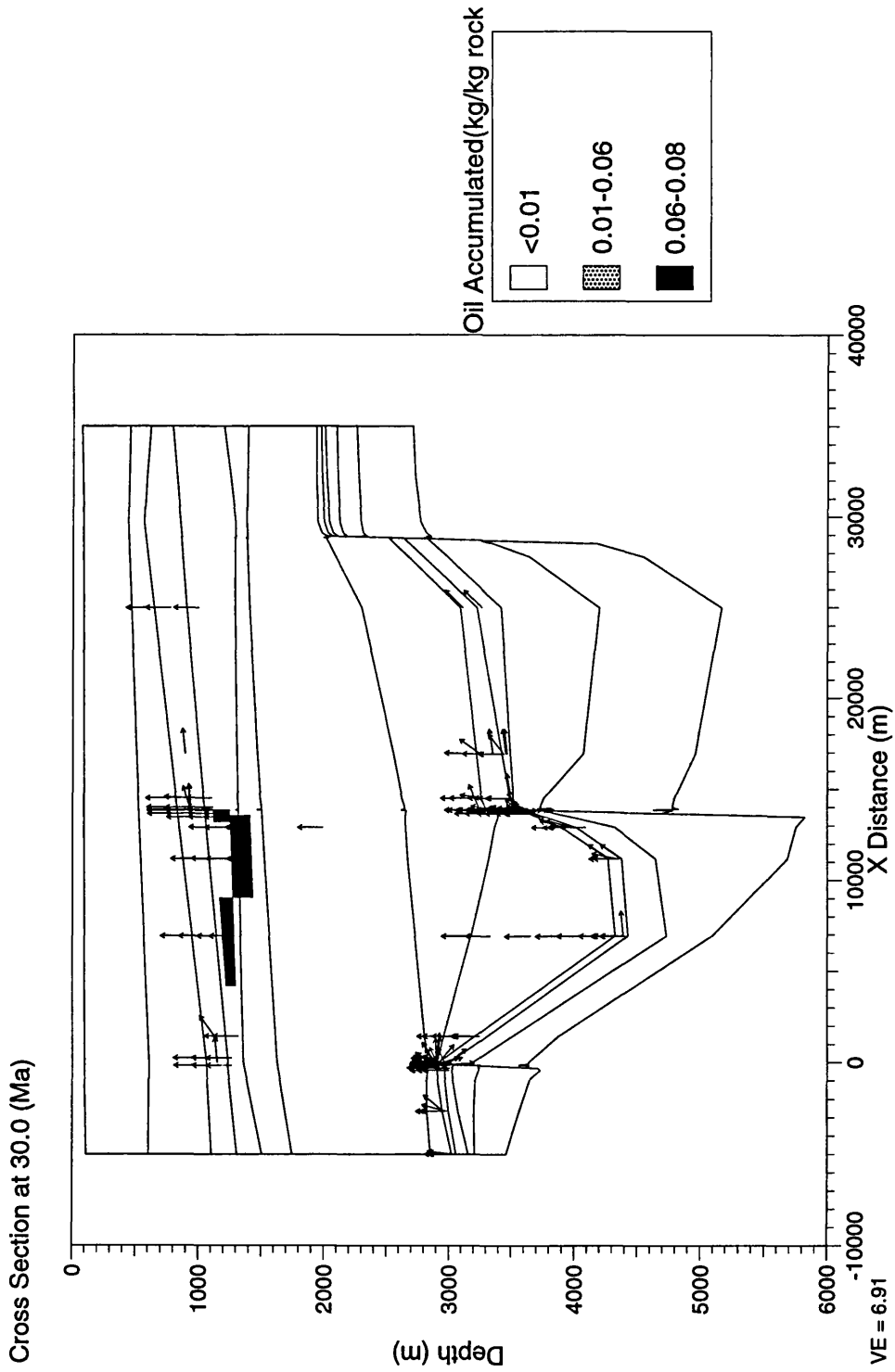


Figure 5.37 Oil migration and accumulation in open-fault model at 30 Ma. Permeable faults allow earlier emplacement of hydrocarbons in the Palaeocene sandstones, as hydrocarbons are not retained in the Jurassic sandstones.

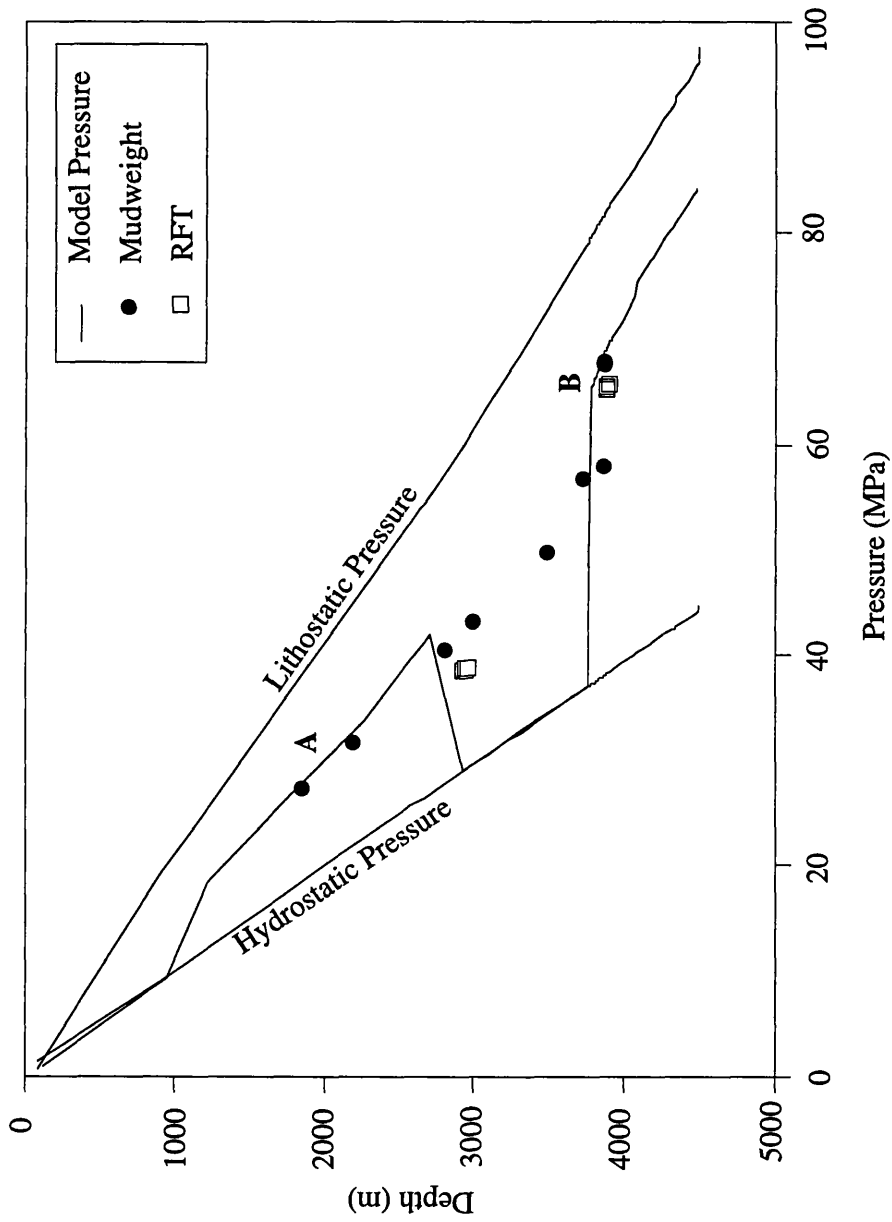
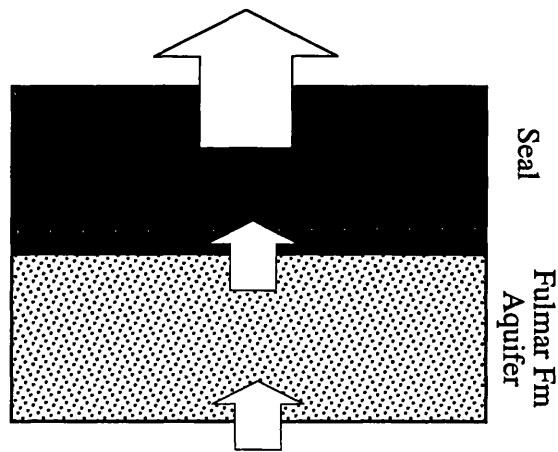


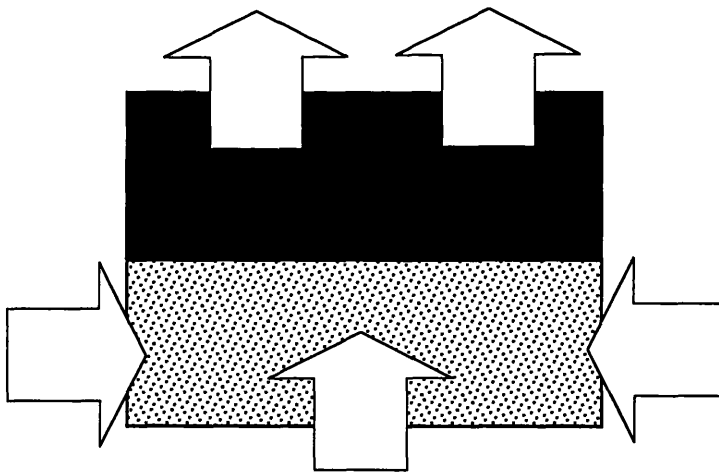
Figure 5.38 Modelled and observed pressure-depth profiles in well 23/27-6 for low-permeability mudstones. Lowering the permeability of mudstones leads to high pressures in the Tertiary shales in this well (A). Model pressures exceed mudweight (which provides a constraint for maximum pressure). Model pressures exceed mudweight and measured pressure in the Jurassic (B). This low-permeability model cannot be considered valid, and the "base-case" model of Figure 5.21 is preferred.

(A) One-dimensional analysis of flow through pressure seal reveals that flux is too great due to high permeability (calibrated to seal pressures) and thinness of seal



High observed overpressures cannot be explained simply by the restriction of vertical fluid flow through low-permeability seals

The dynamic flow of fluid through the pressure seal requires that pressure beneath the seal is dynamically maintained



(B) Two-dimensional analysis reveals that lateral flow of fluid from thick, undercompacted off-structure regions allows dynamic maintenance of overpressure at the observed levels, with no requirement for ultralow-permeability seals

Figure 5.39

Summary cartoon of model investigation findings

Table 4.1 Model input lithological parameters (refer to Appendix for algorithms)

One-Dimensional Model Lithological Input

	Initial Porosity (A)	Initial Porosity (B)	Porosity reduction factor (A)	Permeability reduction factor (B)	Fraction A	Initial Permeability (mD)	Permeability Power	Density (g/cm ³)	Thermal Conductivity (W/m ³ *degC)	Heat Capacity (kJ/m ³ *degC)
<i>High-permeability models (from Bethke 1985 and Person & Garven 1992)</i>										
Sandstone	0	0.45	0	1.35E-08	0	2.70E+04	5.5	2.64	4.4	2800
Siltstone	0.55	0	-0.8	0	1	1.01E-01	5.5	2.64	2	2650
Shale	0.6	0	-0.6	0	1	1.01E-02	5.5	3	1.5	2100
Chalk	0.1	0	-0.5	0	1	2.70E+04	5.5	2.72	2.9	2600
<i>Low-permeability models</i>										
Shale	0.4	0	-0.6	0	1	1.01E-02	5.5	2.64	1.5	2100
Chalk	0.1	0	-0.5	0	1	1.00E-04	5.5	2.72	2.9	2600

Two-Dimensional Model Lithological Input

	Sandstone	Siltstone	Shale*	Limestone
Porosity	0.45	0.55	0.6	0.6
Reciprocal Compaction	1.75	2.2	2.4	1.5
Exponential Compaction	0.27	0.41	0.51	0.22
Density (g/cm ³)	2.64	2.64	2.7	2.72
Grain Size (mm)	0.5	0.0156	0.0004	0.5
Matrix Conductivity (W/m ³ *deg C)	4.4	2	1.5	2.9
Capacity (kJ/m ³ *deg C)	2800	2650	2100	2600
Vertical Permeability (mD)*	30000	100	100*	5000
Porosity Reduction Factor (A)	0.00012	0.00023	0.0003	0.00019
Permeability Reduction Factor (B)	7	6	6	6
Fracture Gradient	0.99	0.99	0.99	0.99
Irreducible Water Saturation	0.2	0.4	0.4	0.2
Permeability Anisotropy	1	0.2	0.2	0.5
Thermal Conductivity Anisotropy	1	1	1	1

* To produce a low-permeability model in Section 5.5.6(c), initial shale permeability was lowered to 1mD. This produced an invalid model.

Table 5.2 *Hydrocarbon Generation Parameters*

All data taken from Cornford (1994)

Formation	Kerogen Type	TOC (%)
Kimmeridge Clay	Type II	10
Heather	Type III	3

Table 5.3 *Sensitivity analysis results*

Model	Observed formation pressure (MPa) in Fulmar sandstone, well 22/30a-1	Modelled formation pressure (MPa) in Fulmar sandstone, well 22/30a-1	Observed formation pressure (MPa) in Fulmar sandstone, well 23/27-6	Modelled formation pressure (MPa) in Fulmar sandstone, well 23/27-6
Base-case	99	99	65	65
Discontinuous Fulmar	99	99	65	65
Palaeocene siltstone	99	99	65	65
Open Faults	99	99	65	65
Low-K aquitard	99	99	65	70

Chapter Six

Overpressure-related aspects of diagenesis in the Central Graben

- 6.1 Introduction**

- 6.2 Current conceptual models of diagenesis**
 - 6.2.1 *Diagenesis and overpressure*
 - 6.2.2 *Review of diagenesis of the Fulmar sandstones*
 - 6.2.3 *Summary*

- 6.3 Authigenic illite and overpressure in the Central Graben**
 - 6.3.1 *Methodology and results*
 - 6.3.2 *Discussion*
 - (i) *Graben Margins*
 - (ii) *Graben Centre*
 - 6.3.3 *Conclusions*

- 6.4 Overpressure and porosity distribution in the Central Graben**
 - 6.4.1 *Methodology*
 - 6.4.2 *Results*
 - 6.4.3 *Discussion*
 - 6.4.4 *Conclusions*

- 6.5 Conclusions: a model for Central North Sea overpressure-related diagenesis**

6.1 Introduction

The previous chapters have demonstrated that overpressure in the Central Graben today is the expression of a dynamic fluid flow system. The processes controlling this dynamic system have been active throughout the history of the basin, and have led to the present-day characteristics of the system. It is the aim of this chapter to examine the impact of the overpressure systems in the Central Graben, past and present, on sandstone diagenesis.

To achieve this aim, an investigation of aspects of sandstone diagenesis has been integrated with the quantitative basin model presented in Chapter 5. This novel approach has delivered unexpected and informative insights into the links between diagenesis and fluid flow.

This approach has involved two principal projects:

- The integration of potassium-argon ages of authigenic illite from Fulmar sandstones with the quantitative model of the hydrogeological evolution of the basin.
- The analysis of the links between measured and modelled overpressure and the measured porosity distribution in the Fulmar sandstones.

Due to the diversity and complexity of sediment diagenesis, it is necessary to precisely define the aims and the methodology employed in this chapter. It is the aim of this chapter to present selected aspects of sediment diagenesis related to overpressure in the Central Graben. It is not the aim of this chapter to present a detailed diagenetic scheme for the Jurassic sandstones of the Central Graben; such work is outwith the scope of this study and has been undertaken elsewhere (Wilkinson *et al.*, in prep (b); Wilkinson *et al.*, 1994a; Wilkinson & Haszeldine, in prep (a); Wilkinson *et al.*, in prep (c); Wilkinson *et al.*, 1994b).

The isotopic and petrographic analyses presented in this chapter are products of work carried out at Glasgow University as part of a larger multi-disciplinary study of Fulmar Fm. diagenesis (Wilkinson *et al.*, 1994b). The isotopic and petrographic data have been conducted by other workers at Glasgow (Wilkinson *et al.*, 1994b). It must be emphasised that this data has not been gathered or reproduced by the present study. It is the aim of this chapter to present *interpretations* of this data by the author. The interpretations, concepts and models presented in this chapter are the work of the

author.

The selection of the diagenetic aspects under investigation by this project, and accordingly the analytical methodology employed, has been achieved through a review of existing literature. This has allowed construction of initial hypotheses regarding the links between overpressure and diagenesis.

6.2 Current conceptual models of diagenesis

Diagenesis can be defined as "the sum total of processes that bring about changes in a sedimentary rock subsequent to its deposition in water" (Berner, 1980). Diagenesis of clastic sediments has attracted considerable research interest due to the economic significance of the phenomena involved in sediment porosity and permeability change. Accordingly it is associated with a detailed literature. Unfortunately, despite lengthy investigation, there is no consensus on the geological and geochemical controls of mineral dissolution and precipitation in the subsurface. A simplistic overview of diagenetic studies reveals three principal schools of thought:

- Diagenesis is primarily determined by the initial composition of the sediments. Diagenetic reactions occur as a consequence of burial and heating of minerals. These reactions occur as minerals become thermodynamically unstable and form new, stable minerals (Bjørlykke, 1984; Dypvik, 1983; Giles & Boer, 1990; Giles & de Boer, 1989; Hower *et al.*, 1976; Irwin *et al.*, 1977). Diagenesis is seen as occurring in a largely closed system. Diagenetic minerals are locally sourced from the dissolution of unstable minerals or from intraformational pressure solution. It is contended that the low porosity inferred for deep regions of sedimentary basins precludes large-scale fluid movement.
- Diagenesis occurs as a response to the perturbation of porewaters by fluid flow, and the introduction of reactive fluids and exotic solutes (e.g. (Haszeldine *et al.*, 1992). Examples are the vigorous flushing of sandstones by meteoric waters (e.g. Longstaffe, 1984), and the introduction of hot corrosive waters due to basin compaction (e.g. McLaughlin, 1994).

A third school may be perceived as a subset of the second case:

- Diagenesis is controlled by organic-inorganic reactions, particularly those associated with the maturation of kerogen, the expulsion of oil, and the generation

of organic acids from source rocks. Hydrocarbons are advanced as a cause of diagenetic alteration (e.g. Edman & Surdam, 1986; Emery *et al.*, 1993; Helgeson *et al.*, 1993; Seewald, 1994) and as a method of halting or slowing diagenetic reactions (Gluyas *et al.*, 1993).

It should be noted that the three primary controls on diagenesis detailed above are all theoretically valid mechanisms; indeed, it is possible that all mechanisms may be active at stages in the evolution of the basin. Recent model investigations (Harrison & Tempel, 1993) have suggested that short time-scale, episodic diagenetic events are superimposed upon continuous diagenetic changes.

6.2.1 Diagenesis and overpressure

The previous chapters have demonstrated that overpressure is an expression of restricted fluid flow, and that overpressure controls the migration and entrapment of hydrocarbons. Accordingly, aspects of diagenesis that are controlled by the flow of water or hydrocarbons will be affected by overpressure. Thermodynamic aspects of diagenesis that occur solely as a result of changes in temperature upon burial will not be greatly affected by overpressure. Overpressure will play a role in hydrogeologically closed systems in that low effective stresses between grains reduce pressure solution. This may limit internal sourcing of material for quartz cements (Swarbrick, 1994), although temperature is identified as the principal control on pressure solution (Bloch, 1991). Fluid pressure influences the solubility of minerals, both directly and through the changes in formation water chemistry due to the pressure-controlled dissolution of gas in water. Increased pressure favours silicate dissolution (Bruton & Helgeson, 1983).

Swarbrick (1994) developed a generalised model, based on the Northern North Sea, demonstrating that diagenesis occurs preferentially during periods of hydropressure, and that regional overpressure retards diagenesis due to the inhibition of fluid flow (Fig 6.1). Quartz fluid inclusion data were interpreted to suggest formation under near-hydrostatic pressure. Coeval authigenic illite was radiometrically dated and integrated with a basin model to demonstrate a coincidence of illite diagenesis with hydropressure. The modelling methodology of Swarbrick (1994) is flawed due to the use of uncoupled fluid flow and compaction algorithms. The reliability of palaeotemperatures inferred from fluid inclusions has also been questioned (Osborne & Haszeldine 1994). Retardation of diagenesis due to overpressure in the North Sea has been advanced by McAuley *et al.* (1993). A hydrogeological control on illite

growth has also been proposed by Hamilton *et al.*, (1992). Haszeldine *et al.*, 1992, and Small *et al.*, 1992).

The most widely documented effect on diagenesis by overpressure is in porosity change. Sections 4.2 and 5.5.4 have shown that overpressure strongly affects the distribution of porosity in Central Graben shales, with anomalously high porosities inferred for overpressured shales. Similar patterns may be demonstrated by overpressured sandstones (e.g. Jansa & Urrea, 1992; Leonard, 1993; Ramm & Bjorlykke, 1994) where high porosities are preserved in overpressured zones.

Diagenetic processes have also been advanced by some authors as causes of overpressure, either by expansive clay mineral reactions or by reductions in aquitard permeability due to diagenetic cementation (Hunt, 1990; Whelan *et al.*, 1994). By contrast, in this study, diagenetic reactions have been inferred to play no role in causing overpressure in the Central Graben (Section 3.5), or in retaining fluids (Section 2.4). It must of course be recalled that direct observation of the mineralogy of the pressure seal is prevented by the absence of core.

6.2.2 Review of diagenesis of the Fulmar sandstones

Simplified versions of the paragenetic sequence for the Fulmar sandstones in the Central Graben have been presented by several authors (Fig 6.2). The diagenesis of the Fulmar Field (well 30/17b-5 in Fig 1.3) has been presented by Stewart (1986) and Saigal *et al* (1992). Important authigenic cements are dolomite, quartz overgrowth, illite, ankerite and albite, with significant dissolution of dolomite and feldspar (Stewart, 1986). Late pyrite and bitumen are noted. Heavy-oil residues have a deleterious effect on sandstone porosity and permeability. A similar simplified diagenetic sequence has been presented by Wilkinson *et al* (1994a) for the Fulmar sandstone in well 29/10-2 (Fig 6.2). The diagenesis of the Fulmar-equivalent sandstones of the Ula field, in the Norwegian Central Graben, has been presented by Nedkvitne *et al* (1993) (Fig 6.2). All three studies show similar diagenetic sequences despite widely varying present-day overpressures. An important divergence is that the Fulmar field shows no evidence of feldspar or dolomite dissolution. This is attributed to isolation from meteoric flushing (Saigal *et al.*, 1992). A second important dissimilarity is the absence of authigenic clays in the Ula field (Nedkvitne *et al.*, 1993), despite important feldspar dissolution. Authigenic albite is proposed as a sink for the products of feldspar dissolution (Nedkvitne *et al* 1993).

Quartz may be coeval with illite in 29/10-2 (Wilkinson *et al* 1994a). Quartz cement makes up <4% of whole rock volume in Fulmar and up to 5% volume in Ula, despite Ula being at 14.8 MPa overpressure and Fulmar at only 7.6 MPa overpressure. Silica for quartz cement is derived locally from pressure solution in Fulmar (Saigal *et al* 1992). It appears that quartz cements are not greatly affected by overpressuring in the Graben. Nedkvitne *et al* (1993) used petroleum and aqueous fluid inclusions to suggest that cementation has occurred from 2.5km burial depth, and has continued to the present-day burial depth of 3.4km. Similarly, quartz cementation at or close to present-day reservoir temperatures is suggested by Saigal *et al* (1992) from aqueous fluid inclusions. Note that inference of timing and duration of quartz cementation relies on the adequacy of fluid inclusion palaeotemperatures, which can be questioned (see Osborne & Haszeldine, 1994). Accordingly a closer correlation between burial depth (and thus temperature) and quartz cementation than between overpressure and quartz cementation is suggested from this data. This suggests that overpressure has not exerted a major control on the sequence of diagenetic mineral changes that have occurred in the Central Graben.

The effects of oil emplacement on diagenetic processes in the Fulmar Field have been presented by Saigal *et al* (1992). This study suggested that quartz cementation and albitization of K-feldspars were strongly effected by oil emplacement in the late Miocene. A simplification of the diagenetic sequence, extracted from these publications, is presented in Fig 6.2.

6.2.3 Summary

From this review, it is possible to direct attention to processes where any links between diagenesis and overpressure can be tested with this thesis. These may be expressed as initial hypotheses that may be tested in the Central Graben.

- The timing of diagenetic events may be influenced by overpressure due to possible retardation of fluid movement by overpressure. This may be tested by integration of K-Ar dates with basin models (Swarbrick 1994).
- Porosity may be strongly influenced by overpressure. This can be tested by integration of porosity data with the descriptive model of overpressure advanced in Chapter 3.

Both these initial hypotheses integrate efficiently with the multi-disciplinary,

quantitative approach employed in previous chapters.

6.3 Authigenic illite and overpressure in the Central Graben

A principal cause of reservoir deterioration is the growth of diagenetic minerals as the reservoir is buried. The presence of fibrous authigenic illite is particularly unfavourable, as it can disastrously reduce the permeability of the reservoir. Due to the economic importance of this mineral, it has been the subject of intense research by geoscientists during the past three decades (Boles & Franks, 1979; Burst, 1959; Hamilton *et al.*, 1989; Powers, 1959).

Illite is a common authigenic mineral that is suitable for radiometric age-dating. This allows an absolute age to be determined and located within the framework of relative ages of a typical diagenetic sequence (e.g. Haszeldine *et al* 1992). Illite age-dating thus allows integration of diagenetic observations into the quantitative hydrogeological framework constructed by the basin model in Chapter 4. Unfortunately there is no consensus on the significance of the radiometric age recorded by authigenic illite; equally there is no agreement on what process initiates illite growth. Growth of illite has been proposed to be a temperature-dependent process, occurring as the basin sediments are progressively buried (Hamilton *et al* 1989). Illite age-dates have been noted to be broadly coincident with hydrocarbon migration (Burley & Flisch, 1989; Glassman *et al.*, 1989; Hamilton *et al.*, 1992), allowing some authors to propose a direct geochemical link (Liewig *et al* 1987), or to suggest a link to increased fluid flow rates (Hamilton *et al* 1989). Experimental work (Small, 1993) suggests that fibrous illite growth is enhanced in the presence of organic acids, again suggesting a link to source rock maturation. Illite is sometimes postulated as being coeval with quartz cementation of reservoirs (Emery *et al.*, 1993); accordingly the illite age-date may record the timing of other diagenetic processes.

6.3.1 Methodology and Results

Three wells on a west-east cross section have been examined: well 29/10-2, on the "Puffin" horst on the western margin of the Graben; well 22/30a-1, on the axial Forties-Montrose High; and well 23/27-6, on the eastern margin of the Graben. The location of the study wells are shown in Fig 6.3.

Petrographic analysis, separation and dating of authigenic illite has been carried out by

Wilkinson and co-workers (see Wilkinson *et al* 1994b). The aim is to separate and date the finest (and thus most recent) illite. Their methodology is detailed here to allow assessment of the validity of the K-Ar date recorded for illite. The procedure for extraction, purification and K-Ar age-dating presented in Hamilton *et al* (1989) has been followed. The extraction of a K-Ar date from illite requires isolation of the illite from the sandstone core, size separation, purity assessment and the analysis of pure separates for radiogenic argon (Hamilton *et al* 1989). The <0.1 micron size fraction of illite has been isolated and the purity of the separate assessed by x-ray diffraction and a transmission electron microscope (TEM) study, following the procedure of Hamilton *et al* (1989). Scanning and transmission electron microscope images of the illite from the three study wells are presented in Fig 6.4. X-ray diffraction analysis is presented in Fig 6.5. These analyses show that the separates analysed are composed of pure illite with no contamination from other minerals. The TEM image shows that the separate contains only illite with the fibrous, lath-like shape typical of authigenic illite growth. Contamination from detrital illite (resulting in a spuriously old age for authigenic growth) can thus be considered not to have affected the results. Details of the methodology and illite petrography are reported in Wilkinson *et al* (1994a). The systematics and methodology of the K-Ar geochronometer are discussed by Faure (1987).

The commercial basin models BasinMod™ 1-D and BasinMod™ 2-D have been used to simulate the subsidence, compaction and fluid flow of the Central Graben (Chapter 5). The data used to construct the models has been presented in Chapter Four. One-dimensional simulations of the subsidence of wells 22/30a-1, 29/10-2 and 23/27-6 have been presented in Section 5.4. For insight into the palaeo-hydrogeology of the Graben, it is necessary to turn to the two-dimensional model presented in Section 5.5. The subsidence, compaction and pressure of wells 22/30a-1 and 23/27-6 have been simulated using the two-dimensional model BasinMod™ 2-D. The excellent agreement achieved between the simulations of pressure and porosity using BasinMod™ 2-D, and observed data from well logs has been presented in Section 5.5.4. The impact of uncalibrated variables such as fault permeability on the model results has been presented in Section 4.5.6. As the two-dimensional model adequately reproduces the observed pressures at the present-day, it can serve here in this diagenetic study as a guide to the palaeo-pressure and palaeo-fluid flow regimes of the basin.

The K-Ar ages of illite for each well are presented in Table 6.1. Authigenic illite in the two wells on the margins of the Graben have a late Cretaceous age. Illite in well 22/30a-1 has an Oligocene age. The K-Ar ages are integrated with the burial history of the wells in Fig 6.6. The evolution of modelled overpressure through time for the

study wells 22/30a-1 and 23/27-6 is presented in Fig 6.7, adapted after Figs 5.27 and 5.28.

6.3.2 Discussion

The measurement of late-Cretaceous illites on the margins of the Graben and younger Oligocene illite in the deeper axial well is counter-intuitive if depth-temperature criteria are considered. In the Northern North Sea Hamilton *et al* (1992) suggest that illite begins to form at 75°C. Here in the Central Graben illite seems to have grown earliest in the cooler, shallower wells and latest in the deeper, hotter central well. Decrease of illite age with increasing depth has been noted for shales in the Texas Gulf Coast (Eberl, 1993). This pattern of illite ages has been related to illite recrystallisation below 4km burial depth. It is suggested that this recrystallisation has not occurred in the study wells, as the Central Graben is cooler than the Gulf Coast: temperatures of 200°C at 4200m are recorded in the Gulf Coast (Mello *et al.*, 1994), compared to 150°C in the Central Graben (Fig 4.2). Thus, assuming illite recrystallisation can occur in sandstones, the study wells would appear to be much cooler than the 200°C temperature threshold for recrystallisation defined by Eberl (1993), and the illite can be assumed to be an authigenic precipitate.

The temperature of the Fulmar Fm. during the time represented by the illite dates has been simulated using BasinMod™. Illite dates in well 29/10-2 occur at a simulated temperature of 55°C (Fig 5.7). Illite dates in well 23/27-6 similarly occur at a simulated temperature of 55°C (Fig 6.8). These simulated temperatures are close to the kinetic illitisation threshold of 60°C defined from laboratory experiment by Small, (1993). Thus there is good agreement between model, observation and experiment. However, the later illite dates in well 22/30a-1 occur at a temperature of 100°C.

It would appear from these results that illite growth is not simply a temperature-dependent reaction. It is necessary to examine the fluid history of the basin in more detail to explain the observed pattern of illite dates.

(i) Graben Margins

The similarity of illite age-dates in the Graben margin wells is noted, as is the coincidence of these dates with the commencement of rapid late Cretaceous-Tertiary subsidence in the Graben centre (Fig 6.6). Rapid subsidence and compaction of the

shale-rich Graben sediments implies the expulsion of compactional porewaters from the Graben. Expulsion of porewaters during late Cretaceous subsidence would have caused an increase in fluid flow rates and a change in the physico-chemical conditions in the carrier bed sandstones. This fluid flow would decrease as the compaction rate of the Graben sediments decreases with increasing burial (Sclater & Christie, 1980).

Why should illite dates show a relationship to changing fluid flow rates? A hydrogeological influence on illite growth has been proposed by previous workers. Hamilton *et al* (1992), in an empirical study of Northern North Sea illites, suggest a link to increased fluid flow rates (due to the perturbation of the hydrogeology by migrating oil), with illite growth favoured by increased water-rock ratio. The hydrogeological simulation presented above suggests similar patterns of illite growth to that of Hamilton *et al* (1992). It is unlikely that illite growth in the Central Graben was related to the advective import or export of dissolved inorganic solutes, as compactional flow rates are slow (Magara, 1987) and fluids chemically equilibrate with the rock during movement (Giles & de Boer, 1989). An open system is not intrinsically required: there were sufficient inorganic components of illite (potassium, aluminium and silica) locally present within the Fulmar sandstones (Wilkinson *et al* 1994a) to grow authigenic illite in a closed chemical system. The link to fluid flow must lie elsewhere.

The presence of organic acids, notably oxalic acid, has been demonstrated as being favourable to the growth of fibrous illite in laboratory experiments (Small, 1993). Organic-rich mudstones of the Upper Jurassic Kimmeridge Clay and Heather formations may be 1 km thick in the Graben immediately adjacent to the structures penetrated by wells 29/10-2 and 23/27-6 (Figs 1.5 and 1.6). It is suggested that the compaction of adjacent organic-rich source rocks will introduce organic acid-rich fluids into the sandstone. Thus these mudstones provide a local source of organic acid-rich compactional fluids (Cornford, 1994) during early maturation during the period of illite growth.

Liquid hydrocarbons may also be sourced from the mudstones. Illite dates in the Northern North Sea have been suggested to record filling of the reservoir with hydrocarbons (Hamilton *et al* 1989). The timing of the onset of hydrocarbon generation in the Central Graben is suggested to be 60 Ma with peak generation at 20 Ma (Section 5.5.5). However, this timing is poorly constrained by the data used to construct the models (see Section 5.5.5). The timing of hydrocarbon generation in the Central Graben has been investigated by two previous studies. The onset of hydrocarbon generation in the E. Forties Basin source kitchen is suggested to be lower

Palaeocene (65 Ma) with peak oil generation in the lower Oligocene (38 Ma) by Barnard & Bastow (1991). Cornford (1994) suggests a mid-Cretaceous (70 Ma) date for the onset of oil generation in the Central Graben with peak generation at 25 Ma. Illite dates of 84-58 Ma would appear to predate the onset of hydrocarbon generation in the Central Graben source kitchens, and undoubtedly predate peak oil generation and migration (Cornford 1994; see also Figures 5.30 and 5.31). This is an important difference from the Northern North Sea studies of Hamilton *et al* (1989, 1992).

It is here inferred that the *timing* of entry of organic acids into the sandstones will be controlled by the basin subsidence (Fig 6.6). Peak flux of organic acids into the reservoir, and thus peak flux of "nutrients" for illite growth, will correspond to the peak expulsion of compactional waters from local source rocks. Compaction and expulsion of compactional waters occurred in the late Cretaceous - early Tertiary as the mudstone-dominated Graben depocentres began to subside (Fig 6.6). Local cessation of illite growth occurs when the supply of "nutrients" is exhausted (Hamilton *et al* 1992). Cessation of illite growth (that is, the youngest illite) is preserved as the K-Ar date recorded for the well. Illite growth was sustained for a timespan of 26 Ma in 29/10-2, reflecting a sustained flux of compactional porewaters through the sandstone. As the Graben sediments progressively compacted and fluid flow rates decreased, illite growth ceased (Fig 6.9).

(ii) Graben Centre

The 30-33 Ma illites of the axial well, 22/30a-1, do not show such a clear relationship to basin subsidence. Despite deep burial, high temperatures and an abundance of inorganic components for illite growth, illite dates record only a brief interval of Oligocene growth. Why was illite growth in this well so late? It is suggested that the answer to this question lies with the hydrogeological conditions of the well.

It should be noted that the absence of K-Ar dates that show a late Cretaceous age from illite in the axial well may be an artefact of the sampling approach employed by Wilkinson *et al* (1994b). The sampling is biased towards the finest, most recent illite. Illite exhibiting a late Cretaceous age may have been excluded from the separated and dated sample in favour of finer Oligocene illite. It is therefore possible that illite exhibiting an 85-65 Ma age-date may exist in this well.

Modelling of the pressure history of this well provides a clue to the palaeohydrological situation of the axial structure. Illite ages on the Graben margins *predate*

the modelled onset of overpressure, but illite ages in the axial well occur *during* overpressured conditions (Fig 6.7). Well 22/30a-1 has a complex pressure history; variations in the magnitude of modelled overpressure developed in the well occur due to variations in Tertiary subsidence and sedimentation rates. Decreases in sedimentation rate lower the overpressure in the well. The model (Fig 6.7) indicates that the cell has been overpressured since at least 40 Ma. The model suggests that pressures have never returned to hydrostatic. This result appears robust with respect to variation in model parameters (Section 5.5.6). Nevertheless, overpressure is low (5-8 MPa) at 35 Ma, and rapidly increases from 30 Ma to the present day.

The illite dates in 22/30a-1 coincide with the modelled onset of high levels of overpressure, which have continued to the present day. Modelled high overpressure suggests that the low permeability of the aquitard is restricting the rate of fluid flow during rapid Cenozoic burial. As aquitard permeability decreases during Cenozoic burial, and sub-aquitard overpressure increases, the rate of fluid flow will consequently decrease. Restriction of fluid flow and lower fluid flow rates suggest a lower water-rock ratio. Lower water-rock ratio and thus a reduced supply of advected organic nutrients will retard illite growth (Hamilton *et al* 1992; Small 1993). Similar "system closure" to nutrient supply was proposed for illite in the Northern North Sea by Haszeldine *et al.* (1992) Thus the latest illite date recorded in this well marks the cessation of illite growth. As in the margin wells, illite age-dates in the axial well coincide with a hydrogeological event.

It is possible to link the views of Hamilton *et al* (1989) to this hydrogeological model, to suggest that hydrocarbons may have migrated from adjacent mature source rocks into the reservoir at this time. This timing of oil emplacement is supported by the model of Figure 5.31. Hydrocarbon migration, like water flow, will be retarded by overpressure. The combination of organic catalyst and fluid flow provides the physico-geochemical trigger for illite growth in the same manner as discussed above for the Graben margins. It is suggested that the K-Ar date measured for Central Graben illites represents latest illite growth in an environment of decreasing water-rock ratios caused by overpressure.

The complex control of fluid flow by overpressure in the Central Graben suggests that overpressured sandstones will not show simple relationships between authigenic illite ages and source rock maturity as was predicted by Hamilton *et al* (1992). Illite also does not correlate to episodes of hydropressure (Fig 6.1, Swarbrick 1994). The model for illite growth in the Central Graben is shown in Figure 6.9

6.3.3 Conclusions

In this section empirical measurements of the dates of sandstone diagenesis have been linked to a quantitative, model-driven interpretation of basin fluid processes. This approach has allowed recognition that:

- a) Illite growth on the margins of the Graben was coincident with the onset of rapid basin subsidence in the late Cretaceous and records the entry of organic acid-bearing fluids that had been expelled laterally from compacting organic-rich source rocks. The onset of rapid subsidence of the Central Graben marks a major change in the physico-chemical characteristics of the basinal fluids; this change is recorded by the growth of authigenic illite. Illite dates represent the cessation of illite growth as the supply of organic acids from adjacent compacting source rocks slowed.
- b) Illite age-dates in the axial well immediately predate the modelled onset of high overpressure. Pressurisation of the sandstones reduces water-rock ratio. Thus the illite ages represent cessation of illite growth, which occurred as the supply of organic acids from compacting source rocks slowed.
- c) A measured K-Ar illite date represents the local cessation of illite growth, triggered by the local cessation of rapid fluid flow in the Graben. This differs for different structures in the Central Graben. This link between a datable diagenetic event in the rock and a hydrogeological event may provide a powerful tool in validating computer simulations of basin hydrogeology.

This analysis of illite in the Central Graben demonstrates the power of a multi-disciplinary approach to diagenesis. Empirical measurement of authigenic illite has been linked to quantitative hydrogeological simulation. This has allowed the recognition of a hydrogeological control on the growth of illite. This approach allows new insight into the processes of water-rock interaction occurring in the Central Graben.

6.4 Overpressure and porosity distribution in the Central Graben

The processes of porosity preservation and generation in sandstones are of considerable commercial interest because of the implications for the porosity development of petroleum reservoirs. Sandstones have an initially high porosity upon deposition. This initial, primary porosity is reduced during burial compaction as the

effective vertical stress on the sandstone increases. Overpressured porefluids may restrict the compaction of the pore space by reducing the effective vertical stress acting on the rock (Section 2.5). Accordingly, overpressured sandstones may have a higher porosity than hydro pressured sandstones. This effect has been observed in many basins, including the North Sea (Ramm & Bjorlykke, 1994).

However, the processes of porosity change on sandstones are complex. As well as the change in fluid volume that occurs as primary pore space is compacted, sandstones can undergo a change in solid volume due to mineral dissolution and precipitation. Mineral dissolution forms pore space that is termed "secondary porosity". Numerous studies have described the petrographic features produced by secondary porosity formation and have speculated as to the cause of mineral dissolution. Dissolution has been attributed to the effect of water enriched in organic acids (e.g. Surdam & Crossey, 1985); to acid porewaters generated in the zone of abiotic decarboxylation reactions (Curtis, 1978); or to the slow equilibrium dissolution of thermodynamically unstable feldspar (Giles & de Boer, 1989). The timing of secondary porosity formation has been a source of some debate: many authors have ascribed secondary porosity formation to deep burial diagenesis (e.g. (Jansa & Urrea, 1992). However, the secondary porosity formed in deep diagenesis may be balanced by porosity infilled by authigenic minerals precipitated (e.g. Giles & Boer, 1990). This results in no net gain in porosity, merely a redistribution. Alternatively, the products of mineral dissolution may be removed from the sandstone. This increases the porosity of the sandstone. Because of the difficulty of moving large quantities of solute out of a sandstone during deep burial, some authors have suggested that the majority of secondary porosity must form during shallow burial under the influence of meteoric water flushing, when large volumes of water are available for solute transport (e.g. Bjorlykke, 1984), or due to seismic pumping of large volumes of water (Sibson *et al.*, 1975).

Whether porosity is primary or secondary, the preservation of void space at great depths in a sedimentary basin requires support of the void space by a combination of rock strength and overpressured pore fluid. Without the low effective stress generated by overpressure, porosity will compact. Thus it is possible to advance the hypothesis that in the Central Graben, high porosity will be observed in overpressured sandstones.

To test this hypothesis, porosity measurements on Fulmar Fm. sandstones have been collated to provide a regional analysis of the porosity distribution in the Jurassic of the Central Graben. The results of a petrographic study of the Upper Jurassic Fulmar Formation (Wilkinson *et al* 1994b) are used to gain insight into the nature of the

porosity in the sandstones. This data has been integrated with the model of Central North Sea pressure distribution detailed in Chapter 3. The porosity data has also been combined with the results of the quantitative modelling of porosity development and overpressure patterns presented in Chapter 5, to allow conclusions regarding the timing of porosity change to be drawn. A model is presented to describe the interaction of overpressure, porefluid flow patterns and secondary porosity development.

6.4.1 Methodology

Government-released porosity and permeability data for Fulmar Fm. sandstones in the Central Graben, derived from helium injection in conventional cores, were assimilated. Helium-injection porosity data is frequently available from three or four core plugs for each metre of core. The arithmetic mean was calculated from all measurements on a core to give a single porosity value for the Fulmar Fm. in each well, which is useful for modelling (see Fig 6.14). Petrographic examination of core chips was conducted as part of a larger multi-disciplinary study of the regional diagenesis of the Fulmar Formation of the south Central Graben (Wilkinson *et al* 1994b). This petrographic examination has not been conducted or verified by the present author. The results of this analysis form useful corroboration of the model-based interpretation of porosity presented below.

The evolution of porosity in wells 22/30a-1 and 23/27-6 has been simulated using the two-dimensional basin model presented in Section 5.5. The validity, calibration and sensitivity of the model to unconstrained variables is discussed in detail in Section 5.5.6. Porosity is dependent on the effective stress acting on the rock, related to depth and pore pressure. The simulation calculates the effective stress acting on the rock. Overpressure increases in the Fulmar sandstones during rapid Tertiary burial, and so the effective stress acting on the rock is lower than in hydro pressured conditions. Non-ideal compaction (such as grain support and compaction-resistant frameworks) are neglected here.

The basin model employed simulates the compaction of primary porosity. It is a purely physical model (see Section 5.2), and so can take no account of geochemical changes in the rock. Accordingly, modelled decrease of primary porosity is non-reversible (see Appendix), as is probable in nature (de Marsily, 1986). However, as discussed above, porosity in sandstones can increase due to changes in solid volume upon mineral dissolution. Thus, in an examination of sandstone porosity, it is useful to introduce the concept of a "reversible" porosity related to the effective vertical stress acting on the

rock to represent dissolution effects.

A rock buried in a homogenous, subsiding basin undergoes a monotonous increase in effective stress due to increased loading, assuming no increase in fluid volume (as has been demonstrated by the one-dimensional quantitative analysis presented by Luo and Vasseur, 1992). The rate of increase of effective stress acting on a rock buried in a subsiding basin is dependent on the pore fluid pressure. Overpressure allows a lower effective vertical stress to act on the rock compared to equivalent depths in hydro pressured conditions. However, the one-dimensional conceptualisation of effective stress (Luo & Vasseur, 1992) does not take the structure of the basin into account. Section 3.7 suggests that hydraulic communication between deep regions and the shallow crests of fault blocks may exist in the Central Graben (Fig 3.27). Section 4.4 has developed this concept to show that the effective stress on sandstones in crestal positions may undergo a *decrease* as overpressure increases in the basin (Fig 4.15). Crests of fault blocks in the Central Graben are currently in a state of very low effective stress, due to the proximity of pore pressures to the minimum stress. In addition, Section 4.3 has suggested that overpressure in the Central Graben may be due to hydrocarbon generation in addition to disequilibrium compaction. The increase in fluid volume (and accompanying overpressure) due to hydrocarbon generation may cause a decrease in effective stress from previously higher values throughout the overpressured regions of the Graben. Thus decreases in effective stress may occur in the Central Graben (Fig 6.10).

Low effective stress due to overpressuring allows the support of higher porosity. If effective stress undergoes a decrease, porosity may theoretically increase (Fig 6.11). It is useful to consider the maximum porosity sustainable for a given effective stress. The porosity-effective stress relationship (Lerche, 1990; see Appendix) is used to approximate a reversible model maximum porosity, equivalent to the porosity in the sandstone at the modelled effective stress *in hydro pressured conditions* (Fig 6.12). The model porosity resulting from this approach is a "virtual" porosity that is the maximum porosity the stress state in the rock can support at the modelled depth and pressure. This is termed the Maximum Potential Porosity (MPP). The MPP of an overpressured sandstone is equal to the porosity of a hydro pressured sandstone at much shallower burial (Fig 6.12).

The observed porosity must be less than or equal to MPP. It is hypothesised that secondary porosity can increase to fill the virtual field in a manner governed by rates of geochemical reactions and export of solutes from the sandstone (Fig. 6.13).

6.4.2 Results

A regional overview of measured porosity distribution is presented in Fig 6.14. Available porosity data is shown in Table 6.2. The modelled porosity, modelled overpressure and MPP for wells 23/27-6 and 22/30a-1 are presented in Figure 6.15 and Figure 6.16 (after Figs 5.27 and 5.28), with the measured porosity data for comparison.

The majority of the secondary porosity in the Fulmar sandstone in the Central Graben was produced by the dissolution of potassium feldspar (Wilkinson *et al.*, in prep (b); Wilkinson & Haszeldine, in prep (a); Wilkinson *et al.*, 1994b). Fig 6.18 shows SEM images of secondary pore space in deeply-buried Fulmar sandstones. Note that petrographical identification of secondary pore space is difficult and the textural criteria are not fully agreed (Giles *et al.*, 1992). Thus petrographic analysis frequently underestimates the importance of this diagenetic effect. Important volumes of feldspar may be dissolved during burial of a sandstone. Fig 6.17 shows the reduction in feldspar content with increasing depth in the Fulmar sandstones in the Central Graben (after Wilkinson *et al.* (c) in prep). Up to 30% of the total volume of the rock has been lost. This loss of feldspar may lead to an increase in total porosity or merely a redistribution of porosity (Giles *et al.* 1992). Fig 6.18 shows thin sections of representative Fulmar sandstones; high porosity is clearly shown for well 22/30a-1.

6.4.3 Discussion

Sandstone porosity generally declines with increasing depth in the Central Graben. A decreasing trend of 4% porosity /km can be defined from wells 30/17b-5, 23/27-6, 29/10-2 and 30/1c-3 (Fig 6.14). Well 23/27-6 can be taken to be representative of the majority of wells within the south Central Graben, so that the porosity type and abundance are typical for the Fulmar Formation at the sampled burial depth (Fig 6.14). The 4%/km porosity-loss trend defined from these four wells is identical to the porosity loss gradient of empirical compaction curves for hydro pressured sandstones (Baldwin & Butler, 1985). The trend forms a close match to empirical sandstone compaction curves defined from the Northern North Sea (Emery *et al.*, 1993). Two wells are anomalous with respect to this porosity trend. Well 22/27a-1 and, more significantly, well 22/30a-1, have exceptionally high mean and maximum porosity for the burial depth.

The anomalous porosity in these wells is unlikely to be the result of depositional variations such as variations in grain size or facies. All porosity data in Fig 6.14 is from the shallow-shelf Fulmar sandstones, so there is no gross variation in the depositional environment of the sandstones. Wells 29/10-2 and 30/17b-5 contain a complete section of the Fulmar Fm, with all facies preserved (Donovan *et al.*, 1993). The grain size of the Fulmar Fm. generally coarsens upwards (Stewart 1986). The coarsest facies is preserved in both wells 29/10-2 and 30/17b-5. However, these wells do not exhibit anomalously high porosity. Thus it is not possible that the two anomalous wells (22/30a-1 and 22/27a-1) contain a coarse facies with high porosity that is missing in the other wells. In addition, the observed paragenetic sequence in the anomalous wells 22/30a-1 and 22/27a-1 is not unusual (Wilkinson *et al* 1994b).

Can the high porosity in the anomalous wells be correlated to overpressure? The initial hypothesis to be examined by this study is that high porosity will be encountered in highly-overpressured sandstones. Fulmar Fm. sandstones in both wells 22/30a-1 and 22/27a-1 are highly overpressured (Section 3.3.5). However, well 29/10-2 is also highly overpressured (Section 3.3.5), but does not exhibit anomalously high porosity. Thus the anomalous porosity in wells 22/30a-1 and 22/27a-1 cannot be solely related to the high overpressure in these wells.

The quantitative model of the compaction of porosity in the Central Graben simulates the complex inter-relationships between porosity and overpressure. Fig 6.15 illustrates the difference in present-day porosity, and also the relationship to MPP for well 23/27-6. The present-day mean porosity of 21.5% is approximately equal to the modelled primary porosity of 22%. The MPP has slightly increased above the model primary porosity due to overpressuring in the rapid, regional Plio-Pleistocene burial (Fig 6.6). Hence the simplest explanation of the present-day porosity is that compaction reduced the porosity to its current levels. There has been no increase in porosity above the compacted primary porosity. This suggests that no solute export has occurred (Fig 6.19). Secondary porosity is inferred to exist in well 23/27-6 (Wilkinson *et al* 1994b). However, this secondary porosity had no impact on the total porosity of the rock. Thus the secondary porosity in well 23/27-6 is re-distributional (Giles *et al* 1992).

The porosity evolution in well 22/30a-1 must be more complex. The modelled evolution of porosity in this well (Fig 6.16) shows that the onset of high overpressure in the late Tertiary effectively halts compaction of the sandstone in well 22/30a-1. However, arrestation of compaction occurs relatively late in the geohistory of the basin. Much primary porosity has been lost. For the present-day observed porosity of 30-32% to be preserved primary porosity would require arrestation of compaction at

70Ma. This would require pore pressures equal to minimum stress to exist from the Late Cretaceous to the present day. This is not supported by the quantitative model. Accordingly, it is hypothesised that the high porosities observed in the Central Graben cannot be preserved primary porosity. Petrographic analysis confirms that the porosity is secondary (Wilkinson *et al* 1994b). However, secondary porosities of 30-38% can only be sustained at 4600m burial depth by simultaneous pressuring of developing voids. Without fluid pressure support, void space would compact.

The model suggests that the axial fault block began to become overpressured at 40Ma (Fig 6.16). Overpressure was low and fluctuated until 30Ma, when accelerating subsidence and decreasing seal permeability caused overpressure to gradually rise to the present-day high values (Section 4.5). In the Oligocene, the sediments were at 2700m (Fig 6.6). Modelled porosity had decreased due to compaction to values of 22% (Fig 6.16). However present-day mean porosities are 10-13% higher than this minimum value, such that 10-13% porosity must have been formed during deep burial in the late Cenozoic. Petrographic evidence strongly supports the dissolution of potassium feldspars as the porosity generating process (Wilkinson *et al* 1994b). A deficit of reaction products (e.g. albite and illite) implies open-system conditions during feldspar dissolution, with the export of the reaction products (aluminium and potassium, see Wilkinson *et al* (b), in prep) from the sandstone. The quantitative model of overpressure presented in Section 5.5 suggests that these open-system conditions occurred during a time when the sandstone was overpressured (Fig 6.16).

How can an overpressured sandstone be an open chemical system? The answer to this question clearly depends upon the perception of overpressure. If overpressure is regarded as being generated within a sealed box (a pressure cell), then removing solute is difficult (other than by the geologically slow process of diffusion). However, if overpressure is regarded as a dynamic phenomenon, which can be maintained despite fluid loss to structurally higher and less-overpressured units (Section 3.5), then the movement of solutes is more easily accounted for. The dynamic model suggests that vertical fluid flow is focused at Leak Points. This flow is driven by overpressure. Indeed, the dynamic regulation of overpressure by hydrocarbon generation suggested in Section 4.3 (and by Engelder & Fischer, 1994) suggests that *extremely* high fluid flow rates may be sustained at Leak Points as a *consequence* of overpressure. The geochemically open-system behaviour of overpressured reservoirs has been noted by Helgeson *et al* (1993).

It is this porefluid-flow which is hypothesised to be responsible for the removal of both reservoired hydrocarbons (Section 3.7) and the products of feldspar dissolution

within well 22/30a-1, and hence for the anomalously high present-day porosities (Fig 6.19).

Well 29/10-2 is also suggested to be a highly-overpressured Leak Point in Section 3.5. However, it does not exhibit anomalous maximum porosity (Fig 6.14). Why should this well differ from wells 22/30a-1 and 22/27a-1? A detailed examination of the pressure-depth profile of this well reveals that the Palaeocene sandstones and the Cretaceous Chalk are overpressured in this well (Fig 3.13). Additionally, the Fulmar sandstone is sealed by a thicker accumulation of Lower Cretaceous and Upper Jurassic shales than in wells 22/30a-1 and 22/27a-1. These two factors will reduce vertical fluid flux, as the vertical potentiometric gradients across the transition zone overlying this Leak Point are less extreme than those of well 22/30a-1. Lower rates of vertical fluid flow can transport less solutes. It is thus more difficult to remove dissolution products. This means that the geochemical system is only partly open. Dissolution products may be re-precipitated within the sandstone. This results in re-distributional porosity, as described above.

The diagenetic processes that have formed the secondary porosity in the Fulmar sandstones are strongly affected by the complexities of the fluid flow systems in the region, and are not solely effected by depth, temperature, mineralogy or by the overpressure within the Fulmar Fm. itself. The pressure-controlled export of solutes from the Fulmar Fm. echoes the inferred patterns of hydrocarbon migration (Section 3.6). The quantification of these patterns (Section 5.5.6a) also suggested that overpressure in the Palaeocene inhibited vertical fluid flow.

It should be noted that the quantitative model of overpressure suggests that very high overpressures within the south Central Graben only occurred within the last 5Ma, as a result of Plio-Pleistocene burial. The model suggests that effective stress has only been reduced to very low levels in the recent geological past. As the formation of secondary porosity by silicate hydrolysis (i.e. feldspar dissolution) is not an instantaneous process, the present-day porosity may not be the maximum that could be developed. In other words, secondary porosity may *still be forming at present day* within the Fulmar Formation as the porosity increases towards the MPP.

The recognition that possibly 10-15% of the rock in the crest of Leak Point cells has been removed during the recent development of secondary porosity raises two important questions: how has the void space been filled by fluid, and where have the solutes gone?

Focusing of compactional flow may occur through Leak Points. Rock volume loss has only occurred at localised zones in the basin, and so fluid transfer from deeper regions of the Graben into leak points may fill the void space. Fluid pressures in adjacent regions to Leak Points are close to, but not equal to, minimum horizontal stress. The adjacent regions will thus undergo small, but finite, decrease in porosity due to Plio-Pleistocene sediment loading. The expelled fluid cannot move vertically due to the overlying Kimmeridge Clay pressure seal (Section 4.3), and so all fluid expulsion will take place laterally, towards the Leak Point. The areal extent of the secondary porosity zone cannot be defined from single wells. However, it seems likely that this extraordinary focusing of fluid flow at Leak Points may explain the fluid volume increase. Additionally, Section 4.3 suggests that additional fluid has been generated in the deep subsurface. This has been caused by hydrocarbon generation in the sub-seal regions of the Central Graben while material was being exported through the pressure seal. While the pressure-volume-temperature relationships of hydrocarbon generation remain poorly constrained (Section 4.3), it is clear that fluid volume is generated during gas generation, and that this alone may explain the increase in fluid volume necessary in the Central Graben.

The eventual fate of the solutes from the sub-seal sandstones is intriguing. Pressure and temperature changes across transition zones may allow precipitation of solutes above the seal from vertically-streaming flow (Harrison 1994; Bruton & Helgeson 1983). Precipitation of solutes above the transition zone has been noted in the Louisiana Gulf Coast (Whelan *et al.*, 1994). This cannot be assessed in the Central Graben as the transition zone has not yet been cored. However, the upper regions of the transition zone form the most likely theoretical sink for the missing reaction products. Stratigraphically and structurally-higher regions of the basin may also form a sink for reaction products Stewart (1995).

6.4.4 Conclusions

1. Mean sandstone porosity in the Central Graben can exceed that predicted for compacted primary porosity. This extra porosity is secondary in origin.
2. To maintain high porosities requires the support of developing voids by high porefluid overpressure. Without overpressure, the porosity will compact.
3. Solute export is required to allow enhancement of porosity by secondary porosity. This occurs preferentially at Leak Points with thin seals, sharp transition zones,

and overlying hydro pressured sediments.

4. Numerical modelling of the overpressure and porosity development of the Fulmar Formation sandstones within the south Central Graben enables the time of formation of anomalous secondary porosity within well 22/30a-1 to be constrained: it formed during the Plio-Pleistocene regional burial, i.e. within the last 5Ma, and probably within the last 2Ma. It is probable that secondary porosity after feldspar is still forming in this well at the present day.
5. Porefluid flow can take place within an overpressured sandstone, and consequently significant volumes of solute can be transported during deep burial diagenesis.
6. To understand diagenetic patterns within the south Central Graben, an understanding of the overpressure development, structural configuration and porefluid flow paths is essential. Deep burial diagenesis within the south Central Graben is not an isochemical process, such that the export of solute is a major control upon the distribution of porosity. Quantitative simulation of the hydrogeological and geodynamic evolution of the basin serves as an invaluable framework for discussing the dynamic evolution of porosity.

The summary model for the evolution of porosity in the Fulmar sandstone is shown in Fig 6.19.

6.5 Conclusions: A model for Central North Sea overpressure-related diagenesis

Overpressure in the Central North Sea has been shown by the case studies detailed above to play an active role in illite growth and secondary porosity generation (Fig 6.20). This role is based on the dynamic nature of overpressure proposed in Chapter 3. This is in sharp contrast to previous studies, which stress the static nature of overpressure and its passive retardation of cementation. The research detailed above demonstrates that:

- Overpressure controls the timing of some diagenetic events by controlling fluid flow rates. This is exemplified by illite age-dates which coincide with changes in the hydrogeological regime of the Graben. A physico-geochemical control on diagenesis is implied.

- Overpressure provides a mechanism for forming and preserving secondary porosity at Leak Points.
- Overpressure distribution controls hydrocarbon migration by providing potentiometric gradients. Diagenetic reactions catalysed by organic-inorganic interactions (e.g. Helgeson *et al* 1993) will be affected by pressure distribution.

These observations allow formulation of a composite model of overpressure-related diagenesis. The model can be proposed for a regional scale (Fig 6.20). Quartz cementation and feldspar dissolution occur in response to burial and heating essentially independent of overpressure. Fluid flow has triggered illite growth in the Graben sandstones by controlling the movement of organic acid-bearing fluids. Overpressure in the Graben aids the development of high porosities, but not due to arrestation of compaction. High *secondary* porosities are developed in sandstones on structurally-controlled regional Leak Points. In these locations the sandstones can undergo reductions in effective stress, due to hydraulic communication with deep regions. Low effective stress may lead to hydraulic fracturing of the seal, permitting vertical flow of hydrocarbon and aqueous fluids. These flows may remove the dissolution products of feldspar as solutes through the pressure seal. This results in the creation of additional porosity within the sandstone. Where this export of solutes cannot freely occur, porosities are low despite high overpressure, due to growth of clay. The model rests on the recognition of the dynamic nature of Central North Sea overpressure.

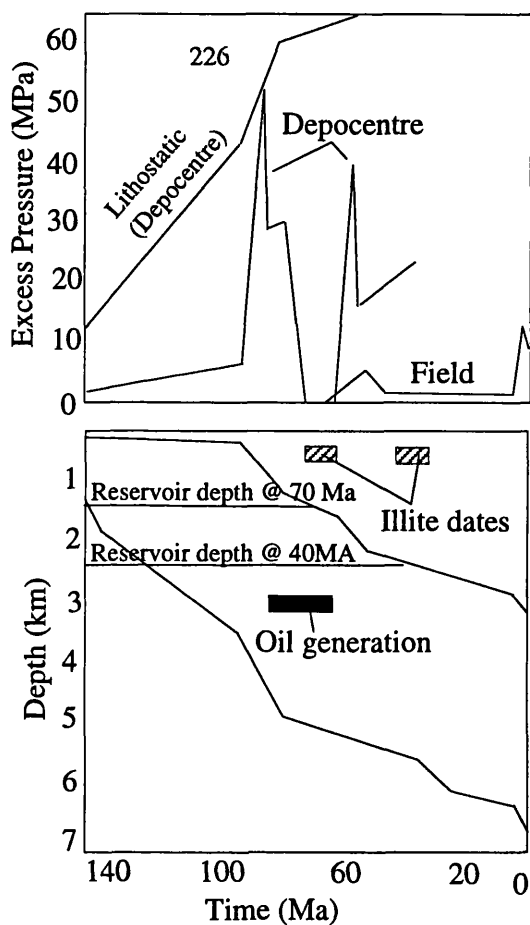
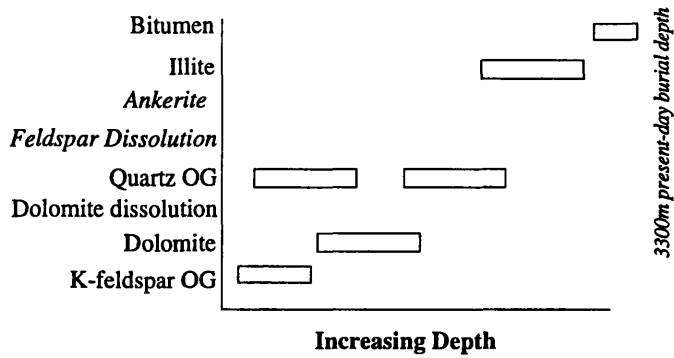


Figure 6.1 Relationship between illite dates and modelled overpressure evolution in the NW Hutton Field, Northern North Sea (after Swarbrick 1994).

Illite dates coincide with modelled episodes of hydropressure (or low overpressure). High overpressure is inferred to restrict fluid movement and inhibit diagenesis. The models used are flawed due to the use of uncoupled fluid flow and compaction algorithms. However, the hypothesis presented is intriguing.

Fulmar Field

(after Stewart 1986 and Saigal et al 1992)

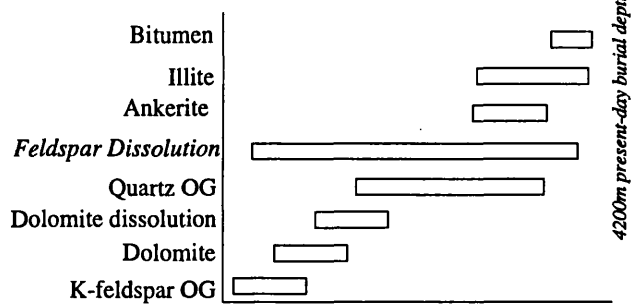


West

Low overpressure

29/10-2

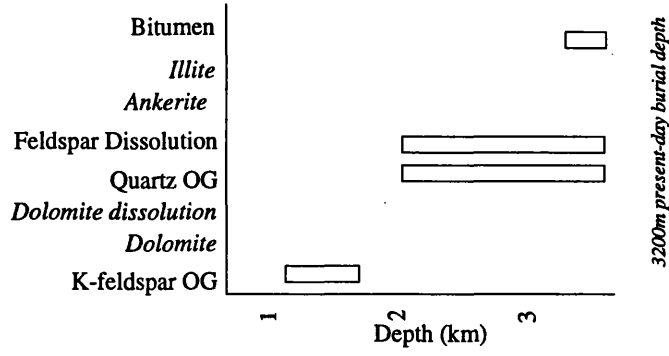
(after Wilkinson 1994)



High overpressure

Ula Field

(after Nedkvitne et al 1993)



Low overpressure

East

Figure 6.2 Published diagenetic sequences for the Fulmar sandstones in the Central Graben

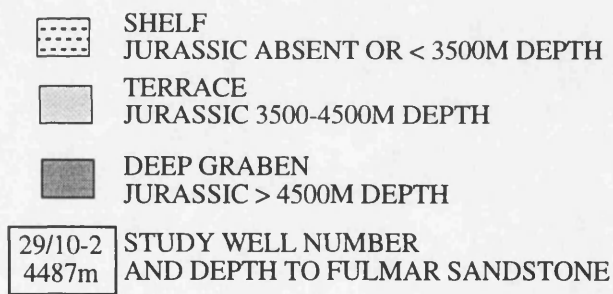
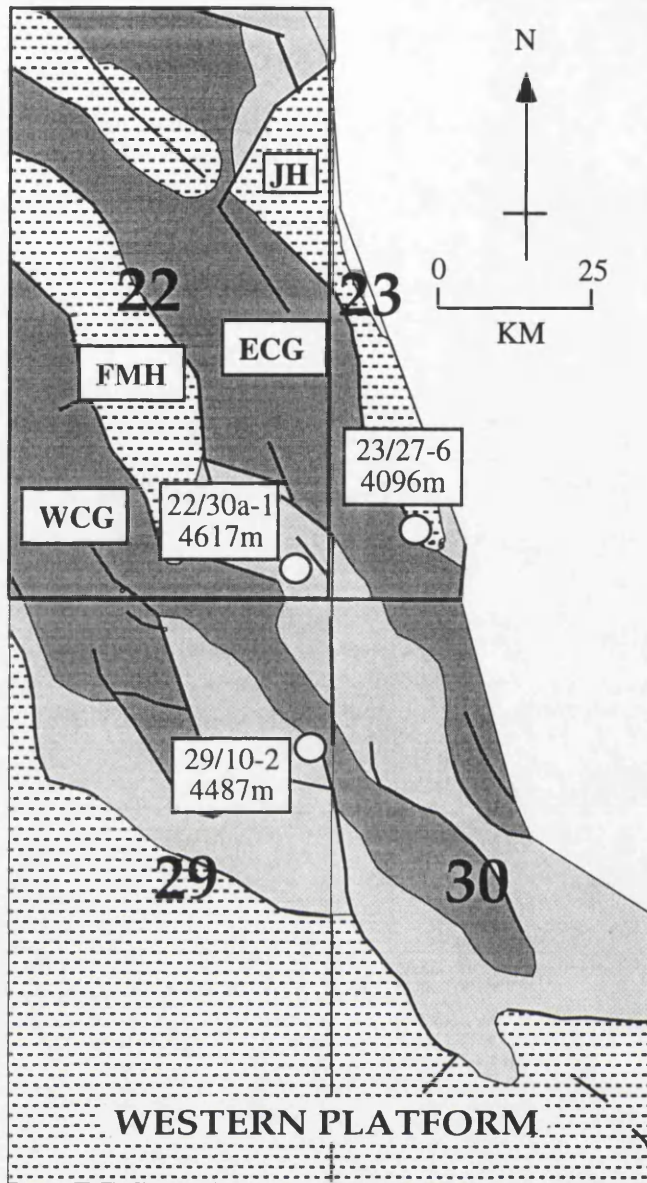


Figure 6.3 Location of study wells
 EFB: East Forties Basin; WCG: West Central Graben;
 FMH: Forties-Montrose High

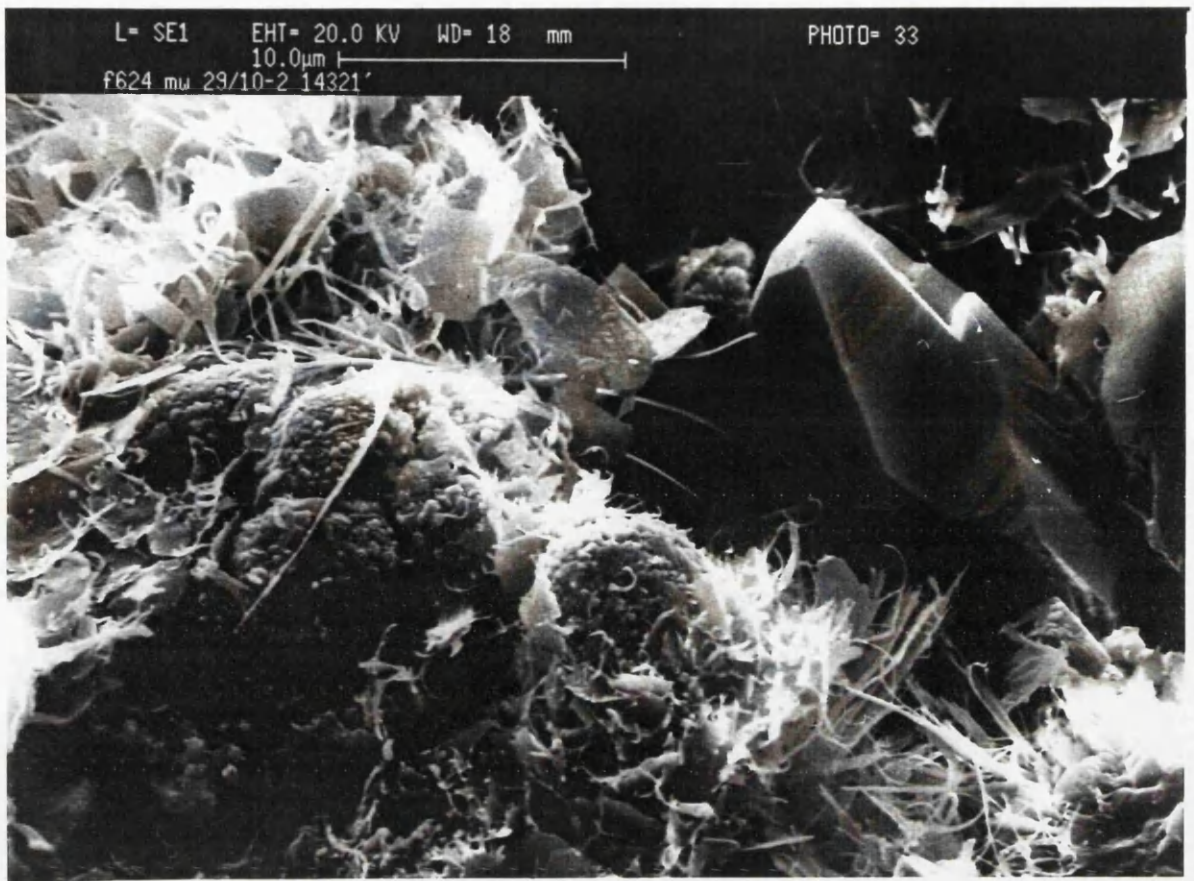


Figure 6.4 Scanning Electron Microscope (A) and Transmission Electron Microscope (B) images of authigenic illite in Fulmar Fm. from well 29/10-2. Note the characteristic "hairy" morphology and lath-like crystal shape typical of authigenic illite.

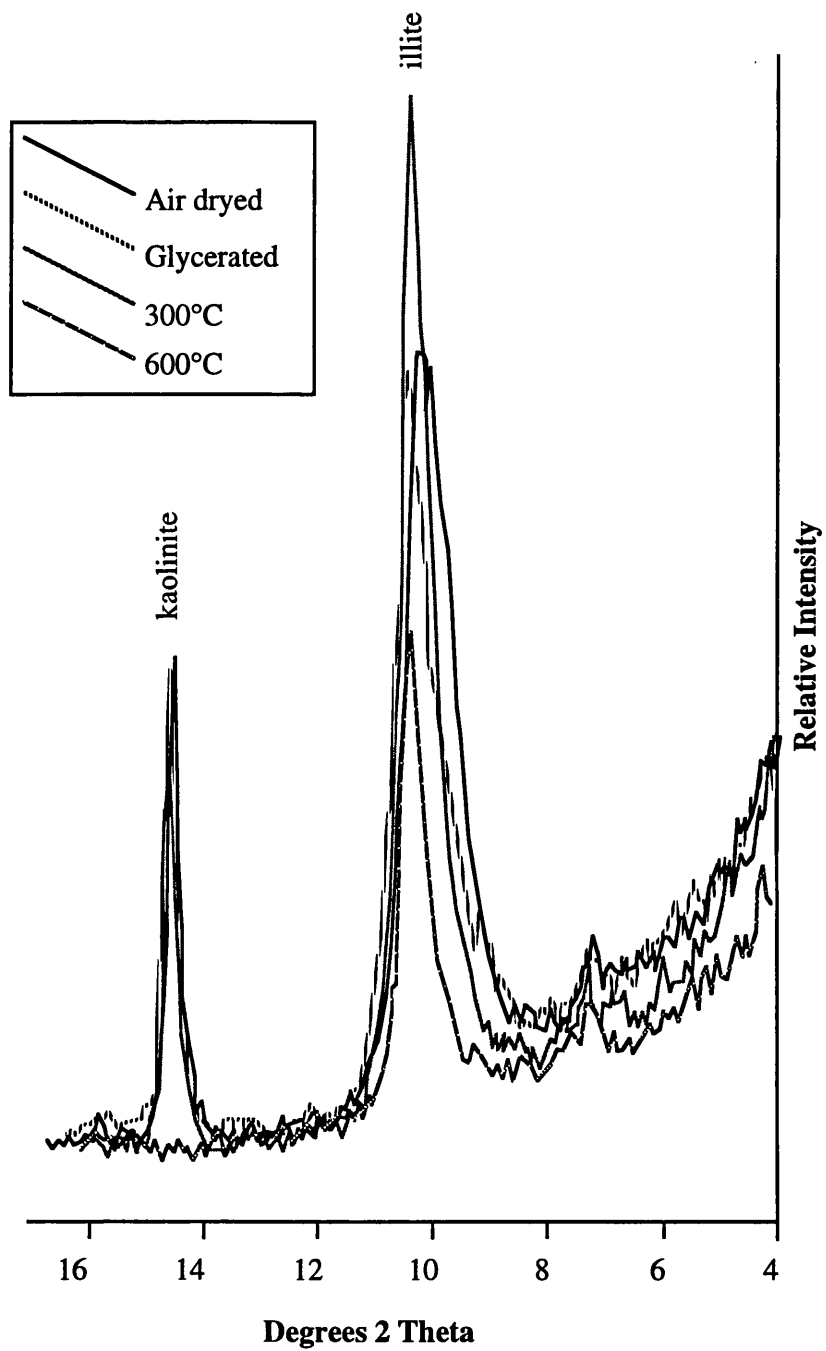


Figure 6.5 X-ray diffraction patterns for <10 micron clay fraction for Central Graben Fulmar sandstone

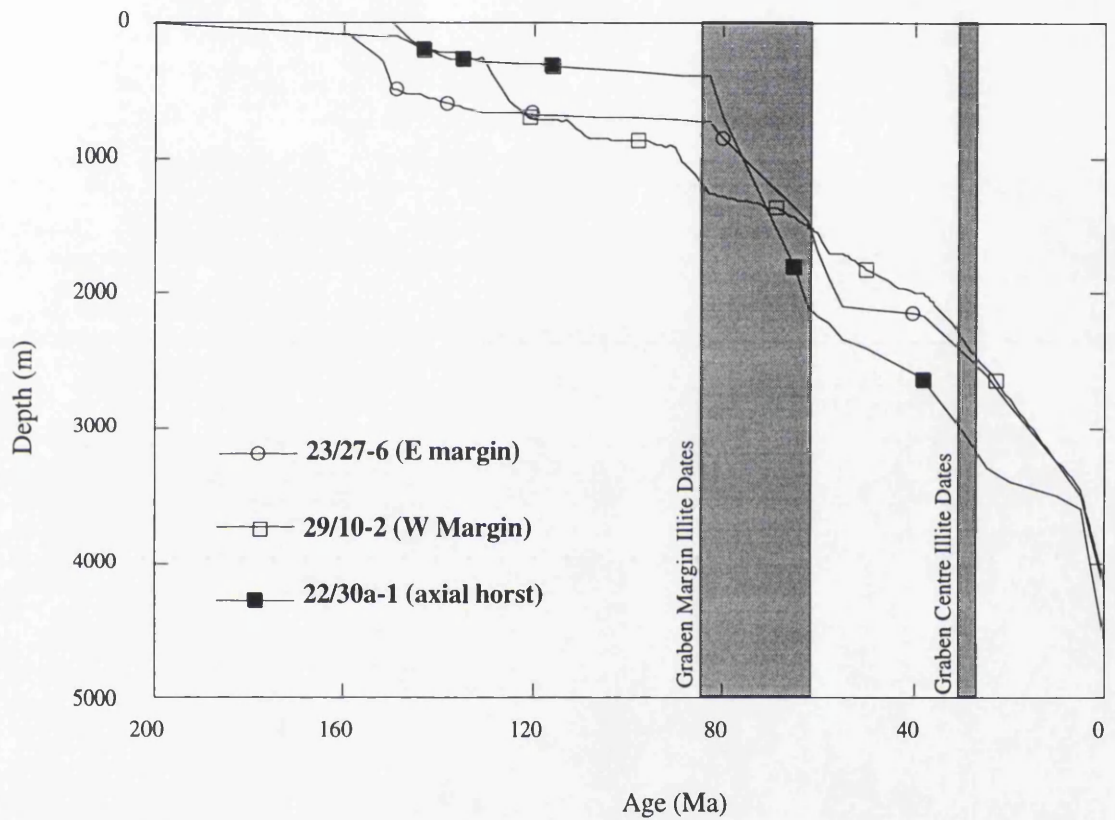


Figure 6.6 Modelled subsidence curves for the study wells 22/30a-1, 23/27-6 and 29/10-2. Shaded regions illustrate K-Ar ages of authigenic illite. Unusually, the deeper, hotter axial well 22/30a-1 contains the youngest illite. The Central Graben began to subside rapidly in the early Tertiary. The compacting sediments will have expelled pore water vertically and onto the basin margins. Illite ages on the basin margins are coincident with this subsidence and compaction.

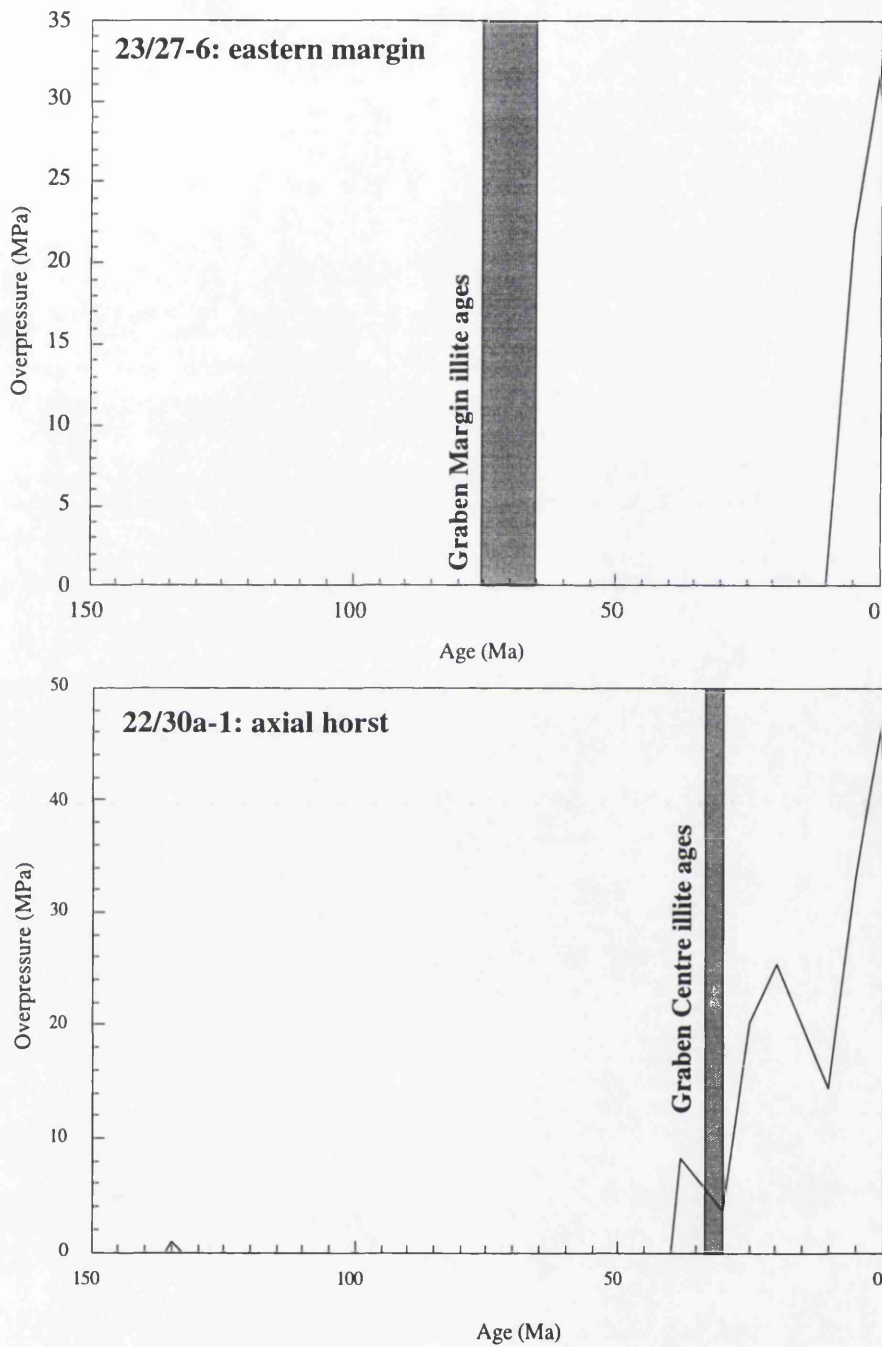


Figure 6.7 Simulated overpressure for wells 22/30a-1 and 23/27-6, with illite dates. Illite dates from the Graben margins coincide with hydro pressured conditions. Illite dates in the Graben centre coincide with fluctuating overpressured conditions and mark the onset of high overpressure. A link to decreasing water-rock ratio is suggested.

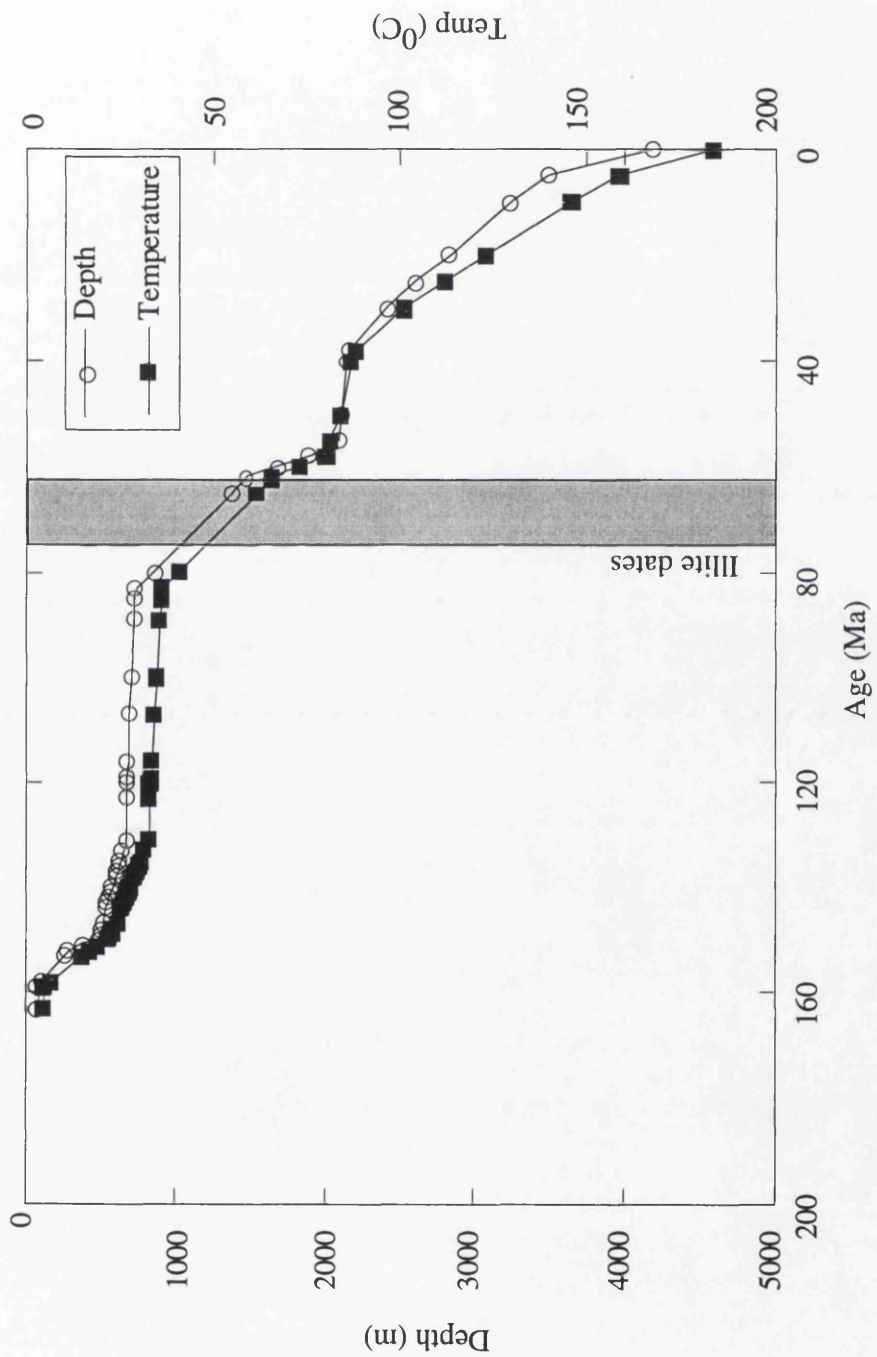
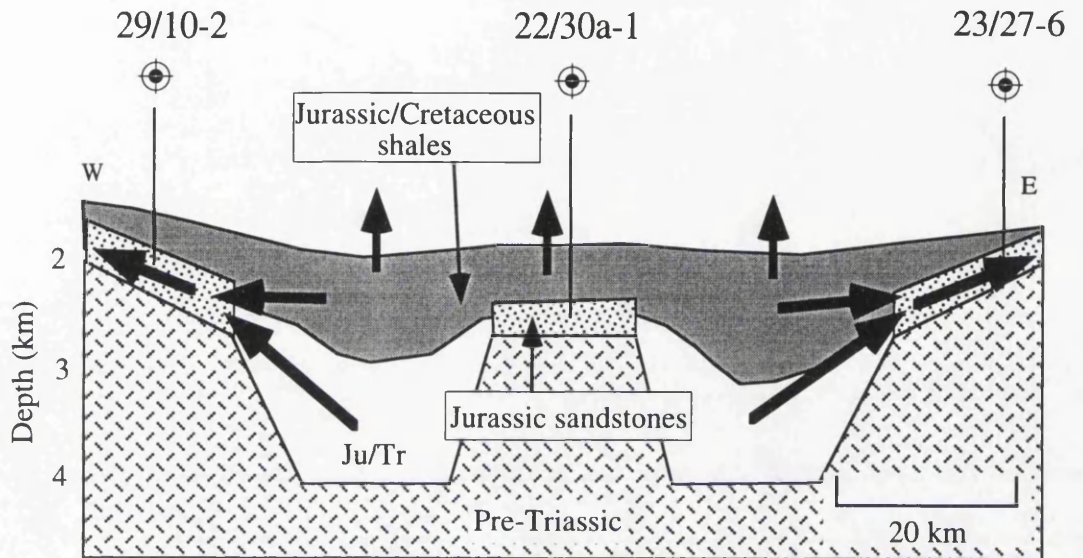


Figure 6.8 Modelled depth of burial and temperature of Fulmar Fm. in well 23/27-6. Illite dates suggest growth began at 55-60°C, equivalent to the kinetic threshold defined by Small *et al* (1994)

Late Cretaceous:
Illite grows on margins after compactional fluids and organics enter margin sandstones.



Oligocene/Eocene:
Illite grows in central well as overpressure controls flow rates and entry of organic-rich fluids into axial horst

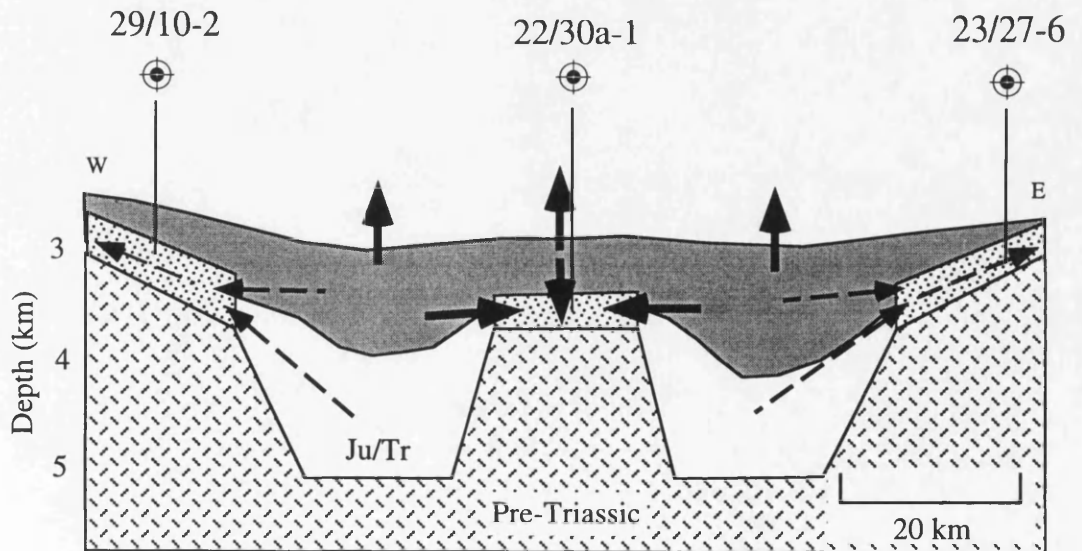


Figure 6.9 Summary cartoon of relationship between structure, overpressure and illite growth

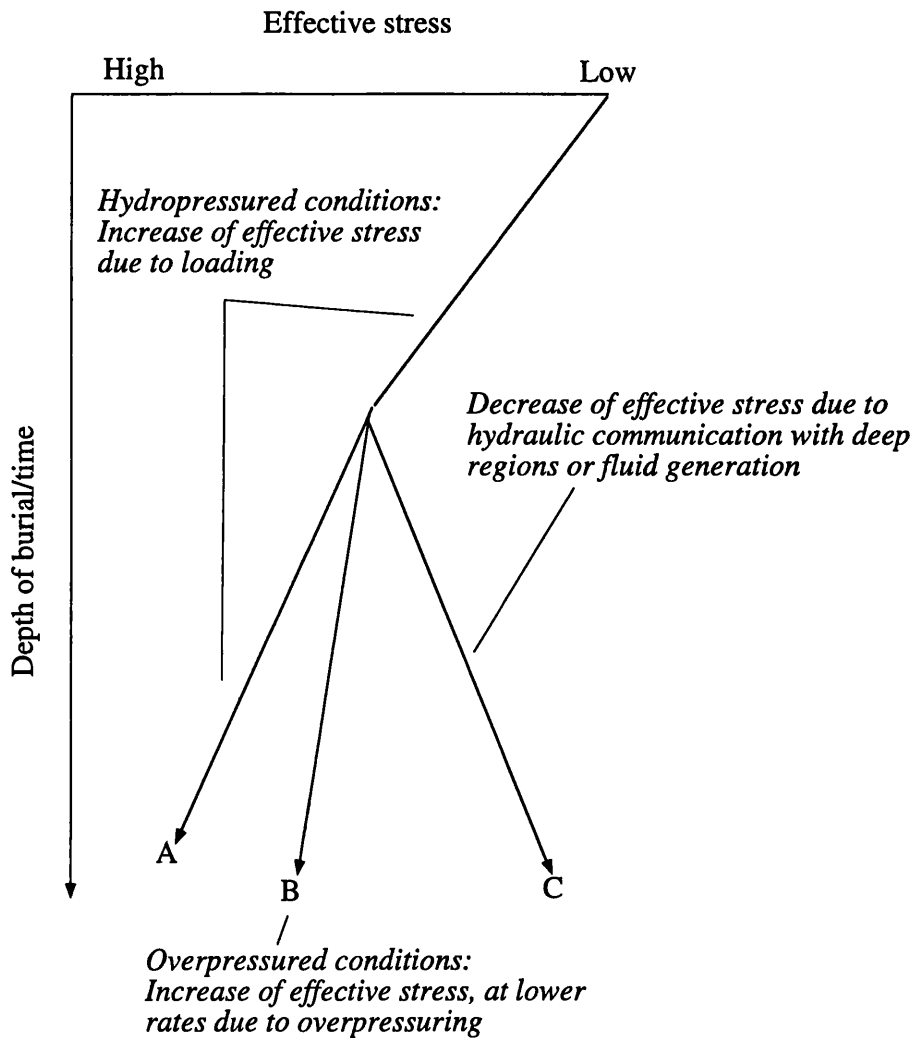


Figure 6.10 Evolution of effective stress with time. Effective stress due to loading shows a monotonous increase (A). The rate of this increase is dictated by the pore fluid pressure. Effective stress increases more slowly in overpressured regions (B). However, the structural complexity of the Graben may lead to reduction of effective stress in structurally-elevated regions that are in hydraulic communication with deeper regions (C). Additionally, fluid generation at depth may decrease the effective stress.

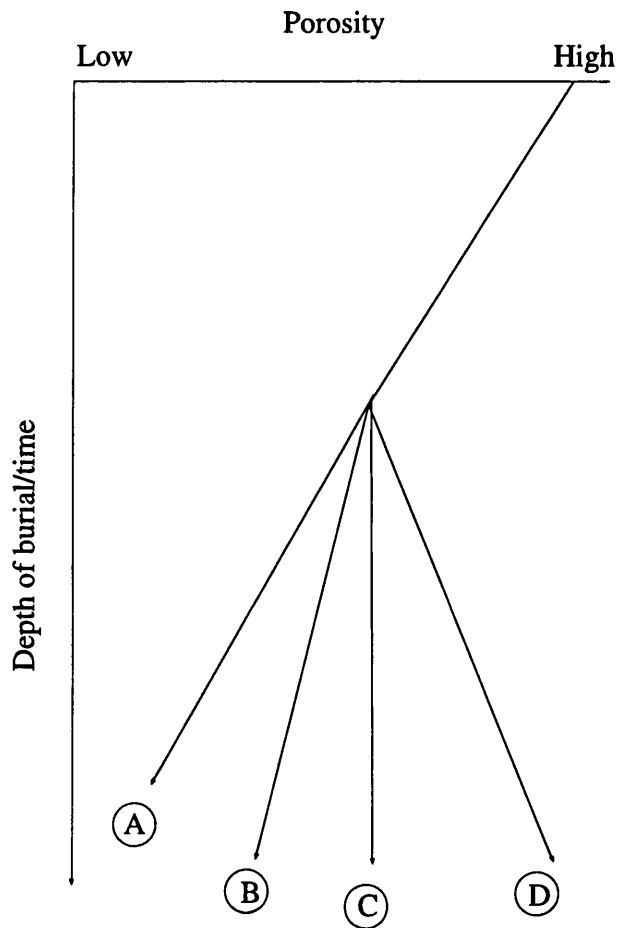


Figure 6.11 Relation of porosity to changes in effective stress.

- Ⓐ Effective stress increases in hydro pressured conditions. Porosity decreases.
- Ⓑ Effective stress increases in over pressured conditions. Porosity decreases, but at a lower rate than in hydro pressured conditions.
- Ⓒ Effective stress remains constant. For example, pore pressure equals minimum stress. No porosity change occurs.
- Ⓓ Effective stress decreases due to structural effects or fluid generation. Porosity may increase if solutes can be exported from the sandstone

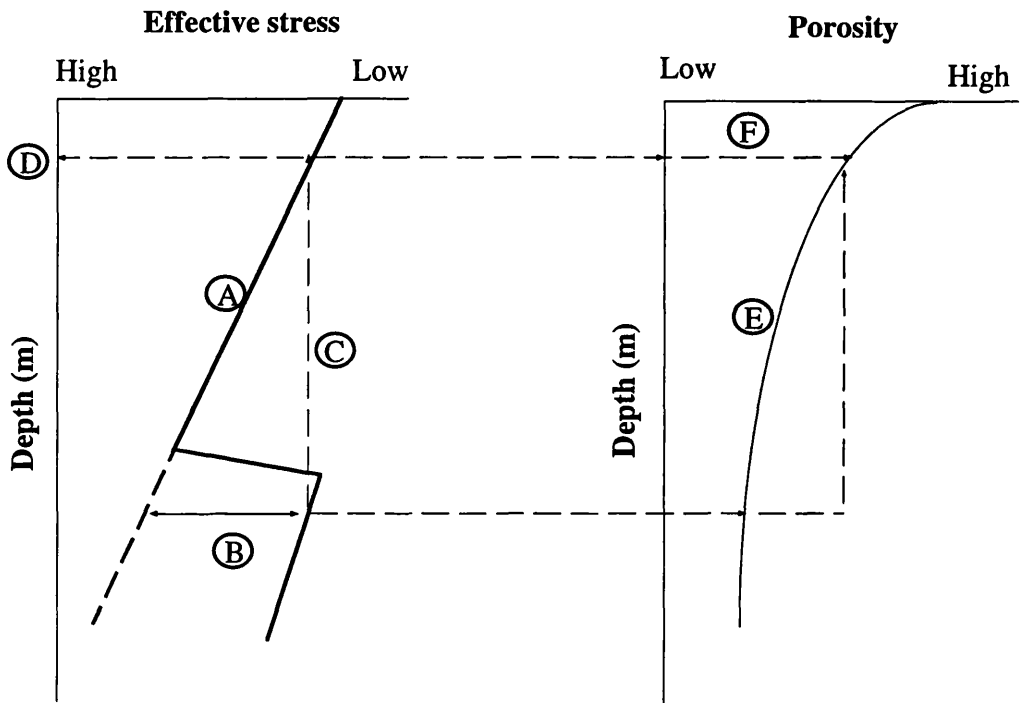


Figure 6.12 Effective stress and the maximum potential porosity concept

- Ⓐ Effective stress increases with increasing depth if porefluid is hydro pressured.
- Ⓑ If porefluid is overpressured, effective stress is less at that depth than in hydro pressured conditions.
- Ⓒ Effective stress in overpressured cells is equivalent to effective stress at much shallower burial in hydro pressured conditions Ⓓ
- Ⓔ Porosity declines with depth in hydro pressured conditions
- Ⓕ Low effective stress in pressure cells theoretically allows a porosity to be supported that is equivalent to the porosity at much shallower depths. This is the Maximum Potential Porosity for that depth-pressure condition.

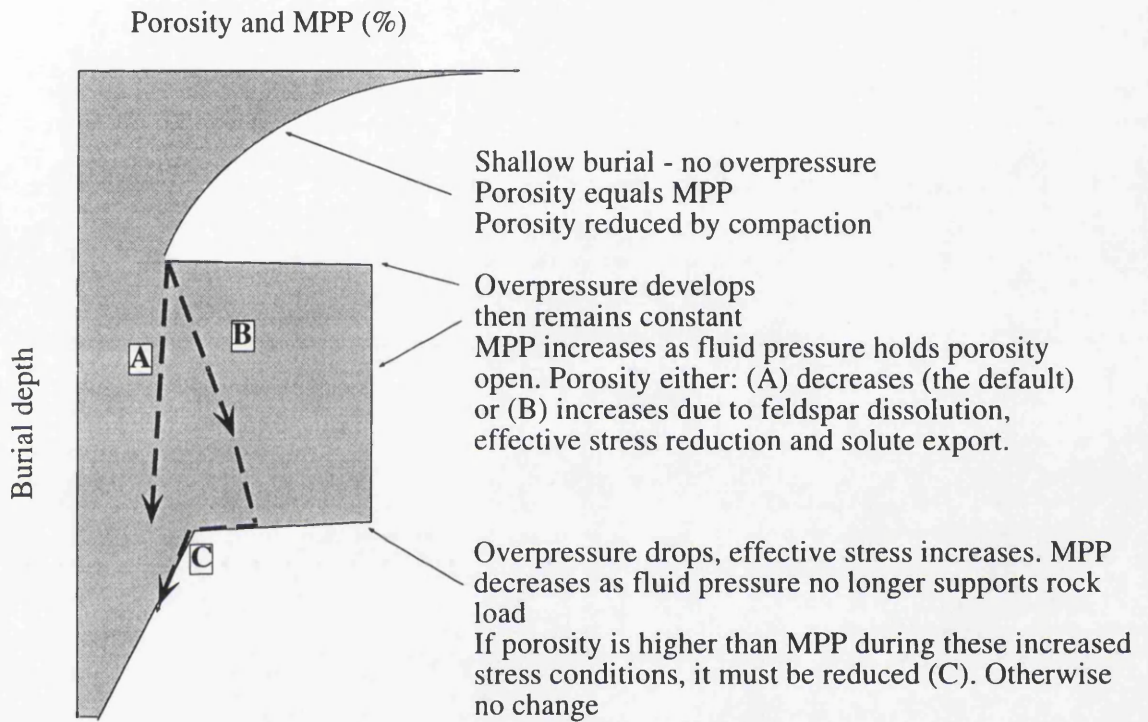


Figure 6.13 The concept of Maximum Potential Porosity (MPP) and the relationship between porosity and overpressure

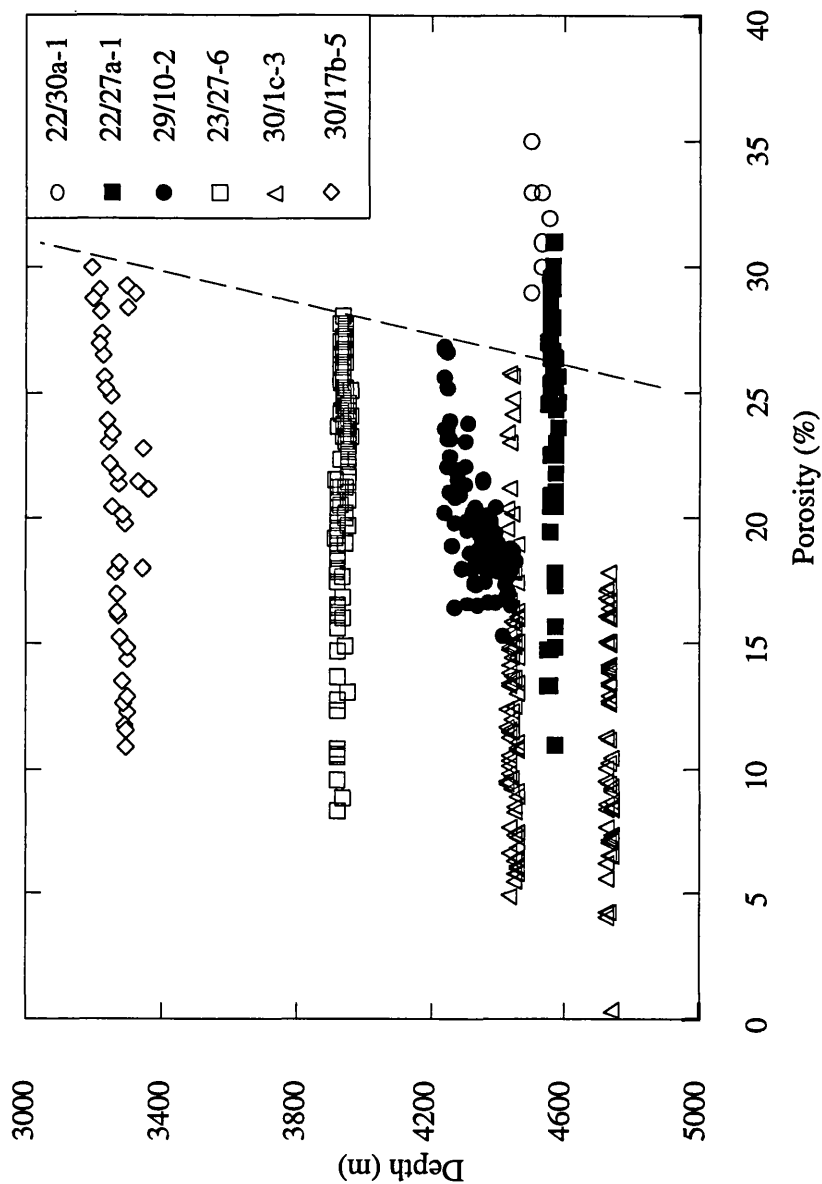


Figure 6.14 Porosity data from helium injection on conventional cores in the Fulmar Fm. sandstones in the Central Graben. Porosity shows a decreasing trend with increasing depth. Wells 22/30a-1 and 22/27a-1 are anomalous with respect to this trend, and contain unusually high maximum porosity for their depth. This anomaly is unrelated to facies changes or grain size. Dashed line shows the porosity trend in the Central Graben, coincident with equilibrium compaction curve of primary porosity in sandstones of the Northern North Sea (Emery *et al* 1993). Data for 30/17b-5 from Stewart (1986).

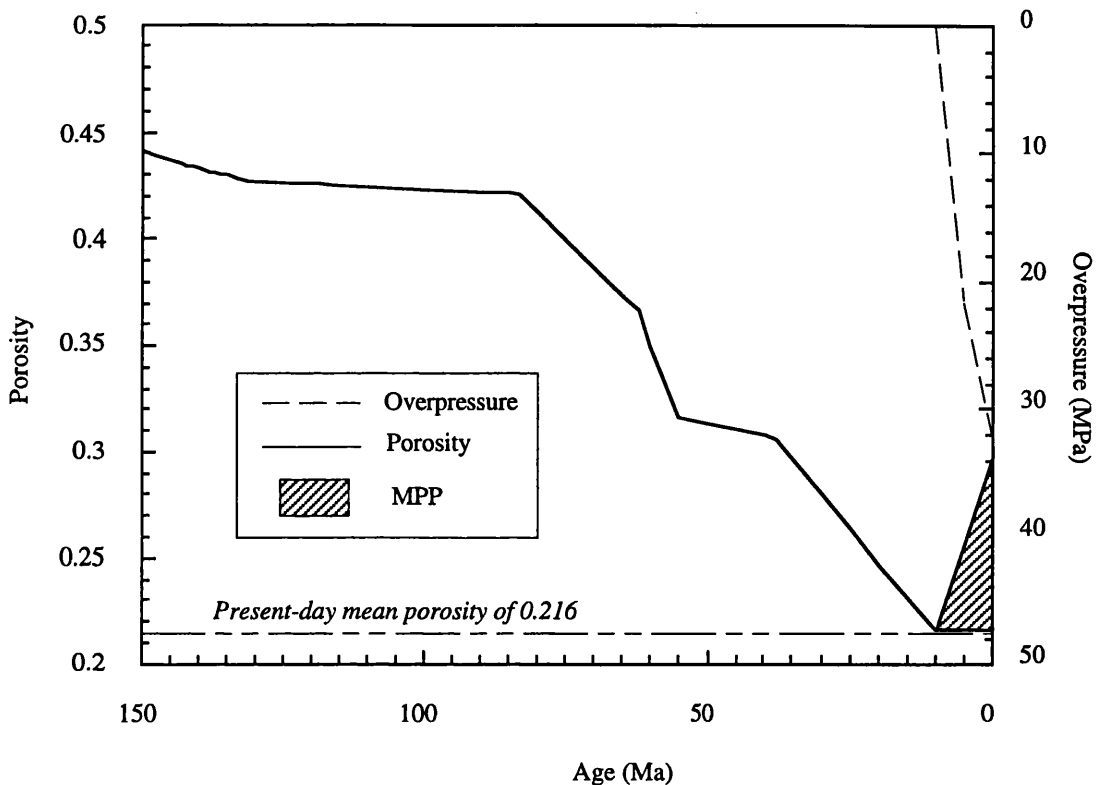


Figure 6.15 Modelled overpressure and porosity, and calculated MPP, for Fulmar Fm. in well 23/27-6.

Compaction as a response to increasing loading during Cenozoic burial leads to porosity loss. Overpressure increases to high levels in the Quaternary, inhibiting compaction and allowing MPP to increase. However, the measured present-day mean porosity in this well is close to the modelled value for compacted primary porosity. This suggests that secondary porosity has not allowed total porosity to increase towards the "virtual" MPP. The measured porosity remains near the compacted primary porosity, and no enhancement of porosity has occurred. Dissolution of feldspar must be balanced by precipitation of minerals within the reservoir, with no solute export.

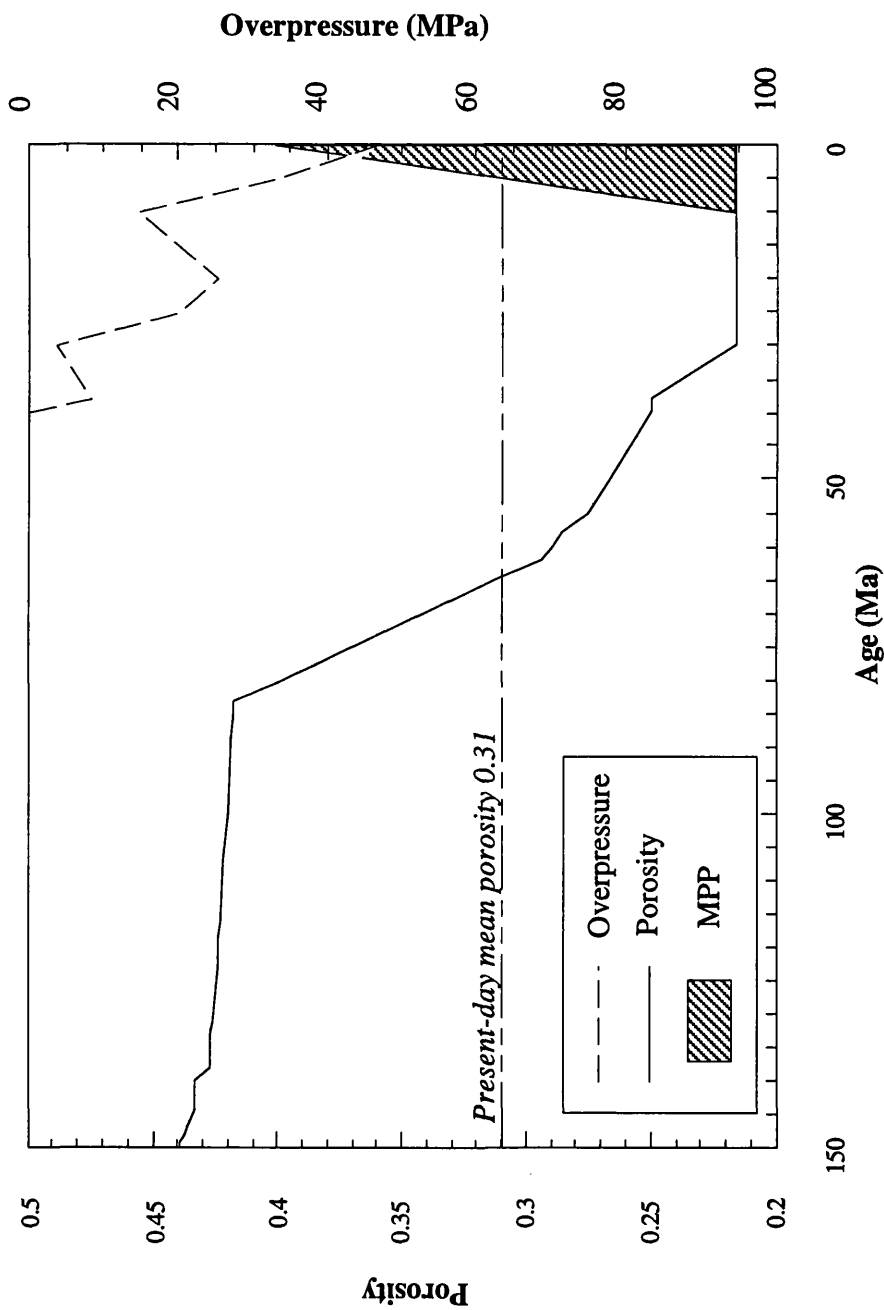


Figure 6.16 Modelled porosity and overpressure for Fulmar Fm. in well 22/30a-1, with calculated MPP

Porosity decreases and overpressure increases during rapid Cenozoic burial. High levels of overpressure retard compaction from Oligocene-present. However, much primary porosity has already been lost by this time. MPP increases in the Quaternary as effective stress is reduced in this well due to high overpressure and hydraulic communication with deep regions. The anomalously high present-day porosity is the result of secondary porosity increasing towards the MPP. Solute export from this Leak Point well allows enhancement of porosity.

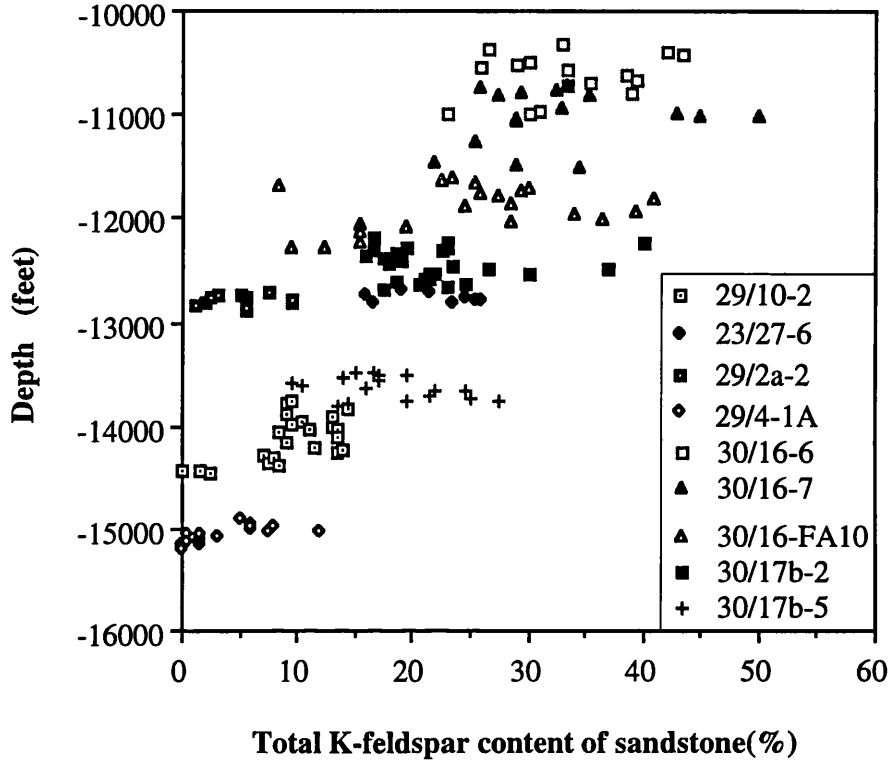


Figure 6.17 Distribution of feldspars as a function of depth in Fulmar Fm. sandstones of the Central Graben (after Wilkinson et al (b) in prep).

A trend of decreasing feldspar abundance with increasing depth can be clearly defined in the Central Graben. The feldspar abundance cannot be related to facies changes. This relationship indicates steady decomposition of feldspars with increasing depth and temperature.

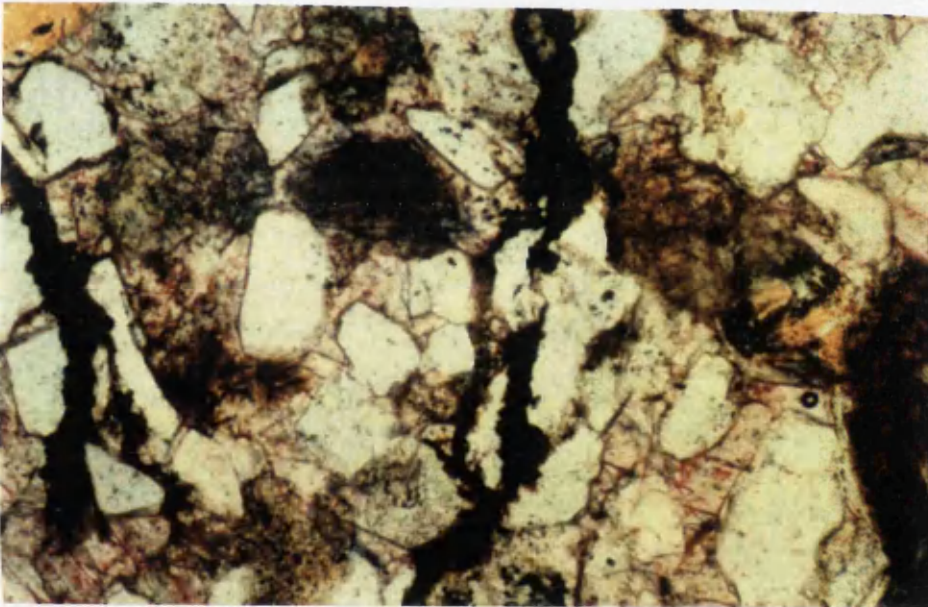
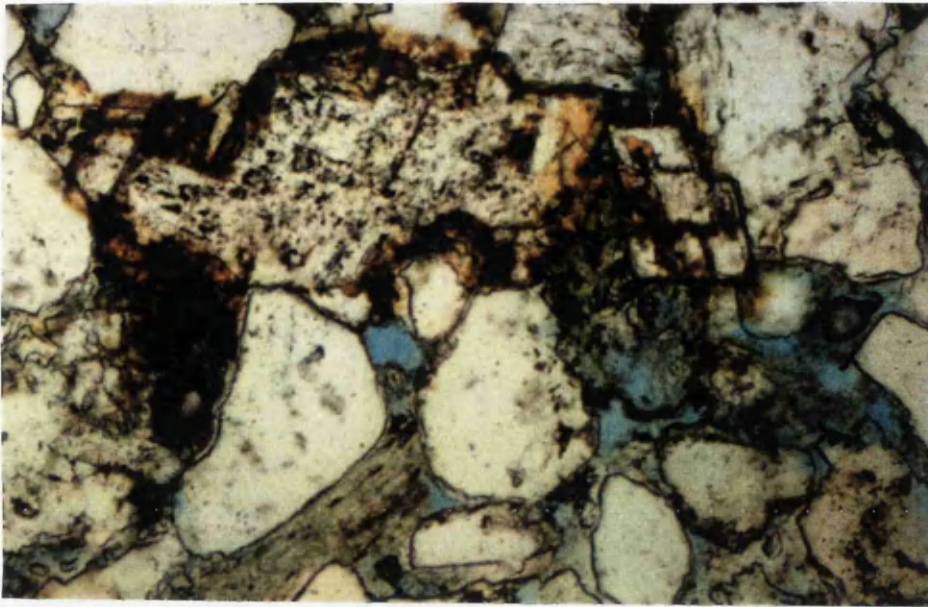


Figure 6.18. Fulmar Fm. porosity: (A) Thin section of well 22/30a-1. Field of view is 0.7mm. High porosity is clearly shown by the blue resin filling pore space. (B) Thin section of well 29/10-2. Field of view is 0.7mm. Porosity is lower than in well 22/30a-1. (C) Scanning Electron Microscope image of corroding feldspar forming secondary porosity in Fulmar Fm. (All images from Wilkinson et al (1994b)).

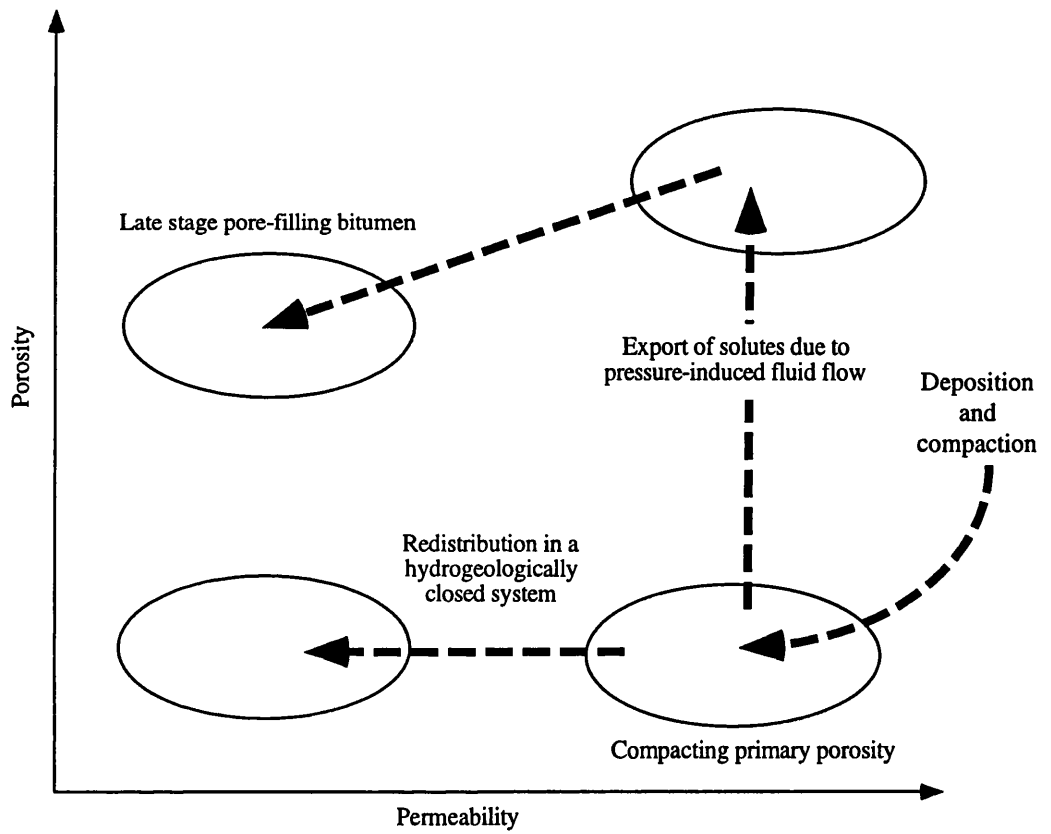


Figure 6.19 Evolution of Fulmar sandstone porosity and permeability during late diagenesis (modified after Wilkinson et al, 1994b). Overpressure controls the present-day porosity.

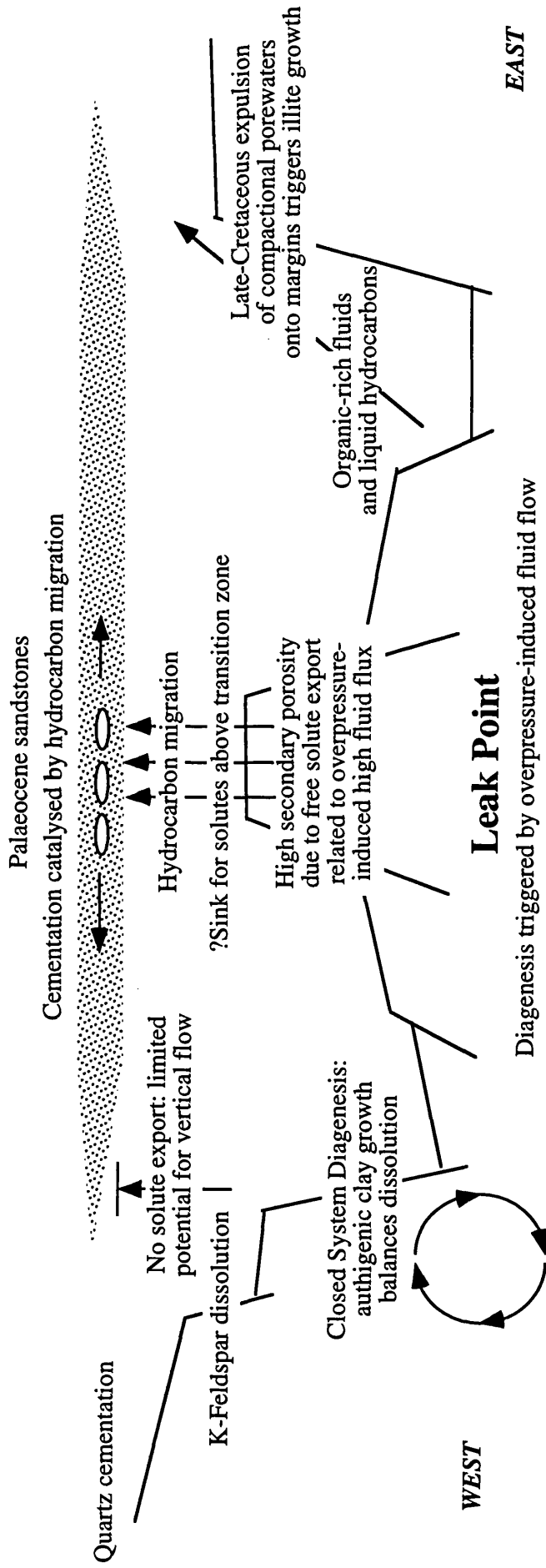


Figure 6.20 Summary cartoon for overpressure-related diagenesis in the Central Graben

Table 6.1 Radiogenic K-Ar age-dates from Central Graben illites (from Wilkinson et al 1994b)

Sample Depth (m)	Sample Weight (g)	Radiogenic $^{40}\text{Ar}/10^6 \text{ mol g}$	Radiogenic % ^{40}Ar	K (Wt%)	Age (Ma) +/- 1 σ
22/30a-1					
5011.7	0.02264	3.987	42.67	7.09	32.1 +/- 1.0
5016.4	0.02547	4.042	44.79	6.9	33.5 +/- 1.0
5019.7	0.0241	3.613	32.44	6.73	30.7 +/- 1.2
23/27-6					
4172.4	0.02345	6.939	49.81	6.02	65.3 +/- 1.8
4198.1	0.02345	7.3	46.89	5.52	74.7 +/- 2.2
4526.1	0.0293	10.18	62.24	6.83	84.0 +/- 2.1
4549.6	0.02882	9.187	63.41	7.33	70.8 +/- 1.7
4566.9	0.01325	9.067	43.57	6.88	78.8 +/- 2.4
4599.2	0.03895	8.588	64.55	7.49	64.9 +/- 1.6
4599.2	0.02982	8.209	57.88	7.28	63.9 +/- 1.6
4694.7	0.04067	7.352	56.98	7.11	58.7 +/- 1.5

Table 6.2 Statistical analysis of helium porosity measured on Fulmar Fm. sandstone conventional cores, Central Graben
In these wells, Fulmar Fm. is similar in facies and grain size.

	30/1e-3	29/2a-2	29/1e-2	23/27-6	22/30a-1	22/27a-1
Minimum	0.40000001	3.7	15.3	8.3000002	27	11
Maximum	25.7999999	26	26.9	28	35	31
Sum	2088	1013.2	1698.8	2754.08	1118	1456.8
Points	188	65	86	126	36	59
Mean	11.106383	15.587692	19.753488	21.857778	31.055556	24.691525
Median	10.25	16.299999	19.2	23.299999	31	25.799999
RMS	12.276118	16.179721	19.90694	22.364212	31.141701	25.113687
Std Deviation	5.243816	4.3704801	2.4814464	4.7512843	2.3475756	4.6247569
Variance	27.497606	19.101096	6.1575761	22.574703	5.5111111	21.388376
Std Error	0.38244459	0.54209134	0.26758124	0.42327805	0.3912626	0.60209206
Skewness	0.42039188	-0.9016408	1.0381347	-1.0340759	-0.03058162	-1.1596824
Kurtosis	-0.21809522	0.89790666	0.85949666	0.45261725	-0.80580125	0.58758019

Chapter Seven

Conclusions

7.1	Introduction
7.2	Research Conclusions
7.2.1	<i>The distribution of overpressure in the Central Graben</i>
7.2.2	<i>Origins of overpressure</i>
7.2.3	<i>Development of a quantitative process-based model</i>
7.2.4	<i>Overpressure and diagenesis</i>
7.3	Thesis methodology: steps forward
7.4	Further work suggested by this thesis
7.5	Concluding statement

7.1 Introduction

In Chapter One, the state of knowledge of Central North Sea overpressure was reviewed, and a series of research aims delineated. These were:

- to describe the distribution of overpressure in the region;
- to identify pressure seals and define pressure cells;
- to identify the mechanisms of pressure seal formation;
- to identify the origins of overpressure in the region;
- to examine the possible links between overpressure and diagenesis;
- to test the static and dynamic paradigms of overpressure (Section 2.8).

The pursuit of these aims has been achieved through a multi-disciplinary approach linking observational data from diverse sources and quantitative simulation of basin hydrogeological processes. This final chapter has two aims:

- To summarise the findings of this research and to present a series of conclusions. These conclusions will be placed in the context of previous studies. This allows demonstration of the fresh insight into geological processes presented by this thesis.
- To discuss assumptions, perceived weaknesses and implications of the approach taken that deserve further investigation.

7.2 Research conclusions

7.2.1 *The distribution of overpressure in the Central Graben*

Chapter Three comprised a detailed integrated analysis of an overpressured basin. Pressure data has been derived from RFT measurements, mudweight and gas levels. Protocols for the interpretation of pressure information have been presented. Overpressure has been delineated for several stratigraphic units in the Central Graben. Overpressure is inferred below 1500m depth in the thick Cenozoic mudstones. A reversion to hydrostatic pressure is found in the underlying Palaeocene sandstones and the Cretaceous Chalk in the north of the Graben. Pressure in the Palaeocene sandstones and Cretaceous Chalk increases towards the south of the Graben. This is controlled by the depositional distribution of the Palaeocene sandstones. These form a regionally extensive aquifer acting as a permeable "drain"

across the northern basin. The sandstones become thin and discontinuous, and regional permeability is lowered towards the south.

Overpressure rises in the muddy base of the Chalk Group and in the Lower Cretaceous-Upper Jurassic mudstones. High pressures are observed in the Jurassic sandstones beneath this low-permeability aquitard. Extremely rapid rises in pressure define pressure seals, which occur in the Kimmeridge Clay Fm. or at the top of the permeable Jurassic sandstones. The Jurassic sandstones are divided into pressure cells, which are bounded laterally by faults and sedimentary discontinuities. Extremely high pressures are observed in permeable sandstones on structurally-elevated horsts, where pressures may approach the minimum stress. Deeper, adjacent structures may be contained within the same pressure cell as the elevated horsts.

These detailed observations suggest that hydraulic continuity exists between deeply-buried regions in the Graben and relatively shallow regions on the axial horst. A dynamic model of the pressure distribution is proposed. This model of hydraulic communication explains the distribution and magnitude of overpressure in the region. Structurally-elevated shallow regions exhibit fluid pressures close to the minimum stress; deeper regions have fluid pressure far from the minimum stress. These shallow zones are termed "Leak Points". Vertical fluid flow is favoured at "Leak Points" due to high fluid pressure, thin aquitards and possible hydraulic fracturing of the seal.

The "Leak Point" model describes the location of pressure seals in the Graben. In on-structure "Leak Points", highest overpressures occur in the permeable sandstone. Pressures are elevated above the pressure in overlying mudstones due to hydraulic communication with deeper regions. In off-structure cells, sandstones exhibit overpressures equal to or less than overlying mudstones. Highest overpressures occur in the Kimmeridge Clay source rock overlying the permeable sandstone, which marks the upper boundary of the pressure cell. Pressure seals are controlled by lithostratigraphy and structure, and not by cementation or depth as has been previously proposed for the region (Hunt 1990, Leonard 1993).

The overpressure distribution has been proposed as a control on hydrocarbon entrapment in the region. Hydrocarbon accumulation in the Cretaceous Chalk requires overpressure in the overlying Palaeocene sandstones. In the Jurassic, Leak Points are unfavourable sites for hydrocarbon retention. Deeper structures in hydraulic communication with Leak Points contain hydrocarbons.

The Leak Point model is intrinsically a dynamic model. The distribution of overpressure in the region is controlled by lithology and structure, and so fits the hydraulically-continuous "dynamic" paradigm. The pressure distribution does not fit the "static" paradigm. Pressure seals are not at a constant depth. The requirement for fluid flow in Leak Points stresses the dynamic nature of overpressure in the region.

7.2.2 Origins of overpressure

In Chapter Four, interpretation of sonic and density wireline logs has identified anomalously high porosity in the overpressured Lower Cretaceous and Jurassic rocks of the Central Graben. This is interpreted as preserved primary porosity. This suggests that the energy disequilibrium in the study area has been caused by disequilibrium compaction. However, sharp increases in pressure in the Kimmeridge Clay Fm., a gas-mature source rock, are also noted. This coincidence suggests that hydrocarbon generation contributes to the overpressure in the region. Additionally, the increase of minimum stress (derived from leak-off tests) above the overpressured cells suggests fluid generation. Thus overpressure in the Central Graben may be due to both external effects (disequilibrium compaction due to rapid loading) and internal effects (fluid generation due to hydrocarbon generation).

The relative influences of disequilibrium compaction and hydrocarbon generation on overpressure cannot be assessed in the present study. This is due to the complexity of the hydrocarbon generation process. Several facets of the process are still poorly understood. One of these facets is the dissolution of gas in water and in oil; another is the hydrocarbon expulsion efficiency of the Kimmeridge Clay Fm. Without accurate quantification of these processes, the fluid volume increase during hydrocarbon generation cannot be quantitatively assessed. However, a three-stage qualitative model of the influence of the Kimmeridge Clay Fm. pressure seal on the basin hydrogeology was presented. A composite model of overpressure generation in the region was developed. Aquathermal pressuring and clay mineral dehydration have previously been proposed as possible causes of Central Graben overpressure (Gaarenstroom *et al.* 1993). These are rejected in Chapter Four, as the physical conditions necessary for their influence are not met in the Central Graben.

Overpressure results from physico-geochemical effects operating on a microscopic (pore) scale; these microscopic effects give rise to basin-scale pressure cell structures.

7.2.3 Development of a quantitative process-based model

Chapters Three and Four presented a model of Central Graben overpressure based primarily on observational data. Chapter Five synthesised these diverse, detailed observations in a quantitative basin model of the Graben, leading to a process-based quantitative description of the basin hydrogeology.

A one-dimensional basin model was used to examine the relationship between subsidence rate, porosity change and seal permeability reduction. These models found that the pressures in the Jurassic sandstones in the Central Graben cannot be attributed solely to the restriction of vertical flow through the pressure seal. This is in marked contrast to the results of previous model investigations of the Central North Sea and other overpressured basins worldwide (e.g. Mudford *et al.* 1991). The regional aquitard formed by Cretaceous Chalk and Jurassic mudstones is too thin and too permeable to provide the necessary barrier to fluid flow. Mudweights in the aquitard provide an observed upper limit to constrain model pressures in the aquitard, and thus to constrain model aquitard permeability. The one-dimensional model allowed evaluation of the model sensitivity to variation in constrained and unconstrained input parameters. It was found that the available data was sufficient to simulate pressure, but was inadequate for quantitative simulation of hydrocarbon generation.

A two-dimensional basin model was used to build on the one-dimensional model results by examining the role of lateral flow beneath the regional aquitard. This model adequately reproduced the observed pressure distribution and magnitude in two calibrant wells using standard empirical functions for rock properties. The model quantified and reiterated the role of lateral flow beneath the pressure seal controlled by geological structure. This supported the observations made in the preceding chapters. The adequate description of the present-day overpressure systems by the model allowed insight into the palaeo-overpressure systems and the probable timing of the onset of overpressure, suggesting that overpressure has been caused by disequilibrium compaction due to rapid Cenozoic sedimentation linked to the low permeability of the mudstone-dominated basin. Overpressure in the Fulmar Fm. began at 40 Ma in the axial structures of the graben and at 10 Ma on the margins of the Graben. Quantification of hydrocarbon generation and its role in overpressuring was hindered by the inadequacy of the data and the possible inadequacy of the equations used to simulate this complex process. However, the model qualitatively supported the model of hydrocarbon entrapment advanced in

Chapter Three. It suggested that hydrocarbon generation is insignificant in causing overpressure in the Graben because observed pressures could be simulated through disequilibrium compaction alone.

7.2.4 Overpressure and diagenesis

Chapter Six has shown that the development of a model for the hydrogeology of the region allows new insights into sediment diagenesis. Quantitative observation of the diagenesis of the Fulmar Fm. in the Central Graben has been integrated with the quantitative model of basin hydrogeology developed in Chapter Five.

A hydrogeological control on the growth of authigenic illite has been advanced. Basin subsidence leads to increased fluid flow rates. K-Ar dates from authigenic illite in wells on the eastern and western margins of the Graben coincide with the onset of rapid subsidence in the Graben. Rapid subsidence may have caused increased fluid flow rates and the influx of organic acids from adjacent mudrocks into the margin sandstones. As the compaction of the Graben continued, fluid flow slowed and illite growth ceased. Cessation of illite growth is preserved as the illite K-Ar date for the well. In contrast, a well on the axial horst of the Graben contains illite with an Oligocene age-date. This date coincides with the onset of high overpressure in the well. This coincidence suggests illite dates represent cessation of illite growth as overpressure reduces fluid flow rates. Advection of organic acids or hydrocarbons that may be essential for illite growth will similarly be reduced by overpressure. Fluid flow rates in the Central Graben are controlled by the complex interplay of subsidence, porosity change, and overpressuring. The positioning of dates of authigenic illite growth in a structural-hydrogeological framework has shed new light on the geological causes of illite growth.

A hydrogeological control has also been proposed for the development of secondary porosity in the Graben. It is conventional that overpressure allows the preservation of primary sandstone porosity (e.g. Ramm, 1994). In Chapter Six it was suggested that overpressure also allows support of developing voids. The structurally-controlled fluid flow systems expressed by the pressure distribution control the export of solutes through the pressure seal. Solute export occurs preferentially at Leak Points. Thus at Leak Points, overpressure allows the support of secondary porosity and the export of solutes from the sandstone, leading to high porosities at great depths in the Central Graben.

These patterns provide a new, original insight into the diagenesis of the region. Some aspects of sediment diagenesis in deep burial should be considered in tandem with the hydrogeology of those sediments. Consequently, some aspects of diagenesis should be placed in the context of basin structure and basin evolution. The basin-scale distribution of pressure affects the pore-scale distribution of porosity.

7.3 Research methods: steps forward

This thesis has demonstrated that maximising the use of pressure data is essential to characterise overpressure in a region. Pressure data can be derived from mudweight in addition to RFT pressures. Integration with geological data (principally lithostratigraphy and structure) has allowed the construction of a detailed depiction of the overpressure in the region. Analysis of pressure data on a well-by-well basis has led to a description of the pressure systems that differs fundamentally from previous studies (e.g. Cayley 1987; Hunt 1990; Leonard 1993; Gaarenstroom *et al.* 1993). These previous studies have focused on the description of basin-scale patterns, from which erroneous inferences have been made regarding the reservoir-scale distribution of pressure, the fixed depth and horizontal morphology of pressure seals, and the static geological nature of these seals. The new approach has also allowed accurate calibration of aquitard pressures in basin models. This calibration is fundamental for the validity of the models. Maximising the data available for model calibration through multi-well coverage and detailed pressure and log data has allowed rigorous model construction.

Use of RFT pressures from reservoirs alone to delineate pressure-depth trends results in errors. Regional plots of reservoir pressures against depth also leads to erroneous conclusions. A study of the overpressure systems cannot be abstracted from a detailed consideration of the regional geology. Regional trends are tempting to infer, but may have no basis in areas of complex lithological and structural variation such as the Central Graben.

7.4 Assumptions made in the research

This research approach has made three principal assumptions. Firstly, it is assumed that fluid flow can occur in deeply-buried mudstones in the Central North Sea. This fundamental assumption requires that (a) mudstones have a non-zero permeability, and (b) that Darcy's Law applies to these deep mudstones. Accordingly it has been

assumed that the presence of potential energy gradients across mudstones will drive fluid flow through the rock. The applicability of this fundamental Law has not been demonstrated. There is a growing body of work that suggests Darcy flow does not occur in clay-rich sediments until a threshold hydraulic gradient is reached (Swartzendruber 1962; Byerlee 1990; Bernardiner & Protopas 1994). Note that this threshold gradient occurs for a wetting-phase fluid and is distinct from familiar capillary entry pressures for non-wetting phase fluids (e.g. Watts, 1987). Threshold gradients may be formed by the dynamic properties of molecularly thin liquid films (Israelachvili *et al.* 1988). Neuzil (1995) has suggested that hydraulic gradients sufficient to overcome threshold gradients do not commonly occur in sedimentary basins. However, the evidence for threshold gradients is controversial, as experiments are not always reproducible even with identical rocks (Byerlee 1990, Neuzil 1995). This has led to speculation that threshold gradients may be experimental artifacts (Byerlee 1990). The role of threshold gradients, and thus the crucial applicability of Darcy's Law to deeply-buried mudstones, remains unresolved (Neuzil 1995).

This thesis has found that simulation of the fluid flow in shale layers replicates the observed pattern of pressure in those layers, suggesting that Darcy's Law is valid in this region. Darcy's Law has also been assumed to apply to faults. If Darcy's Law is shown to be inapplicable to deeply-buried mudstones, a major re-evaluation of the hydrogeology of sedimentary basins will be required. However, the findings of this thesis will not be absolutely refuted. If fluid flow cannot occur through the matrix porosity of mudstones, then it will occur in fractures. These fractures will be preferentially located in regions of low effective stress, which in the Central Graben will be formed by the Leak Points defined in Chapter Three. Thus flow will occur by Darcy's Law through the matrix of the sub-seal sandstones towards structurally-elevated zones. Vertical flow in fractures will aid solute transport and hydrocarbon migration through the seal. However, the timing of hydrocarbon migration through the seal will be altered, and will require open fractures.

The second assumption is a corollary of the first. It is assumed that the Graben sediments are able to compact. Compaction provides the driving force for Darcy flow, and Darcy flow through mudstones allows compaction. It has been assumed that the porosity change associated with this compaction is controlled by physical loading and effective stress. Compaction is the great unknown in the description of sedimentary basins (Giles *et al.* 1994). This assumption is fundamental to the current understanding of fluid flow and overpressure in basins. It has been noted in Section 3.2 that direct examination of the porosity of mudstones in the Gulf Coast (Hunt *et*

al. 1994) suggests that compaction is not occurring. Examination of the compaction processes of North Sea sandstones (Emery *et al.* 1993) suggests that the change in porosity observed with depth is primarily the result of cementation, not increased loading. Similarly, petrophysical analysis of mudstones from the Venture basin of Canada (Katsube *et al.* 1994) demonstrated that, at depths below 2000m, cementation and not compaction lowers shale permeability and porosity. If it is demonstrated that porosity change is chemically-mediated and not primarily controlled by physical loading, a paradigm shift in basin hydrogeology will be required.

The third assumption made in this thesis is the neglect of lateral stresses and their effect on fluid pressure and porosity. Lack of data makes assessment of the magnitude of lateral stresses in the Central Graben difficult. Models that couple fluid flow, compaction, and rock mechanics do not yet exist. This may be attributed to the three-dimensionality necessary to assess stress state in the crust. Bour *et al.* (1995) have attempted a two-dimensional qualitative analysis of the role of lateral stress in overpressuring in a SE Asian basin. Three-dimensional basin models will be necessary for quantitative assessment of the role of lateral stresses.

These three assumptions have usefully allowed the use of basin models to describe and quantify the hydrogeological regime in the Central Graben. The model replicates the observed distribution of overpressure in the region; however, the causes of this distribution are subject to the above assumptions. As stated in Chapter Five, the complex models presented are subject to refutation by new data, as are all scientific models (Popper 1963; Oreskes *et al.* 1994).

7.5 Further work suggested by this thesis

The thesis presented in the previous chapters may be improved by additional data acquisition, and by an improved theoretical understanding of the causal mechanisms of overpressure.

- **Additional data** acquisition should be focused on non-sandstone intervals of the well. Porosity and permeability data from mudstones will provide data for calibration of the existing forms of basin model and may provide new insights into the processes of porosity change. Increased areal coverage, with the availability of multiple wells in a structure, will become available as the central North Sea matures as an exploration province. Additional useful information will

include a depiction of possible variations in the formation water salinity across the basin, which will allow refinement of the understanding of hydraulic head in the basin (Fig 3.26). Increased information on the three-dimensional stress state in the Central Graben (from earthquake foci and borehole breakouts) should be gathered. Refinement of the structure of the Graben by the availability of three-dimensional seismic sections will aid the integration of pressure data and structure.

- **3D basin modelling.** The possibility of three-dimensional structural analysis raises the possibility of three-dimensional simulation of the basin hydrogeology. Advances in computer power will enable efficient three-dimensional basin modelling, which will refine the two-dimensional model presented in Chapter Four. Integrating stress and rock mechanics of the basin with the fluid flow and compaction models will lead to a fuller description of the processes affecting fluid pressure in the region.
- **Palaeopressure measurement.** In addition to widening the scope of observation in terms of depth and area, observations of the pressure regime in the geological past may be made through improvement of derivation of palaeopressures from fluid inclusions (Mullis 1979). This may allow calibration of a basin model for additional time periods if sufficient accurate data is derived. The method requires validation with respect to the trapped hydrocarbon compositions in the inclusions. Hydrocarbons may alter composition after trapping in inclusions (Larter & Mills 1991) and may not reflect original pressures of trapping. Additionally, the technique depends on the integrity of aqueous fluid inclusions (see Osborne & Haszeldine 1994).
- **Application to other basins.** Integration of quantitative models of basin hydrogeology with quantitative analysis of sediment diagenesis has allowed fresh insight into the controls on diagenesis. Similar controls may be observed in other basins. Application of the methodology developed in this thesis will test the hypotheses advanced in Chapter Six.
- **Hydrocarbon generation.** The principal area of uncertainty in overpressure mechanisms is the role of hydrocarbon generation. If compaction proves to be of less significance than implied by this project, hydrocarbon generation may prove to be a main overpressure mechanism. Quantification of this role through an improved understanding of the interaction between generation, expulsion, solution and compressibility for various hydrocarbon types will aid further

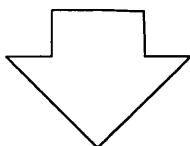
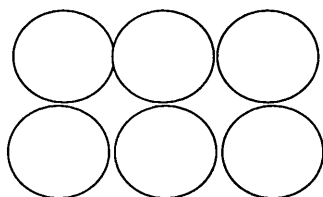
research in deciphering this problem. This quantification may be attempted through laboratory experiment (Ungerer *et al.* 1983) and numerical simulation (Lerche 1990; Bredehoeft *et al.* 1994).

Thus it is envisaged that understanding of overpressure in the Earth's crust will advance through a combination of increased observation, quantitative simulation and laboratory experiment.

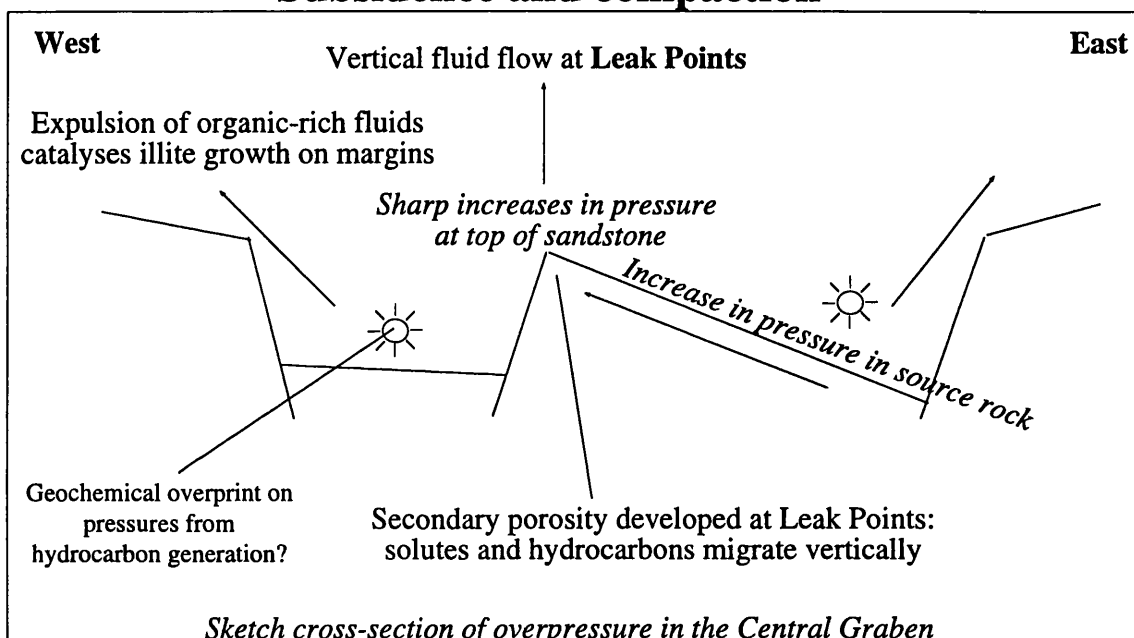
7.6 Concluding statement

This thesis has demonstrated that a diverse series of hydrogeological observations in the Central North Sea may be reconciled if overpressure is perceived as a dynamic phenomenon in the Earth's crust. Despite the static implications of the terminology applied to overpressure ("seals" and "sealed compartments"), on a geological timescale an overpressured basin is a dynamic, continually-changing system. Overpressure results from a wide range of interacting processes in the shallow crust operating on both a microscopic (pore) scale, and on a macroscopic (basin) scale. In turn, the phenomenon of overpressure also affects the crust in a series of complex interactions between geochemical reactions, fluid flow and sediment compaction (Fig 7.1). Pore-scale alterations build basin-scale structures such as cells and seals, and these basin-scale structures in turn effect pore-scale changes in the basin. This thesis has delineated and quantified these interacting processes in the study region. The complexity of overpressure reflects the complexity of the dynamic geological environment.

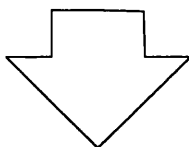
Pore-scale changes produce basin-scale patterns



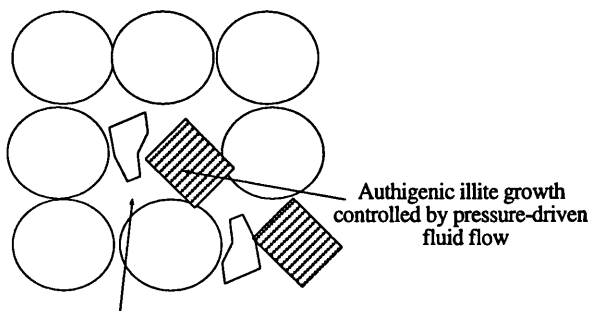
Subsidence and compaction



Basin-scale patterns of overpressure control the reservoir-scale distribution of pressure



Basin-scale patterns of overpressure in turn produce pore-scale changes in the rock



Secondary porosity regulated by overpressure support of voids and overpressure-driven export of solutes from Leak Points.

Figure 7.1 Summary

Bibliography

- Anderson, E.M. (1951). The dynamics of faulting and dyke formation with application to Britain. Oliver & Boyd, Edinburgh, 320pp.
- Andrews-Speed, C.P., Oxburgh, E.R. & Cooper, B.A. (1984). Temperatures and depth-dependent heat flow in western North Sea. *Bulletin of the American Association of Petroleum Geologists*, **68**, No. 11, 1764-1781.
- Audet, D.M. & Fowler, A.C. (1992). A mathematical model for compaction in sedimentary basins. *Geophysical Journal*, **110**, 3, 577-590.
- Audet, D.M. & McConnell, J.D.C. (1992). Forward modelling of porosity and pore pressure evolution in sedimentary basins. *Basin Research*, **4**, 147-162.
- Bailey, R.C. (1994). Fluid trapping in mid-crustal reservoirs by H₂O-CO₂ mixtures. *Nature*, **371**, 238-240.
- Baldwin, B. & Butler, C.O. (1985). Compaction curves. *Bulletin of the American Association of Petroleum Geologists*, **69**, 622-626.
- Barker, C. (1990). Calculated volume and pressure changes during the thermal cracking of oil to gas in reservoirs. *Bulletin of the American Association of Petroleum Geologists*, **74**, 8, 1254-1261.
- Barker, C. (1972). Aquathermal pressuring- role of temperature in development of abnormal-pressure zones. *Bulletin of the American Association of Petroleum Geologists*, **56**, No. 10, 2068-2071.
- Barnard, P. & Bastow, M. (1991). Petroleum generation, migration, alteration, entrapment and mixing in the Central and Northern North Sea. In: England, W. & Fleet, A. (eds.), *Petroleum Migration*. Geological Society Special Publication No.59, The Geological Society, London, 167-190.
- Bernardiner, M.G. & Protopas, A.L. (1994). Progress on the theory of flow in geologic media with threshold gradient. *Journal of Environmental Science and Health, Part A- Environmental Science and Engineering*, **29**, No. 1, 249-275.

- Berner, R.A. (1980). Non-marine sediments. In: Berner, R.A. (eds.), *Early Diagenesis, a Theoretical Approach*. Princeton Univ. Press, Princeton, N.J., 206-224.
- Berry, F.A.F. (1973). High fluid potentials in California Coast ranges and their tectonic significance. *Bulletin of the American Association of Petroleum Geologists*, **57**, No. 7, 1219-1249.
- Berry, M.J. & Mair, J.A. (1977). The nature of the Earth's crust in Canada. In: Heacock, J.G. (eds.), *The Earth's crust, its nature and physical properties. Geophysical Monograph No. 20*, American Geophysical Union, 319-348.
- Bethke, C.M. (1986). Inverse hydrologic analysis of the distribution and origin of Gulf Coast-type geopressed zones. *Journal of Geophysical Research-Solid Earth and Planets*, **91**, No. NB6, 6535-6545.
- Bethke, C.M. (1985). A numerical model of compaction-driven groundwater flow and heat transfer and its application to the palaeohydrology of intracratonic sedimentary basins. *Journal of Geophysical Research* **90**, No. B8, 6817-6828.
- Bingham, M.G. (1964). A new approach to interpreting rock drillability. *Oil and Gas Journal*, **62**, No. 46, 148-150.
- Biot, M.A. (1941). General theory of three-dimensional consolidation. *Journal of Applied Physics*, **12**, 155-164.
- Birchwood, R.A. & Turcotte, D.C. (1994). A unified approach to geopressure, low-permeability zone formation, and secondary porosity formation in sedimentary basins. *Journal of Geophysical Research*, **99**, No. B10, 20050-20058.
- Bjørlykke, K. (1993). Fluid flow in sedimentary basins. *Sedimentary Geology*, **86**, 137-158.
- Bjørlykke, K. (1984). Formation of secondary porosity: how important is it? In: McDonald, D.A. & Surdam, R.C. (eds.), *Clastic Diagenesis. American Association of Petroleum Geologists Memior 37*, American Association of Petroleum Geologists, 277-286.

- Bloch, S. (1991). Empirical prediction of porosity and permeability in sandstones. *Bulletin of the American Association of Petroleum Geologists*, **75**, 1145-1160.
- Boles, J. & Franks, S. (1979). Clay diagenesis in the Wilcox sandstones of SE Texas- implications of smectite diagenesis on sandstone cementation. *J. Sediment. Petrol.*, **49**, 55-70.
- Bour, O. & Lerche, I. (1994). Numerical Modelling of abnormal fluid pressures in the Navarin Basin, Bering Sea. *Marine and Petroleum Geology*, **11**, No. 4, 491-500.
- Bour, O., Lerche, I. & Grauls, D. (1995). Quantitative models of very high fluid pressure- the possible role of lateral stresses. *Terra Nova*, **7**, No.1, 68-79.
- Bowers, G.L. (1994). Pore pressure estimation from velocity data: accounting for overpressure mechanisms besides undercompaction. *SPE Drilling and Completion Journal*, **10**, 2, 89-95.
- Bradley, J.S. (1975) Abnormal formation pressure. *Bulletin of the American Association of Petroleum Geologists*, **59**, 6, 957-973.
- Bredehoeft, J., Wesley, J. & Fouch, T. (1994). Simulations of the origin of fluid pressure, fracture generation, and the movement of fluids in the Uinta Basin, Utah. *Bulletin of the American Association of Petroleum Geologists*, **78**, No. 11, 1729-1747.
- Bredehoeft, J.D. & Hanshaw, B.B. (1968). On the maintenance of abnormal fluid pressures, I: thick sedimentary sequences. *Geological Society of America Bulletin*, **79**, 1097-1106.
- Bruton, C. & Helgeson, H. (1983). Calculation of the chemical and thermodynamic consequences of differences between fluid and geostatic pressure in hydrothermal systems. *American Journal of Science*, **283-A**, 540-588.
- Buhrig, C. (1989). Geopressured Jurassic reservoirs in the Viking Graben: modelling and geological significance. *Marine and Petroleum Geology*, **6**, 31-48.
- Burley, S.D. & Flisch, M. (1989). K-Ar geochronology and the timing of detrital I/S clay illitization and authigenic illite precipitation in the Piper and Tartan Fields, Outer Moray Firth, UK North Sea. *Clay Minerals*, **24**, 285-316.

Burley, S.D. (1993). Models of burial diagenesis for deep exploration plays in Jurassic fault traps of the Central and Northern North Sea. *In: Parker, J. (ed) Petroleum Geology of Northwest Europe*. The Geological Society, London, 1353-1375.

Burnham, A.K. & Sweeney, J.J. (1989) A chemical-kinetic model of vitrinite maturation and reflectance. *Geochimica Cosmochimica Acta*, **53**, 2649-2657.

Burrus, J., Osadetz, K., Gaulier, J.M., Brosse, E., Doligez, B., Choppin de Janvry, G., Barlier, J. & Visser, K. (1993). Source rock permeability and petroleum expulsion efficiency: modelling examples from the Mahakam Delta, the Williston Basin and the Paris Basin. *In: Parker, J. (ed.) Petroleum Geology of North West Europe*. The Geological Society, London, 1317-1331.

Burrus, J., Kuhfuss, A., Doligez, B. & Ungerer, P. (1991). Are numerical models useful in reconstructing the migration of hydrocarbons? A discussion based on the Northern Viking Graben. *In: England, W.A. & Fleet, A.J. (eds) Petroleum Migration*. Geological Society Special Publication No.59, The Geological Society, London, 89-109.

Burst, J. (1959). Post diagenetic clay mineral-environmental relationships in the Gulf Coast Eocene. *Clays and Clay Minerals*, **6**, 327-341.

Burst, J.F. (1969). Diagenesis of Gulf Coast clayey sediments and possible relation to petroleum migration. *Bulletin of the American Association of Petroleum Geologists*, **53**, 73-93.

Byerlee, J. (1990). Friction, overpressure and fault normal compression. *Geophysical Research Letters*, **17**, 2109-2112.

Carlin, S. & Dainelli, J. (in press). Pressure regimes in the Adriatic Basin, Italy. *In: Law, B.E. & Ulmishek, G. (eds.), Abnormal pressures in hydrocarbon environments*. American Association of Petroleum Geologists, Tulsa, OK., USA.

Cartwright, J. (1994). Episodic basin-wide fluid expulsion from geopressured shale sequences in the North Sea basin. *Geology*, **22**, 447-450.

- Cavanagh, A. (1995). *A two-dimensional modelling investigation of the Central Graben, North Sea*. Unpublished B.Sc. thesis, Glasgow University.
- Cayley, G.T. (1987) Hydrocarbon migration in the central North Sea. *In: Glennie, J.B. and Brooks, K. (eds) Petroleum Geology of North West Europe*, 549-555.
- Chiarelli, A. & Duffaud, F. (1980). Pressure origin and distribution in Jurassic of Viking Basin (United Kingdom-Norway). *Bulletin of the American Association of Petroleum Geologists*, **64**, No. 8, 1245-1266.
- Cornford, C. (1994). The Mandal-Ekofisk (!) Petroleum System in the Central Graben of the North Sea. *In: Magoon, L. & Dow, W. (eds) The Petroleum systems- from source to trap: American Association of Petroleum Geologists Memoir No. 60*, American Association of Petroleum Geologists, Tulsa, OK, USA. 290-314.
- Coyner, K., Katsube, T., Best, M. & Williamson, M. (1993). Gas and water permeability of tight shales from the Venture Gas Field, offshore Nova Scotia. *In: Current Research, Part D: Geological Survey of Canada*. 129-136.
- Curtis, C.D. (1978). Possible links between sandstone diagenesis and depth-related geochemical reactions occurring in enclosing mudstones. *Journal of the Geological Society, London*, **135**, No. 1, 107-117.
- Da-Jun, P. & Yun-Ho, L. (in press). Generation of abnormal pressure in the Sichuan Basin. *In: Law, B.E. & Ulmishek, G. (eds.), Abnormal pressures in hydrocarbon environments*. American Association of Petroleum Geologists, Tulsa, OK, USA.
- Dahlberg, E.C. (1982). *Applied Hydodynamics in Petroleum Exploration*. Springer-Verlag, New York, 161 pp.
- de Caritat, P., Bloch, J.D., Hutcheon, I.E. & Longstaffe, F.J. (1994). Compositional trends of a Cretaceous foreland basin shale (Belle Fourche Formation, Western Canada Sedimentary Basin): diagenetic and depositional controls. *Clay Minerals*, **29**, 4, 503-526.
- de Marsily, G. (1986). *Quantitative Hydrogeology*. Academic Press, San Diego, 440pp.

- Deming, D. (1994) Factors necessary to define a pressure seal. *Bulletin of the American Association of Petroleum Geologists*, **78**, 6, 1005-1010.
- Dewers, T. & Ortoleva, P. (1994). Nonlinear dynamical aspects of deep basin hydrology: fluid compartment formation and episodic fluid release. *American Journal of Science*, **294**, 713-755.
- Dickinson, G. (1953). Geological aspects of abnormal reservoir pressures in Gulf Coast Region of Louisiana. *Bulletin of the American Association of Petroleum Geologists*, **37**, 410-432.
- Donovan, A.D., Djakic, A.W., Ioannides, N.S., Garfield, T.R. & Jones, C.R. (1993) Sequence stratigraphic control on Middle and Upper Jurassic reservoir distribution within the UK Central North Sea. In: Parker, J. (ed) *Petroleum Geology of NW Europe*. The Geological Society, London, 251-270.
- Duppenbecker, S.J., Dohmen, L. & Welte, D.H. (1991). Numerical modelling of petroleum expulsion in two areas of the Lower Saxony Basin, Northern Germany. In: England, W.A. & Fleet, A.J. (eds) *Petroleum Migration*. Geological Society Special Publication No.59, The Geological Society, London, 47-64.
- Dypvik, H. (1983). Clay mineral transformation in Tertiary and Mesozoic sediments from the North Sea. *Bulletin of the American Association of Petroleum Geologists*, **67**, No. 1, 160-165.
- Eberl, D. (1993). 3 zones for illite formation during burial diagenesis and metamorphism. *Clays and Clay Minerals*, **41**, No. 1, 26-37.
- Edman, J. & Surdam, R. (1986). Organic-inorganic interactions as a mechanism for porosity enhancement in the Upper Cretaceous Ericson sandstone, Green River Basin, Wyoming. In: Gautier, D. (ed.), *Roles of organic matter in sediment diagenesis: SEPM Special Publication No.38*. 85-110.
- Emery, D., Smalley, P. & Oxtoby, N. (1993). Synchronous oil migration and cementation in sandstone reservoirs demonstrated by quantitative description of diagenesis. *Phil. Trans. R. Soc. Lond.*, **344**, 115-125.

Engelder, T & Fischer, M.P. (1994) Influence of poroelastic behavior on the magnitude of minimum horizontal stress, S_h , in overpressured parts of sedimentary basins. *Geology*, **22**, 949-952.

Engelder, T. (1993). *Stress regimes in the lithosphere*. Princeton University Press, Princeton, New Jersey, 449pp.

England, W., MacKenzie, A., Mann, D. & Quigley, T. (1987). The movement and entrapment of petroleum fluids in the subsurface. *Journal of the Geological Society*, **144**, 327-347.

Faure, G. (1987). *Principles of isotope geology*. John Wiley and Sons, New York, 589pp.

Ferry, J.M. & Dipple, G.M. 1991. Fluid flow, mineral reactions and metasomatism. *Geology*, **19**, 211-214.

Fleming, C.G. (in prep) *Thermal anomalies in the North Sea*. Unpublished PhD thesis, Glasgow University, Glasgow, Scotland.

Forbes, P.L., Ungerer, P. & Mudford, B.S. (1992). A two-dimensional model of overpressure development and gas accumulation in Venture Field, Eastern Canada. *Bulletin of the American Association of Petroleum Geologists*, **76**, No. 3, 318-338.

Fowles, J. & Burley, S. (1994). Textural and permeability characteristics of faulted, high-permeability sandstones. *Marine and Petroleum Geology*, **11**, No. 5, 608-623.

Fripiat, J. & Letellier, M. (1984). Microdynamic behaviour of water in clay gels below the freezing point. *Journal of Magnetic Resonance*, **57**, No. 2, 279-286.

Funing, L. (in press). Overpressure in the Yinggehai Basin, South China Sea. In: Law, B.E. & Ulmishek, G. (eds.), *Abnormal pressures in hydrocarbon environments*. American Association of Petroleum Geologists, Tulsa, OK., USA.

Galloway, W.E. (1984). Hydrogeologic regimes of sandstone diagenesis. In: McDonald, D.A. & Surdam, R.C. (eds), *Clastic Diagenesis*. *American Association of Petroleum Geologists Memoir 37*, American Association of Petroleum Geologists, Tulsa, OK, USA, 3-14.

- Gaarenstroom, L., Tromp, R., de Jong, M. & Brandenburg, A. (1993). Overpressures in the Central North Sea: implications for trap integrity and drilling safety. In: Parker, J. (ed.), *Petroleum Geology of Northwest Europe: Proceedings of the 4th Conference*. The Geological Society, London, 1305-1313.
- Garven, G. & Freeze, R. (1984). Theoretical analysis of the role of groundwater flow in the genesis of stratabound ore deposits 1: mathematical and numerical model. *American Journal of Science*, **284**, No. 10, 1085-1124.
- Garven, G. (1989). A hydrogeologic model of the formation of the giant oil sands deposit in the Western Canadian sedimentary basin. *American Journal of Science*, **289**, 105-166.
- Gibson, R. (1994). Fault-zone seals in siliciclastic strata of the Columbus Basin, offshore Trinidad. *Bulletin of the American Association of Petroleum Geologists*, **78**, No. 9, 1372-1385.
- Giles, M.R. & de Boer, R.B. (1990). Origin and significance of redistributive secondary porosity. *Marine and Petroleum Geology*, **7**, 378-397.
- Giles, M.R. & de Boer, R.B. (1989). Secondary porosity: creation of enhanced porosities in the subsurface from the dissolution of carbonate cements as a result of cooling formation waters. *Marine and Petroleum Geology*, **6**, 261-269.
- Giles, M.R., Stevenson, S., Martin, S.V., Cannon, S.J.C., Hamilton, P.J., Marshall, J.D. & Samways, G.M. (1992). The reservoir properties and diagenesis of the Brent Group; a regional perspective. In: Morton, A.C., Haszeldine, R.S., Giles, M.R. & Brown, S. (eds.), *Geology of the Brent Group*. Geological Society of London, London, UK. 289-328.
- Giles, M.R., Indrelid, S.L., & James, D.M.D. (in press). Compaction: the great unknown in basin modelling. In: Duppenbecker, S. & Iliffe, J. (eds.) *Basin Modelling*. Geological Society Special Publication, The Geological Society, London.
- Glassman, J.R., Clark, R.A., Larter, S., Briedis, N.A. & Lundegard, P.D. (1989). Diagenesis and hydrocarbon accumulation, Brent Sandstone (Jurassic) Bergen high area, North Sea. *Bulletin of the American Association of Petroleum Geologists* **73**, 1341-1360.

Gluyas, J., Robinson, A., Emery, D., Grant, S. & Oxtoby, N. (1993). The link between petroleum emplacement and sandstone cementation. *In: Parker, J. (ed.), Petroleum Geology of North West Europe*. The Geological Society, London, 1395-1403.

Goloshubin, G.M. & Galchenko, A.I. (in press). Character of manifestation, model of formation, and prediction of abnormally high reservoir pressure in rocks of the Tyumen producing region, Wets Siberia. *In: Law, B.E. & Ulmishek, G. (eds.), Abnormal pressures in hydrocarbon environments*. American Association of Petroleum Geologists, Tulsa, OK., USA.

Gran, K., Bjørlykke, K. & Aagaard, P. (1992). Fluid salinity and dynamics in the North Sea and Haltenbanken basins derived from well log data. *In: Hurst, A., Griffiths, C. & Worthington, P. (eds.), Geological applications of wireline logs II*. Geological Society Special Publication No. 65, The Geological Society, London, 327-388.

Grauls, D & Cassagnol, C. (1993). Identification of a zone of fluid pressure induced fractures from log and seismic data- a case history. *First Break*, **11**, 2, 1-10.

Greenwood, P.J., Shaw, H.F. & Fallick, A.E. (1994). Petrographic and isotopic evidence for diagenetic processes in Middle Jurassic sandstones and mudrocks from the Brae area, North Sea. *Clay Minerals*, **29**, 4, 637-650.

Hamilton, P., Giles, M. & Ainsworth, P. (1992). K-Ar dating of illites in Brent Group reservoirs: a regional perspective. *In: Morton, A., Haszeldine, R., Giles, M. & Brown, S. (eds.), Geology of the Brent Group*. Geological Society Special Publication No. 61, 377-400.

Hamilton, P., Kelley, S. & Fallick, A. (1989). K-Ar dating of illite in hydrocarbon reservoirs. *Clay Minerals*, **24**, 215-231.

Harrison, W. & Tempel, R. (1993). Diagenetic pathways in sedimentary basins. *In: Horbury, A.D. & Robinson, A.G. (eds.), Diagenesis and basin development*, American Association of Petroleum Geologists Studies in Geology No. 36, Tulsa, OK. 69-86.

Haszeldine, R., Brint, J., Fallick, A., Hamilton, P. & Brown, S. (1992). Open and restricted hydrologies in Brent Group diagenesis: North Sea. *In: Morton, A.,*

Haszeldine, R., Giles, M. & Brown, S. (eds.), *Geology of the Brent Group*. Geological Society Special Publication No. 61, 401-419.

Hedberg, H. D. (1980). Methane generation and petroleum migration. In: Roberts, W.H. & Cordell, R.J. (eds.), *Problems of petroleum migration*. American Association of Petroleum Geologists studies in geology No.10, American Association of Petroleum Geologists, Tulsa, OK., USA. 179-206.

Helgeson, H.C., Knox, A.M., Owens, C.E. & Shock, E.L. (1993). Petroleum, oilfield waters, and authigenic mineral assemblages: Are they in metastable equilibrium in hydrocarbon reservoirs? *Geochimica et Cosmochimica Acta*, **57**, 3295-3339.

Henriet, J.P., de Batist, M. & Verschuren, M. (1991). Early fracturing of Palaeogene clays, southernmost North Sea: relevance to mechanisms of primary hydrocarbon migration. In: Spencer, A.M. (ed.), *Generation, accumulation and production of Europe's hydrocarbons*. Oxford University Press, Oxford, 217-227.

Herman, Z., Weil, W. & Mleczko, A. (in press). Abnormal pressures in Poland-origin and prediction. In: Law, B.E. & Ulmishek, G. (eds.), *Abnormal pressures in hydrocarbon environments*. American Association of Petroleum Geologists, Tulsa, OK., USA.

Hermanrud, C. (1994). Uncertainties in basin modelling- magnitudes and implications (abstract), *Proceedings of the Geological Society Conference on Basin Modelling*. The Geological Society, London.

Hodgson, N.A., Farnsworth, J. & Fraser, A.J. (1992). Salt-related tectonics, sedimentation and hydrocarbon plays in the Central Graben, North Sea, UKCS. In: Hardman, R. (ed.) *Exploration Britain: geological insights for the next decade*. Geological Society Special Publication No. 67, The Geological Society, London. 31-64.

Hoiland, O., Kristensen, J. & Monsen, T. (1993) Mesozoic evolution of the Jaeren High area, Norwegian Central North Sea. In: Parker, J. (ed) *Petroleum Geology of NW Europe*. The Geological Society, London. 1189-1196.

Holm, G. (in press). The Central North Sea: a dynamic hydrocarbon charging system. In: Law, B. & Ulmishek, G. (eds.), *Abnormal pressures in hydrocarbon environments*. American Association of Petroleum Geologists, Tulsa, OK., USA.

Hower, J., Eslinger, E.V., Hower, M.E. & Perry, E.A. (1976). Mechanisms of burial metamorphism of argillaceous sediments: 1. mineralogical and chemical evidence. *Bulletin of the Geological Society of America*, **87**, 725-737.

Hubbert, M.K. & Rubey, W.W. (1959). Role of fluid pressures in mechanics of overthrust faulting: I. Mechanics of fluid-filled porous solids and its application to overthrust faulting. *Geological Society of America Bulletin*, **70**, 115-166.

Hubbert, M.K. (1940). The theory of ground-water motion. *Journal of Geology*, **68**, No. 8, 785-944.

Hunt, J.M. (1990). Generation and migration of petroleum in abnormally-pressured fluid compartments. *Bulletin of the American Association of Petroleum Geology*, **74**, No. 1, 1-12.

Hunt, J.M., Whelan, J.K., Eglinton, L.B. & Cathles, L.M. (1994). Gas generation- a major cause of deep Gulf Coast overpressures. *Oil and Gas Journal*, **92**, 29, 59-63.

Israelachvili, J.N., McGuiggan, P.M. & Homola, A.M. (1988). Dynamic properties of molecularly thin liquid films. *Science*, **240**, 189-191.

Irwin, H., Coleman, M.L. & Curtis, C.D. (1977). Isotopic evidence for several sources of carbonate and distinctive diagenetic processes in organic rich Kimmeridgian sediments. *Nature*, **269**, 209-213.

Jansa, L.F. & Urrea, V.H.N. (1992). Geology and diagenetic history of overpressured sandstone reservoirs, Venture gas field, offshore Nova Scotia, Canada. *Bulletin of the American Association of Petroleum Geologists*, **74**, 10, 1640-1658.

Jorden, J.R. & Shirley, O.J. (1966). Application of drilling performance data to overpressure detection. *Journal of Petroleum Technology*, **28**, No. 11, 1387-1394.

Katsube, T.J. & Williamson, M.A. (1994). Effects of diagenesis on shale nano-pore structure and implications for sealing capacity. *Clay Minerals*, **29**, 451-461.

- Keller, M.B. (in press). Abnormally high reservoir pressure in subsalt rocks of the southeastern Peri-Caspian Basin. *In: Law, B.E. & Ulmishek, G. (eds.), Abnormal pressures in hydrocarbon environments*. American Association of Petroleum Geologists, Tulsa, OK., USA.
- Knipe, R.J. (1993). The influence of fault zone processes and fault zone diagenesis on fluid flow in sedimentary basins. *In: Robinson, A.G. (ed.), Diagenesis and basin development*. Studies in Geology, American Association of Petroleum Geologists, Tulsa, OK. 135-153.
- Larter, S. & Mills, N. (1991). Phase-controlled molecular fractionations in migrating petroleum. *In: England, W. & Fleet, A. (eds) Petroleum Migration*. Geological Society Special Publication No.59, The Geological Society, London, 137-148.
- Law, B.E. & Dickinson, W.W. (1985). Conceptual model for origin of abnormally pressured gas accumulations in low-permeability reservoirs. *Bulletin of the American Association of Petroleum Geologists* **69**, 8, 1295-1304.
- Law, B.E. & Ulmishek, G. (eds) in press. *Abnormal pressures in hydrocarbon environments*. American Association of Petroleum Geologists, Tulsa, OK., USA.
- Leonard, RC. (1993) Distribution of sub-surface pressure in the Norwegian Central Graben and applications for exploration. *In: Parker, J. (ed.) Petroleum Geology of North West Europe*. The Geological Society, London, 1295-1304.
- Lerche, I. (1990). *Basin Analysis- Quantitative Methods, Volume 1*. Academic Press Inc, San Diego, 562 pp.
- Leythausen, D, Radke, M & Schaefer, RG. (1984). Efficiency of petroleum expulsion from shale source rocks. *Nature*, **311**, 745745-748.
- Liewig, N., Clauer, N. & Sommer, F. (1987). Rb-Sr and K-Ar dating of clay diagenesis in Jurassic Sandstone Oil Reservoir, North Sea. *Bulletin of the American Association of Petroleum Geologists*, **71**, No. 12, 12.
- Lindgreen, N. (1987). Molecular sieving and primary migration in Upper Jurassic and Cambrian source rocks. *In: Brooks, J. & Glennie, K. (eds) Petroleum geology of NW Europe*. Graham & Trotman, London, 248-256.

- Lindholm, C.D., Bungum, J., Bratli, R.K., Aadnoy, B.S., Dahl, N., Torudbakken, B. & Atakan, K. (1995) Crustal stress in the Northern North Sea as inferred from borehole breakouts and earthquake focal mechanisms. *Terra Nova*, **7**, 1, 51-59.
- Liu, G. & Roaldset, E. (1994). A new decompaction model and its application to the Northern North Sea. *First Break*, **12**, No. 2, 81-89.
- Longstaffe, F. (1984). The role of meteoric water in diagenesis of shallow sandstones: stable isotope studies of the Milk River aquifer and gas pool, SE Alberta. In: McDonald, D. & Surdam, R. (eds.), *Clastic Diagenesis*. American Association of Petroleum Geologists Memoir 37, Tulsa, OK,
- Luo, M., Baker, M. & LeMone, D. (1994). Distribution and generation of the overpressure system, eastern Delaware Basin, Western Texas and Southern New Mexico. *Bulletin of the American Association of Petroleum Geologists*, **78**, No. 9, 1386-1405.
- Luo, X & Vasseur, G. (1992). Contributions of compaction and aquathermal pressuring to geopressure and the influence of environmental conditions. *Bulletin of the American Association of Petroleum Geologists*, **76**, 10, 1550-1559.
- Luo, X. & Vasseur, G. (1993). Contributions of compaction and aquathermal pressuring to geopressure and the influence of environmental conditions: reply. *Bulletin of the American Association of Petroleum Geologists*, **77**, 11, 2011-2014..
- Mackenzie, A.S., Price, I., Leythaeuser, D., Muller, P., Radke, M. & Schafer, R.G. (1987). The expulsion of petroleum from Kimmeridge Clay source rocks in the area of the Brae oilfield, UK continental shelf. In: Brooks, J. & Glennie, K. (eds) *Petroleum Geology of North West Europe*. Graham & Trotman, London, 865-877.
- Magara, K. (1968). Compaction and migration of fluids in Miocene mudstone, Nagaoka Plain, Japan. *Bulletin of the American Association of Petroleum Geologists*, **52**, 12, 2466-2501.
- Magara, K. (1987). Fluid flow due to sediment loading- an application to the Arabian Gulf region. In: Goff, J. & Williams, B. (eds.), *Fluid flow in Sedimentary Basins and Aquifers*. Geological Society Special Publication No 34, 19-28.

- Malysheva, V.V.(1994). Abnormally high pressures in Upper Cretaceous rocks of the Middle Caspian Basin (abstract). *Proceedings of the American Association of Petroleum Geologists Hedberg Conference on Abnormal Pressures*, Golden, Colorado, USA.
- Mann, M.D. & Mackenzie, A.S. (1990). Prediction of pore fluid pressures in sedimentary basins. *Marine and Petroleum Geology*, 7, No. 1, 55-65.
- Mann, U. (1993). An integrated approach to the study of primary petroleum migration. In: Parnell, J. (ed) *Geofluids: origin, migration and evolution of fluids in sedimentary basins*. Geological Society Special Publication No. 78, The Geological Society, London, 233-260.
- McAuley, G., Burley, S. & Johns, L. (1993). Silicate mineral authigenesis in the Hutton and NW Hutton fields: implications for sub-surface porosity development. In: Parker, J. (ed.), *Petroleum Geology of North West Europe*. The Geological Society, London, 1377-1394.
- McLaughlin, O. (1992). *Isotopic and textural evidence for diagenetic fluid mixing in the South Brae oilfield, North Sea..* Unpublished PhD thesis, Glasgow University, Glasgow, Scotland.
- Meissner, F. (1988). Petroleum geology of the Bakken formation, Williston Basin, North Dakota and Montana. In: Beaumont, E. & Foster, N. (eds) *Geochemistry. Treatise of Petroleum Geology Reprint series, No.8*, American Association of Petroleum Geologists, Tulsa, OK.
- Meissner, F.F. (1980). Examples of abnormal fluid pressure produced by hydrocarbon generation. *Bulletin of the American Association of Petroleum Geologists*, 64, 4, 749.
- Mello, U.T., Karner, G.D. & Anderson, R.N. (1994) A physical explanation for the positioning of the depth to the top of overpressure in shale-dominated sequences in the Gulf Coast basin, United States. *Journal of Geophysical Research*, 99, B2, 2775-2789.
- Meyer, B.L. & Nederlof, M.H. (1984). Identification of source rocks on wireline logs by density/resistivity and sonic transit time/resistivity crossplots. *Bulletin of the American Association of Petroleum Geologists*, 68, 2, 121-129.

Miller, T.W. & Luk, C.H. (1993). Contributions of compaction and aquathermal pressuring to geopressure and the influence of environmental conditions: Discussion. *Bulletin of the American Association of Petroleum Geologists*, **77**, 11, 2006-2010.

Montel, F, Caillet, G, Pucheu, A & Caltagirone, JP. (1993). Diffusion model for predicting reservoir gas losses. *Marine and Petroleum Geology*, **10**, 51-57.

Mouchet, J.P. & Mitchell, A. (1989). *Abnormal Pressures While Drilling*. Manuels techniques elf aquitaine, Boussens, France, 264 pp.

Mudford, B. (in press). Modelling the interplay of pressure evolution, fluid flow and thermal maturity evolution in the Mahakam Delta. *In: Duppenbecker, S. & Illife, J. (eds.), Basin Modelling*. The Geological Society, London.

Mudford, B.S., Gradstein, F.M., Katsube, T.J. & Best, M.E. (1991). Modelling 1D compaction-driven flow in sedimentary basins: a comparison of the Scotian Shelf, North Sea and Gulf Coast. *In: England, W.A. & Fleet, A.J. (eds.), Petroleum Migration*. Geological Society Special Publication No. 59, The Geological Society, London, 65-85.

Muir-Wood, R. (1988). *Shear waves show the Earth is a bit cracked*. *New Scientist*, **18**, April 21st 1988, 44-48.

Mullis, J. (1988). Rapid subsidence and upthrusting in the Northern Appenines, deduced by fluid inclusions studies in quartz crystals from Poretta Terme. *Schweizerische Mineralogische und Petrographische Mitteilungen*, **68**, 157-170.

Nashaat, M. in press. Abnormal pressure at the Nile Delta and North Sinai Basins, Egypt. *In: Law, B.E. & Ulmishek, G. (eds.), Abnormal pressures in hydrocarbon environments*. American Association of Petroleum Geologists, Tulsa, OK., USA.

Nedkvitne, T., Karlsen, D., Bjørlykke, K. & Larter, S. (1993). Relationship between reservoir diagenetic evolution and petroleum emplacement in the Ula field, North Sea. *Marine and Petroleum Geology*, **10**, 255-270.

Neuzil, C.E. (1995) Abnormal pressures as hydrodynamic phenomena. *American Journal of Science*, **295**, 742-786.

Oknova, N.S. (in press). Geologic causes of abnormally high reservoir pressure in the Timan-Pechora Basin. *In: Law, B.E. & Ulmishek, G. (eds.), Abnormal pressures in hydrocarbon environments*. American Association of Petroleum Geologists, Tulsa, OK., USA.

Okui, A., Hara, M. & Matsubayashi, H. (in press). Overpressuring in the Akita Basin, Japan. *In: Law, B.E. & Ulmishek, G. (eds.), Abnormal pressures in hydrocarbon environments*. American Association of Petroleum Geologists, Tulsa, OK., USA.

Oreskes, N. & Belitz, K. (1994). *Modelling complex systems: What can be done?* Proceedings of the Chapman Conference on Hydrogeology, Lincoln, New Hampshire.

Oreskes, N., Shrader-Frechette, K. & Belitz, K. (1994). Verification, validation and confirmation of numerical models in the earth sciences. *Science*, **263**, 641-646.

Ortoleva, P. & Al-Shaieb, Z. (eds) (1995) *Basin Compartments and Seals*. American Association of Petroleum Geologists Memoir 61, Tulsa, OK., USA.

Ortoleva, P. (1993). Self-organisation and nonlinear dynamics in sedimentary basins. *Phil. Trans. R. Soc. Lond.*, **344**, 171-179.

Osadetz, K.G., Brooks, P. & Snowdon, L.R. (1992). Oil families and their sources in the Canadian Williston Basin (SE Saskatchewan and SW Manitoba). *Bulletin of Canadian Petroleum Geology*, **40**, 254-273.

Osborne, M. & Haszeldine, R.S. (1992). Fluid inclusions in diagenetic quartz record oil field burial temperatures, not precipitation temperatures. *Marine and Petroleum Geology*, **10**, 271-278.

Park, A., Maxwell, M., Mu, J. & Ortoleva, P. (1995). *Chaotic basin fluid migration patterns*. (abstract). Proceedings of the American Association of Petroleum Geologists Annual Convention, Houston, Tx. USA.

Payne, D.L. & Park, A.J. (1995). *Modelling diagenetic reservoir modifications during basin evolution, offshore Norway*. (abstract). Proceedings of the American Association of Petroleum Geologists Annual Convention, Houston, Tx., USA.

- Pearson, M.J. & Small, J.S. (1988). Illite-smectite diagenesis and palaeotemperatures in Northern North Sea Quarternary to Mesozoic shale sequences. *Clay Minerals*, **23**, 2, 109-132.
- Pekot, L.J. & Gerril, G.A. (1987). Ekofisk. In: Spencer, A.M. (ed.) *Geology of the Norwegian Oil and Gas fields*. Graham & Trotman, London, 73-87.
- Penge, J., Taylor, B., Huckerby, J.A. & Munns, J.W. (1993) Extension and salt tectonics in the East Central Graben. In: Parker, J. (ed) *Petroleum Geology of NW Europe*. The Geological Society, London. 1197-1210.
- Pepper, A.S. (1991). Estimating the petroleum expulsion behaviour of source rocks: a novel approach. In: England, W. & Fleet, A. (eds) *Petroleum Migration*. Geological Society Special Publication No. 59, The Geological Society, London, 9-32.
- Person, M. & Garven, G. (1992). Hydrologic constraints on petroleum generation within continental rift basins- theory and application to the Rhine Graben. *Bulletin of the American Association of Petroleum Geologists*, **76**, No. 4, 468-488.
- Platte River Associates Inc (1995). *BasinModTM User's Handbook*. PRA Inc, Denver, USA.
- Popper, K.R.(1963). *Conjectures and refutations: the growth of scientific knowledge*. Routledge & Kegan Paul.
- Powers, M. (1959). Adjustment of clays to chemical change and the concept of the equivalence level. *Clays and Clay Minerals*, **6**, 309-326.
- Powley, D.E. (1990) Pressures and hydrogeology in petroleum basins. *Earth-Science Reviews*, **29**, 215-216.
- Powley, D.E. (1980). *Pressures, normal and abnormal*. American Association of Petroleum Geologists Advanced Exploration Schools, 38 pp.
- Price, J, Dyer, R, Goodall, I, McKie, T, Watson, P & Williams, G. (1993) Effective stratigraphical subdivision of the Humber Group and the Late Jurassic evolution of the UK Central Graben. In: Parker, J. (ed) *Petroleum Geology of NW Europe*. 1, The Geological Society, London, 443-458.

Ramm, M. & Bjørlykke, K. (1994). Porosity-depth trends in reservoir sandstones: assessing the quantitative effects of varying pore pressure, temperature history and mineralogy, Norwegian Shelf data. *Clay Minerals*, **29**, No. 4, 475-490.

Rattee, R.P. & Hayward, A.B. (1993) Sequence stratigraphy of a failed rift system: the Middle Jurassic to Early Cretaceous basin evolution of the Central and Northern North Sea. In: Parker, J. (ed) *Petroleum Geology of NW Europe*. The Geological Society, London, 215-249.

Reynolds, T. (1994) Quantitative analysis of submarine fans in the Tertiary of the North Sea Basin. *Marine and Petroleum Geology*, **11**, 2, 202-207.

Rieke, H.H. & Chilingarian, G.V. (1974). *Compaction of argillaceous sediments*. Developments in sedimentology No.16, Elsevier, Amsterdam, 424pp.

Roberts, A., Price, J. & Olsen, T. (1990). Late Jurassic half-graben control on the siting and structure of hydrocarbon accumulations: UK/Norwegian Central Graben. In: Hardman, R. & Brooks, J. (eds.), *Tectonic Events Responsible For Britain's Oil and Gas Reserves*. Geological Society of London Special Publication No 55, 229-257.

Saigal, G., Bjørlykke, K. & Larter, S. (1992). The effects of oil emplacement on diagenetic processes- examples from the Fulmar reservoir sandstones, Central North Sea. *Bulletin of the American Association of Petroleum Geologists*, **76**, No. 7, 1024-1033.

Sclater, J. & Christie, P. (1980). Continental stretching: an explanation of the post mid-Cretaceous subsidence of the central North Sea basin. *Journal of Geophysical Research*, **85**, 3711-3739.

Sears, R.A., Harbury, A.R., Protoy, A.J.G. & Stewart, D.J. (1993) Structural styles from the Central Graben in the UK and Norway. In: Parker, J. (ed) *Petroleum Geology of Northwest Europe: Proceedings of the 4th Conference*. The Geological Society, London, 1231-1244.

Seewald, J. (1994). Evidence for metastable equilibrium between hydrocarbons under hydrothermal conditions. *Nature*, **370**, 285-287.

Sibson, R.H., Moore, M. & Rankin, A.H. (1975). Seismic pumping - a hydrothermal fluid transport mechanism. *Journal of the Geological Society of London*, **131**, 653-659.

Small, J. (1993). Experimental determination of the rates of precipitation of authigenic illite and kaolinite in the presence of aqueous oxalate and comparison to the K-Ar ages of authigenic illite in reservoir sandstones. *Clays and Clay Minerals*, **41**, No. 2, 191-208.

Small, J., Hamilton, D. & Habesch, S. (1992). Experimental simulation of clay precipitation within reservoir sandstones 2: mechanism of illite formation and controls on morphology. *Journal of Sedimentary Petrology*, **62**, No. 3, 520-529.

Smith, R.I., Hodgson, N. & Fulton, M. (1993) Salt control on Triassic reservoir distribution, UKCS Central North Sea. In: Parker, J. (eds) *Petroleum Geology of NW Europe*. The Geological Society, London. 547-558.

Spencer, C. (1987). Hydrocarbon generation as a mechanism for overpressuring in the Rocky Mountain Region. *Bulletin of the American Association of Petroleum Geologists*, **71**, No. 4, 368-388.

Stewart, D. (1986). Diagenesis of the shallow marine Fulmar formation in the Central North Sea. *Clay Minerals*, **21**, 537-564.

Stewart, R.N. (1995). Diagenesis of the Palaeocene submarine fans in the North Sea. Unpublished PhD thesis, University of Glasgow, Glasgow, Scotland.

Surdam, R.C. & Crossey, L.J. (1985). Organic-inorganic reactions during progressive burial: key to porosity and permeability enhancement and preservation. *Phil. Trans. Roy. Soc. London, Series A*. **315**, 135-156.

Swarbrick, R.E. (1994). Reservoir diagenesis and hydrocarbon migration under hydrostatic palaeopressure conditions. *Clay Minerals*, **29**, No. 4, 463-474.

Swartzendruber, D. (1962). Non-Darcy flow behavior in liquid-saturated porous media. *Journal of Geophysical Research*, **67**, No. 13, 5205-5213.

Symington, W., Huang, J., Green, K., Pottorf, R. & Summa, L. (1994). *Multi-disciplinary approach to modelling secondary migration, a Central North Sea*

example (abstract). Proceedings of the American Association of Petroleum Geologists Annual Convention, Denver, Colorado, USA.

Tang, J. & Lerche, I. (1992). Analysis of the Beaufort-mAckenzie Basin, Canada - burial, thermal and hydrocarbon history. *Marine and Petroleum Geology*, **9**, No.5, 510-525.

Taylor, J.C.M. (1984) The Late Permian-Zechstein. *In: Glennie, K.W. (ed.) Introduction to the Petroleum Geology of the North Sea*, Blackwell Scientific Publications, London, 61-84.

Terzaghi, K. (1943). *Theoretical Soil Mechanics*. John Wiley & Sons, New York.

Thorne, J. & Watts, A. (1989). Quantitative analysis of North Sea subsidence. *Bulletin of the American Association of Petroleum Geologists*, **73**, No. 1, 88-116.

Tiggert, V. & Al-Shaieb, Z. (1990). Pressure seals: their diagenetic banding patterns. *Earth-Science Reviews*, **29**, 227-240.

Toth, J., Maccagno, M.D., Otto, C.J. & Rostron, B.J. (1991). Generation and migration of petroleum from abnormally pressured fluid compartments: Discussion. *Bulletin of the American Association of Petroleum Geologists*, **75**, No. 2, 331-335.

Trewin, N. & Bramwell, M. (1991). The Auk field, Block 30/16, UK North Sea. *In: Abbotts, I. (ed.), United Kingdom Oil and Gas Fields, 25 years commemorative volume*. Geological Society Memoir No.14, The Geological Society, London, 227-236.

Ungerer, P., Behar, E. & Discamps, D. (1981). Tentative calculation of the overall volume expansion of organic matter during hydrocarbon genesis from geochemistry data. Implications for primary migration. *In: Meyer, J (ed.) Advances in Organic Geochemistry*. John Wiley & Sons, New York.

Ungerer, P., Burrus, J., Doligez, B., Chenet, P.Y. & Bessis, F. (1990). Basin Evaluation by integrated two-dimensional modeling of heat transfer, fluid flow, hydrocarbon generation and migration. *Bulletin of the American Association of Petroleum Geologists*, **74**, No. 3, 309-335.

Van Balen, R & Cloetingh, S. (1994) Tectonic control of the sedimentary record and stress-induced fluid flow: constraints from basin modelling. *In: Parnell, J. (ed) Geofluids: origin, migration and evolution of fluids in sedimentary basins.* Geological Society Special Publication No. 78, The Geological Society, London, 9-26.

Van Wagoner, J.C., Mitchum, R.M., Campion, K.M. & Rahmanian, V.D. (1990). Siliciclastic sequence stratigraphy in well logs, cores and outcrops. *American Association of Petroleum Geologists Methods in Exploration Series, No.7.* American Association of Petroleum Geologists, Tulsa, OK., USA, 55pp.

Wakefield, L.L., Droste, H., Giles, M.R. & Janssen, R. (1993) Late Jurassic plays along the western margin of the Central Graben. *In: Parker, J. (ed) Petroleum Geology of NW Europe.* The Geological Society, London. 459-468.

Waldrop, M.M. (1993). *Complexity.* Viking, London, 380pp.

Watts. (1987). Theoretical aspects of cap-rock and fault seals for single- and two-phase hydrocarbon columns. *Marine and Petroleum Geology, 4,* 274-307.

Weedman, S.D., Brantley, S.L. & Albrecht, W. (1992). Secondary compaction after secondary porosity: Can it form a pressure seal? *Geology, 20,* No. April 1992, 303-306.

Wensaas, L., Shaw, H.F., Gibbons, K., Aagaard, P. & Dypvic, H. (1994). Nature and causes of overpressuring in mudrocks of the Gullfaks area, North Sea. *Clay Minerals, 29,* 4, 139-450.

Whelan, J.K, Eglinton, L.B. & Cathles, L.M. (1994) Pressure Seals- Interactions with organic matter, experimental observations, and relation to a "hydrocarbon Plugging" hypothesis for pressure seal formation. *In: Ortoleva, P. & Al-Shaieb, Z. (eds) Basin Compartments and Seals.* American Association of Petroleum Geologists Memoir 61, American Association of Petroleum Geologists, Tulsa, OK. USA. 125-153.

Whelan, J.K., Kennicutt, M.C., Brooks, J.M., Schumacher, D. & Eglinton, L.B. (in press). Organic geochemical indicators of dynamic fluid flow processes in petroleum basins. *Bulletin of the American Association of Petroleum Geologists.* .

Wilkinson, M. (1990). Concretionary cements in Jurassic Sandstones, Isle of Eigg, Inner Hebrides. *In: Parnell, J. (eds.), Basins of the Atlantic Seaboard: Petroleum Geology, Sedimentology and Evolution.* Geological Society of London Special Publications, Geological Society of London, London.

Wilkinson, M., Fallick, A., Keaney, G., Haszeldine, R. & McHardy, W. (1994a). Stable isotopes in illite: the case for meteoric water flushing within the Upper Jurassic Fulmar sandstones, UK North Sea. *Clay Minerals*, **29**, No. 4, 567-574.

Wilkinson, M., Haszeldine, R.S., Osborne, M., Keaney, G., McKeown, C. & Darby, D. (1994b). Diagenesis of the Fulmar sandstones in the Central Graben. *Elf Enterprise Caledonia Internal Report*, Aberdeen, UK.

Wilkinson, M. & Haszeldine, R.S. (in prep (a)). Aluminium loss from overpressured Jurassic sandstones, Central North Sea.

Wilkinson, M., Darby, D. & Haszeldine, R.S. (in prep (b)). Late secondary porosity associated with overpressure leak-off: evidence from the Fulmar formation, UKCS.

Wilkinson, M., Haszeldine, R.S. & Fallick, A.E. (in prep (c)). Diagenesis of the Fulmar sandstones in the UK Central Graben.

Williamson, M.A. & Smyth, C. (1992). Timing of gas and overpressure generation in the Sable Subbasin, offshore Nova Scotia. *Bulletin of Canadian Petroleum Geology*, **40**, No. 2, 151-169.

Williamson, M., Coflin, K., King, S., Desroches, K., Moir, P., McAlpine, K.D., & Wray, A. (1994). A hydrocarbon charge model of the Hibernia drainage area, Jeanne D'Arc basin, offshore Newfoundland. *Energy Exploration and Exploitation*, **12**, No.4, 295-323.

Wilson, M.S., Gunneson, B.G., Honore, R. & Enrico, R. (in press). Characteristics of abnormally pressured compartments in the southern Piceance Basin, Colorado. *In: Law, B.E. & Ulmishek, G. (eds.), Abnormal pressures in hydrocarbon environments.* American Association of Petroleum Geologists, Tulsa, OK., USA.

Wyllie, M.R.J. (1956). Elastic wave velocities in heterogeneous and porous media. *Geophysics*, **21**, 1, 41-70.

Wyllie, M.R.J. (1958). An experimental investigation of factors affecting elastic wave velocities in porous media. *Geophysics*, **23**, 3, 459-493.

Yardley, B.W.D. & Valley, J.W. 1994. How wet is the Earth's crust? *Nature*, **371**, 205-206.

Yassir, N. & Bell, J. (1994). Relationships between pore pressure, stresses, and present-day geodynamics in the Scotian Shelf, offshore eastern Canada. *Bulletin of the American Association of Petroleum Geologists*, **78**, No. 12, 1863-1880.

Ziegler, K., Sellwood, B. & Fallick, A. (1994). Radiogenic and stable isotope evidence for age and origin of authigenic illites in the Rotliegend, southern North Sea. *Clay Minerals*, **29**, No. 4, 555-566.

Zoback, M.D., Apel, R., Baumgartner, J., Brudy, M., Emmerman, R., Engeser, B., Fuchs, K., Kessels, W., Rischmuller, H., Rummel, F. & Vernick, L. (1993). Upper-crustal strength inferred from stress measurements to 6km depth in the KTB borehole. *Nature*, **365**, 633-635.

Appendix

Mathematical foundation of BasinMod™

Chapters Five and Six have used quantitative basin models to gain insight into the hydrogeological systems of the Central Graben. The models used are the BasinMod™ system. BasinMod™ is a commercial one- and two-dimensional basin modelling software package developed by Platte River Associates Ltd. It is the purpose of this Appendix to present the mathematical foundation of this software package. This will allow evaluation of the adequacy of the governing equations, and the likely impact of this adequacy on the errors in the results presented in Chapter Five.

1D modelling has become the industry standard for maturity modelling. 2D models are a more recent development, but are already becoming established. The BasinMod™ system is favoured by geoscientists in the oil industry due to several factors. Their modular form allows the user to focus on aspects of the petroleum system of particular relevance to the desired end. The developers have devoted a great deal of effort to graphics, allowing far greater ease of use than comparable models. Unlike TEMISPACK or CIRF.B (see Section 5.2), BasinMod™ does not use novel algorithms to describe geological processes. Instead, existing published algorithms (from many authors) are encoded into the model. This emphasis on software development over scientific advancement has contributed to BasinMod™'s position as the industry leader. Significantly, BasinMod™ is continually updated and improved in the light of regular feedback from the end-users.

As a piece of commercial (and expensive) software, portions of BasinMod™ are confidential. The numerical solution (see Bethke, 1985) and finite-difference methodology employed are confidential and cannot be reproduced in this thesis. However, all algorithms used to describe the geological processes under investigation are derived from the scientific literature. Accordingly, the empirical adequacy of the governing equations has been extensively peer-reviewed.

This study has used BasinMod™ 1-D release versions 3.23 and 4.2, and BasinMod™ 2-D release versions 0.5 and 1.28.

Both 1D and 2D packages have a common mathematical foundation. The models comprise a burial history and fluid flow module; a heat transfer module; and a hydrocarbon generation and expulsion module. These modules will be discussed below. Basin modelling is by definition a complex exercise, encompassing many diverse geological disciplines. Thus this Appendix will only provide a brief discussion of the mathematical description embodied in the model. For further

details, the reader is referred to the BasinMod™ User's Handbook (Platte River Associates 1995). Symbols used in equations are contained in Table A1.

A.1 Burial History and Fluid Flow

1D and 2D models have used a coupled fluid-flow and compaction methodology based on Darcy's Law and the concept of effective stress (Section 2.1). The premise is that restricted fluid flow will lead to restricted sediment compaction. The fluid-flow and compaction equations combine a mass conservation equation with a state equation of mass and the equation of transportation (Darcy's Law). This allows simulation of how the porosity, permeability, fluid viscosity, density, and the amount, rate and direction of fluid flow vary with time. The formulation is identical to that of Bethke (1985) and Lerche (1990). The equations are formulated as finite difference approximations and applied to a finite difference grid of a cross section of the basin (Fig 5.19)

Note that the mass conservation equations (Bethke 1985) do not take into account any alteration of volume due to geochemical reactions. Such reactions have been shown to be extremely important in affecting the pore volume of sandstones (Emery et al 1993). The equations of Bethke (1985) have also been criticised (Audet & McConnell, 1994) for failing to present a 2D momentum balance for stresses. Thus the role of lateral stresses in changing pore volume cannot be addressed.

Simulation of porosity reduction is perhaps the most vital element of the model for pressure modelling. As discussed in Section 4.2 and 7.4. porosity change is poorly understood. Many empirical studies suggest an exponential relationship between depth and porosity (e.g. Rubert & Hubbey 1959, Bethke 1985). In BasinMod, porosity reduction is governed by the effective stress acting on the sediment (Bethke 1985) as described by

$$\phi = \phi_i \exp \left[A \frac{\sigma - \sigma_i}{\sigma_i} \right] \dots\dots\dots(i)$$

Thus compaction is related to pore fluid pressure. A is a lithology-dependent fit coefficient. Initial sediment porosity ϕ_i is taken from Bethke (1985). Both A and ϕ_i are plausible, standard values (see the BasinMod™ User's Handbook (Platte River

Associates 1995), Bethke, 1985 and Person & Garven, 1992, and Tables 5.1 and 5.2). Standard compaction curves under hydrostatic conditions are shown in Fig A.1 for each lithology.

Permeability is also vital to the simulation of pressure and fluid flow. The reduction of permeability upon compaction of the sediments is simulated by a power function (Lerche 1990).

$$K = \left(\frac{K_i}{\phi_i^B} \right) \phi^B \dots\dots\dots(ii)$$

Again, values of K_i and B are plausible, standard values for each lithology. Parameters A and B in equations (i) and (ii) are presented in Tables 5.1 and 5.2. Initial permeability K_i is varied to achieve calibration to pressures (see Section 5.3). The relationship between porosity and permeability for each standard lithology is shown in Figure A.2. There is no completely accepted method of simulating permeability, which leads to the necessity of the calibration process discussed in Section 5.2. There is a world-wide dearth of in-situ measured permeabilities for mudstones, which are critical for fluid flow. Moreover, sandstone permeabilities are often mediated by geochemical processes. Thus it is difficult to judge the empirical adequacy of this equation, despite its importance in controlling simulated fluid flow.

A.2 Heat transfer

The heat transfer equation is used to solve for the basin temperature distribution resulting from heat conduction and advective heat transfer (Bethke 1985). Heat flow is simulated using the fully compacted coordinate form (Lerche 1990):

$$\left(\frac{\partial H_r}{\partial T} + \frac{\partial H_f}{\partial T} \right) \frac{\partial T}{\partial t} = \gamma \frac{\partial}{\partial x} \left(k_x \frac{\partial T}{\partial x} \right) + \frac{\partial}{\partial \xi} \left(\frac{k_z}{\gamma} \frac{\partial T}{\partial \xi} \right) \dots\dots\dots(iii)$$

$$- \frac{\gamma \rho c K_x}{\mu} \frac{\partial P_x}{\partial x} \frac{\partial T}{\partial x} - \frac{\gamma \rho c K_z}{\mu \gamma^2} \left[\frac{\partial P_x}{\partial \xi} + g \xi \gamma \frac{\partial P_n}{\partial \xi} \right] \frac{\partial T}{\partial \xi}$$

$$\text{and } H = T(\rho_f c_f e + \rho_r c_r) \dots\dots\dots(iv)$$

A.3 Hydrocarbon generation and expulsion

Kerogen maturity is calculated using the Lawrence Livermore National Laboratory "easy Ro" equation (Burnham & Sweeney 1989). This methodology is based on kerogen kinetic parameters derived from geological studies and laboratory analogues and is valid for vitrinite reflectance values of between $R_o = 0.3\%$ and $R_o = 4\%$. Primary hydrocarbon expulsion from source rocks is simulated using the pressure-fracture expulsion model of Duppenbecker *et al* (1991). The premise of this approach is that pore pressure increases when petroleum is generated from kerogen due to the difference in densities. If pore pressure is high enough to overcome capillary pressure or to fracture the rocks, then the hydrocarbons are expelled. Sections 5.4.4 and 5.5.5 have shown that the data available to this project is insufficient for quantitative simulation of hydrocarbon generation. It should also be noted that almost all aspects of hydrocarbon generation, expulsion and migration are poorly understood in quantitative precision (Mann 1994). Accordingly quantitative simulation of these processes is undoubtedly subject to considerable uncertainty in the underlying conceptualisation and the empirical adequacy of the governing equations.

Volumetric changes occur when kerogen transforms into oil and gas. These volumetric changes may alter pore pressure. BasinMod™ 2-D calculates the pressure increase due to the generation of hydrocarbons using the equations of Lerche (1990). Generation pressure is determined from the temperature, sediment porosity, liquid density, liquid compressibility and rate of kerogen transformation. Sediment porosity increases as solid kerogen is transformed to hydrocarbon fluid. This approach is necessarily a simplification of a highly complex process (see Section 4.3). It is noted that the simulated pressure resulting from compaction disequilibrium, with a minor component of generation pressure, forms an adequate match to observed pressures in the Central North Sea (Section 5.5.4). However, the test of a model is its adequacy in reproducing the observed geological phenomena. These equations should be tested in other basins such as the Piceance Basin where overpressure is believed to be due to hydrocarbon generation (Spencer 1987).

A.4 Boundary Conditions

In the 2D models used in Chapter Five, the lateral and basal boundaries of the model are assumed to be closed, i.e. that no flow occurs. Pressure is zero at the upper model boundary (the sediment surface).

A.5 Faults

BasinMod™ applies a "Leak Fraction" to simulate the permeability of a fault. In the 2D models of Chapter Five, faults were treated as either *closed* (a barrier to fluid flow, where "Leak Fraction" =0), or as *open* (a highly permeable conduit, where Leak Fraction = 1). For these conditions

$$\text{Closed faults: } K = K_f$$

and if $K_f > 0.1$ mD, then the model assumes $K_f = 0.1$ mD;

if $K_f < 0.1$ mD, then the actual value of K_f is used.

$$\text{Open faults: } K = 10 K_f$$

and if $K_f > 1.0$ mD, then the actual value of K_f is used;

if $K_f < 1.0$ mD, then the model assumes $K_f = 1.0$ mD.

Thus fault permeability changes over time as the faulted lithology compacts. Actual values of fault permeability used in "open" and "closed" fault models are shown in Figure A.4. This is clearly a very simple approximation to the highly complex behaviour of fluid flow in faults. For example, modelled faults in mudstones do not take into account "shale smears" which may lower permeability below that of adjacent formations. Similarly, permeable faults which contain open fractures may be considerably more permeable than assumed in the model. The model values of 1 mD for an open fault and 0.1 mD for a closed fault are arbitrary and do not appear to be based on any geological observation. Faults are considered to be so fundamental to fluid flow in the crust (e.g. Bredehoeft *et al* 1994) that this simplification by BasinMod™ may be viewed as a serious failing. Quantifying the permeability of fault zones will allow a major step forward in the correspondence between basin models and geological reality.

A.6 Multiphase Fluid Flow

Three-phase fluid flow in the model is governed by a series of partial differential equations derived from Darcy's Law. Water is assumed to be the wetting phase, and so flow of oil and gas is controlled by relative permeability and capillary pressures (Lerche 1990).

$$\frac{\partial}{\partial t}(\rho_w e S_w) = \gamma \frac{\partial}{\partial x} \left(\frac{K_x K_w \rho_w}{\mu_w} \frac{\partial P_w}{\partial x} \right) + \frac{\partial}{\partial \zeta} \left(\frac{K_z K_w \rho_w}{\gamma_w} \frac{\partial P_w}{\partial \zeta} \right) + q_w$$

$$\frac{\partial}{\partial t}(\rho_o e S_o) = \gamma \frac{\partial}{\partial x} \left(\frac{K_x K_o \rho_o}{\mu_o} \frac{\partial P_o}{\partial x} \right) + \frac{\partial}{\partial \zeta} \left(\frac{K_z K_o \rho_o}{\gamma_o} \frac{\partial P_o}{\partial \zeta} \right) + q_o$$

$$\frac{\partial}{\partial t}(\rho_g e S_g) = \gamma \frac{\partial}{\partial x} \left(\frac{K_x K_g \rho_g}{\mu_g} \frac{\partial P_g}{\partial x} \right) + \frac{\partial}{\partial \zeta} \left(\frac{K_z K_g \rho_g}{\gamma_g} \frac{\partial P_o}{\partial \zeta} \right) + q_g \quad \dots\dots\dots(v)$$

and where

$$S_w + S_o + S_g = 1.0 \quad \dots\dots\dots(vi)$$

Capillary pressure of oil and gas is calculated as:

$$P_{c_m} = C \frac{1.0}{(1.0 - S_{w_{IRR}} - S_m) \phi \gamma} \quad \dots\dots\dots(vii)$$

Table A.1 Symbols used in equations

ρ = density (g/cm^3)	s = effective stress (MPa)
f = porosity	s_i = initial effective stress (MPa)
f_i = initial porosity	T = temperature ($^{\circ}\text{C}$)
K = permeability (mD)	k = thermal conductivity
K_i = initial permeability (mD)	c = thermal capacity
A = porosity reduction factor	H = enthalpy (J)
B = permeability reduction factor	q = source term
K_f = fault permeability (mD)	P = pressure (MPa)
K_{f0} = permeability if no fault present (mD)	P_x = excess pressure (MPa)
g = gravitational constant	z = rock matrix thickness (m)
m = viscosity (Pa/s)	$S_{w_{\text{irr}}}$ = irreducible water saturation
t = time (s)	g = grain size (mm)
e = void ratio	x = distance in lateral (x) direction (m)
S = saturation	z = distance in vertical (z) direction (m)
S_m = saturation of the mth fluid	

Subscripts

Subscript w refers to water
 Subscript o refers to oil
 Subscript g refers to gas
 Subscript r refers to rock
 Subscript f refers to fluid
 Subscript x refers to lateral (x) direction
 Subscript z refers to vertical (z) direction

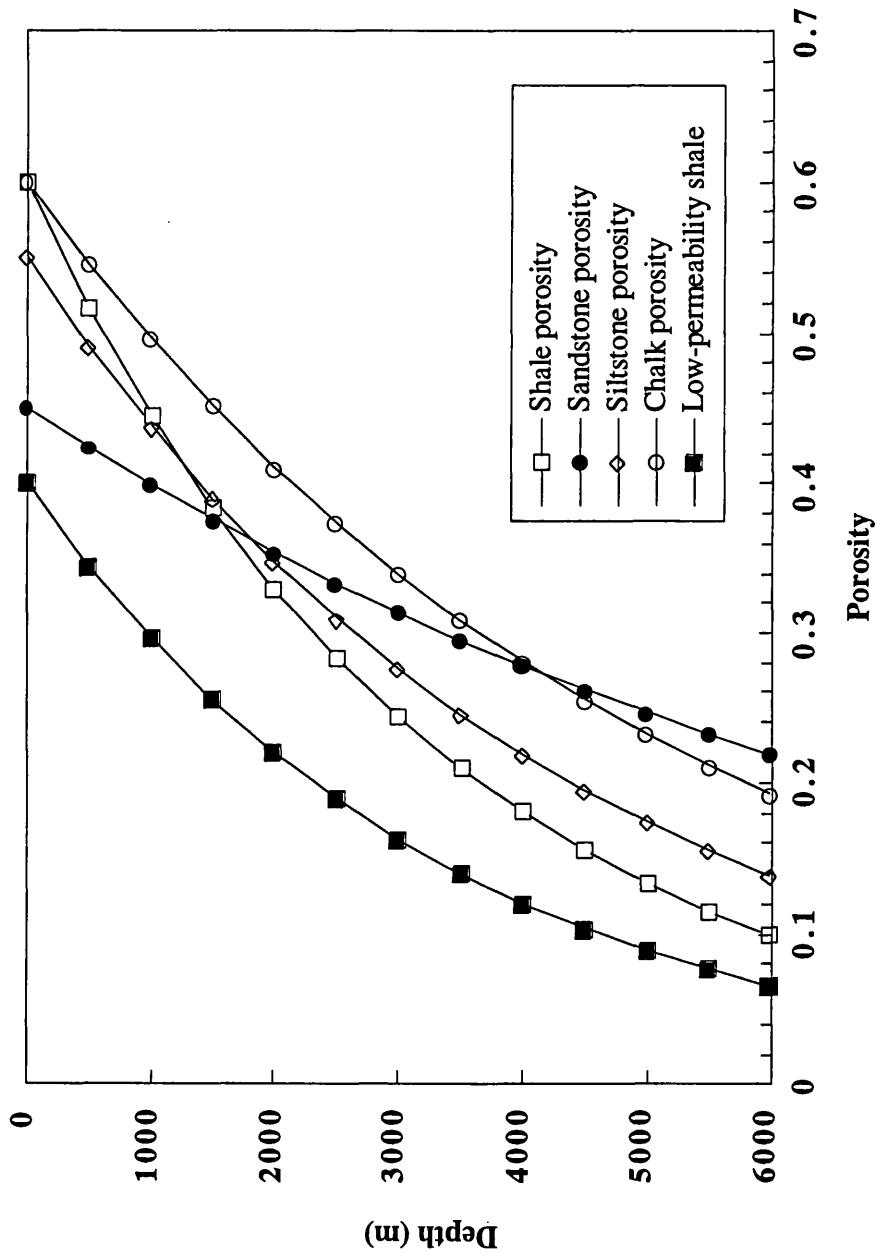


Figure A.1 Sediment compaction curves used in BasinMod (in hydro pressured conditions) Each rock type compacts from an initial value (from Bethke, 1985 and Person & Garven (1992)) according to the exponential equation (i), from Bethke (1985).

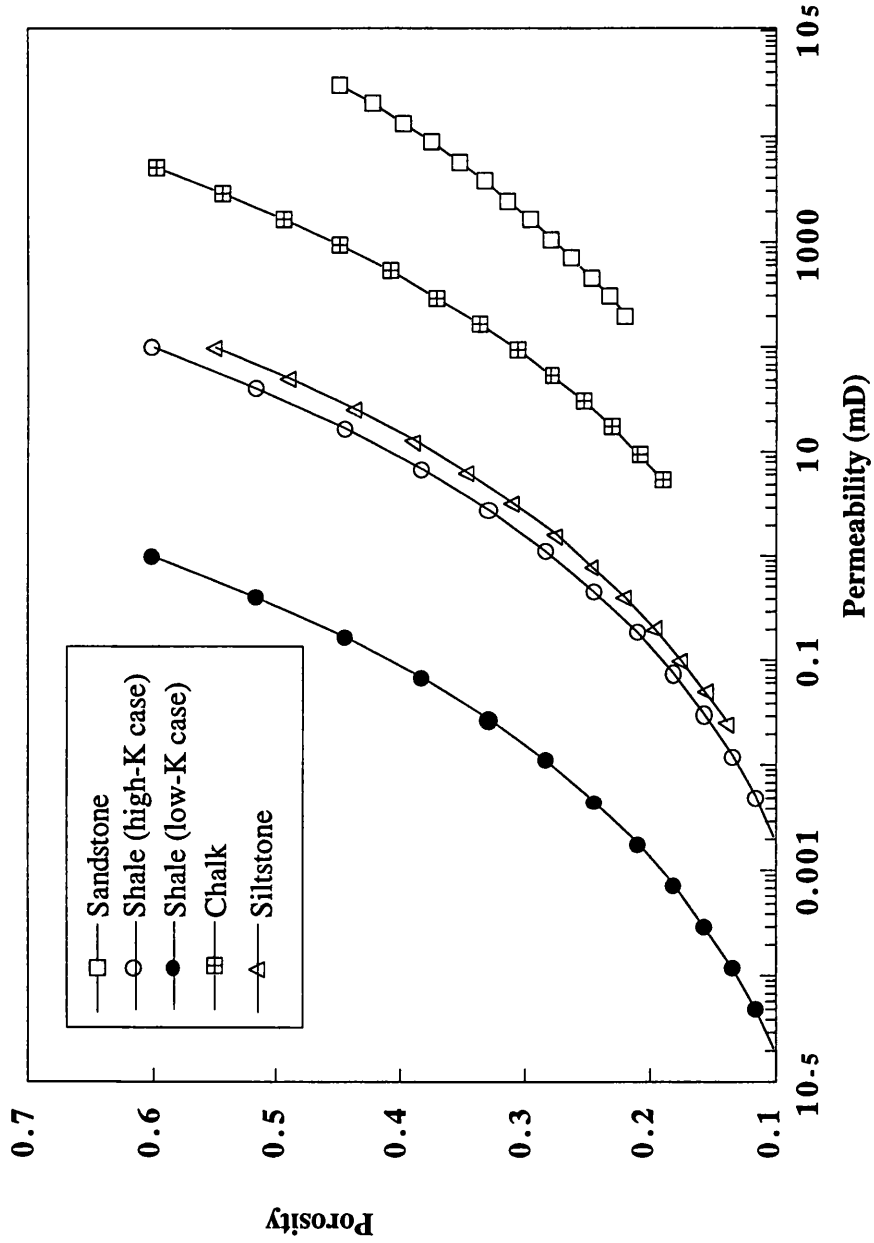


Figure A.2 The relationship of vertical permeability to porosity in BasinMod. Permeability decreases from an initial high value according to Lerche's Power Law (equation (ii), from Lerche, 1990). Initial sediment permeability from Person & Garven 1990. Initial permeability of shale was varied to produce a low-permeability model.

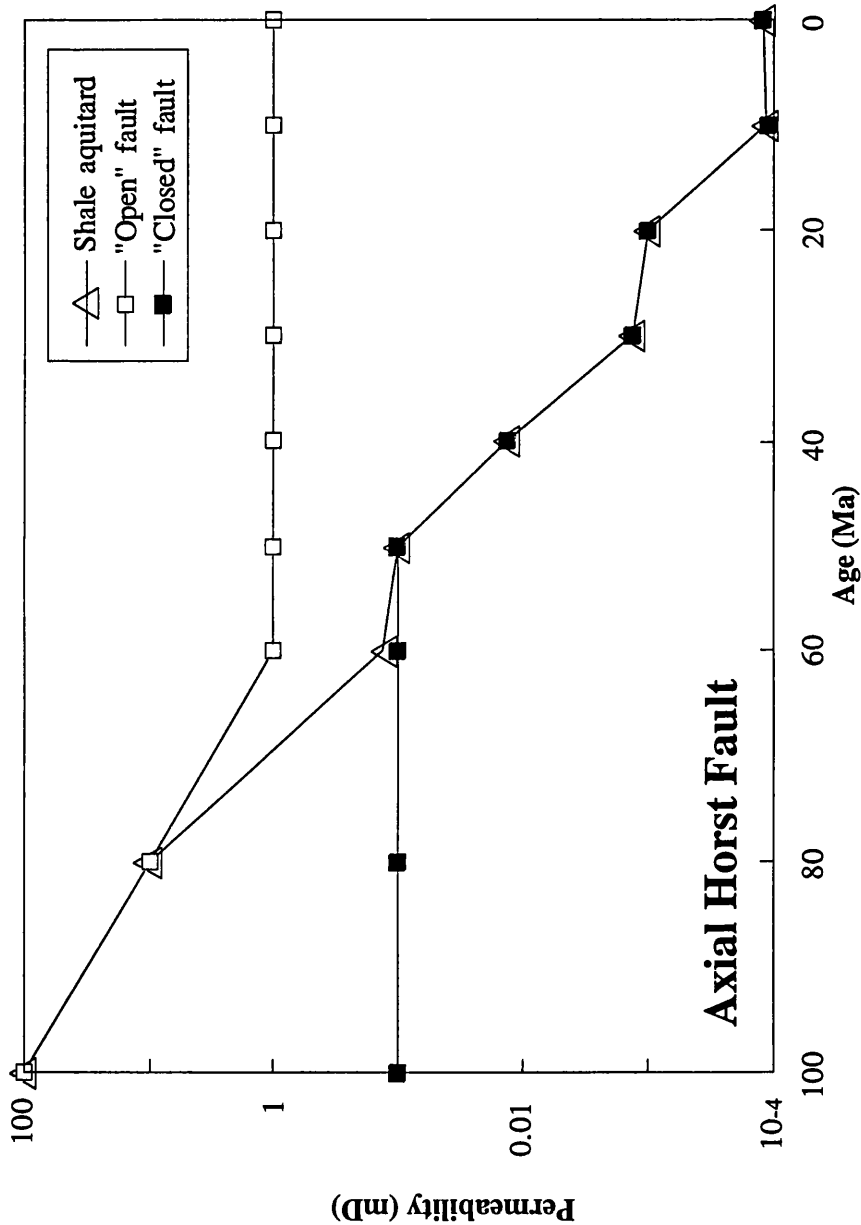


Figure A.3 Modelled fault permeability. Fault permeability in BasinMod depends on the permeability of the faulted rocks. Open and closed faults have been modelled according to the relationship in Section A.5. An "open" fault has a low (1mD) permeability during the Cenozoic. This low permeability does not significantly enhance fluid flow through the aquitard, as the faults do not fully pierce the aquitard. The low-permeability case is equivalent to an unfaulted aquitard during the Cenozoic. Fault permeability has no effect on overpressure distribution in this model (see Section 5.5.6).